Discovery of Pro-Inflammatory Cytokine Inhibitors from Bacterial Strain for the Treatment of Renal Inflammation

THESIS

Submitted in partial fulfillment

of the requirements for the degree of

DOCTOR OF PHILOSOPHY

by

KIRTI

ID No 2016PHXF0030H

Under the Supervision of

Prof. A. SAJELI BEGUM

&

Under the Co-supervision of

Prof. ONKAR KULKARNI

Pilani | Dubai | Goa | Hyderabad

BIRLA INSTITUTE OF TECHNOLOGY AND SCIENCE, PILANI

2020

BIRLA INSTITUTE OF TECHNOLOGY AND SCIENCE, PILANI

CERTIFICATE

This is to certify that the thesis titled "**Discovery of Pro-Inflammatory Cytokine Inhibitors from Bacterial Strain for the Treatment of Renal Inflammation**" submitted by **Kirti** ID No **2016PHXF0030H** for award of Ph.D. of the Institute embodies original work done by ~~him~~/her under my supervision.

Signature of the Supervisor:

Name in capital letters: Prof. A. SAJELI BEGUM

Designation: Associate Professor and Head

Department of Pharmacy

Date:

Signature of the Co-supervisor:

Name in capital letters: Prof. ONKAR KULKARNI

Designation: Associate Professor

Date:

Abstract

Imbalance of pro-inflammatory cytokines and anti-inflammatory cytokines turns out to be the key regulator in the development process of pathological disorders. Molecules that target pro-inflammatory cytokines have shown positive results in alleviating inflammatory disorders. Therefore, development of small molecule inhibitors particularly those derived from natural sources which targets key pro-inflammatory cytokines namely TNF-α, IL-6 and IL-1β may improve the current approach of treatment of chronic inflammatory condition. Literature reports reveal that *Pseudomonas* species and their metabolites have shown beneficial effects in attenuating inflammatory diseases. With this background, attempts were made to discover low molecular weight cytokine-inhibitory molecules from a *Pseudomonas* species, isolated from rhizospheric soil of groundnut plant.

In Phase I, culture broth extract of *Pseudomonas* sp. ABS-36 (PCBE) was prepared in bulk. Then the pro-inflammatory cytokine inhibition potential of PCBE was evaluated by LPS-induced *in vitro* model using RAW 267.4 cells. PCBE was found to inhibit the production of TNF-α, IL-6 and IL-1β by 88.67%, 94.15% and 63.76%, respectively at 500 μg/mL with IC_{50} values of 73.66, 95.49 and 132.09 μg/mL respectively. Also, results of Griess assay revealed the protective role of PCBE in downregulating nitric oxide (NO) levels by 53.47% at 500 μg/mL. The significant inhibition effect shown by PCBE motivated us to continue the evaluation of the chemical constituents responsible for the activity, through which anti-inflammatory drug lead molecules could be discovered.

Thus, in phase II, the chemical constituents of PCBE were isolated through chromatographic techniques. Around twenty compounds (**1** – **20**) were isolated in pure form. In phase III, the structure of all twenty compounds were elucidated using various spectroscopic methods. The compounds (**1** – **20**) were characterized as cyclic dipeptides namely cyclo(Val-Pro) (**1**), cyclo(Leu-Pro) (**2**), cyclo(Val-Leu) (**3**), cyclo(Phe-Pro) (**4**), cyclo(Val-Phe) (**5**), cyclo(Ile-Phe) (**6**), cyclo(Leu-Ile) (**7**), cyclo(Leu-Leu) (**8**), cyclo(Leu-Hydoxy-Pro) (**9**), cyclo(Pro-Tyr) (**10**), cyclo(Ala-Pro) (**11**), cyclo(Gly-Pro) (**12**), cyclo(Gly-Phe) (**13**), cyclo(Ala-Phe) (**14**), cyclo(Ala-Ile) (**15**), cyclo(Gly-Tyr)(**16**), cyclo(Ala-Tyr) (**17**), cyclo(Val-Tyr) (**18**), cyclo(Leu-Tyr) (**19**) and cyclo(Ala-Ala) (**20**). This is the first report of isolation of cyclic dipeptides **1**–**3**, **5**–**8**, **10**, **11** and **13**–**20** from this source.

In Phase IV, the proline-based cyclic dipeptides **1**, **2**, **9-12** which were identified as the major metabolites secreted by *Pseudomonas* sp. ABS-36 were screened for their anti-inflammatory potential using *in vitro* LPS assays. The suppressive effect of all six compounds was found to be more effective against IL-1β secretions compared to TNF-α and IL-6 in ELISA assays with IC_{50} values ranging between 7.5 and 12.6 μg/mL. Also, the compounds exhibited significant reduction in the levels of IL-6 with IC_{50} values ranging from 7.8-18.0 μg/mL. Compounds, cyclo(Val-Pro) (**1**) and cyclo(Leu-Pro) (**2**) attenuated TNF-α levels with IC_{50} values of 22.61 and 22.85 μg/mL, respectively. Parallelly, cyclic dipeptides **1**, **2**, **9**, **10**, **11** and **12** also showed downregulation of NO levels by 38.8%, 40.8%, 55.2%, 60.7%, 53.5% and 31.0%, respectively with no cytotoxic activity on RAW 264.7 cells. Thus, proline based cyclic dipeptides were found to exhibit pan cytokine inhibition effect by downregulating major pro-inflammatory cytokines IL-1β, TNF-α and IL-6 when tested under various cell-based assays.

In phase V, the effect of these six cyclic dipeptides **1**, **2**, **9**, **10**, **11** and **12** were then tested under acute *in vivo* model of renal inflammation using oxalate crystal induction. At 50 mg/kg oral dose, cyclo(Val-Pro) (**1**) demonstrated 57% reduction of plasma IL-1β protein expression and 35.2% decline in blood urea nitrogen level. Further, compound **1** attenuated renal injury as depicted by significant reduction of mRNA expressions of IL-1β ($P < 0.01$) and kidney injury marker-1 ($P < 0.001$) and alleviation of histology of renal tissue. Compound cyclo(Val-Pro) (**1**) significantly downregulated mRNA gene expression of pro-inflammatory cytokines and protein expression of IL-1β at 100 μM in *in vitro* mechanistic study.

On observing the beneficial role of cyclo(Val-Pro) (**1**) and cyclo(Leu-Hydroxy-Pro) (**9**) in attenuating oxalate-induced renal injury, they were further evaluated at different doses of 25, 50 and 75 mg/kg doses under renal ischemic reperfusion model. Both the compound significantly lowered plasma IL-1β levels at 50 and 75 mg/kg dose with $P<0.05$. A significant downregulation of mRNA expression levels of pro-inflammatory cytokines (TNF-α, IL-6 and IL-1β) and kidney injury markers (KIM-1, NGAL, α-GST, π-GST) was observed at 75 mg/kg dose ($P<0.05$). Likewise, tubular injury index was significantly improved at 75 mg/kg doses. However, treatment with 25 mg/kg dose exhibited only marginal protection in attenuating ischemic injury. *In vitro* mechanistic study done using antimycin-induced ischemia in NRK-52 E cell lines showed marked attenuation in cell survivability rate in MTT as well as Flow cytometry assays. Also significant reduction of pro-apoptotic protein Bax and elevation of anti-apoptotic protein BCL2 were observed in cyclo(Val-Pro) (**1**) and cyclo(Leu-Hydroxy-Pro) (**9**) treated cells.

Further, the most effective compound cyclo(Val-Pro) (**1**) was tested in chronic renal injury model of unilateral ureter ligation (UUO) at 50 mg/kg body weight oral dose. Renal tissues were evaluated for the protein expression of fibrotic markers using western blot analysis. Cyclo(Val-Pro) (**1**) showed significant abrogation of renal fibrosis by lowering the expression of α-SMA, TGF-β and collagen-1. Histopathological studies using sirius staining also indicated the protective role of cyclo(Val-Pro) (**1**) in alleviating renal fibrosis. The *in vitro* mechanistic study done using TGF-β induced fibrotic model in NRK-49F cell lines, showed significant improvement in cell survivability rate.

In conclusion, *Pseudomonas* sp. (ABS-36) has been identified as a new source for seventeen cyclic dipeptides **1-3**, **5-8**, **10**, **11** and **13-20**. *Pseudomonas sp.* (ABS-36) has been found to secrete non-cytotoxic pan-cytokine inhibitory proline-based cyclic dipeptides (**1**, **2** and **9-12**) exhibiting protective effect in oxalate-induced renal nephropathy. This is the first study which has explored the effect of cyclic dipeptides in renal inflammation. Further, cyclo(Val-Pro) (**1**), identified as the most active compound attenuating ischemic renal injury and renal fibrosis is reported as a newer anti-inflammatory lead. Further, pharmacokinetic studies are warranted to corroborate the efficacy of *in vitro* and *in vivo* studies.

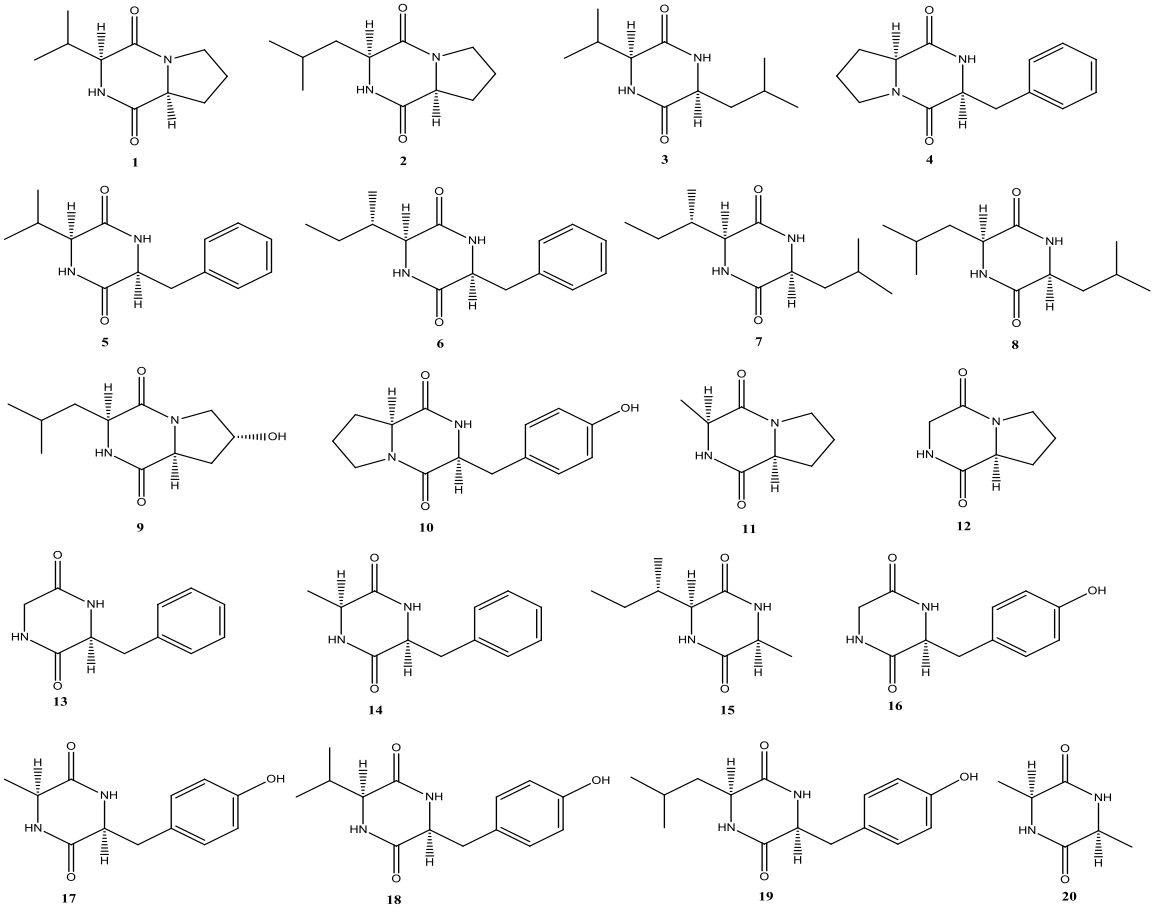

Declaration

I hereby declare that, the present work embodied in this thesis entitled, ***""Discovery of Pro-Inflammatory Cytokine Inhibitors from Bacterial Strain for the Treatment of Renal Inflammation"*** was carried out by me during the course of investigation (August 2016-November 2020) under the direct supervision and guidance of Prof. A. Sajeli Begum and co-supervision of Dr. Onkar Kulkarni, Department of Pharmacy, BITS-Pilani, Hyderabad campus, Hyderabad, India. This work has not been done / submitted in part or full to any other university or institute for award of any degree or diploma and is not concurrently submitted in candidature for any other degree.

Name: Kirti

Date:

Place:

Acknowledgements

First and foremost, praises and thanks to the God, the Almighty, for his showers of blessings throughout my research work to complete the research successfully. Then I would like to owe my gratitude to all those people who have made this thesis possible and because of whom my research experience has been one that I will cherish forever.

I would like to express my deep and sincere gratitude to my research supervisor, **Prof. A. Sajeli Begum**, Associate Professor, Department of Pharmacy, BITS Pilani Hyderabad Campus, for her guidance which supported the thesis work for its on-time completion. My immeasurable appreciation for **Prof. Onkar Kulkarni**, for the help and support extended throughout my thesis with his patience and knowledge, while allowing me the room to work in my own way. I feel amazingly fortunate to have him as my co-advisor, for encouraging my research work and allowing me to grow as a scientist. The advices received from both of them on my career and research have been priceless.

I would also like to extend my deepest regards for **Prof D. Sriram** and **Prof Arti Dhar**, who acted as my Doctoral Advisory Committee (DAC) members and gave valuable comments whenever needed. My sincere thanks to all faculty members for providing necessary support to accomplish my research work. I am grateful to Department of Pharmacy, BITS Pilani Hyderabad Campus for providing well infra structure and Prof **Arti Dhar** (DRC) for her invaluable support.

I would also like to thankfully acknowledge **Dr. S. Ameer Basha**, Associate Professor, Professor Jeyashankar Telangana State Agricultural University, Hyderabad for providing bacterial strain. My special thanks to **Prof. Yoshinori Fujimoto**, Meiji University, Japan for extending help in spectral analysis.

It's my privilege to express our deep sense of gratitude to **Prof. Souvik Bhattacharyya**, Vice Chancellor, **Prof. G Sundar**, Director and **Prof. Vamsi Krishna Venuganti**, Associate Dean, Academic Graduate Research Division, BITS-Pilani Hyderabad Campus, for their support to do my research work.

A special word of thanks to my Friends **Pravesh Sharma, Srashti Goel, Priyanka Reddy, Purbali, Pragya** for providing overwhelming support all throughout my PhD thesis work. I would like to thank my fellow research scholars **Kalyani, Yamini, Nikhila, Kavitha,**

Prakruti, Lakshmi Soukya, Suresh Babu, Girdhari Roy, Shubham, Vishnu, Himanshu for providing work friendly environment. My heartfelt thanks to the supporting staff and lab technician **Ms Sunitha, Ms Saritha, Ms Rekha, Mr Rajesh, Mr Mallesh, Mr Kumar, Mr Upallaiyah** and **Mr Narsimha** for their extraordinary support whilst providing chemicals and reagents during the hour of need.

I thank CSIR (09/1026(0019)/2017-EMR-I) for awarding the JRF/SRF and DST (EMR/2016/002460) for funding the work. I express my tearful and heartfelt gratitude to all the small animals that were sacrificed for the benefit of mankind.

Last but not the least, I thank my parents and my brother Kartik for standing with me at every step during my PhD. I am greatly indebted to my father, who has strained every nerve in educating me and to my mother for her blessings.

Table of Contents

List of Tables

List of Figures

Abbreviations

α-SMA	alpha-Smooth Muscle Actin
α-GSH	alpha-Glutathione S Transferase
Ala	Alanine
APS	Ammonium Per Sulfate
Arg	Arginine
Asn	Asparagine
Asp	Aspartic acid
brs	Broad singlet
BSA	Bovine Serum Albumin
BUN	Blood Urea Nitrogen
cDNA	Complimentary deoxyribonucleic acid
$CHCl_3$	Chloroform
Col-1	Collagen-1
Cq	Cycle quantification
Cys	Cysteine
d	doublet
dd	double doublet
ddd	doublets of doublet
DEPC	Diethyl pyrocarbonate
DMEM	Dulbecco's Modified Eagle Medium
DMSO	Dimethyl Sulfoxide

ELISA	Enzyme Linked Immunosorbent Assay
EtOAc	Ethyl acetate
EtOH	Ethanol
FBS	Fetal Bovine Serum
GAPDH	Glyceraldehyde-3-phosphate dehydrogenase
Gln	Glutamine
Glu	Glutamic acid
Gly	Glycine
H & E	Hematoxylin and Eosin
His	Histidine
HPLC	High Performance Liquid Chromatography
IAEC	Institutional animal ethics committee
ICAM	Intercellular cell adhesion molecule
IC_{50}	Half maximal inhibitory concentration
Ile	Isoleucine
IL-1ra	Interleukin 1 receptor antagonist
IL-1β	Interleukin 1 beta
IL-6	Interleukin 6
iNOS	Inducible Nitric Oxide Synthase
KIM-1	Kidney Injury marker
LPS	Lipopolysaccharides
Leu	Leucine
Lys	Lysine
m	multiplet

mAb	Monoclonal antibody
MeOH	Methanol
Met	Methionine
mRNA	Messenger Ribonucleic Acid
MS	Mass Spectrum
MTT	[3-(4,5-dimethylthiazol-2-yl)-2,5-diphenyltetrazolium bromide]
m/z	Mass/Charge
NFκB	nuclear factor kappa light chain enhancer of activated B cells
NGAL	Neutrophil gelatinase associated lipocalin
NMR	Nuclear magnetic resonance
NO	Nitric oxide
P.	*Pseudomonas*
π-GSH	Pi- Glutathione S transferase
PBS	Phosphate buffer saline
Phe	Phenylalanine
Pro	Proline
ppm	Parts Per Million
PVDF	Polyvinylidene difluoride
RIPA	Radioimmunoprecipitation assay buffer
RTPCR	Real time polymerase chain reaction
SDS	Sodium dodecyl sulfate
SDS-PAGE	Sodium dodecyl sulfate poly acrylamide gel electrophoresis
SEM	Standard Error of Mean
Ser	Serine

t	triplet
sTNF	Soluble TNF
TBST	1X Tris-Buffered Saline, 0.1% Tween
TEMED	N,N,N′,N′-Tetramethylethylenediamine
TFA	Trifluoroacetic acid
Thr	Threonine
TLC	Thin Layer Chromatography
TMB	3,3′,5,5′-Tetramethylbenzidine
TNF-α	Tumor necrosis factor-alpha
TNFR	TNF receptor
TGF-β	Tumor growth factor-beta
Trp	Tryptophan
Tyr	Tyrosine
TLR	Toll like receptor
Val	Valine

SYMBOLS

°C	Degree Celsius
µg	Microgram
h	Hours
kDa	Kilodalton
MHz	Megahertz
Nm	Nanometer
µL	Microlitre
mL	Millilitre

μM	Micromolar
mM	Millimolar
δ	delta

Chapter 1

Introduction

Inflammation refers to the immune response of the host towards stimuli such as injury, pathogenic invasion, exposure to irradiation or any chemical substance. It involves series of cellular and molecular events that occur in a coordinated manner in order to mitigate the underlying pathophysiology to resolve inflammation. The events of inflammation can be summarised as follows (Chen *et al.* 2018).

- Ligand binding to pattern recognition receptor (PRR)
- Activation of signaling pathways
- Release of inflammatory mediators
- Recruitment of inflammatory effectors

Recognition by PRRs: PRR involves toll-like receptor (TLR), C-type lectin receptor (CLR), retinoic acid inducible gene like receptor (RLR) and nod like receptor (NLR), expressed by both immune as well as non-immune cells. These receptors get activated upon exposure to pathogen associated molecular patterns (PAMPs) and damage associated molecular pattern (DAMPs), which further stimulate the intracellular signaling cascade (Chen *et al.* 2018).

Signal transduction pathways: PRRs activate numerous signaling pathways such as NFκB, MAPK (ERK1/2, p38 MAPK, JNK), JAK/STAT which further effectuate the inflammation by releasing inflammatory mediators (Ashley *et al.* 2012, Mendes *et al.* 2018).

Inflammatory mediators: These include cytokines, chemokines, adhesion molecules (ICAM, VCAM), prostaglandins, leukotrienes, histamine (Mendes *et al.* 2018). They serve as biomarker for early diagnosis of disease. Cytokines modulate inflammatory process by series of interactive reactions. Dysregulation of levels of pro-inflammatory cytokines (IL-6, TNF-α, IL-1β, IL-8, IL-12, Interferons) and anti-inflammatory cytokines (IL-4, IL-10, IL-11, TGF-β) can lead to devastating effects such as organ dysfunctioning, haemodynamic changes and ultimately leads to fatality (Ashley *et al.* 2012, Abdulkhaleq *et al.* 2018).

Recruitment of inflammatory effector cells: The first cells to reach the site of inflammation are neutrophils, followed by monocytes, natural killer T-cells, T-lymphocytes, B-lymphocytes and mast cells (Ryan 1977). Monocytes get differentiated to macrophages and dendritic cells that are recruited to the site of inflammation *via* chemotaxis. Macrophages play crucial role in the inflammatory process by undergoing phagocytosis, presenting antigen to T-cell and mediating inflammation by the release of cytokines and various growth factors (Abdulkhaleq *et al.* 2018).

Resolution of inflammation is a well-orchestrated process whereby, chemokine gradient fades overtime. Release of chemicals such as lipoxin suppresses neutrophil recruitment (Brenner *et al.* 2003) and stimulation of Fas receptors mediated apoptosis of the affected cells (Serhan *et al.* 2005, Chen *et al.* 2018).

Acute kidney injury (AKI) indicates abrupt decline in kidney function as a result of structural and functional impairment (Makris *et al.* 2016). It is associated with significant elevation in the levels of serum creatinine, blood urea nitrogen (BUN) and reduced glomerular filtration rate (Bagga *et al.* 2007). AKI is a major risk factor for the development for chronic renal injury, cardiac complications and ultimately leading to mortality (Chawla *et al.* 2014). Inflammatory signals interfere with renal microcirculation activation, particularly endothelial cells and leukocytes sustain the production of tubular toxins (ROS) which results in the local amplification of pro-inflammatory factors and oxidative stress (Mihai *et al.* 2018). There is a growing evidence which suggests that pro-inflammatory cytokines play pathogenic role in the progression of AKI. These are produced as a consequence of activation of transcription factors (such as NFκB, HSP-1, HIF-1), which further stimulate chemokine production that recruit neutrophils, monocytes, etc., (Jang *et al.* 2009). Numerous findings have unveiled the beneficial effect of neutralization of pro-inflammatory cytokines in renal inflammatory disorders. Thus, targeting pro-inflammatory cytokines will be helpful to improve the currently available therapeutic intervention for the treatment of renal inflammation.

Natural products particularly those derived from microbial origin have emerged out as prominent therapeutic candidates for the treatment of various disorders. Literature shows a myriad of secondary metabolites isolated from microbes exhibiting anticancerous, antiinflammatory, antidiabetic, antituberculosis, antimalarial, antifungal activities, etc. (Pandey 2019). Several species of *Pseudomonas* have shown to produce wide array of secondary metabolites and other proteins that exhibit pharmacological activity. Secondary metabolites released by *P. fluorescens* and *P. aeruginosa* have revealed antifungal activity (Altaee *et al.* 2017, Hameed *et al.* 2018). Metabolites of marine *Pseudomonas* sp. (N11) significantly attenuated neutrophil-mediated inflammatory disorders by inhibiting p38 MAP kinase, JNK, and calcium pathways (Yang *et al.* 2014). *P. aeruginosa*-derived secondary molecules such as pyocyanine, pyoverdins, phenazines pyochelin, paerucumarin, pseudoveridin have shown prominent biological activities (Hira *et al.* 2017). Report by Khan *et al.* and Hira *et al.* documented bioactive secondary metabolites isolated from *P. aeruginosa*, targeting specifically pro-inflammatory cytokines (Khan *et al.* 2015, Hira *et al.* 2016).

Therefore, *Pseudomonas* sp. turns out to be an interesting source for discovering drug leads. On observing the cytokine inhibition effect exhibited by the culture broth extract of *Pseudomonas sp*. ABS 36 strain in our preliminary study, it was selected for the exhaustive study to discover pro-inflammatory cytokine inhibitors for the treatment of renal inflammation.

In the present research work, the culture broth extract of *Pseudomonas sp*., ABS 36 strain was assessed for the *in vitro* cytokine inhibitory capability. The metabolites of the culture broth extract were isolated, purified and their structures were characterized. Thereafter, the major pure compounds isolated from the culture broth extract were subjected for *in vitro* studies followed by extensive evaluation under acute renal inflammatory models. Further, the compound that exhibited highly potent anti-inflammatory activity was investigated for possible mechanistic pathway and was also tested for its efficiency in alleviating chronic renal inflammation.

Chapter 2

Literature Review

2.1.Inflammation

Inflammation is a complex biological phenomenon initiated upon microbial invasion or any kind of injury and is associated with the release of inflammatory mediators such as cytokines, chemokines, prostaglandins, leukotrienes, vasoactive amines (Chen *et al.* 2018). Perturbations in the levels of proinflammatory cytokines (tumour necrosis factor-alpha (TNF-α), interleukin-6 (IL-6) and interleukin-1beta (IL-1β)) and antiinflammatory cytokines (IL-1Ra, IL-4, IL-10, IL-13, TGF-β) lead to unresolved injury (Ashley *et al.* 2012) which further progresses towards the development of chronic inflammatory diseases like chronic obstructive pulmonary diseases, inflammatory bowel syndrome, atherosclerosis, Alzheimer disease, neuroinflammation, heart disease, renal inflammation., rheumatoid arthritis, cancer, etc. (Kumar *et al.* 2020).

Inflammatory process is stimulated upon recognition of various pathogen associated molecular patterns (PAMPs) and disease associated molecular patterns (DAMPs) by soluble as well as membrane bound mediators that brings multiple factors into action. Release of inflammatory mediators *via* NFκB, inflammasomal, p38MAP kinase and JAK/STAT signaling pathways induces dilation of the blood vessels which increases blood supply, enhances vascular permeability and increases the expression of cell adhesion molecules (Mendes *et al.* 2018). Cytokines mediated conformational changes cause arrest and adhesion of neutrophils to endothelium, which then migrate through transendothelial region to the site of injury. Monocytes mature to form macrophages once they leave blood stream and enter tissues. Upon stimulation they produce various cytokines, complement proteins and oxidative stress that mediate inflammatory response (Abdulkhaleq *et al.* 2018). Pro-inflammatory and antiinflammatory cytokine levels affect the extent of tissue injury and resolution after injury.

2.2.Acute kidney injury

Acute kidney injury (AKI) involves rapid deterioration of renal morphology and excretory functions that lead to accumulation of nitrogenous waste and electrolyte imbalances (Mehta *et al.* 2007). Dysregulation of kidney functioning results from ischemia, crystal nephropathy or sepsis, hypoxia, nephrotoxicity, consequently activating the inflammatory response, tubular obstruction, necroptosis and apoptosis. AKI is more prevalent amongst hospitalised inpatients, particularly those admitted in ICU (Makris *et al.* 2016). Kidney injury involves continuous decline in renal efficiency, increased risk of development of cardiovascular diseases and mortality. Based on etiologies AKI can be classified as prerenal characterised by azotaemia,

intrinsic kidney disease (involving acute tubular necrosis, glomerular nephritis, interstitial as well as vascular nephritis) and postrenal obstruction of urinary tract (Figure 2.2) (Fry *et al.* 2006). Acute renal injury can be classified based on AKIN (Acute Kidney Injury Network) (Table 2.2.1) and RIFLE (Risk, Injury, Failure, Loss and End stage) criteria (Table 2.2.2) (McDaniel *et al.* 2015, Makris *et al.* 2016).

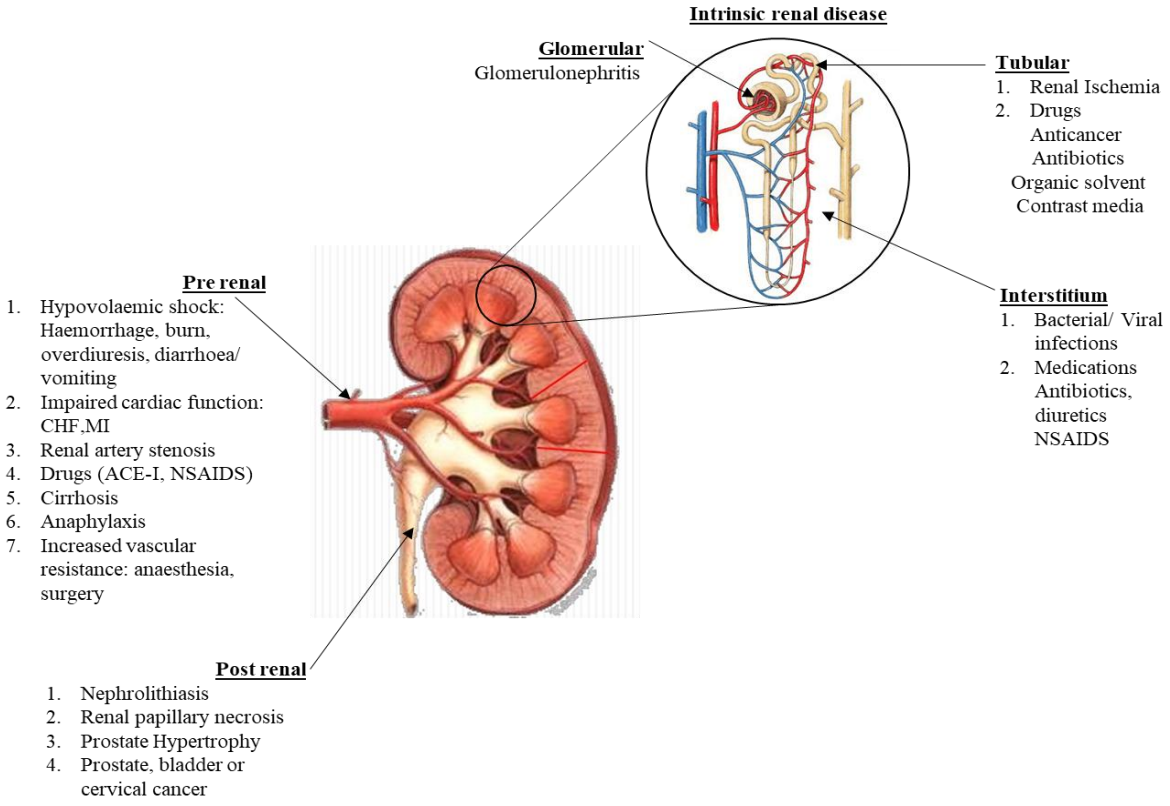

Figure 2.2: Etiology of kidney disease (Fry *et al.* 2006)

Table 2.2.1: Classification of AKI as per AKIN criteria

Stages	Serum Creatinine (Scr)	Urine output
1	1.5- 2-fold increase by 0.3 mg/dL from baseline	Less than 0.5 mL/kg/h for 6 h
2	2-3- fold increase from baseline	Less than 0.5 mL/kg/h for 12 h
3	More than 3-fold increase from baseline or ≥4.0 mg/dL with an acute rise of ≥0.5 mg/dL	Less than 0.3 mL/kg/h for 24 h or anuria for 12 h

Ref: McDaniel *et al.* 2015

Table 2.2.2: Classification of AKI as per RIFLE criteria

RIFLE	Serum Creatinine (Scr) and Glomerular filtration rate (GFR)	Urine output
Risk	1.5-fold increase in serum creatinine or GFR reduced by >25% from baseline	Less than 0.5 mL/kg/h for 6 h
Injury	2-fold increase in serum creatinine or GFR reduced by >50% from baseline	Less than 0.5 mL/kg/h for 12 h
Failure	3-fold increase in serum creatinine or GFR reduced by >75% from baseline	Less than 0.3 mL/kg/h for 24 h or anuria for 12 h
Loss	Complete loss of function for more than 4 weeks	
End-stage kidney disease	Complete loss of function for more than 3 months	

Ref: McDaniel *et al.* 2015

Biomarkers of AKI includes serum creatinine, BUN levels, Kidney injury marker (KIM-1), neutrophil gelatinase associated lipocalin (NGAL), α-GST, π-GST, sodium hydrogen exchanger isoform 3 (NHE-3) (Trof *et al.* 2006). NGAL is markedly upregulated in injured epithelia to induce reepithelization and activate heme oxygenase-1 (Devrajan 2008). Expression level of KIM-1 significantly increased in proximal tubule following ischaemic and nephrotoxic drugs induced injury (Han *et al.* 2002). KIM-1 is a type-1 membrane protein that plays a crucial role in epithelial cell adhesion, growth and differentiation. α-GST and π-GST are cytoplasmic enzymes found in proximal and distal tubular epithelial cells and tubular injury results in their increased excretion (McMohan *et al.* 2010). NHE-3 is the most abundant sodium transporter present in apical membrane of proximal tubule, thin and thick ascending loop of Henle. Presence of NHE-3 in urine indicates tubular injury (Sole *et al.* 2011).

Stimulation of various pattern recognition receptors (PPRs) such as TLR, CLR, NLR, RLR by pathogen associated molecular pattern (PAMPs) and damage associated molecular pattern (DAMPs) such as histones, HSP, HMGB-1 present on both immunologic and non-immunologic cells triggers inflammatory signaling cascade (Rabb *et al.* 2016). Various cytokines and chemokines released as an outcome of stimulation of PRRs further lead to vascular (vascular dilation, increase in blood flow and vascular permeability) and cellular

events (recruitment of neutrophils and macrophages to the site of inflammation). These events amplify oxidative stress as well as local inflammatory responses (Ortega *et al.* 2010). Intracellular ATP rapidly degrades to hypoxanthines and xanthines under hypoxic condition, generating highly reactive superoxides and hydroxyl radicals. Thereafter, these reactive species damage epithelial cell characterised by degraded actin cytoskeletal, loss of tubular brush border, polarity loss and ultimately advances towards apoptotic and necrotic cell death (Bonventre *et al.* 2011). Renal damage increases BUN levels, serum creatinine level and decreases glomerular filtration rate (GFR) (Bagga *et al.* 2007).

AKI rapidly progresses to chronic kidney injury (CKI) with accelerated fall in GFR, persistent interstitial fibrosis, epigenetic modification, microvascular rarefaction and finally approaches end stage renal disease (ESRD) (Fiorentino *et al.* 2018). Renal injury can revert to normal by proliferation of tubular cells along with redeployment of Na+/K + ATPase and integrin to the apical side or there could be irreversible loss to kidney caused as a result of necroptosis and apoptosis of tubular epithelial cells (Wilson *et al.* 2000).

Table 2.2.3: Drugs available for the treatment of kidney injury

Antiapoptotic/ antinecrotic	Caspase inhibitors Nonselective caspase inhibitors Selective caspases 3 and 7 inhibitors Selective caspase 1 inhibitors Minocycline Guanosine Pifithrin-α PARP inhibitor
Anti-inflammatory	Sphingosine 1 phosphate analog Adenosine 2A agonist α-MSH IL-10 iNOS inhibitor Fibrate PPAR-γ agonist Minocycline Activated protein C
Antisepsis	Insulin Activated protein C Ethyl pyruvate
Growth factor	Recombinant erythropoietin Hepatocyte growth factor
Vasodilator	Carbon monoxide release compound and bilirubin Endothelin antagonist Fenoldopam, ANP

Ref: (Jo *et al.* 2007)

2.3 Chronic Kidney Injury (CKI) is a major health problem affecting approximately 10–12% of the population worldwide and is 16th most leading cause of mortality worldwide. CKI is more prevalent in people >65 years of age, 50% of elderly population exhibit the signs of renal dysregulation, associated with high morbidity and mortality (Chen *et al.* 2018). CKI is a heterogenous disorder associated with increased risk of cardiovascular complications, hyperlipidemia, anemia and metabolic bone disorders, development of insulin resistance, end stage renal diseases (ESRD) and death (Romagnani *et al.* 2017, Raj *et al.* 2020). CKI can be characterised by persistent abnormality in renal histology or debilitated renal excretory function with glomerular filtration rate (GFR) of less than 60 mL/min/1.73 m^2, atleast 30 mg albuminuria for 24 h, or renal injury markers with hematuria or polycystic or dysplastic kidneys for more than 3 months (Chen *et al.* 2019).

2.4 Role of TNF-α in renal injury

Role of TNF-α has been implicated in the pathogenesis of various renal disorders such as LPS-induced acute renal failure, lupus nephritis, glomerulonephritis, cisplatin nephrotoxicity, kidney stones, renal insufficiency following a cardiac surgery (Meldrum *et al.* 1999). TNF-α, 17kD polypeptide exerts its proinflammatory activity through TNFR1, TNFR2, p38 MAP kinase, NFκB and TNF transcription factors, consequently increasing its own levels as well as of other inflammatory mediators (IL-1β, TGF-β, IL-6) (Donnahoo *et al.* 1999).

TNFR1-deficient and TNFR2-deficient mice have demonstrated protection against glomerulonephritis. TNF-α exerts its immunostimulatory activity by increasing the expression of MHC class 1 and class 2 adhesion molecules, ICAM, VCAM, E- selectin, MIF (macrophage migration inhibitory inhibition factor) that promotes rapid adhesion as well as recruitment of neutrophils in kidney (Khan *et al.* 2005). Neutralization of TNF-α by TNF-α antibodies and knockout of TNFR1 and 2 have shown significant protection in cisplatin induced nephrotoxicity (Ramesh *et al.* 2002) and crescentic glomerulonephritis (Khan *et al.* 2005, Timoshanko *et al.* 2003). Also, study by Mulay *et al.* showed that inhibition of TNFR signaling failed to induce chronic kidney disease with oxalate rich diet in TNFR1 and TNFR2 knockout mice. Inhibition of TNF-α reduced the expression of crystal adhesion molecules (annexin II and CD 44) in renal epithelial cells (Mulay *et al.* 2017).

TNF-α intervene kidney injury by increasing levels of vasoconstrictive peptides (platelet activating factor (PAF), endothelin-1, prostaglandins) which lowers glomerular filtration rate or GFR, by inducing the expression of adhesion molecules like ICAM on mesangial cells and

E-selectin on glomerular endothelial cells which promotes rapid adhesion of neutrophils and macrophages or can directly exert cytotoxic action through apoptosis (Daemen *et al.* 1999). TNF-α mediates apoptosis by binding to Fas receptor or TNFR1 and interaction with TRADD (TNF receptor associated death domain) and FADD (Fas receptor associated death domain) triggers RIP (receptor interacting protein) which activates endonucleases to cleave DNA (Donnahoo *et al.* 1999). TNF-α arbitrated renal fibrosis by enhancing TGF-β, which contributes to glomerular sclerosis and fibrosis of interstitium by increasing extracellular matrix synthesis, myofibroblast proliferation, collagen deposition in unilateral obstruction model (Meldrum *et al.* 2007, Guo *et al.* 2001). Neutralisation of TNF-α with PEG-sTNFR1 resulted in downregulation of NFκB, which further decreased TGF-β mediated inflammatory cascade (Therrien *et al.* 2012).

2.5 Role of IL-1β in renal injury

IL-1β is a pleiotropic cytokine which mediates its inflammatory response by acting on IL-1Rt1 receptor present on nearly all types of cells. Elevated levels of IL-1β and IL-1R have been implicated in exacerbated proteinuria, reduction in creatinine clearance, progression of tubulostitial injury, crescent formation in human glomerulonephritis and mice lupus nephritis model (Tesch *et al.* 1997, MnIAs, N. E. 1995). IL-1β induces the expression of macrophage colony stimulating factor (M-CSF), PGE2, endothelin-1, adhesion molecules (ICAM, CD11a/CD18, CD11b/CD18, CD11c/CD18, VCAM) consequently increasing macrophage and neutrophil infiltration (Tesch *et al.* 1997, MnIAs, N. E. 1995, Tang *et al.* 1994). Treatment with IL-1 receptor antagonist (IL-1Ra) abrogated glomerular necrosis, crescent formation, reduced glomerular hypercellularity by inhibiting mesangial cell proliferation and prevented macrophage, T-cell infiltration (Lan *et al.* 1993). Neutralisation of IL-1β with soluble receptor type-1 (sIL-TRt1) resulted in alle*via*tion of LPS mediated renal injury (Karkar *et al.* 1995).

Upregulation of IL-1β and IL-1Rt1 has been observed in both glomerular and tubulointerstitium of diabetic patients and anti-IL-1β IgG upregulated mRNA expression levels of WT-1 and synaptopodin (podocyte markers), alle*via*ted KIM-1 and NGAL (kidney injury markers) and downregulated fibrotic markers (α-SMA and collagen-1) (Lei *et al.* 2019). Findings of Haq *et al.* showed that IL-1 Ra and IL-1 knockout mice mitigated injury in renal ischemia reperfusion model by reducing polymorphonuclear leukocyte (PMN) infiltrations as a result of downregulation of CD11a/CD18 expression on leukocytes and ICAM-1 levels on endothelial cells (Haq *et al.* 1998). Furthermore, IL-1β inhibition decreased MCP-1

(Monocytes chemotactic protein-1) and MIP-1 (Macrophage infiltration inhibitory protein) expressions (Furuichi *et al.* 2006). Also, IL-1R deficient mice attenuated calcium oxalate induced renal nephropathy (Mulay *et al.* 2012) and rhabdomyolysis induced renal injury (Komada *et al.* 2015).

Study by Masola *et al.* showed that blockade of IL-1β using human monoclonal antibody, canakinumab inhibited epithelial to mesenchymal transition (EMT) in renal epithelial cells (Masola *et al.* 2019). IL-1β exerts profibrotic effect by inducing TGF-β synthesis, enhancing fibroblast proliferation, neutrophil diapedesis, increasing lymphocyte mediated cytokine synthesis and upregulation of fibrotic markers (collagen-1, fibronectin, α-SMA). Studies show that IL-1β is important for release of TGF-β and its downstream effect such as increased deposition of extracellular matrix protein and inhibiting molecules that degrades matrix protein (Fan *et al.* 2001).

2.6 Role of IL-6 in renal injury

IL-6, a proinflammatory cytokine, act mainly by binding to α-chain of membrane bound IL-6 receptor (mbIL-6R) or soluble IL-6 receptor (sIL-6R). Ligand binding induces homodimerization of gp 130 (a membrane glycoprotein) and then, activates associated tyrosine kinase (JAK1, JAK2, Tyk 2) (Scheller *et al.* 2006, Su *et al.* 2017). Further, these kinases induce transcription of STAT 1 and STAT 3 and signaling *via* Ras/Raf cascade (Scheller *et al.* 2006, Su *et al.* 2017, Pecoits-Filho *et al.* 2003). IL-6/IL-6R axis has been implicated in the pathogenesis of several renal inflammatory diseases (Nechemia-Arbely *et al.* 2008). Therefore, IL-6 acts as a major target for the development of therapeutic intervention for renal disorders. Therapies either target cytokine directly (clazakizumab, olokizumab) or alpha subunit of IL-6R (tocilizumab, sarilumab) (Jones *et al.* 2015). IL-6 deficient mice exhibited resistance to mercuric chloride induced and ischemic reperfusion induced renal injury. IHC studies showed localisation of IL-6 in outer medulla of kidney (Nechemia-Arbely *et al.* 2008, Kielar *et al.* 2005).

Horii *et al.* evaluated the involvement of IL-6 in mesangial glomerulonephritis. In their findings they observed that rIL-6 stimulated mesangial cell growth in *in vitro* and urine samples of glomerulonephritis patients showed significant elevation of IL-6 (Horii *et al.* 1989). Furthermore, Il-6 inhibition in Lupus nephritis halted B-cell proliferation by downregulating CD5 expression (Garaud *et al.* 2009), reduced mesangial volume, proteinuria and improved GFR (Jones *et al.* 2015, Horii *et al.* 1989, Kiberd *et al.* 1993). Human and murine evidences

also suggested IL-6 as the key cytokine involved in Ang-II mediated downstream signaling of chronic kidney disease (Zhang *et al.* 2012). Ang-II enhances fibrosis by elevating signaling response of tubular epithelial cells to TGF-β. IL-6 augments TGF-β_1 receptor trafficking to non-lipid raft pools. Thus, aggravating its fibrotic response (Zhang *et al.* 2005).

Table 2.6: Therapies targeting pro-inflammatory cytokines

Drug	**Target**	**Indications**
Etanercept	TNFR2	Arthritis, psoriasis, spondylitis
Infliximab	IgG/k mAb	Arthritis, psoriasis, spondylitis, Ulcerative colitis, Crohn's disease
Adalimumab	IgG1/k mAb	Arthritis, psoriasis, spondylitis, Ulcerative colitis, Crohn's disease
Certolizumab	PEGylated Fab fragment	Crohn's disease, Arthritis, Spondylitis
Golimumab	IgG1/k mAb	Arthritis, Spondylitis, Ulcerative colitis
XPro1595, XENP345	sTNF inhibitor	-
R1antTNF, DMS5540, TROS, ATROSAB	TNFR1 antagonist	-
Tocilizumab REGN88 (SAR153191) ALX-0061	IL-6 receptor-specific mAb targeting soluble and membrane-bound interleukin-6 receptor	Castleman's disease, Juvenile idiopathic arthritis, Rheumatoid arthritis, Relapsing polychondritis, Ankylosing spondylitis, Type II diabetes Rheumatoid arthritis, ankylosing spondylitis Rheumatoid arthritis
CDP6038 (Olokizumab) CNTO136 (Sirukumab) CNTO328 (cCLB, Siltuximab) ALD518 (BMS-945429) C326	IL-6 specific mAb targeting IL-6	Rheumatoid arthritis Rheumatoid arthritis Castleman's disease Multiple myeloma, anticancer Rheumatoid arthritis, Non-small cell lung-cancer-related fatigue and cachexia Crohn's disease

FE301	Soluble gp130-Fc fusion protein targeting IL-6/sIL-6R	Crohn's disease
Tofacitinib, Ruxolitinib, Baricitinib (INCB-28050), GLPG-0634, AC430	Targeting Janus kinases (JAKs) downstream of gp130/IL6ST	Rheumatoid arthritis
Canakinumab ACZ885	anti-IL-1 β	Type 1 Diabetes, Schnitzler Syndrome Rheumatoid arthritis
Anakinra (Kineret)	IL-1ra	Type 1 Diabetes, Chronic kidney disease, arthritis,
Rilonacept	(IL-1 Trap)	Type 1 Diabetes, autoinflammatory syndrome

Ref: (Fischer *et al.* 2015, Zhang 2011, Jones *et al.* 2015)

2.7 Role of TGF-β in renal injury

TGF-β is a pleotropic cytokine, which is present ubiquitously and plays prominent role in cell development, differentiation, tissue repair as well as maintaining the homeostasis of cell. TGF-β superfamily comprises TGF-β, activin, BMPs, growth and differentiation factors (Bottinger 2007). TGF-β exists in three isoforms (1,2 and 3), which are synthesized as inactive form bound to latent TGF-β binding protein (Lan 2011). The most abundant isoform found in mammals is TGF-β1. Key regulatory step in TGF-β activity is the stimulation besides transcription of TGF-β. TGF-β receptor includes two families of protein receptor type I (TβRI) and type II (TβRII). TGF-β binding to TβRII actuates heteromeric complex formation with type 1 receptor. Resulting complex phosphorylates serine and threonine residues of TβRI and TβRI kinase further phosphorylates R-Smads (small mothers against decapentaplegic) which activates canonical Smad 2/3 pathway. Phosphorylated R-Smads forms complex with Smad 4 and translocates to nucleus to control transcription of the target gene. Other non-canonical pathways through which TGF-β modulates the expression of target genes includes mitogen-activated protein kinases (MAPKs) (extracellular regulated kinases (ERKs), p38, Jun kinase, small GTP binding proteins (Ras, Rho1, Rac 1, cdc 42) and integrin-linked kinase (ILK) (Bottinger 2007).

TGF-β acts at multiple levels in renal injury such as glomerular, tubulointerstitial and vascular. TGF-β overexpression has been observed in glomerulosclerosis and tubulointerstitial renal fibrosis. TGF-β promotes glomerulosclerosis by initiating thickening of glomerular basement

membrane through hypertrophy and matrix synthesis while apoptosis mediated detachment of podocytes from basement membrane. (López-Hernández *et al.* 2012, Schnaper et al, 2009). TGF-β mediates fibrosis by upregulating the production of matrix proteins, decreasing their degradation and by promoting transformation of tubular epithelial cells to fibroblast (Lan 2011).

TGF-β induces epithelial-to-mesenchymal transition by stimulating epithelial cells to lose tight junctions, adherens junction, apical basal polarity and acquire migratory activity with more expression of α-SMA and extra cellular matrix proteases like MMP-2 and MMP-9. TGF-β inhibited cyclin kinase dependent mitosis and IL-1β secretions in cultured tubular epithelial and mesenchymal cells (Biernacka *et al.* 2011, Schnaper et al, 2009). Findings suggests that TGF-β upregulates α-SMA through Rho A activation and vimentin expression through ZEB-1, ZEB-2 induction (Wendt *et al.* 2009). Also, TGF-β induced collagen synthesis by altering miR-192 levels in UUO (Chung *et al.* 2010). Neutralization of TGF-β with antibodies (1D11, α-T), oligonucleotides, TGF-β, soluble TβRII or receptor kinase inhibitors effectively abrogated renal fibrosis (Miyajima *et al.* 2000, Fukasawa *et al.* 2004, Liang X *et al.* 2016). Together these reports suggest putative role of TGF-β in effectuating renal fibrosis.

2.8 Models of Renal Injury

2.8.1 Sodium oxalate induced crystal nephropathy model in mice

Idiopathic renal stone affect about 8% population globally, 72% patient retain calcium oxalate while 14.7% have phosphate oxalate, while small portion of struvite, uric acid, and cysteine are also observed as renal stones. Monohydrate form of calcium oxalate dominantly retains in renal parenchyma as compared to dihydrate form due its physiochemical properties (Bilbault, Héloïse *et al.* 2016). Supersaturation of urine with mineral metabolites or insoluble drugs leads to crystal deposition and this accumulation and retention under the influence of environmental factors or pH influence nephrocalcinosis (Khan *et al.* 2016, Tattevin *et al.* 2013). Crystal nephropathy is divided into 3 types based on crystal retention region in urinary system (Type1) vascular crystal embolism causing renal ischemia (Type2) supersaturation of crystal extra and intratubular damaging tubular epithelial cells (TECs) (Type 3) accumulation of crystals in collecting duct cause obstructive nephropathy (Mulay *et al.* 2017). Adherence of oxalate crystals to tubular region is also governed by osteopontin (OPN) and Tamm-Horsfall protein (THP) which is abundantly expressed by tubular cells (Khan et al 1997).

Accumulated crystals in renal tubules behave as dangerous foreign particles for localized epithelial cells and trigger inflammatory pathway through NACHT, LRR and PYD domains-containing protein (NLRP)3 inflammasome. NALP3 along with ASC activate caspase-1 resulting in maturation of IL-1β and IL-18 in macrophages and dendritic cells. Cytokine and chemokine drive migration of phagocytic immune cells towards interstitial compartment to clean crystal granuloma through phagocytosis (Mulay *et al.* 2017, Mulay *et al.* 2014).

Cellular observation says that tubular cells start internalizing crystals (<10 μm) in order to be digested by lysosomes causing release of free calcium in cytosol inducing necrosis, overload of calcium destabilizes lysosome membrane, triggering necroptosis and generation of reactive oxygen sepsis (ROS) which is a key feature of acute kidney injury (AKI) (Tan *et al.* 1972, Liu *et al.* 2014, Huang *et al.* 2015). Damage-associated molecular patterns (DAMPs) released through necroptosis (ATP, histones, mitochondrial DNA, uric acid, etc) damage neighbouring tubular cells amplifing tubular damage (Allam *et al.* 2014). Chronic activation of innate immunity in renal parenchyma through NLRP3/ IL-1β /IL-18 axis cause loss of nephron, and effect kidney performance (Ludwig-Portugall I *et al.* 2016).

Along with immune cells crystal granuloma activate fibroblast to secrete extra cellular matrix (collagen 1&3) to fill damaged epithelial cells and stimulate TGF- β to amplify the situation through Smad pathway results end stage renal failure followed by fibrotic kidney (Ludwig-Portugall I *et al.* 2016).

Markers of kidney fibrosis are serum creatinine, albuminuria, and low glomerular filtration rate (GFR) and persistence of these markers are characterized as chronic kidney disease (CKD) (Zhong *et al.* 2017). Crystal nephropathy model in rodents is induced through administration of glyoxylate, ethylene glycol, sodium oxalate, hydroxy-L-proline, ammonium oxalate or oxalate rich diet which gets metabolised into oxalate and retain in renal tubules (Khan et al 1997).

2.8.2 Ischemic reperfusion renal injury model

Acute kidney injury (AKI) arises through multiple abnormalities like hypo perfusion (prerenal), structural deformities to renal parenchyma (intrinsic renal), obstructive nephropathy (post renal) followed by hypoxia which leads to morbidity and mortality. Ischemia/reperfusion injury (IRI) is prerenal arterial obstruction of blood supply followed by refurbishment of blood and restoration of oxygen (Malek *et al.* 2015). IRI can be manifested through sepsis induced

hypotension, vasoconstrictive drugs, trauma, kidney transplant, renal losses, congestive heart failure (Sharfuddin *et al.* 2011).

Hypoxia interrupts the electron transport in mitochondria leading to decline in ATP production with cellular morphology disruption especially in proximal convoluted tubules (PCT). ATP dependent sodium-potassium pumps, calcium pumps, sodium–hydrogen exchanger pumps, fails to maintain haemostasis of sodium, calcium, hydrogen in PCT causing hyperosmolarity, leading to water influx in cytoplasm which results in cell swelling and tubular atrophy, invasion of immune cells, membrane disruption (Wu *et al.* 2018, Nauta *et al.* 1991). Restoration of blood supply triggers enzymatic action of xanthine oxidase to catalyze hypoxanthine to xanthine and later into uric acid leading to generation of hydrogen peroxide (H_2O_2) along with superoxides ($O^{2\bullet-}$), thus producing oxidative stress burden following initiation of cytokine cascade with expression of adhesion molecule ICAM-1 and P-selectin (Lee *et al.* 2014).

Necrosis of epithelial cell during IRI is supported by ROS, cell swelling, membrane disintegration, oxidative stress and mitochondrial dysfuntioning (Linkermann A *et al.* 2013) IRI activate apoptotic pathway intrinsically through procaspase-9 which is governed by BCL2 family while procaspase-8 *via* extrinsic pathway and death receptors (FAS and FADD) located on cell surface (Bonegio *et al.* 2002, Guo *et al.* 2004). Enhanced ROS and NF-κB transcription factor during IRI also encourage phosphorylation of RIPK3 which significantly induces necroptosis (Wong *et al.* 2010).

Necroptic tubular epithelial cells (TECs) rapidly trigger innate immunity resulting in secretion of pro-inflammatory cytokines (IL-6, IL-1β and TNF-α) and chemokines (IL-8, C5a which regulate infiltration of neutrophils and macrophages to eliminate cell debris (Thurman *et al.* 2007, De Vries *et al.* 2003). Increased expression of TLR-4 and TLR-2 was also observed in IRI which worsen the situation *via* mediating production of inflammatory cytokines and chemokines (Wolfs *et al.* 2002).

Activated macrophage secreting TGF-β1 during IRI leads to activation of fibroblasts to proliferate and migrate towards the damaged region and secrete extracellular matrix (collagen1/3, fibronectin, α-SMA) and restore the function. Prolonged damage induces excessive proliferation of fibroblasts ultimately leading to extensive fibrosis with dense tissue scar formation and leading to incomplete recovery finally progressing towards end stage renal failure (Ghaly Ahmed *et al.* 2010).

2.8.3 Unilateral ureter obstruction model

Obstructive nephropathy (ON) is a clinical problem which arises due to obstruction in urine flow leading to hydronephrosis and consequently damage of renal parenchymal (Ucero, Alvaro *et al.* 2010). Obstruction deformities common in children are ureterovesical junction obstruction, urethral atresia, posterior urethral valves while in adults acquire obstruction through nephrolithiasis, prostatic obstruction and ureteral strictures (Ravanan *et al.* 2007, Abou El-Ghar *et al.* 2008).

Obstructive nephropathy increases hydrostatic pressure in renal tubules causing stretching of tubular cells, increased mechanical stress on tubular cells resulting in apoptosis and increased expression of pre-apoptotic factors along with enhanced renin angiotensin system (RAS), oxidative stress, and endothelin-1 (Chevalier *et al.* 2010, Ucero *et al.* 2014, Sinha *et al.* 2012, Kahn *et al.* 1997). Obstructive nephropathy induced tubular atrophy and oxidative stress stimulate several cytokines which advocate transcription of NF-κβ. Orchestrated infiltration of neutrophils, macrophage and NF-κβ enforce translation of pro-inflammatory cytokines (IL-1β, IL-6, TNF- α) adhesion molecules (VCAM, ICAM, selectin) and several chemokines (MCP-1, IL-8, RANTES) (Abbas *et al.* 2018, Grande *et al.* 2010).

Cytokine-driven infiltration of macrophage and dendritic cells into interstitial region encourage fibroblast activation and proliferation, resulting in interstitial fibrosis. Chronic obstruction nephropathy induces RAS system which aggravates fibrosis by eliciting TGF-β/Smad signaling and Wnt/β-catenin pathway (Chevalier *et al.* 2009, Hosseinian *et al.* 2017). Along with other destructive phenomena generation of reactive oxygen species (ROS), depletion of ATP, mitochondrial damage, ischemia and hypoxia contribute in obstructive nephropathy (Blondin *et al.* 1975).

In addition to inflammation and interstitial fibrosis, epithelial tubular cells, and endothelial cells acquire mesenchymal phenotype through epithelial–mesenchymal transition (EMT). Along with other epithelial cells, pericytes also undergo myofibroblast transition and starts migrating towards interstitium to secrete extracellular matrix (collagen, α-smooth muscle actin) (Chevalier *et al.* 2009).

Surgical obstruction is a most common method used for unilateral ureteral obstruction (UUO) model in rodents. UUO induced CKD developed in rodents in 1-2 weeks and severe renal

parenchymal damage with interstitial fibrosis and tubular atrophy was noticed due to hydronephrosis. Neonates show more damage to UUO than adults with progressive reduction in glomerular filtration rate and renal blood flow observed within 24 h (Vaughan *et al.* 2004). UUO model preferred to unravel different biomarkers which sequentially interplay in progression of chronic kidney disease.

2.9 *Pseudomonas*

Pseudomonas comprises a myriad of more than 60 species of gamma proteobacteria with widespread occurrence in environment like soil, water, plant surface and animals. *Pseudomonas* species have attracted great deal of attraction because of its remarkable ecological and metabolic diversity, capability to produce enormous array of structurally diverse secondary metabolites exhibiting wide ranging biological activities, biochemical versatility and simplicity of the condition required for their growth (Gross *et al.* 2009, Palleroni 2015). Pseudomonads are capable of producing siderophores (complexing agents that increases availability of inorganic Fe $^{3+}$) (pyoverdins, pyochelins, paerucumarin), cyclic lipopeptides, numerous non-ribosomally derived peptides, phytotoxins and polyketides (Budzikiewicz 1993).

Pyoverdins are yellow-green fluorescent and strain specific siderophores which acquire Fe (III) ions from the environment that serve as intercellular signaling to control gene expression. It comprises a dihydroxy-quinoline chromophore attached to 6–12 amino acids peptide chain and a dicarboxylic acid or its amide (Gross *et al.* 2009, Palleroni 2015, Budzikiewicz 1993). Pyochelins are condensation product of cysteine and salicylic acid, which act as tetravalent ligand for iron complexation. Compounds pseudomonine contains salicylic acid and two heterocyclic amino acid molecules. Secondary metabolites produced by *Pseudomonas* species play vital role in defence against competitors and predators, virulence and nutrient acquisition (Gross *et al.* 2009, Hira *et al.* 2017). Findings of Mezaache-Aich *et al.*, revealed antimicrobial potential of secondary metabolites isolated from *Pseudomonas* species against all pathogenic fungi and bacteria like *Bacillus subtilis* and *Paracoccus paratrophus* (Mezaache-Aich *et al.* 2016).

Literature on the secondary metabolites produced by *Pseudomonas* species are described in Table 2.9 and Figure 2.9.

Table 2.9: Secondary metabolites produced by *Pseudomonas* species

S. No.	Compound	Producer	Biological Activity
1	Pyochelin, Paerucumarin, Pseudoveridin	*P. aeruginosa*	-
2	Safracin	*P. fluorescens A2-2*	Antitumor
3	Tabtoxin	*P. synringae*	-
4	Pyrrolnitrin	*P. fluorescens*, *P. aurantiaca BL915*, *Pseudomonas* species	Antifungal, Antimycotic
5	Indole-3-acetic acid	*Pseudomonas* species	-
6	Syringofactin	*P. synringae*	-
7	Orfamides	*P. fluorescens*	-
8	Polyketide and Fatty acids Mupirocin (Pseudomonic acid) 2,4-Diacetylphloroglucinol (DAPG) 2,5-Dialkylresorcinols	 *P. fluorescens NCIMB 10586* *P. fluorescens* *P. aurantiaca BL915*	 Antibacterial Antibacterial/ Antihelmentic Antibacterial/ Antifungal
9	Cyclic Lipopeptides Syringomycin, Syringopeptin Arthrofactin Massetolides Putisolvin	*P. synringae* *Pseudomonas species MIS38* *P. fluorescens SS101*, *Pseudomonas species MF-30* *P. putida PCL 1445*	 - - - -
10	Pseudomonine	*P. fluorescens AH2* *P. fluorescens WCS374* *P. entomophila L48*	-
11	Cyclic peptide polyketides Syringolin, Coronatine Pyoluteorin	 *P. synringae*	 -

	Pederin	*P. aeruginosa, P. fluorescens Pf-5, Pseudomonas species M18* *Pseudomonas species*	Cytotoxic
12	Rhizoxins	*P. fluorescens Pf-5*	-
13	Phenazines: Pyocyanin (5-N-methyl-1-hydroxyphenazine) Phenazine-1-carboxylic acid, 2-hydroxyphenazine-1-carboxylic acid and Phenazine-1-carboxamide 1-Hydroxypenazine, Phenazine-1-carboxylic acid phenazine-1-carboxylic acid 2,8-dihydroxyphenazine	*P. chlororaphis, P. fluorescens, P. aeruginosa* *P. aeruginosa* *P. chlororaphis, P. fluorescens* *Pseudomonas species strain ICTB-745* *Pseudomonas aurantiaca PB-St2*	Antibiotic/ Antitumor/ Antiparasitic - Antifungal Insecticidal Anticancer, Antifungal (Mehnaz *et al.* 2013)
14	Quinolone	*P. aeruginosa*	Antibacterial
15	Hydrogen cyanide (HCN)/ Prussic acid	*Pseudomonas species*	Inhibitor of cytochrome c oxidase and other mettaloproteins
16	2,4,6-trihydroxyacetophenone (THA)	*P. brassicacearum*	Antifungal
17	Aldoxime dehydratase	*P. cholororaphis*	Involved in carbon-nitrogen triple bond synthesis
18	Rhamnolipids Rhamnolipid 1		

	Rhamnolipid 2	*Pseudomonas species strain ICTB-745*	Antifeedant/ Insecticidal
19	Cyclo(L-Leu-L-Pro)	*P. aeruginosa*	Antiinflammatory
20	Cyclo(L-Pro-L-Tyr)	*P. fluorescens*	Inhibition of TNF-α
21	Cyclic dipeptides	*P. fluorescens*	Antifungal
22	Proline-based cyclic dipeptides, cyclo(Gly-L-Pro), cyclo(L-Pro-L-Phe), cyclo(trans-4-hydroxy-L-Pro-L-Phe) and cyclo(trans-4-hydroxy-L-Pro-L-Leu)	*P. aeruginosa*	Inhibition of TNF-α

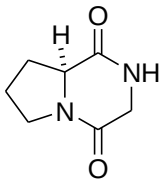

Cyclo(Gly-Pro)

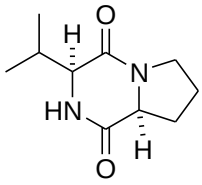

Cyclo(Val-Pro)

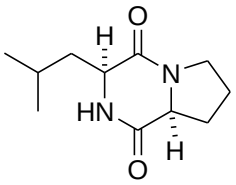

Cyclo(Leu-Pro)

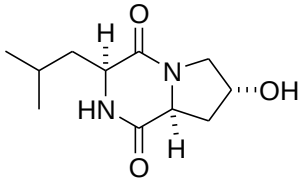

Cyclo(Leu-Hydroxy Pro)

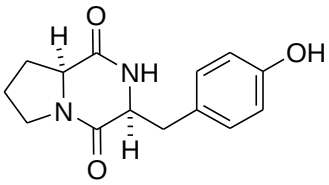

Cyclo(Pro-Tyr)

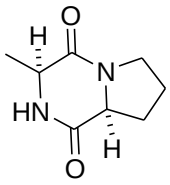

Cyclo(Pro-Al)

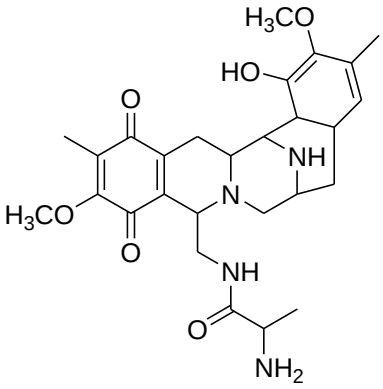

Safracin

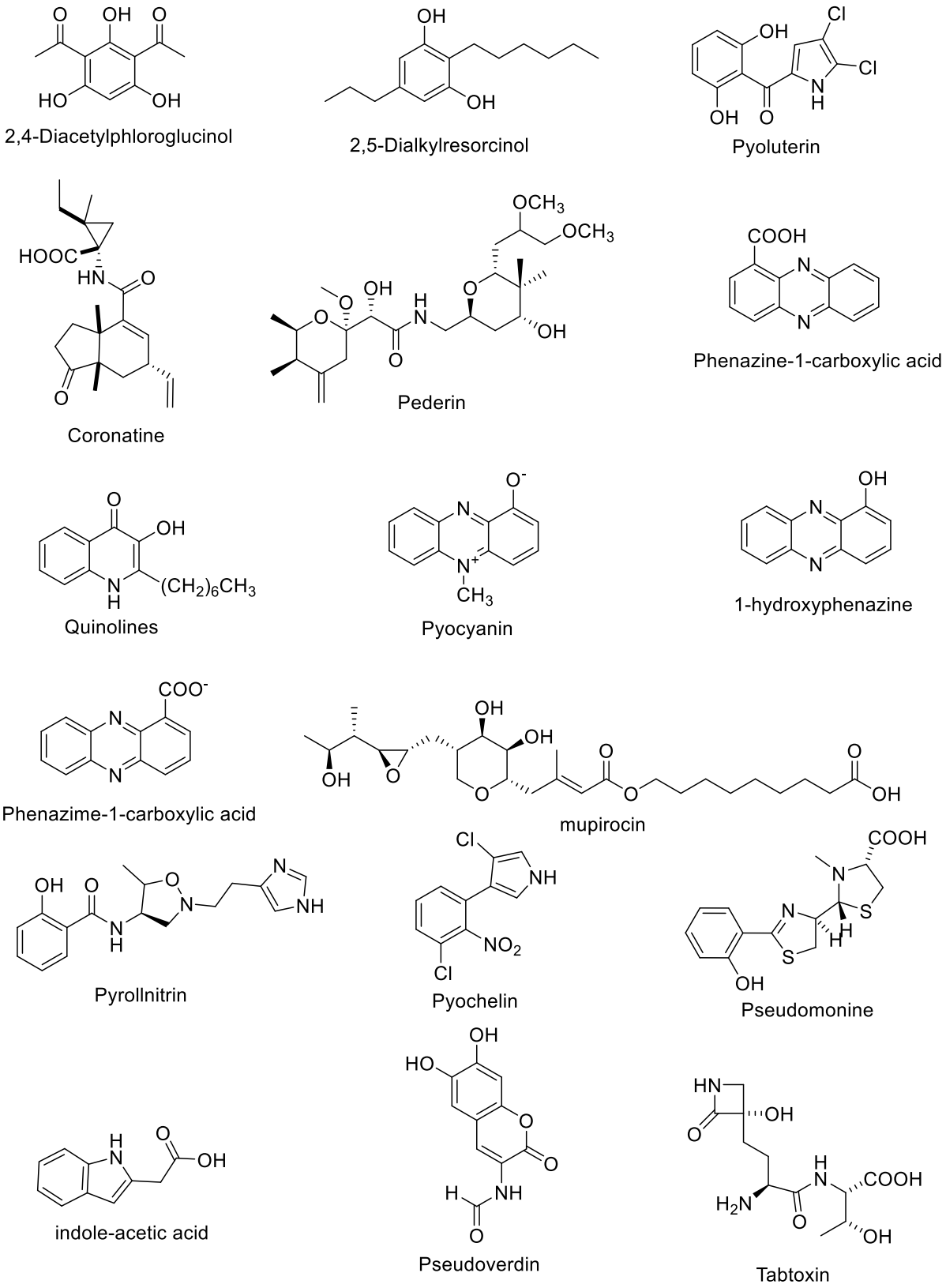

Figure 2.9 Structure of secondary metabolites produced by various *Pseudomonas* species

Pseudomonas aeruginosa

Pseudomonas aeruginosa is an opportunistic human pathogen that can be found ubiquitously in nature. It is mainly a gram negative, rod shaped soil bacterium with 1-5 μm length and 0.5-1.0 μm width, which produces an enormous spectrum of proteins and secondary metabolites. It utilizes aerobic respiration for its metabolism and anaerobically uses nitrates and other electron acceptors. It breaks down polycyclic aromatic hydrocarbons and produces lectins, rhamnolipids, phenazines, quinolones and hydrogen cyanide (Lindeberg *et al.* 2008).

Secondary metabolites of *P. aeruginosa* and their biological effects

Secondary metabolites produced by *P. aeruginosa* stimulates host's specific as well as non-specific defence mechanisms. Several findings of *in vivo* and *in vitro* studies revealed that heat-killed *P. aeruginosa* or bacterial lyophilizate inhibits immune responses in vivo as well as in vitro. Furthermore, exoproteins such as alkaline proteases and elastase are inhibited T-lymphocyte and natural killer cell functions (Ulmer *et al.* 1990). Pyocyanine (N-methyl-1-hydroxyphenazine) is a blue phenazine pigment of 210.23 g mol^{-1} molecular weight, typically characterized as virulence factor of *P. aeruginosa*, exhibited both immune-stimulatory as well as inhibitory effects. Ulmer, *et al.* and his colleagues found that pyocyanine at low concentrations of less than 0.1 μg/ml enhanced the proliferation of B and T-lymphocytes and also augmented the secretion of antibodies by B-lymphocytes (Ulmer *et al.* 1990). Also, study on murine macrophages, demonstrated downregulation of TNF-α, IL-1β and nitric oxide levels upon treatment with pyocyanine (Marreiro de Sales-Neto *et al.* 2019). Thus, pointing towards its positive role in immunosuppressant activity. Further, experiment by Laxmi *et al.* focussing on the extraction, characterization and study of the biological activity of the *P. aeruginosa* BTRY1 derived pyocyanin revealed the antioxidant potential with no cytotoxicity on L929 fibroblast cell line and human red blood cells (Laxmi *et al.* 2016). Other derivatives of phenazines isolated from *P. aeruginosa* like 1-hydroxyphenazine and phenazine-1-carboxylic acid showed their effect by modulating oxidative pathway (Denning *et al.*2003).

P. aeruginosa mediates communication among bacteria about population size or behavioural transformation from symbiosis to virulence by producing small diffusible molecules known as quorum sensing signal molecules (QSSM), chemically recognised as *N*-acylhomoserine lactones (AHL) and quinolones comprising *N*-(3-oxododecanoyl)-L-homoserine lactone (3-oxo-C12-HSL) and *N*-butanoyl-L-homoserine lactone (C4-HSL), two major AHL's and *N*-(3-oxohexanoyl)-L- homoserine lactone (3-oxo-C6-HSL) and *N*-hexanoyl-L-homo- serine lactone (C6-HSL) as two minor AHL's along with 2-heptyl-3-hydroxy-4 (1*H*)-quinolone (PQS) (Hooi, DS *et al.* 2004). In an experimental model of LPS stimulated RAW264.7

macrophages, 3-oxo-C12-HSL at 50 μM concentration suppressed TNF-α levels and substantially increased anti-inflammatory cytokine IL-10 without affecting the cell *via*bility (Glucksam-Galnoy, 2013). Findings also showed that *P. aeruginosa* derived 3-oxo-C12-HSL modulated host immune system by aggravating proliferation of T-lymphocytes and upregulating TLR2/TLR4 expression along with the significant reduction of TNF-α (Bao *et al.* 2017). Moreover, 3-oxo-C12-HSL treatment impaired the regulation of NFκB and suppressed NFκB mediated cytokine release (Kravchenko VV *et al.* 2008) and inhibited degranulation as well as mediator release from primary mast cells (Khambati *et al.* 2017). Altogether these studies revealed antiinflammatory potential of *P. aeruginosa* derived QSSM.

Exotoxin-A, a major extracellular product of *P. aeruginosa* lowered TNF-α levels by 90% at 100 ng/ml along with the reduction in the levels of IL-1β, IL-1α and IFN-γ. Also, exotoxin -A release suppressed lymphocyte proliferation (Staugas *et al.* 1992). Report by Rupesh *et al.*, on marine bacteria in the Bay of Bengal near Andaman and Nicobar Island, identified as *P. aeruginosa* demonstrated decline in proliferation of LPS induced Peripheral Blood Mononuclear cells (PBMCs) by crude ethyl acetate extract of *P. aeruginosa* with IC_{50} of 12 μg/ml (Rupesh *et al.* 2012). Similar study by Rukaiyya Khan *et al.* on ethyl acetate extract of *P. aeruginosa* attenuated mRNA expression levels of TNF-α in lipopolysaccharide stimulated RAW macrophages (Khan *et al.* 2015). Hoque and his colleague's work identified *Pseudomonas aeruginosa* FARP72 as a potential source of secondary metabolites with antibacterial property (Hoque *et al.* 2019).

Jarvis and Johnson first reported the isolation of potential anionic biosurfactants rhamnolipids from *P. aeruginosa* in 1949 (Jarvis and Johnson 1949). In another study, Mono- and di-rhamnolipids isolated from *P. aeruginosa* MR01 showed potent cytotoxic action against MCF cancer cell lines with IC_{50} values of 25.87 μg/ml and 31.00 μg/ml. Also, mRNA levels of tumor regulating p53 gene significantly upregulated upon treatment with 30 μg/ml concentration of rhamnolipids. Thus, demonstrating significant potential to be used as natural therapeutic anticancer agent (Rahimi *et al.* 2019).

Therefore, literature findings indicated vast capability of *P. aeruginosa* to produce secondary metabolites of biological importance.

2.10 Cyclic dipeptides

Cyclic dipeptides also known as 2,5-diketopiperazine, or piperazine-2,5-dione consists of a six-membered ring containing two amide linkages where the two nitrogen atoms and the two carbonyls are at opposite positions in the ring. Cyclic dipeptides demonstrate inherent property

of chemical and enzymatic stability, and structural and conformational specificity (Hernandez Padilla *et al.* 2017).

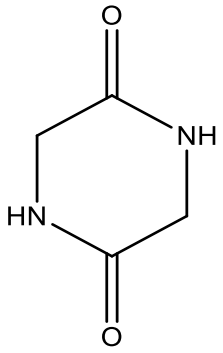

Figure 2.10.1: Basic structure of cyclic dipeptides

Cyclo (His-Pro) is reported to be endogenously present in brain, GIT, prostate and body fluids, derived from the metabolism of thyroid releasing hormone (Prasad *et al.* 1995). Numerous studies have demonstrated neuroprotective role of Cyclo (His-Pro) mediating its action through Nrf2-NFκB pathway. It stimulates Nrf2, a transcription factor that upregulates the expression of antioxidants (HO-1), along with the suppression of iNOS, gp91 phox, 47 phox gene and NFκB activity (Grottelli *et al.* 2016, Belleza *et al.* 2014). Cyclo (His-Pro) also showed protection to hypoxic PC-12 cells by activating p38 MAPK and mitigating phosphorylation of ERK1/2, protein kinase C (Minelli *et al.* 2006).

Several findings reveal the pharmaceutical potential of cyclic dipeptides, particularly the ones originated from microbes. *P. aeruginosa* PAO1 derived cyclic dipeptides Cyclo (L-Pro- L-Tyr), cyclo(L-Pro-L-Phe), cyclo(L-Pro-L-Val) showed antiproliferative capacity by preventing phosphorylation of akt and S6k kinases (Hernandez *et al.* 2017). Cyclo (L-Pro-D-Val), cyclo (L-Pro-L-Tyr) isolated from *Bacillus* sp. HC001 and cyclo (L-Pro-D-Leu) from *Piscicoccus* sp. 12L081 effectively ameliorated LPS induced expression of HMGB-1 in sepsis (Lee *et al.* 2016). While in another experiment, these cyclic dipeptides inhibited LPS-induced adhesion and migration of leukocytes across endothelial cells (Kang *et al.* 2016). Cyclic dipeptides isolated from *Streptomyces* sp. namely cyclo(L-Pro-L-Val), cyclo(L-lle-D-Pro), cyclo(L-Leu-L-Pro) and cyclo(D-Pro-L-Phe) significantly attenuated the levels of inflammatory mediators (TNF-α and IL-6) (Nalli *et al.* 2017).

Cyclo (Gly-Pro) showed protection in paw edema model by attenuating nociceptive behaviour and inflammatory responses (Ferro *et al.* 2015). Cyclic dipeptides originated from *Achromobacter* species demonstrated antiinflammatory potential by augmenting the expression of antiinflammatory cytokines IL-10 and IL-4 (Deepa *et al.* 2015). Khan *et al.* showed the isolation of proline based cyclic dipeptides from *Pseudomonas aeruginosa* ABS-

36 strain with vast antiinflammatory capability that significantly abrogated the levels of TNF-α. Furthermore, the pharmacological activity shown by cyclic dipeptides has been summarised in Table 2.10

Table 2.10: Pharmacological profile of cyclic dipeptides

S.no	Cyclic dipeptide	Source	Biological activity	Reference
1.	Cyclo(Leu-Pro)	*Brevibacillus laterosporus*	Antimicrobial	Khaled *et al.* 2017
2.	Penicimutide Cyclo(L-Val-L-Pro), Cyclo(L-Ile-L-Pro), Cyclo(L-Leu-L-Pro), Cyclo(L-Phe-L-Pro)	*Penicillium purpurogenum* G59	Cytotoxicity against HeLa cells	Wang *et al.* 2016
3.	Cyclo(his-pro)	-	CNS stimulant	Wilber 1995
4.	cyclic-L-proline-L-alanine dipeptide	-	Treatment of skin wounds esp burns	Chen *et al.* 2016
5.	Cyclo(L-Pro–L-Leu)	*Pseudomonas putida* MCCC 1A00316	Nematicidal activity	Zhai *et al.* 2019
6.	Cyclo(Gly-Pro)	-	Antinociceptive antiinflammatory	Ferro *et al.* 2015
7.	Cyclo(Gly-L-Pro), Cyclo(L-Pro-L-Phe), Cyclo(trans-4-hydroxy-L-Pro-L-Phe) Cyclo(trans-4-hydroxy-L-Pro-L-Leu)	*Pseudomonas aeruginosa* ABS-36	Antiinflammatory	Khan *et al.* 2015
8.	Cyclo(L-Pro-L-Tyr) Cyclo(D-Pro-L-Tyr)	*Streptomyces* sp. strain 22-4	Antibacterial	Wattana-Amorn *et al.* 2016
9.	14-hydroxycyclopeptine	*Aspergillus* sp. SCSIOW2	Reduced NO production	Zhou *et al.* 2016
10.	Cycloprolylglycine	-	Antihypoxic, nootropic, and anxiolytic effects	Kolyasnikova *et al.* 2015
11.	Cyclo(valine-valine)	-	Cholera treatment	Vikram *et al.*2014

12.	Cyclo(Leu-Gly)	-	Blocked haloperidol-induced dopamine receptor supersensitivity	Bhargawa et al 1980
13.	Cyclo(L-Pro-L-Phe)	Seaweed aflatoxin c-f-3	Phosphodiesterase inhibitors	Jin *et al.* 2013
14.	*cis*-cyclo(L-Val-L-Pro) *cis*-cyclo(L-Phe-L-Pro)	*Lactobacillus plantarum* LBP-K10	Antifungal Inhibited proliferation of Influenza A virus	Kwak *et al.* 2014 Kwak *et al.* 2013
15.	Cyclo(D-Tyr-D-Phe) Cyclo(L-Leu-D-Arg) Cyclo(D-Pro-L-Leu), Cyclo(D-Pro-L-Met) Cyclo(D-Pro-L-Phe) Cyclo(L-Pro-L-Met)	*Bacillus* sp. N strain	Antioxidant Antibacterial Anticancer Antifungal Antimycobacterial	Kumar *et al.* 2014 Nishanth *et al.* 2014a Nishanth *et al.* 2014b
16.	Cyclo(13,15-dichloro-L-Pro-L-Tyr)	-	Antiinflammatory	Saleki *et al.* 2013
17.	Cyclo(His-Gly) Cyclo(His-Ala)	-	Anticancer	Kilian *et al.* 2013
18.	Cycloprolylglycine	-	Neuroprotective Nootropic anxiolytic	Kolisnikova *et al.* 2012
19.	1-demethylhyalodendrin tetrasulfide brevicompanine B.	-	Antimalarial	Pérez-Picaso *et al.* 2012
20.	Cyclo(L-Cys-L-Leu)	-	Antioxidants	Furukawa *et al.* 2012
21.	Cyclo(His-Pro)	-	Antidiabetic	Ra *et al.* 2012
22.	Cyclo(L-Leu-L-Tyr)	-	Protection in Postischemic myocardial dysfunction	Mitsui-Saitoh *et al.* 2011
23.	Plinabulin	-	Antimicrotubular agent	Yamazaki*et al.* 2011
24.	Cyclo(Phe-Pro)	-	Cholera treatment	Bina *et al.* 2010

25.	Cyclo(Pro-4-hydroxy-Leu)	*Coprinus plicatilis*	Anticancer	Zhao *et al.* 2018
26.	Cyclo(L-Pro-D-Val) (1), Cyclo(L-Pro-L-Tyr) (2) and Cyclo(L-Pro-D-Leu) (3)	1 and 2 isolated from Bacillus sp. HC001 3 from Piscicoccus sp. 12L081	Modulates Secretory Group IIA Phospholipase A2 Antiinflammatory activity Anti-Endothelial cell protein C receptor (EPCR) shedding agent Inhibitory effect on HMGB1 induced sepsis	Choi *et al.* 2016 Kang *et al.* 2016 Jeong *et al.* 2016 Lee *et al.* 2016a Lee *et al.* 2016b
27.	Cyclo (Phenylalanyl-Leucyl) Cyclo (Leucyl-Leucyl)	*Thermoactinomyces* sp. imbas-22	Antibacterial Antifungal	Bratchkov *et al.* 2017
28.	Petrocidin A	*Streptomyces* sp. SBT348	Anticancer	Cheng *et al.* 2017
29.	Cyclo(L-4-OH-Pro-L-Leu), Cyclo(L-Tyr-L-Pro), Cyclo(L-Phe-L-Pro), Cyclo(L-Leu-L-Pro)	*Paludifilum halophilum*	Antimicrobial	Dammak *et al.* 2017
30.	Cyclo-(L-Pro-D-Leu)	*Streptomyces xiamenensis* MCCC 1A01570	Anticancer	Lin *et al.* 2018
31.	Cyclo(L-Pro-D-Ile) Cyclo(L-Pro-L-Phe)	E. *coli* GZ-34	Antimicrobial	Song *et al.* 2018
32.	Cyclo (Pro-DOPA)	*Streptomyces* sp. 8812	Antibacterial, Antifungal Antiproliferative Antioxidant	Solecka *et al.* 2018
33.	Cyclo(L-Ala-L-Ala) Cyclo(L-Ala-D-Ala)	-	Poly (ADP-ribose) polymerase inhibitors	Nilov *et al.* 2018
34.	Cyclo(His-Pro)	-	Treatment of neurodegenerative diseases	Grottelli *et al.* 2016

35.	Cyclo (L-Pro-L-Tyr) Cyclo(L-Pro-L-Phe), Cyclo(L-Pro-L-Val)	*Pseudomonas aeruginosa* PAO1	Antiproliferative	Hernández-Padilla *et al.* 2017
36.	Cyclo(L-Pro-L-Val) Cyclo(L-lle-D-Pro) Cyclo(L-Leu-L-Pro) Cyclo(D-Pro-L-Phe)	*Streptomyces* sp	Antiinflammatory	Nalli *et al.* 2017
37.	Arylidene N-alkoxydiketopiperazine	-	Antitumor	Tian *et al.* 2016
38.	Curromycin A	*Streptomyces* strain RAI364	Anticancer	Hayakawa *et al.* 2016
39.	Cyclo (L-Pro-L-Tyr) Cyclo (L-Pro-L-Phe)	*Pseudonocardia endophytica* VUK-10	Antimicrobial Anticancer	Mangamuri *et al.* 2016
40.	Cyclo(Pro-Tyr) Cyclo(Val-Pro) Cyclo(Pro-Met)	*Pseudomonas aurantiaca*	Antifungal	Mehnaz *et al.* 2013
41.	Cyclo(Val-Pro) Cyclo(Gly-Phe) Cyclo(Phe -Tyr) Cyclo(Leu-Tyr) Cyclo(Val-Leu)	*Streptomyces kunmingensis*	Anticancer	Wei *et al.* 2017
42.	Cyclo(Val-Pro)	*Asperigillus oryzae* *Nigrospora species*	Cytotoxic on HCT-116 cell lines	Shaaban *et al.* 2014 Chen *et al.* 2012
43.	Cyclo(L-4-hydroxy-Pro-L-Ser)	Placental extract	Treatment of contact hypersensitivity	Kim *et al.* 2010

Chapter 3

Objectives and Plan of Work

Objectives

Inflammation refers to complex biological process involving series of events that are triggered upon exposure to antigens or any kind of cellular injury and is associated with the release of various cytokines, chemokines, prostaglandins, leukotrienes etc. Cytokines play a putative role in the development of acute and chronic inflammation. Generally, inflammation is reverted once insult is removed, but the dysregulated levels of pro-inflammatory cytokines and anti-inflammatory cytokines lead to the progression of inflammation to chronic diseases. Thus, drugs intervening pro-inflammatory cytokines could be a potential target for curing renal inflammatory diseases.

Literature review on *Pseudomonas* strain suggests its tremendous potential to secrete numerous secondary metabolites and other molecules that exhibit diverse pharmacological roles such as antifungal, anti-inflammatory, antiproliferative, antioxidant, etc. Based on the literature report (Khan SR *et al.* 2015), *Pseudomonas sp*., ABS 36 strain, isolated from rhizospheric soil was selected for the study to develop small molecular moieties that targets pro-inflammatory cytokines. Currently there exists an unmet demand for novel entities that specifically target these major pro-inflammatory cytokines (TNF-α, IL-1β and IL-6). Small molecular weight natural compounds particularly from microbes have shown tendency to be used as pharmaceutical aid not only because of their biological activity but their possibility of chemical syntheses. In view of these results, an extensive chemical evaluation was planned on *Pseudomonas* sp., ABS 36 strain to isolate and characterize the metabolites, followed by *in vitro* and *in vivo* bio investigation of isolated compounds in renal injury models targeting pro-inflammatory cytokines.

- Evaluation of pro-inflammatory cytokine inhibitory potential of culture broth extract of *Pseudomonas* sp., ABS-36.
- Isolation and characterization of secondary metabolites from the culture broth extract of *Pseudomonas* sp., ABS-36.
- *In vitro* assays on isolated compounds to identify pro-inflammatory cytokine inhibitors targeting IL-1β, TNF-α and IL-6.
- *In vivo* assays of potential compounds using various renal injury model.

Plan of work

The set objectives were implemented through the following phases:

Phase 1: Evaluation of pro-inflammatory cytokine inhibitory potential of culture broth extract (PCBE) of *Pseudomonas* sp., ABS-36 through *in vitro* assay.

- Testing of pro-inflammatory cytokines (TNF-α, IL-1β and IL-6) inhibition effect of PCBE by ELISA and effect on cell viability of LPS stimulated RAW 264.7 cells
- Testing the effect of PCBE on NO production

Phase 2: Isolation of secondary metabolites from PCBE using various chromatographic techniques.

Phase 3: Characterization of secondary metabolites obtained from PCBE using various spectroscopic techniques.

Phase 4: *In vitro* screening of major compounds to identify pro-inflammatory cytokine inhibitors targeting IL-1β, TNF-α and IL-6.

- Testing of pro-inflammatory cytokines (TNF-α, IL-1β and Il-6) inhibition effect of major compounds by ELISA
- Testing the effect of major compounds on NO production
- Testing of cytotoxicity of major compounds

Phase 5: In vivo testing of the potential compounds for treatment of renal injury in various acute and chronic renal injury models

- Evaluation under oxalate induced renal nephropathy model and elaborating the mechanism of action of compound exhibiting prominent protection in *in vivo* model
- Evaluation under renal ischemic reperfusion model and elaborating the mechanism of action of compound exhibiting prominent protection in *in vivo* model using antimycin-induced *in vitro* ischemic model
- Evaluation under chronic renal injury model of unilateral ureteral obstruction and elaborating the mechanism of action of compound exhibiting prominent protection in *in vivo* model using TGF-β-induced *in vitro* fibrotic model

Chapter 4

Materials and Methods

4.1 General

Reagents of analytical and molecular biology grade were used to carry out the study. Mouse RAW 264.7 cell lines, rat NRK-52E kidney epithelial cell lines and rat NRK 49F kidney fibroblast cell lines were obtained from NCCS, Pune, India for carrying out *in vitro* studies. The *Pseudomonas* culture broth extract (PCBE), isolated compounds and standard prednisolone were dissolved in DMSO and added directly to the culture media with final concentration not exceeding 0.1%. Animals (C57/BL6 male mice, 6-8 weeks) were procured from Sai Nath agencies, Hyderabad, India, to carry out the *in vivo* study. Table 4.1a and 4.1b lists the chemicals and instruments used in the course of study.

Table 4.1a: Chemicals and reagents used in the study

Chemicals	Make
Dulbecco modified eagle media (DMEM), Fetal bovine serum (FBS), Antibiotic solution, Diethyl pyrocarbonate (DEPC) water, Dimethyl sulfoxide (DMSO), [3-(4,5-dimethylthiazol-2-yl)-2,5-diphenyltetrazolium bromide] (MTT reagent), Sodium oxalate crystals, N,N,N′,N′-Tetramethylethylenediamine (TEMED), mountant media, King's B media	Himedia Laboratories, India
Organic solvents (Ethyl acetate, isopropanol, methanol, chloroform and acetone)	Finar Limited, India
LPS (*E. coli* serotype 0111:B4), Bay-117082, Tween 20, Bicinchoninic acid and copper sulphate for protein quantification, RIPA lysis buffer, TMB substrate, BCA kit for protein estimation, XTT reagent kit, hematoxylin and eosin staining, Sirius red staining, Primers for TNF-α, IL-1β, IL-6 and GAPDH	Sigma-Aldrich, MO, USA
Glycine, Tris HCL, Ammonium per sulphate, Xylene and Acrylamide/Bisacrylamide	SRL (Sisco research laboratories) Chemicals, India
Paraffin Wax	SD chemicals, India
Silica gel	100–210 or 40–50 μm, Kanto Chemical, Japan
Silica gel 60 F254 glass plate	1.05715.0001, Merck, USA
Calcium oxalate	Alpha Aesar, USA
3 color prestained protein ladder (10-250kDa)	Puregene (Genetix), India

ELISA kits for TNF-α, IL-1β and IL-6 estimations	R & D Biotech India Private Ltd. (India)
Methylcellulose 4000 CPS	S. D. Fine-chem Ltd. Mumbai, India
SYBR Green PCR Master	TB green advantage qPCR Premix, Takara, USA
Trizol reagent, verso cDNA synthesis kit	Thermo Scientific, USA
PVDF membrane	BIO-RAD, laboratories, USA
Primary antibody for Caspase-1, IL-1β, NFκB, TGF-β, α-SMA, collagenase-1, β-actin, Bax, BCL 2, Horseradish peroxidase conjugated secondary antibodies	Biotechne brand, USA
Kit for the estimation of BUN levels (AUTOSPAN Liquid Gold Urea)	Arkray Healthcare Pvt. Ltd., India

Table 4.1b: Instruments used in the study

Instruments	Model/Make
Multiplate reader	Spectromax M4, California, USA
IR	Jasco FT/IR-4200, Maryland, US
MS	LCMS-2020, Shimadzu, Japan
HPLC	LC-8A, Shimadzu, Japan equipped with an ODS column (Inertsil ODS-3, 25 cm×4.6mm i.d., GL Sciences, Japan)
NMR	JNM-AL300, JEOL, Japan
Rotary evaporator	Buchi R-210, Switzerland
Centrifuge	Thermo Scientific, USA
Real time thermal cyclers	iCycleriQ apparatus with iCycler Optical System software (version 3.1), BIO-RAD Laboratories, USA
Enhanced Chemiluminescence detection system (FUSION FX)	Vilber Lourmat, France
Microtome	Jinhua YIDI Medical Appliance CO. Ltd.
Microscope	Leica microsystems
Nano drop spectrophotometer	Eppendorf, Germany
ImageJ software 1.53a	NIH, USA
Graph pad prism 8	GraphPad Software, Inc, San Diego, CA
Western blot apparatus	BIO-RAD Laboratories, USA
Isoflurane chamber	E-Z anaesthesia systems, Braintree scientific, Inc, MA, USA
Flow Cytometer	Becton, Dickinson and company, Franklin lake, NJ

4.2 Preparation of culture broth

Pseudomonas bacteria was isolated from rhizospheric soil of groundnut crop. The isolated colony was identified as *Pseudomonas* species based on the yellow fluorescence observed under UV in King's B media. Also, the bacteria exhibited blue green zone, when cultivated in King's A media which is a characteristic feature of pyocyanin producing *Pseudomonas*. Further, strain identification was done by comparing 16s rDNA sequencing and registered as

ABS-36 strain (GenBank Accession No. KT625586). Identified strain of *Pseudomonas* was then cultivated in King's B media.

Twenty litres of King's B media (comprising proteose peptone, dipotassium hydrogen phosphate, magnesium sulphate heptahydrate and agar) was inoculated with *Pseudomonas* sp. ABS-36 strain pre-culture and allowed to grow at 30 °C for seven days. After 7 days of incubation, small quantity of ethyl acetate (EtOAc) was added to the culture broth to stop the growth. The culture broth was centrifuged at 10,000 rpm for 10 min to separate the supernatant and precipitate. The supernatant was then extracted with EtOAc three times using separating funnel. The collected EtOAc layer was filtered, pooled and evaporated under reduced pressure to yield a dry culture broth extract (PCBE) (13.0 g).

4.3 *In vitro* studies on culture broth

PCBE was tested for its antiinflammatory efficacy using *in vitro* model of LPS-induced RAW 264.7 cell lines. The concentration of pro-inflammatory cytokines (IL-1β, TNF-α and IL-6) were estimated using ELISA assays. The NO levels were estimated using Griess reagent. MTT assay for assessing cell viability was also carried out in order to determine the toxicity of PCBE on RAW cells.

4.3.1 Cell viability studies on LPS stimulated RAW 264.7 cell lines

MTT assay was carried out to determine the cytotoxic effect of PCBE on LPS stimulated cells. It is based on the reduction of yellow coloured water soluble MTT reagent (3-[4,5-dimethylthiazole-2-yl]-2,5-diphenyltetrazolium bromide) to purple coloured formazan crystal by mitochondrial succinate dehydrogenases. Then, the crystals so formed are dissolved in DMSO and percentage of cell viability is calculated based on absorbance obtained spectrophotometrically (Mosmann *et al.* 1983, Kim *et al.* 2019).

RAW 264.7 cells were seeded and allowed to grow in 96-well plate. Then, the cells were pre-treated with the tested concentrations (500, 250, 100, 50, 25, 12.5 µg/mL) of PCBE for 24 h followed by LPS priming. Then, 50 µL of MTT reagent (5 mg/mL dissolved in phosphate buffer saline) was added to each well and allowed to incubate at 37 °C. After 3 h of incubation, the whole media was removed and 100 µL of DMSO was added. Thereafter, absorbance was noted at 570 nm using spectromax multiplate reader. Cell viability was calculated using the equation {100- [(1-T/C) *100]}, where T is the absorbance of PCBE treated group and C is the

absorbance of LPS control group. Further IC_{50} was determined by plotting Logarithmic value of the concentration *Vs.* % Inhibition graph (Van Meerloo *et al.* 2011).

4.3.2 Measurement of IL-1β production using ELISA studies

RAW cells were pre-treated with 500, 250, 100, 50, 25, 12.5 µg/mL concentration of PCBE for one hour, followed by priming with 1 µg/mL LPS. After four hours of LPS induction, cells were stimulated with 250 µg/mL calcium oxalate crystals. The supernatant was collected after 24 h of incubation with LPS to carry out IL-1β estimation using commercially available ELISA kits (Mulay *et al.* 2013, Kumar *et al.* 2019). Briefly, ELISA plates were coated with capture antibody and kept overnight. Following day, plates were blocked using 5% BSA after thorough washing with PBST. After one hour of incubation, again washings were given, samples and standard drug were added to the plate. Then, the samples were removed after two hours of incubation and detection antibody was added for 2 h subsequent to washings. Streptavidin-HRP was added to the plate after extensive washings, followed by the addition of TMB solution. Reaction was stopped by adding 2N H_2SO_4 solution. Subsequently, absorbance was recorded at 450 nm and 540 nm using spectrophotometer (R and D systems 2020).

4.3.3 Estimation of TNF-α and IL-6 levels using ELISA

RAW 264.7 mouse macrophages were grown in complete DMEM media supplemented with 9% FBS and 1% antibiotic solution in a humidified chamber at 37 °C and 5% CO_2. Cells were passaged on every 2-3 days to maintain logarithmic growth. Cells were then plated in 96-well plate at a density of 10,000 cells per well and allowed to incubate in complete DMEM media for 24 h. Further, the media was removed, thorough washings were given using PBS and incomplete DMEM media with 1% antibiotic solution. Thereafter, cells were treated with different concentrations of PCBE (500, 250, 100, 50, 25, 12.5 µg/mL) for 1 h, followed by stimulation using LPS (1 µg/mL). After 24 h of LPS stimulation, the supernatant was collected, centrifuged and used for carrying out ELISA assays for TNF-α and IL-6 estimations as per the manufacturer's protocol (Zhang *et al.* 2008, Bhardwaj *et al.* 2020).

4.3.4 Determination of NO levels

RAW 264.7 macrophages were cultured in 96-well plate and treated with the pre-determined concentrations of PCBE, followed by LPS stimulation. Supernatant was collected after 24 h of induction and then mixed with equal proportion (100µL) of Griess reagent (1% sulfanilamide

and 0.1% naphthylethylenediamine dihydrochloride in 2.5% phosphoric acid). After 10 min of incubation at room temperature absorbance was measured at 540 nm using multiplate reader (Sun *et al.* 2003, Adnan *et al.* 2018).

4.4 Isolation and characterisation of secondary metabolites from PCBE

4.4.1 Isolation of compounds from PCBE

PCBE was subjected for column chromatography on silica gel (100-210 μm) and eluted with EtOAc–MeOH gradient to give fractions 1–7. Fraction 6 (eluted with EtOAc–MeOH (50:1), which exhibited multiple spots under TLC was first selected for purification. It was rechromatographed over silica gel (40-50 μm) eluting with $CHCl_3$–acetone followed by acetone–MeOH gradient. The fraction eluted with $CHCl_3$–acetone (6:1) afforded compound **1** (21 mg) and compound **2** (15 mg) as pure amorphous solid. The fraction eluted with $CHCl_3$--acetone (1:3) was purified by HPLC on an ODS column (solvent, CH_3CN–H_2O (1:4) containing 0.03% TFA, flow 0.5 mL/min, detection 215 nm) to give compound **3** (5.1 mg), compound **4** (7.2 mg), compound **5** (5.5 mg), compound **6** (2.2 mg), compound **7** (2.4 mg) and compound **8** (3.2 mg). The fraction eluted with acetone was separated by preparative TLC (developing solvent, $CHCl_3$–MeOH (95:5)) to afford pure compound **9** (11 mg), compound **10** (19 mg), compound **11** (20 mg). The fraction eluted with acetone–MeOH (8:2) was rechromatographed over silica gel (40-50 μm) elution of column with $CHCl_3$–acetone gradient yielded sub-fractions A (eluted with $CHCl_3$–acetone (20:1)), B (eluted with $CHCl_3$–acetone (20:1.5)), C (eluted with $CHCl_3$–acetone (20:2)), and D (eluted with $CHCl_3$–acetone (20:3)).

Sub-fraction A was suspended in MeOH and the insoluble part was subjected to HPLC (solvent, MeOH–H_2O (2:3) containing 0.03% TFA) to afford compound **12** (9.4 mg) and compound **13** (1.0 mg). The MeOH-soluble part was also separated by HPLC (solvent, MeOH–H_2O (2:3) containing 0.03% TFA) to afford compound **12** (10 mg), compound **13** (8.5 mg), compound **14** (6.3 mg), compound **6** (2.2 mg) and compound **15** (0.9 mg). HPLC separation (solvent, MeOH–H_2O (1:2) containing 0.03% TFA) of the sub-fraction B yielded compound **16** (2.4 mg), compound **17** (2.0 mg), compound **18** (6.1 mg) and compound **19** (1.9 mg). HPLC separation (solvent, MeOH–H_2O (1:2) containing 0.03% TFA) of the sub-fraction C yielded compound **20** (2.1 mg). HPLC purification (solvent, MeOH–H_2O (1:2) containing 0.03% TFA) of the sub-fraction D yielded compound **16** (2.2 mg), compound **17** (7.0 mg) and compound **13** (7.0 mg). Fraction 7 (eluted with EtOAc-MeOH (30:1–10:1)) of the initial silica gel column yielded additional amount (15 mg) of compound **12**.

4.4.2 Characterization of the isolated compounds

All the isolated compounds **1** – **20** were subjected for spectral analysis. Compound **1** was subjected for elaborative analysis (IR, ^{1}H NMR, ^{13}C NMR, DEPT and MS) and was characterised as *cis*-Cyclo(L-Val-L-Pro). ^{1}H NMR and ^{13}C NMR of compounds **1** – **20** were measured by dissolving in either CD_3OD or $CDCl_3$. Compounds **1** – **20** were identified as *cis*-cyclo(L-Val-L-Pro) (**1**), *cis*-cyclo(Leu-Pro) (**2**), *cis*-cyclo(Val-Leu) (**3**), *trans*-cyclo(Phe-Pro) (**4**), *cis*-cyclo(Val-Phe) (**5**), *cis*-cyclo(Ile-Phe) (**6**), *cis*-cyclo(Leu-Ile) (**7**), *cis*-cyclo(Leu-Leu) (**8**), *cis*-cyclo(Leu-hydroxy-Pro) (**9**), *cis*-cyclo(Pro-Tyr) (**10**), *cis*-cyclo(Ala-Pro) (**11**), cyclo(Gly-Pro) (**12**), cyclo(Gly-Phe) (**13**), *cis*-cyclo(Ala-Phe) (**14**), *cis*-cyclo(Ala-Ile) (**15**), cyclo(Gly-Tyr) (**16**), *cis*-cyclo(Ala-Tyr) (**17**), *cis*-cyclo(Val-Tyr) (**18**), *cis*-cyclo(Leu-Tyr) (**19**), *cis*-cyclo(Ala-Ala) (**20**), respectively.

cis-Cyclo(L-Val-L-Pro) (**1**)

^{1}H NMR (400 MHz, $CDCl_3$) δ: 6.03 (1H, brs, NH), 4.10 (1H, t, *J*=7.5 Hz, H-6), 3.95 (1H, brs, H-3), 3.70-3.53 (2H, m, H-9), 2.67-2.63 (1H, m, H-10), 2.41-2.36 (1H, m, H-7a), 2.10-1.89 (3H, m, H-7b, -8), 1.09 (3H, d, *J*=6.9 Hz, H-11), 0.93 (3H, d, *J*=6.9 Hz, H-12). ^{13}C NMR (100 MHz, $CDCl_3$) δ: 170.9 (C-5), 165.0 (C-2), 60.4 (C-3), 58.8 (C-6), 45.2 (C-9), 28.5 (C-10), 28.4 (C-7), 22.4 (C-8), 19.3 (C-12), 16.1 (C-11).

cis-Cyclo(Leu-Pro) (**2)**

^{1} H NMR (300 MHz, $CDCl_3$) δ: 6.70 (1H, brs, NH), 4.12 (1H, t, *J*=7.9 Hz, H-6), 4.02 (1H, dd, *J*=9.0, 3.3 Hz, H-3), 3.66-3.50 (2H, m, H-9), 2.40-2.29 (1H, m, H-7a), 2.19-1.75 (5H, m, H-7b, H-8, H-10a, H-11), 1.54 (1H, ddd, *J*=14.3, 9.0, 5.1 Hz, H-10b), 1.00 (3H, d, *J*=6.6 Hz, H-12), 0.95 (d, *J*=6.3 Hz, H-13). ^{13}C NMR (75 MHz, $CDCl_3$) δ: 172.4 (C-5), 166.2 (C-2), 58.9 (C-6), 53.3 (C-3), 45.4 (C-9), 38.4 (C-10), 28.0 (C-7), 24.5 (C-11), 23.2 (C-12), 22.7 (C-8), 21.2 (C-13).

cis-Cyclo(Val-Leu) (**3**)

^{1}H NMR (300 MHz, CD_3OD) δ: 3.94 (1H, dd, *J*=8.6, 4.4 Hz, H-6), 3.77 (1H, brd, *J*=3.3 Hz, H-3), 2.27-2.16 (1H, m, H-11), 1.93-1.80 (1H, m, H-8), 1.80-1.69 (1H, m, H-7a), 1.64-1.54 (1H, m, H-7b), 1.04 (3H, d, *J*=7.0 Hz, H-12), 0.97-0.93 (9H, m, H-9, -10, -13). ^{13}C NMR (75 MHz, CD_3OD) δ: 171.3 (C-2), 169.7 (C-5), 61.5 (C-3), 54.3 (C-6), 46.0 (C-7), 33.7 (C-11), 25.3 (C-8), 23.6 (C-9), 21.8 (C-10), 19.3 (C-12), 17.8 (C-13).

trans-Cyclo(Phe-Pro) (**4**)

^{1}H NMR (300 MHz, CD_3OD) δ: 7.31-7.15 (5H, m, H-9–13), 4.19 (1H, t, *J*=4.8 Hz, H-6), 3.58-3.48 (1H, m, H-16a), 3.36-3.26 (1H, m, H-16b), 3.18 (1H, dd, *J*=13.5, 4.8 Hz, H-7a), 2.98 (1H, dd, *J*=13.5, 4.8 Hz, H-7b), 2.59 (1H, dd, *J*=10.2, 6.0 Hz, H-3), 2.08-1.99 (1H, m, H-14a), 1.96-1.85 (1H, m, H-15a), 1.71-1.52 (2H, m, H-14b, -15). ^{13}C NMR (75 MHz, CD_3OD) δ: 171.3 (C-2), 167.4 (C-5), 136.7 (C-8), 131.3 (C-9, -13), 129.6 (C-10, -12), 128.5 (C-11), 59.7 (C-6), 59.1 (C-3), 46.1 (C-16), 41.0 (C-7), 29.8 (C-14), 22.5 (C-15).

^{1}H NMR (300 MHz, $CDCl_3$) δ: 7.33-7.18 (5H, m, H-9–13), 6.92 (1H, brs, NH), 4.27 (1H, dd, 9.5, 4.0 Hz, H-6), 3.69- 3.58 (1H, m, H-16a), 3.48-3.35 (1H, m, H-16b), 3.18 (1H, dd, *J*=13.6, 5.9 Hz, H-7a), 3.07 (1H, dd, *J*=13.6, 4.2 Hz, H-7b), 2.92 (1H,dd, *J*=10.4, 6.4 Hz, H-3), 2.21-2.11 (1H, m, H-14a), 1.99-1.86 (1H, m, H-15a), 1.85-1.59 (2H, m, H-14b, -15b). ^{13}C NMR (75 MHz, $CDCl_3$) δ: 169.7 (C-2), 164.9 (C-5), 135.1 (C-8), 129.9 (C-9, -13), 128.7 (C-10, -12), 127.5 (C-11), 58.8 (C-6), 57.7 (C-3), 45.1 (C-16), 40.3 (C-7), 28.8 (C-14), 21.6 (C-15).

cis-Cyclo(Val-Phe) (**5**)

^{1}H NMR (300 MHz, CD_3OD) δ: 7.18-7.31 (5H, m, H-9–13), 4.31 (1H, ddd, *J*=4.8, 4.8, 1.8 Hz, H-6), 3.63 (1H, dd, *J*=4.5, 1.5 Hz, H-3), 3.23 (1H, dd, *J*=13.8, 5.1 Hz, H-7a), 3.02 (1H, dd, *J*=13.8, 4.8, H-7b), 1.70-1.57 (1H, m, H-14), 0.78 (3H, d, *J*=7.3 Hz, H-15), 0.41 (3H, d, *J*=7.0 Hz, H-16). ^{13}C NMR (75 MHz, CD_3OD) δ: 169.4 (C-2, -5), 137.0 (C-8), 131.5 (C-9,13),129.6 (C-10, 12), 128.2 (C-11), 61.3 (C-6), 57.3 (C-3), 40.1 (C-7), 33.3 (C-14), 19.1 (C-16), 17.1 (C-15).

cis-Cyclo(Ile-Phe) (**6**)

^{1}H NMR (300 MHz, CD_3OD) δ: 7.30-7.18 (5H, m, H-9–13), 4.32 (1H, ddd, *J*=4.8, 4.8, 1.5 Hz, H-6), 3.71 (1H, dd, *J*=4.1, 1.8 Hz, H-3), 3.26 (1H, dd, *J*=13.9, 4.9 Hz, H-7a), 2.99 (1H, dd, *J*=13.9, 4.8 Hz, H-7b), 1.49-1.35 (1H, m, H-14), 0.71 (3H, d, *J*=7.3 Hz, H-17), 0.66 (3H, t, *J*=6.2 Hz, H-16), 0.82-0.56 (2H, m, H-15). ^{13}C NMR (75 MHz, CD_3OD) δ: 169.4, 169.2 (C-2, -5), 137.0 (C-8), 131.7 (C-9, -13), 129.5 (C-10, -12), 128.2 (C-11), 60.8 (C-3), 57.2 (C-6), 39.8 (C-14), 39.7 (C-7), 24.7 (C-15), 15.2 (C-17), 12.0 (C-16).

cis-Cyclo(Leu-Ile) (**7**)

^{1}H NMR (300 MHz, CD_3OD) δ: 3.93 (1H, ddd, *J*=9.2, 4.4, 1.1 Hz, H-6), 3.84 (1H, dd, *J*=4.3, 1.1 Hz, H-3), 1.96-1.69 (3H, m, H-7, -11), 1.64-1.46 (2H, m, H-8, -12a), 1.29-1.16 (1H, m, H-

12b), 1.02 (3H, d, *J*=7.0 Hz, H-14), 0.96 (3H, d, *J*=6.6 Hz, H-9), 0.94 (3H, d, *J*=6.2 Hz, H-10), 0.94 (3H, t, *J*=7.3 Hz, H-13). ^{13}C NMR (75 MHz, CD_3OD) δ: 171.2 (C-5), 169.6 (C-2), 60.9 (C-3), 54.3 (C-6), 45.8 (C-7), 40.5 (C-11), 25.9 (C-12), 25.3 (C-8), 23.6 (C-9), 21.9 (C-10), 15.7 (C-14), 12.1 (C-13).

cis-Cyclo(Leu-Leu) (**8**)

^{1}H NMR (300 MHz, CD_3OD) δ: 3.90 (2H, dd, *J*=8.8, 4.8 Hz, H-3,-6), 1.90-1.76 (2H, m, H-8, -12), 1.75-1.55 (4H, m, H-7, -11), 0.97 (6H, d, *J*=6.6 Hz, H-9, -13), 0.95 (6H, d, *J*=6.6 Hz, H-10, -14). ^{13}C NMR (75 MHz, CD_3OD) δ: 171.2 (C-2, -5), 54.7 (C-3, -6), 45.9 (C-7, -11), 25.3 (C-8, -12), 23.6 (C-9, -13), 21.9 (C-10, -14)

cis-Cyclo(Leu-hydroxy-Pro) (**9**)

^{1}H NMR (300 MHz, CD_3OD) δ: 4.54-4.42 (2H, m, H-6, -8), 4.17-4.14 (1H, dd, *J*=3.3, 8.4 Hz, H-3), 3.65 (1H, dd, *J*=12.8, 4.5 Hz, H-9a), 3.43 (1H, d, *J*=12.8 Hz, H-9b), 2.27 (1H, dd, *J*=13.3, 6.5 Hz, H-7a), 2.08 (1H, ddd, *J*=13.3, 11.2, 6.6 Hz, H-7b), 1.94-1.85 (2H, m, H-10a, -11), 1.53-1.48 (1H, m, H-10b), 0.95 (3H, d, *J*=6.3 Hz, H-12), 0.95 (3H, d, *J*=6.3 Hz, H-13). ^{13}C NMR (75 MHz, CD_3OD) δ: 171.6 (C-5), 167.6 (C-2), 67.7 (C-8), 57.3 (C-6), 53.8 (C-9), 53.2 (C-3), 38.0 (C-10), 36.8 (C-7), 24.4 (C-11), 22.0 (C-12), 20.9 (C-13).

cis-Cyclo(Pro-Tyr) (**10**)

^{1}H NMR (300 MHz, $CDCl_3$) δ: 7.52 (1H, brs, C-11-OH), 7.05 (2H, d, *J*= 8.3 Hz, H-9, -13), 6.78 (2H, d, *J*=8.3 Hz, H-10, -12), 6.14 (1H, brs, H-1), 4.23 (1H, m, H-3), 4.08 (1H, t, *J*=7.8 Hz, H-6), 3.70-3.50 (2H, m, H-16), 3.43 (1H, dd, *J*=14.4, 3.6 Hz, H-7a), 2.80 (1H, dd, *J*=9.5, 4.8 Hz, H-7b), 2.39-2.26 (1H, m, H-14a), 2.06-1.80 (3H, m, H-14b, H-15). ^{13}C NMR (75 MHz, $CDCl_3$) δ: 169.7 (C-2), 165.2 (C-5), 155.7 (C-8), 130.3 (C-9, -13), 126.6 (C-11), 116.0 (C-10, -12), 59.1 (C-3), 56.3 (C-6), 45.4 (C-16), 35.9 (C-7), 28.3 (C-14), 22.4 (C-15).

cis-Cyclo(Ala-Pro) (**11**)

^{1}H NMR (300 MHz, $CDCl_3$) δ: 6.94 (1H, brs, H-4), 4.18-4.08 (2H, m, H-3, -6), 3.64-3.50 (2H, m, H-9), 2.41-2.29 (1H, m, H-7a), 2.20-1.73 (3H, m, H-7b, -8), 1.48 (3H, d, *J*=6.9 Hz, H-10). ^{13}C NMR (75 MHz, $CDCl_3$) δ: 170.5 (C-5), 166.4 (C-2), 59.2 (C-6), 51.1 (C-3), 45.4 (C-9), 28.1 (C-8), 22.7 (C-7), 15.9 (C-10).

Cyclo(Gly-Pro) (**12**)

^{1}H NMR (300 MHz, CD_3OD) δ: 4.23 (1H, t, *J*=7.1 Hz, H-6), 4.10 (1H, d, *J*=16.9 Hz, H-3a), 3.73 (1H, d, *J*=16.9 Hz, H-3b), 3.61-3.44 (2H, m, H-9), 2.39-2.22 (1H, m, H-7a), 2.08-1.85 (3H, m, H-7b, -8). ^{13}C NMR (75 MHz, CD_3OD) δ: 172.0 (C-5), 166.5 (C-2), 59.9 (C-6), 47.0 (C-3), 46.3 (C-9), 29.4 (C-8), 23.3 (C-7).

Cyclo(Gly-Phe) (**13**)

^{1}H NMR (300 MHz, CD_3OD) δ: 7.31-7.18 (5H, m, H- 9-13), 4.22 (1H, dd, *J*=4.6, 4.0 Hz, H-6), 3.41 (1H, d, *J*=17.6 Hz, H-3a), 3.24 (1H, dd, *J*=13.5, 4.0 Hz, H-7a), 2.98 (1H, dd, *J*=13.5, 4.6 Hz, H-7b), 2.61 (1H, d, *J*=17.6 Hz, H-3b). ^{13}C NMR (75 MHz, CD_3OD) δ: 170.0 (C-2), 168.7 (C-5), 136.4 (C-8), 131.5 (C-9, 13), 129.6 (C-10, 12), 128.5 (C-11), 57.5 (C-6), 44.6 (C-3), 40.9 (C-7).

cis-Cyclo(Ala-Phe) (**14**)

^{1}H NMR (300 MHz, CD_3OD) δ: 7.33-7.17 (5H, m, H- 9–13), 4.30 (1H, dd, *J*=7.1, 3.6 Hz, H-6), 3.74 (1H, qd, *J*=7.1, 1.1 Hz, H-3), 3.27 (1H, dd, *J*=13.8, 3.6 Hz, H-7a), 2.95 (1H, dd, *J*=13.8, 4.8 Hz, H-7b), 0.50 (3H, d, *J*=7.0 Hz, H-14). ^{13}C NMR (75 MHz, CD_3OD) δ: 170.0 (C-5), 168.7 (C-2), 136.6 (C-8), 131.8 (C-9, 13), 129.5 (C-10, 12), 128.3 (C-11), 57.4 (C-6), 51.7 (C-3), 40.3 (C-7), 20.4 (C-14).

cis-Cyclo(Ala-Ile) (**15**)

^{1}H NMR (300 MHz, CD_3OD) δ: 4.02 (1H, qd, *J*=7.0, 1.5 Hz, H-6), 3.90 (1H, dd, *J*=3.3, 1.2 Hz, H-3), 2.02-1.88 (1H, m, H-8), 1.58-1.44 (1H, m, H-9a), 1.43 (3H, d, *J*=6.9 Hz, H-7), 1.32-1.16 (1H, m, H-9b), 1.01 (3H, d, *J*=7.3 Hz, H-11), 0.94 (3H, t, *J*=7.3 Hz, H-10).

Cyclo(Gly-Tyr) (**16**)

^{1}H NMR (300 MHz, CD_3OD) δ: 7.01 (2H, d, *J*=8.6 Hz, H-9, -13), 6.71 (2H, d, *J*=8.6 Hz, H-10, -12), 4.15 (1H, dd, *J*=4.2, 3.6 Hz, H-6), 3.41 (1H, d, *J*=17.7 Hz, H-3a), 3.14 (1H, dd, *J*=13.9, 3.6 Hz, H-7a), 2.87 (1H, dd, *J*=13.9, 4.2 Hz, H-7b), 2.63 (1H, d, *J*=17.7 Hz, H-3b). ^{13}C NMR (75 MHz, CD_3OD) δ: 170.3 (C-2), 168.8 (C-5), 158.2 (C-11), 132.5 (C-9, -13), 126.6 (C-8), 116.3 (C-10, -12), 57.7 (C-6), 44.7 (C-3), 40.1 (C-7).

cis-Cyclo(Ala-Tyr) (**17**)

^{1}H NMR (300 MHz, CD_3OD) δ: 7.00 (2H, d, *J*=8.4 Hz, H-9, -13), 6.71 (2H, d, *J*=8.4 Hz, H-10, -12), 4.25-4.20 (1H, m, H-6), 3.75 (1H, qd, *J*=7.1, 1.1 Hz, H-3), 3.18 (1H, dd, *J*=13.7, 3.7 Hz, H-7a), 2.84 (1H, dd, *J*=13.7, 4.7 Hz, H-7b), 0.58 (3H, d, *J*=7.0 Hz, H-14). ^{13}C NMR (75

MHz, CD_3OD) δ: 170.7 (C-2), 168.7 (C-5), 158.0 (C-11), 132.8 (C-9, 13), 127.0 (C-8), 116.3 (C-10, 12), 57.6 (C-6), 51.7 (C-3), 39.5 (C-7), 20.4 (C-14).

cis-Cyclo(Val-Tyr) (**18**)

^1H NMR (300 MHz, CD_3OD) δ: 7.02 (2H, d, *J*=8.4 Hz, H-9, -13), 6.69 (2H, d, *J*=8.4 Hz, H-10, -12), 4.25- 4.21 (1H, m, H-6), 3.62 (1H, dd, *J*=4.6, 1.4 Hz, H-3), 3.14 (1H, dd, *J*=13.9, 3.9 Hz, H-7a), 2.92 (1H, dd, *J*=13.9, 4.8 Hz, H-7b), 1.70-1.58 (1H, m, H-14), 0.81 (3H, d, *J*=7.0 Hz, H-16), 0.47 (3H, d, *J*=6.6 Hz, H-15). ^{13}C NMR (75 MHz, CD_3OD) δ: 169.6 (C-5), 169.4 (C-2), 157.9 (C-11), 132.4 (C-9, 13), 127.6 (C-8), 116.3 (C-10, 12), 61.3 (C-3), 57.5 (C-6), 39.3 (C-7), 33.3 (C-14), 19.2 (C-16), 17.2 (C-15).

cis-Cyclo(Leu-Tyr) (**19**)

^1H NMR (300 MHz, CD_3OD) δ: 6.98(2H,d, *J*= 8.4 Hz, H-9, 13), 6.70 (2H, d, *J*=8.4 Hz, H-10, 12), 4.23 (1H, dd, *J*=4.8, 3.7 Hz, H-6), 3.64 (1H, dd, *J*=10.2, 4.3 Hz, H-3), 3.19 (1H, dd, *J*=13.9, 3.7 Hz, H-7a), 2.81 (1H, dd, *J*=13.9, 4.8 Hz, H-7b), 1.49-1.34 (1H, m, H-15), 0.92-0.82 (1H, m, H-14a), 0.74 (3H, d, *J*=6.5 Hz, H-16), 0.14-0.03 (1H, m, H-14b). ^{13}C NMR (75 MHz, CD_3OD) δ: 170.7 (C-5), 169.1 (C-2), 158.1 (C-11), 132.8 (C-9, -13), 127.1 (C-8), 116.4 (C-10, -12), 57.6 (C-6), 54.1 (C-3), 45.2 (C-14), 39.4 (C-7), 24.7 (C-15), 23.4 (C-16), 21.3 (C-17).

cis-Cyclo(Ala-Ala) (**20**)

^1H NMR (300 MHz, CD_3OD) δ: 4.02 (2H, q, *J*=6.9 Hz, H-3, -6), 1.42 (6H, d, *J*=6.9 Hz, H-7, -8). ^{13}C NMR (75 MHz, CD_3OD) δ: 171.5 (C-2, -5), 51.8 (C-3, -6), 20.0 (C-7, -8).

4.5 *In vitro* studies on isolated compounds

Compounds cyclo(Val-Pro) (**1**), cyclo(Leu-Pro) (**2**), cyclo(Leu-hydroxy-Pro) (**9**), cyclo(Pro-Tyr) (**10**), cyclo(Ala-Pro) (**11**), cyclo(Gly-Pro) (**12**) were tested at varying concentrations (3, 10, 30 and 100 μM) for their potential to inhibit pro-inflammatory cytokines using RAW 264.7 macrophage cell lines. Cells were grown in complete DMEM media augmented with 10% FBS and 1% antibiotic solution at 37 °C in a humidified atmosphere. Cells were passaged after confluency is attained and 10,000 cells were seeded in 96-well plate for carrying out cell viability assay, ELISA studies and NO estimation.

4.5.1 Cell viability assay on LPS stimulated RAW 264.7 cell lines

Rapid colorimetric MTT assay was used to assess the effect of compounds on cell viability. Cyclic dipeptides **1**, **2**, **9**-**12** were added to 96-well plate at different concentrations, followed

by LPS stimulation. MTT reagent of 50 µL volume of 5 mg/mL concentration was added to each well and incubated at room temperature for 3 h. DMSO of 100 µL was added after the removal of whole media. Absorbance was measured spectrophotometrically at 570 nm using multiplate reader (Mosmann *et al.* 1983, Kim *et al.* 2019).

4.5.2 ELISA assay for the estimation of TNF-α, IL-6 and IL-1β

RAW 264.7 cells were incubated for one hour with different concentrations of cyclic dipeptides (**1**, **2**, **9**-**12**) i.e. 3 µM, 10 µM, 30 µM and 100 µM. Cells were then stimulated using 1 µg/mL LPS for TNF-α and LPS + 250 µM calcium oxalate crystals for IL-1β estimations. Cell free supernatant was collected after 24 h of stimulation and was subjected to ELISA studies using commercially available ELISA kits as per manufacturer's instruction (R and D systems 2020) and absorbance was noted at 450 nm and 540 nm using spectrophotometer (Zhang *et al.* 2008, Mulay *et al.* 2013).

4.5.3 Measurement of NO levels using Griess assay

Nitrite levels were determined using Griess reagent. Nitrite present in the sample reacts with sulphanilic acid under acidic conditions to form diazonium salts which further couples with 1-napthyl amine to give water soluble pink color azo dye which can be detected spectrophotometrically at 540 nm.

RAW cells were pretreated with different concentrations of isolated compounds as per the experimental protocol, followed by LPS incubation for 24 h. The supernatant of 100 µL volume was then mixed with equal volume of griess reagent and incubated at 37 °C for 10 min. Then the absorbance was recorded spectrophotometrically at 540 nm (Sun *et al.* 2003, Adnan *et al.* 2018).

4.6 *In vivo* evaluation of isolated compounds

All *in vivo* studies were carried out as per the standard protocols approved by Institutional Animal Ethics Committee, BITS-Pilani, Hyderabad Campus with approval number BITS-Hyd/IAEC/2017/10. Animals were maintained in a 12-h dark and light cycle with standard diet and water *ad libitum* throughout the study. Anti-inflammatory efficacy of isolated compounds was tested in acute (calcium oxalate induced renal nephropathy and renal ischemic reperfusion model) as well as chronic model (Unilateral ureteral obstruction model) of renal injury.

4.6.1 Calcium oxalate induced renal nephropathy model

Cyclic dipeptides **1**, **2**, **9-12** were tested for their pro-inflammatory cytokine inhibiting potential using oxalate induced mouse model of renal nephropathy. Briefly, study was carried out in male C57/BL6 mice with weight ranging from 20-25g. Animals were divided into eight different groups (n = 6 in each group) as described in below table:

Table 4.2: Animal grouping in calcium oxalate induced renal nephropathy model

Groups	Treatment
Group 1	Normal Control
Group 2	Disease Control (Oxalate Treated)
Group 3	Cyclo(Val-Pro) (**1**)
Group 4	Cyclo (Leu-Pro) (**2**)
Group 5	Cyclo (Leu-Hydroxy-Pro) (**9**)
Group 6	Cyclo (Pro-Tyr) (**10**)
Group 7	Cyclo (Pro-Ala) (**11**)
Group 8	Cyclo (Gly-Pro) (**12**)

Test compounds were prepared as suspension in methylcellulose and Tween 20 mixture in 9:1 ratio. Mice were kept on overnight fasting with free access to water before the administration of cyclic dipeptides. Compounds were administered at 50 mg/kg using oral gavage (dose volume of 10 mL/kg). After one hour of compound administration, 75 mg/kg sodium oxalate solution was injected through intraperitoneal route. Immediately after giving oxalate, mice were fed with normal diet and water was replaced with 3% w/v sodium oxalate water. Mice were sacrificed to harvest the plasma and kidney tissue samples after 24 h of sodium oxalate administration for further evaluation (Mulay *et al.* 2016, Ahil *et al.* 2019).

4.6.1.1 ELISA and BUN estimations

Plasma isolated from the collected blood samples were estimated for IL-1β levels and blood urea nitrogen levels (BUN) using commercially available kits (Tabacco *et al.* 1979, Ragab *et al.* 2014). In BUN estimations, working reagent was prepared by mixing equal amount of reagent 1 (O-phthalaldehyde) and reagent 2 (NED reagent) provided in the kit and from this 100 µL was added to each well containing 10 µL of sample or standard. Absorbance was recorded at 505 nm using multiplate reader (Arkray Healthcare Pvt. Ltd., India).

4.6.1.2 RTPCR study for estimating inflammatory and kidney injury markers

RTPCR studies were carried out in order to study the gene expression of inflammatory markers (TNF-α, IL-6 and IL-1β) and kidney injury marker (KIM-1). Total RNA was isolated from renal tissue using trizol reagent. Quantification and purity analysis were carried out using nano drop spectrophotometer. The absorbance ratio 260/280 and 260/230 were recorded. The 260/280 ratio ~2.0 and 260/230 ratio between 2.0-2.2 were considered as pure (Thermo Scientific 2020). After purity analysis, cDNA synthesis was carried out using commercially available Verso cDNA synthesis kit (Thermo Scientific). Thereafter, RTPCR studies were carried out with synthesized cDNA using suitable primers for the genes as described in Table 4.3. The Cq values obtained from the instrument for target gene and housekeeping gene were used to calculate δCq values and change in expression levels of target genes were calculated using equation (2^- δδCq). All gene expression was normalized using GAPDH housekeeping gene (Ohshima *et al.* 1998, Ahil *et al.* 2019).

Table 4.3: Primer sequence of TNF-α, IL-6, IL-1β and GAPDH

Gene	Primers	Sequence (5'-3')
TNF-α	Forward	CCGCTCGTTGCCAATAGTGATG
	Reverse	CATGCCGTTGGCCAGGAGGG
IL-6	Forward	GCACTACAGGCTCCGAGATGAA
	Reverse	GCCTCCGACTTGTGAAGTGGTA
IL-1β	Forward	GCACTACAGGCTCCGAGATGAA
	Reverse	GTCGTTGCTTGGTTCTCCTTGT
GAPDH	Forward	AGTGGCAAAGTGGAGATT
	Reverse	GTGGAGTCATACTGGAACA
KIM-1	Forward	TCAGCTCGGGAATGCACA
	Reverse	TGGTTGCCTTCCGTGTCT

4.6.1.3 Histopathological evaluations

Histological evaluations were carried out for renal tissue using hematoxylin and eosin staining. Renal tissues were processed in tissue processor unit and 5 µm sections were taken using semiautomatic microtome, followed by staining of tissue sections with hematoxylin and eosin. Histological scoring was done based on semiquantitative scoring method by quantifying

tubular injury parameters (cast, tubular dilation and tubular necrosis). Scoring was given on a scale of 0-5 (0 for nil damage and 5 for severe damage) (Mulay *et al.* 2013, Ahil *et al.* 2019).

4.6.1.4 *In vitro* mechanistic study

4.6.1.4.1 mRNA expression of pro-inflammatory cytokines

RAW 264.7 cells were plated in a 6-well plate and allowed to grow for 24 h in complete DMEM media. Cells were then treated with the pre-determined concentration (100 µM) of cyclo (Val-Pro) (**1**) for 1 h, followed by priming with 1 µg/mL LPS for TNF-α and IL-6 estimations and LPS + 250 µM calcium oxalate crystals for IL-1β gene expression study. After stimulating for 24 h, total RNA was isolated using trizol reagent and purity determination and quantification were done using nano drop spectrophotometer. After purity analysis, cDNA was synthesized and was subjected to RTPCR using suitable primers (Table 4.3). All Cq values were normalised with housekeeping gene GAPDH (Ahil *et al.* 2019, Weirenga *et al.* 2019).

4.6.1.4.2 Western blot

Mouse macrophages were cultivated in T-25 flask containing complete DMEM media. After 24 h of incubation, cells were treated with 100 µM of cyclo (Val-Pro) (**1**) for 1 h, followed by stimulation with LPS and calcium oxalate crystals for 24 h. Protein was then isolated using RIPA buffer and quantified with BCA kit. 30 µg of quantified protein was loaded into each well for separation of proteins, followed by transfer to PVDF membrane. Subsequently membrane was incubated overnight with primary antibodies for β-actin and IL-1β. Following day, the membrane was kept in respective secondary antibodies and detection was done after extensive washing. Blots were quantified using image J software and protein expression was normalised with β-actin (Weirenga *et al.* 2019).

4.6.2 Renal ischemia reperfusion model

C57BL/6 male mice (6-8 weeks) ranging from 20-25 g were used for conducting this study. Experiment was conducted in two different sets for compounds cyclo(Val-Pro) (**1**) and cyclo(Leu-Hydroxy-Pro) (**9**). Animals were categorised as follows with 6 animals in each group as described in Table 4.4.

Table 4.4: Animal grouping in renal ischemic reperfusion model

Groups	Set-1 Treatment	Set-2 Treatment
Group 1	Normal Control	Normal Control
Group 2	Disease Control (Ischemic control)	Disease Control (Ischemic control)
Group 3	Cyclo (Val-Pro) (**1**) -25 mg/kg	Standard-Bay (10 mg/kg)
Group 4	Cyclo (Val-Pro) (**1**) -50 mg/kg	Cyclo (Leu-Hydroxy-Pro) (**9**) -25 mg/kg
Group 5	Cyclo (Val-Pro) (**1**) -75 mg/kg	Cyclo (Leu-Hydroxy-Pro) (**9**) -50 mg/kg
Group 6	-	Cyclo (Leu-Hydroxy-Pro) (**9**) -75 mg/kg

Cyclo(Val-Pro) (**1**), Cyclo (Leu-Hydroxy-Pro) (**9**) and standard Bay were prepared as suspension in 0.5% methylcellulose and 0.025% Tween 20. The suspension was administered *via* oral route at 10 mL/kg dose volume using an oral gavage one hour prior to the induction. Compounds cyclo(Val-Pro) (**1**) and Cyclo (Leu-Hydroxy-Pro) (**9**) were tested at different doses of 25, 50 and 75 mg/kg body weight. Bay was administered at the dose of 10 mg/kg body weight. Mice were anaesthetized using isoflurane. Thereafter, the left renal artery was clamped for 45 minutes with non-traumatic clamp by making abdominal incision. Wound was covered with cotton soaked in PBS after examining the clamped kidney for the sign of ischemia. After 45 minutes of ischemia, clamp was removed for reperfusion and restoration of blood flow was noted before closure of the wound. Animals were sacrificed after 24 h of injury induction to harvest blood samples and renal tissues for carrying out gene expression study for inflammatory and renal injury markers along with the histopathological evaluations (Sun sang *et al.* 2017, Fang *et al.* 2019).

4.6.2.1 Plasma IL-1β estimations using ELISA

Plasma was isolated from collected blood samples to estimate the levels of IL-1β using commercially available IL-1β ELISA kit. ELISA plates were incubated with capture antibody for overnight and then, plates were blocked using 5% BSA. After one hour of incubation, samples and standard were added to the plate. Then, detection antibody was added to the plate for two hours. Thereafter, Streptavidin-HRP was added followed by incubation with TMB substrate. Finally, reaction was stopped after color development by adding 2N H_2SO_4 solution and the absorbance was recorded at 450 nm and 540 nm using spectrophotometer (R & D systems 2020).

4.6.2.2 mRNA expression study for determining inflammatory and renal injury markers

Trizol reagent was used to isolate RNA from the collected renal tissue and cDNA was synthesized using commercially available cDNA synthesis kit after determining the purity of isolated RNA. Renal damage was assessed by evaluating the mRNA expression levels of the pro-inflammatory cytokines (TNF-α, IL-1β and IL-6) and kidney injury markers such as KIM-1, NGAL, α-GST and π-GST using suitable primers for the genes as described in Table 4.5. All expressions were normalised using housekeeping gene GAPDH (Sakai *et al.* 2019).

Table 4.5: Primer sequence of TNF-α, IL-6, IL-1β, GAPDH, KIM-1, NGAL, α-GSH and π-GSH

Gene	Primers	Sequence (5'-3')
TNF-α	Forward	CCGCTCGTTGCCAATAGTGATG
	Reverse	CATGCCGTTGGCCAGGAGGG
IL-6	Forward	GCACTACAGGCTCCGAGATGAA
	Reverse	GCCTCCGACTTGTGAAGTGGTA
IL-1β	Forward	GCACTACAGGCTCCGAGATGAA
	Reverse	GTCGTTGCTTGGTTCTCCTTGT
GAPDH	Forward	AGTGGCAAAGTGGAGATT
	Reverse	GTGGAGTCATACTGGAACA
KIM-1	Forward	TCAGCTCGGGAATGCACA
	Reverse	TGGTTGCCTTCCGTGTCT
NGAL	Forward	CACCACGGACTACAACCAGTTCGC
	Reverse	TCAGTTGTCAATGCATTGGTCGGTG
α-GSH	Forward	GAGACAACAATCCCACAAGAATAAG
	Reverse	CTTCCTCAAACTCCACTCCAG
π-GSH	Forward	TGTCACCCTCATCTACACCAAC
	Reverse	CAGGGTCTCAAAAGGCTTCAG

4.6.2.3 Evaluation of renal injury by histopathological analysis

Renal tissues were paraffinized after processing for histological evaluations. Then, paraffin blocks were sliced to 5 µm thin sections and stained with hematoxylin and eosin staining. Damage to the histological structure of the kidney was scored using semiquantitative methods based on tubular injury, cast formation and tubular dilation (Chang *et al.* 2016, Sakai *et al.* 2019).

4.6.2.4 *In vitro* mechanistic study

Compounds cyclo(Val-Pro) (**1**) and cyclo(Leu-Hydroxy-Pro) (**9**) were tested using antimycin-induced *in vitro* model of ischemia in rat proximal tubular cells NRK 52E.

4.6.2.4.1 Cell viability studies

Briefly, NRK52E cells were incubated in 37°C supplied with 5% CO_2 and 95% environment air. Cells were seeded in 96 well plate (5000 cells /well) using Dulbecco's Modified Eagle's medium supplemented with 10% FBS. NRK52E cells starved for 12 h with 0.5% FBS. Cells were treated with different concentrations of cyclo(Val-Pro) (**1**) and cyclo(Leu-Hydroxy-Pro) (**9**) (300, 100, 30, 10 and 3 µM) one hour prior to the induction of ischemia. Later, ATP depletion was achieved using antimycin A (3 µM) in glucose free medium for 60 min. Recovery phase was achieved after 1 h with complete DMEM medium and cells were analysed after 24 h using MTT reagent. Absorbance was measured spectrophotometrically using multiplate reader at 570 nm.

4.6.2.4.2 Flow cytometric analysis

For the apoptosis analysis, after administration of 100 µM cyclo(Val-Pro) (**1**) and cyclo(Leu-Hydroxy-Pro) (**9**) NRK 52E cells were stimulated with 3 µM antimycin A for 60 min. Then cells were trypsinized with 0.25% trypsin post recovery phase of 24 h. Cells were then resuspended in PBS after centrifugation and stained with Annexin V-FITC and propidium iodide. Finally, the percentage of apoptotic cells was analysed by flow cytometry

4.6.2.4.3 Western blot

NRK 52E were cultivated in T-25 flask containing complete DMEM media. After 24 h of incubation, cells were treated with 100 µM of cyclo(Val-Pro) (**1**) and cyclo(Leu-Hydroxy-Pro) (**9**) for 1 h, followed by stimulation with 3 µM antimycin A for 1 h. After 24 hours of incubation, protein was isolated using RIPA buffer and quantified with BCA kit. 30 µg of quantified protein was loaded into each well for separation of proteins, followed by transfer to PVDF membrane. Subsequently membrane was incubated overnight with primary antibodies for β-actin, Bax and BCL2. Following day, the membrane was kept in respective secondary antibodies and detection was done after extensive washing. Protein expression was normalised with β-actin (Weirenga *et al.* 2019).

4.6.3 Unilateral ureter obstruction model

The whole study was carried out as per the IAEC approved protocol. C57BL/6 male mice (6-8 weeks) weighing around 20-25g were selected for performing Unilateral Ureter Obstruction (UUO). Animals were divided into four different groups namely normal control, disease control, standard (Bay) group and sample group [cyclo (Val-Pro) (**1**)] while the compound, cyclo (Val-Pro) (**1**) was administered at a dose of 50 mg/kg body weight while 'bay' was administered at 5 mg/kg dose *via* oral route one hour prior to the ligation and treatment was continued on alternate days for 10 days. Thereafter, the animals were anaesthetized using isoflurane. Midline abdominal incision was made to ligate left ureter with silk thread (as shown in Figure 4.1), followed by closure of the wound. Animals were kept under keen observation and animals were sacrificed after tenth day of surgery. Kidney tissues were harvested for studying the impact of treatment on chronic renal injury (Xing *et al.* 2019).

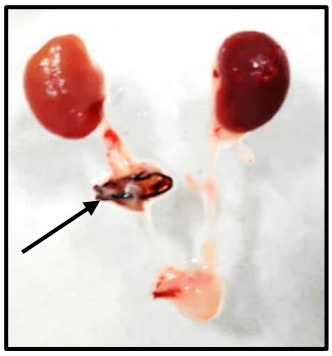

Figure 4.1: Unilateral ligation of left ureter in unilateral ureteral obstruction model. (Arrow indicates the ligated left ureter)

4.6.3.1 Western blot analysis

Tissue was homogenised in RIPA buffer for the isolation of protein from renal tissue. The isolated protein was quantified using BCA kit or bicinchoninic acid kit (Smith *et al.* 1985). Protein concentration was determined from standard curve. Protein was first separated based on their molecular weights by loading 30 µg of quantified protein into each well of SDS page (Composition of stacking gel, resolving gel is given in Table 4.6). Followed by electro transfer of separated proteins to PVDF membrane at 4 °C. Subsequently, membrane was blocked to prevent binding of non-specific proteins using 5% BSA in TBST for one hour and then membrane was incubated with primary antibody for fibrotic markers (α-SMA, TGF-β, collagen-1) and β-actin at 4 °C overnight. The next day, extensive washings were given to the membrane using TBST and then horseradish peroxidase conjugated secondary antibodies was

added. After 1 h of incubation, membrane was washed thoroughly with TBST and then blot was developed using enhanced chemiluminescence detection reagent. The image acquired from system was quantified with Image J software. Normalization of protein expression was done with respect to β-actin expression (Pat *et al.* 2005, Skibba *et al.* 2017).

Table 4.6: Composition of stacking gel and resolving gel for protein separation

12% Resolving gel		**Stacking gel**	
H_2O	3.2 mL	H_2O	2.975 mL
Acrylamide/Bis-acrylamide (30%/0.8% w/v)	4 mL	Acrylamide/Bis-acrylamide (30%/0.8% w/v)	0.67 mL
1.5M Tris(pH=8.8)	2.6 mL	0.5 M Tris-HCl, pH 6.8	1.25 mL
10% (w/v) SDS	100 µL	10% (w/v) SDS	50 µL
10% (w/v) ammonium persulfate	100 µL	10% (w/v) ammonium persulfate	50 µL
TEMED	10 µL	TEMED	5 µL

4.6.3.2 Assessment of renal fibrosis using picro-sirius red staining

Renal tissues were processed to make paraffin blocks. The blocks were sliced to get 5 µm sections using microtome. Sections were dewaxed and rehydrated, followed by staining with hematoxylin and then, counter stained with picro-sirius red for one hour. Again, sections were dehydrated, cleared in xylene and fixed in mountant media. Images were taken using brightfield microscope. Fibrosis was quantified using Image J software (Chevalier *et al.* 2009, Qian *et al.* 2016).

4.6.3.3 *In vitro* mechanistic studies on cyclo (Val-Pro) (**1**)

On perceiving the positive role of cyclo(Val-Pro) (**1**) in fibrotic model, compound was further subjected to TGF-β induced *in vitro* fibrotic model in NRK 49F cell lines at different doses of 300, 100, 30, 10 and 3 µM. Breifly, around 10,000 NRK 49F kidney fibroblasts were seeded in 96 well plate. Cells were pre-treated with different concentrations of the compound, followed by TGF-β (10 ng/mL) stimulation for 48 h. Thereafter, 50 µL of XTT reagent was added into each well for 5 h and absorbance was recorded at 450 nm.

4.7 Statistical Analysis

All values presented in the results were expressed as mean ± SEM. Comparison between the groups was done using one-way ANOVA followed by Dunnett's multiple comparisons with Graph pad prism 8.0 statistical software and $P < 0.05$ was considered as significant.

Chapter 5

Results and Discussions

5.1 *Pseudomonas* strain as potential source of pro-inflammatory cytokines inhibitor

The fluorescing bacterial strain used for the study was earlier identified as *Pseudomonas* species by comparison of 16S rDNA sequence and registered as ABS-36 strain (GenBank Accession No. KT625586) (Khan *et al.* 2015). This bacterium was cultivated in bulk using King's B broth and the culture broth was extracted with EtOAc. The lyophilised culture broth extract (PCBE) was subsequently tested for its pro-inflammatory cytokine inhibitory potential in LPS-induced *in vitro* inflammatory assays.

5.1.1 Cell viability assay of PCBE

MTT assay was carried out in LPS stimulated RAW 264.7 cells at various concentrations (500, 250, 100, 50, 25, 12.5 µg/mL) in order to determine whether the effect of PCBE is due to its cytotoxic nature or anti-inflammatory activity. PCBE at 500 µg/mL showed 62.70 % cell viability with IC_{50} value of 1867.25 µg/mL (Figure 5.1.1) (Table 5.1). Based on the 50% inhibitory concentration found under the cell viability study and pro-inflammatory cytokine inhibitory assay, it can be inferred that the effect of PCBE is due to the anti-inflammatory potential.

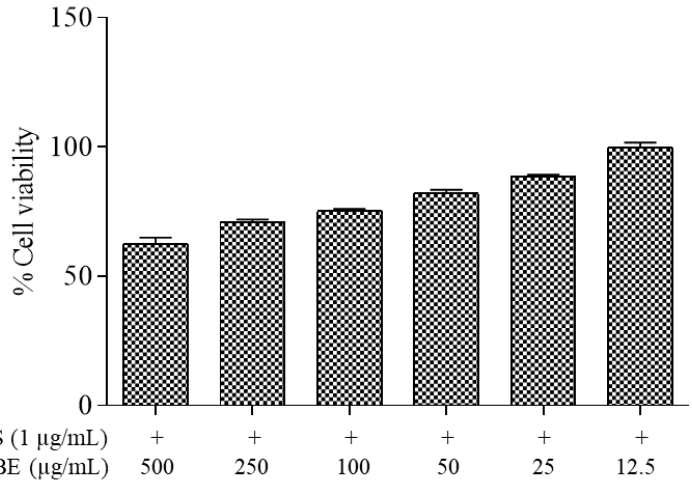

Figure 5.1.1. Cell Viability effect of PCBE on stimulated RAW 264.7 cells. Figure shows the cell viability of RAW 264.7 cells treated with the varied concentration of PCBE, followed by LPS stimulation for 24 h. The values are presented as mean ± SEM from triplicate.

5.1.2 Inhibitory effect of PCBE on LPS and calcium oxalate induced IL-1β release

As per the experimental protocol, RAW 264.7 mouse macrophages were treated with PCBE at predetermined concentrations (based on cytotoxicity study) i.e. 500, 250, 100, 50, 25, 12.5 µg/mL for one hour prior to LPS and calcium oxalate induction. PCBE exhibited IC_{50} value of

95.49 µg/mL and reduced the IL-1β levels by 63.76% at 500 µg/mL concentration. Even at low concentration of 12.5 µg/mL, PCBE reduced the IL-1β levels by 32.81% (Figure 5.1.2).

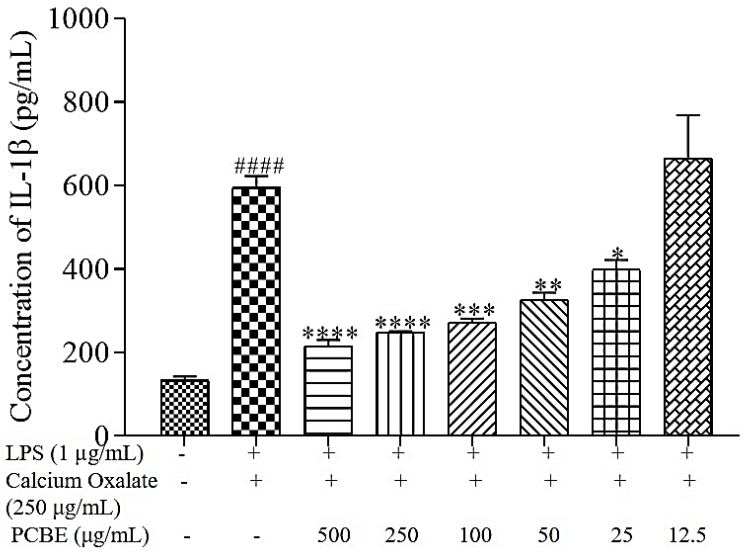

Figure 5.1.2. IL-1β inhibitory effect of PCBE on LPS and calcium oxalate crystal induced RAW 264.7 cells. Cells were treated with the indicated concentrations of PCBE for 1 h and then incubated with LPS (1 µg/mL) and calcium oxalate (250 µg/mL) for 24 h. Supernatant collected after incubation was used for estimating IL-1β levels using ELISA. The values are presented as mean ± SEM from triplicate. $^{####}P < 0.0001$ vs. Normal control, $^{****}P < 0.0001$ vs. LPS and calcium oxalate control, $^{***}P < 0.001$ vs. LPS calcium oxalate control, $^{**}P < 0.01$ vs. LPS calcium oxalate control, $^{*}P < 0.05$ vs. LPS calcium oxalate control.

5.1.3 Effect of PCBE on LPS-stimulated TNF-α and IL-6 levels using ELISA assays

Mouse macrophages were treated with different concentrations of PCBE for one hour prior to LPS induction as per the experimental protocol. PCBE was found to be significantly active against IL-6 and TNF-α demonstrating IC_{50} values of 73.66 µg/mL and 95.49 µg/mL, respectively. PCBE inhibited IL-6 secretion by 94.15% and TNF-α by 88.67% at 500 µg/mL concentration (Figure 5.1.3). Thus, *in vitro* ELISA assays revealed the significant pro-inflammatory cytokine inhibitory potential of PCBE i.e. the culture broth extract of *Pseudomonas sp.* ABS 36 strain.

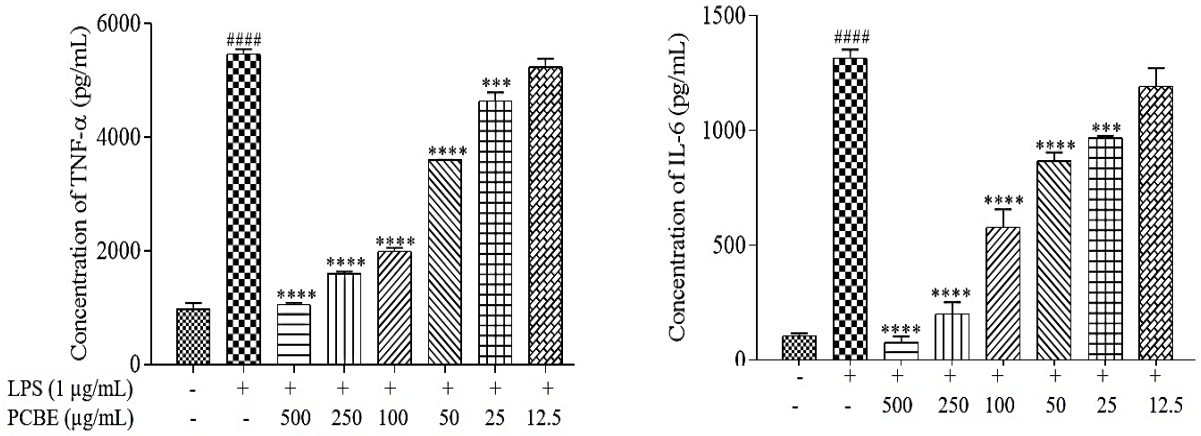

Figure 5.1.3. *In vitro* TNF-α and IL-6 inhibitory effect of different concentrations of PCBE on LPS induced RAW 264.7 cells. Cells were treated with the indicated concentrations of PCBE for 1 h and then incubated with LPS (1 µg/mL) for 24 h. Supernatant collected after incubation was used for estimating TNF-α and IL-6 levels using ELISA. The values are presented as mean ± SEM from triplicate. $^{####}P < 0.0001$ vs. Normal control, $^{****}P < 0.0001$ vs. LPS control, $^{***}P < 0.001$ vs. LPS control.

5.1.4 Inhibition of nitric oxide (NO) production

Upregulated pro-inflammatory cytokines promote the induction of NADPH oxidase, COX-1, COX-2, 2- and 5- lipoxygenase and iNOS, thereby increasing the oxygen consumption and generating reactive oxygen species which subsequently cause various degenerative disorders. Nitric oxide (NO) plays a cardinal role in normal physiological processes like vasodilation and neurotransmission but elevated levels of NO could lead to deleterious effects such as cardiovascular complications, asthma, etc. Therefore, measurement of NO levels was planned in *in vitro* studies using Griess reagent.

PCBE showed 53.47% decline in NO levels at 500 µg/mL concentration with IC_{50} value of 350.05 µg/mL. Even at lowest concentration of 12.5 µg/mL, 30.89% inhibition was observed (Figure 5.1.4). These results supported the pro-inflammatory cytokine inhibitory potential of PCBE.

Table 5.1. presents the comprehensive results of *in vitro* determinations carried out to understand the pro-inflammatory cytokine inhibition effect of PCBE. Ascertaining the significant pro-inflammatory inhibition effect of PCBE, it was realised to be worthy to carry out the chemical investigation to isolate and identify the individual chemical compounds responsible for the activity and thereby develop some anti-inflammatory drug lead molecules.

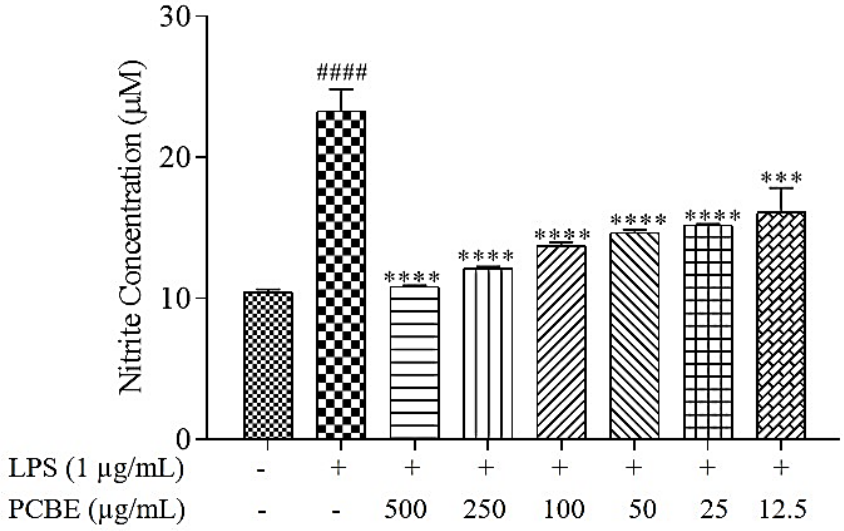

Figure 5.1.4. Inhibition effect of PCBE on LPS induced NO production in RAW 264.7 cells. Cells were treated with the predetermined concentration of PCBE for 1 h and then incubated with LPS (1 µg/mL) for 24 h. Collected supernatant was assessed for NO levels using Griess method. The values are presented as mean ± SEM from triplicate. ####$P < 0.0001$ vs. Normal control, ****$P < 0.0001$ vs. LPS control, *** $P < 0.001$ vs. LPS control.

Table 5.1: Percentage inhibition of pro-inflammatory cytokines (IL-1β, TNF-α and IL-6), NO and cell viability exhibited by PCBE

Concentration of PCBE (µg/mL)	Percentage Inhibition				% Cell viability
	TNF-α	IL-6	IL-1β	NO	
500	88.67±5.32	94.15±4.09	63.76±4.63	53.47±5.02	62.70±6.33
250	70.79±5.38	84.67±1.39	58.26±5.02	47.81±3.27	70.92±6.09
100	63.47±3.02	56.02±5.63	54.17±4.99	41.17±3.92	75.27±5.38
50	34.11±3.21	34.17±2.35	45.11±5.53	37.02±4.82	82.11±3.72
25	15.23±0.27	26.40±1.64	32.81±5.97	34.69±4.97	88.52±1.04
12.5	4.13±2.19	9.34±2.95	ND	30.89±6.77	99.8±3.04
IC_{50} (µg/mL)	95.49	73.66	132.09	350.05	1867.25

ND: Not Detectable

5.2 Isolation and characterisation of secondary metabolites of *Pseudomonas* strain

The bioactive PCBE on repeated chromatographic purification using solvents of increasing polarity yielded twenty compounds (**1** – **20**). The isolation procedure of these compounds is outlined in scheme 1.

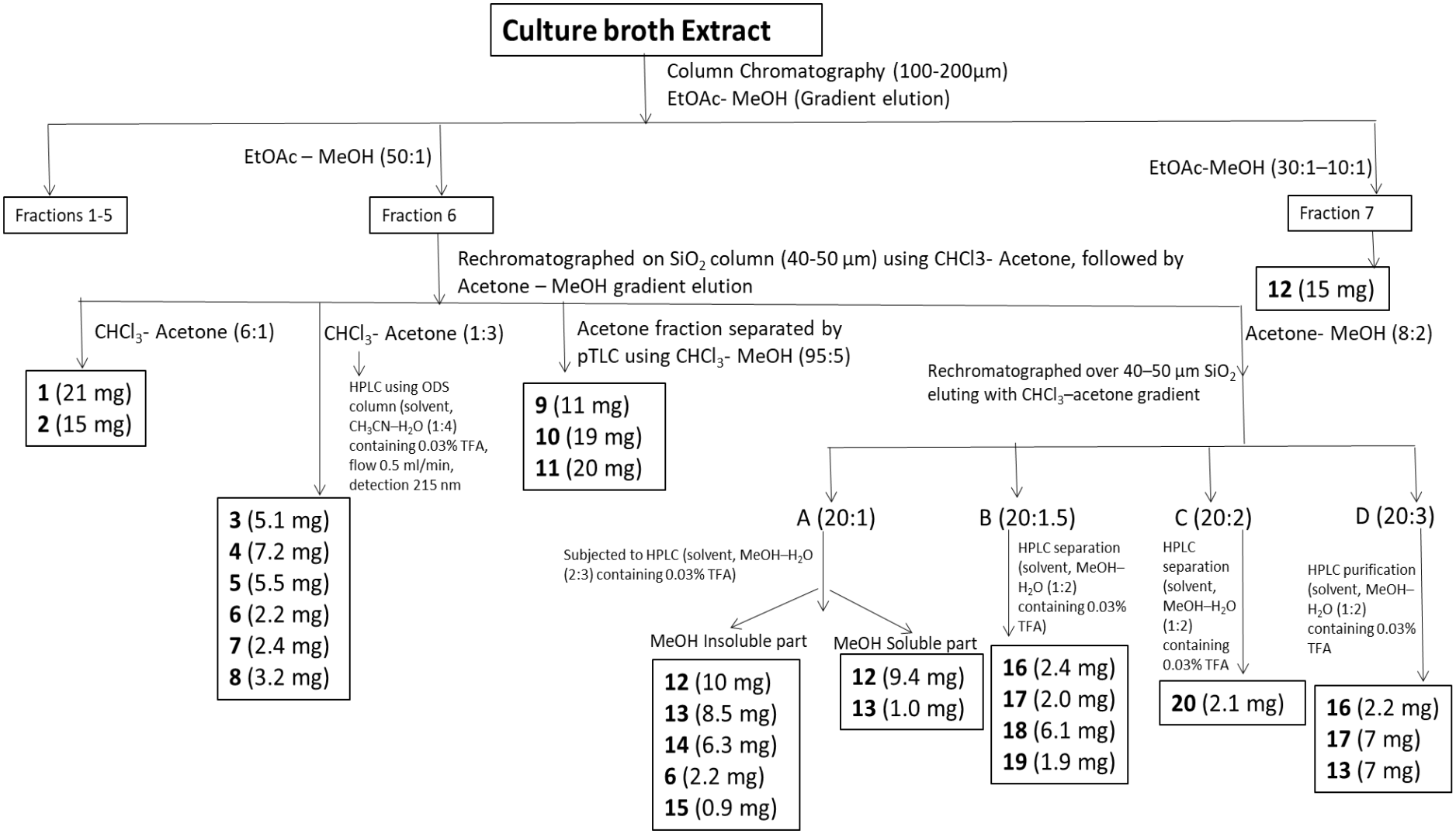

Scheme 1: Isolation of secondary metabolites of *Pseudomonas* strain

5.3 Characterisation of isolated compounds

The structure characterisation of all the isolated compounds were carried out mainly based on proton and carbon NMR analysis. The spectral data of the major compounds i.e. obtained in more than 10 mg (compounds **1**, **2** and **9**-**12**) were selected first for the structure elucidation and the same is discussed in sequel.

5.3.1. Characterisation of compound 12

Compound **12** was obtained as white amorphous powder showing melting point of 178-180 ˚C. The purity of the isolated product was assessed through TLC study using different mobile phase systems ($CHCl_3$: MeOH 8:2, R_f 0.55 and Hexane:EtOAc 9:1, R_f 0.45). Single spot was observed when the plates were sprayed with 10% methanolic sulphuric acid and heated at 110 °C for 10 min. The compound was found to be soluble in MeOH, $CHCl_3$ and EtOAc. It was found to be insoluble in hexane and sparingly soluble in water.

The IR spectrum of compound **12** showed absorption bands at 1678, 1648 (CO str), 1458 (NH-in plane vibration), 1296 (*cis*-CONH) cm^{-1} due to *cis*-amide I band, amide II band and amide III band, respectively (Figure 5.3.1.1). Also absorption bands at 1414 (NH-bending), 1340 (C-N str) and broad band around 3568 - 3114 (N-H str) cm^{-1} confirmed the presence of *cis*-amide groups. All these functionalities were found to be characteristic of diketopiperazines or cyclic peptides.

Compound **12** showed $[M+H]^+$ peak at m/z 155 under ESI-MS analysis (Figure 5.3.1.2). The ^{13}C NMR (75 MHz; CD_3OD) spectrum of compound **12** showed seven distinct carbon signals due to two amide carbonyl groups (CONH, δ_C 166.5 and 172.0 ppm), four methylene groups (δ_C 47.0, 46.3, 29.4 and 23.3 ppm) and one deshielded methine group (δ_C 59.9 ppm) confirming the presence of diketopiperazine with three extended carbon chain in cyclic form (Figure 5.3.1.3). In the 300 MHz ^1H NMR spectrum broad methylene multiplets between δ_H 1.85 – 4.10 ppm integrating for eight protons were observed along with a broad triplet at 4.23 ppm integrating for one proton, which strongly confirmed the diketopiperazine derivative as a proline and glycine based cyclic dipeptide (Figure 5.3.1.4). Further, by correlating the data congregated from MS, ^{13}C NMR and ^1H NMR analysis, compound **12** was identified as cyclo (Gly-Pro) having MF $C_7H_{10}N_2O_2$. The recorded carbon and proton NMR data were found to be in good agreement with that of the reported NMR data of cyclo(Gly-L-Pro) (Campbell *et al.* 2009, Selvakumar *et al.* 2009), through which the stereochemistry of chiral centre at C-6 was also identified as *S*. Further the compound showed $[\alpha]_D$ of -117.7 (c 1.55, MeOH) [reported -

179.58 (c = 8.31mg/mL; EtOH)] and hence was confirmed as cyclo(Gly-L-Pro). The chemical structure of compound **12** was unambiguously identified as **12** as shown below.

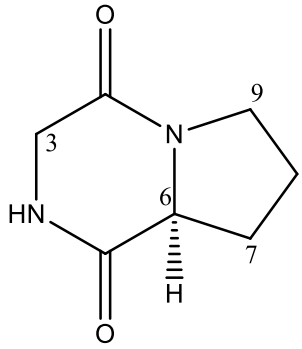

12

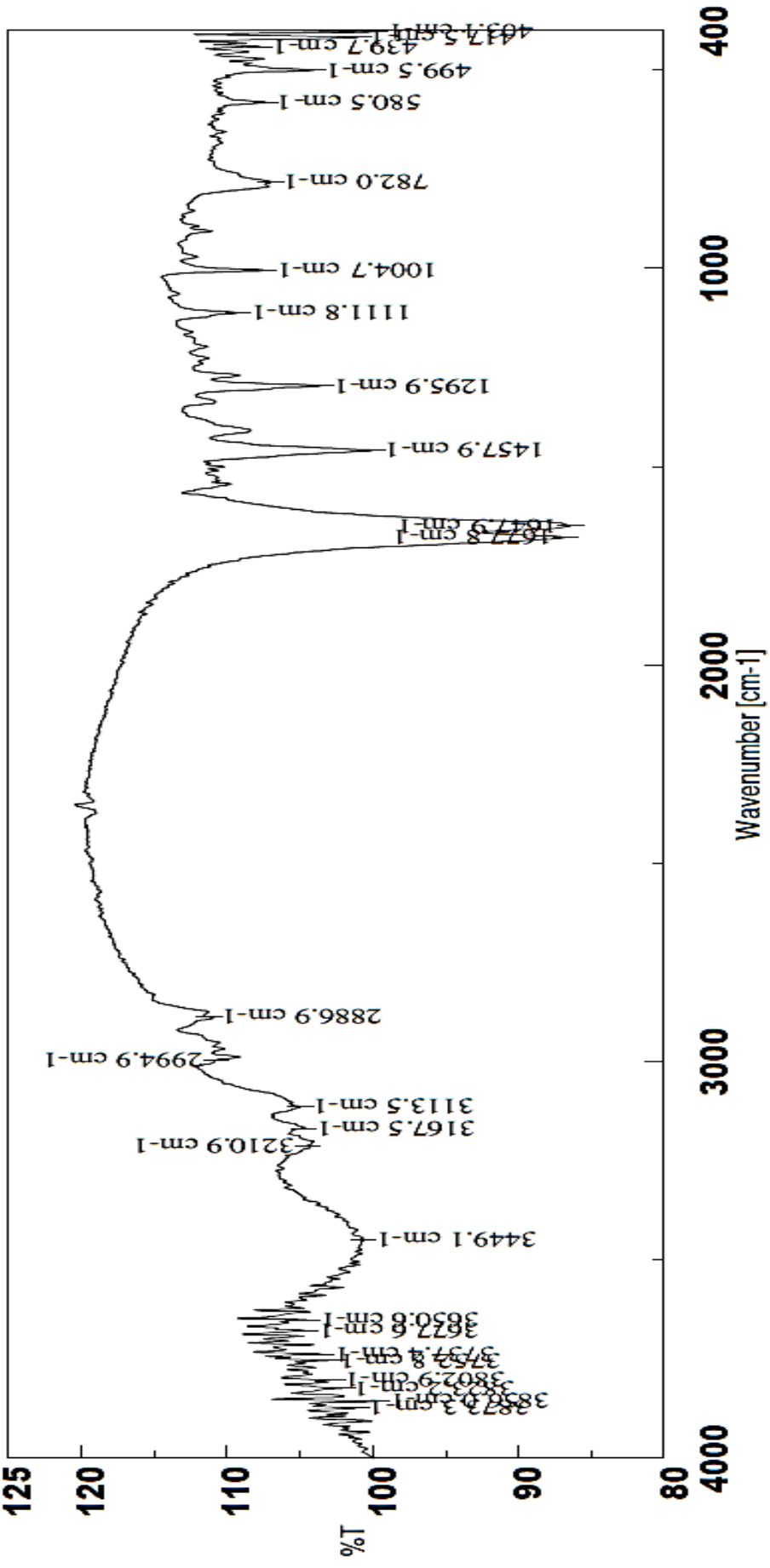

Figure 5.3.1.1 IR spectrum of cyclo(Gly-Pro) (12)

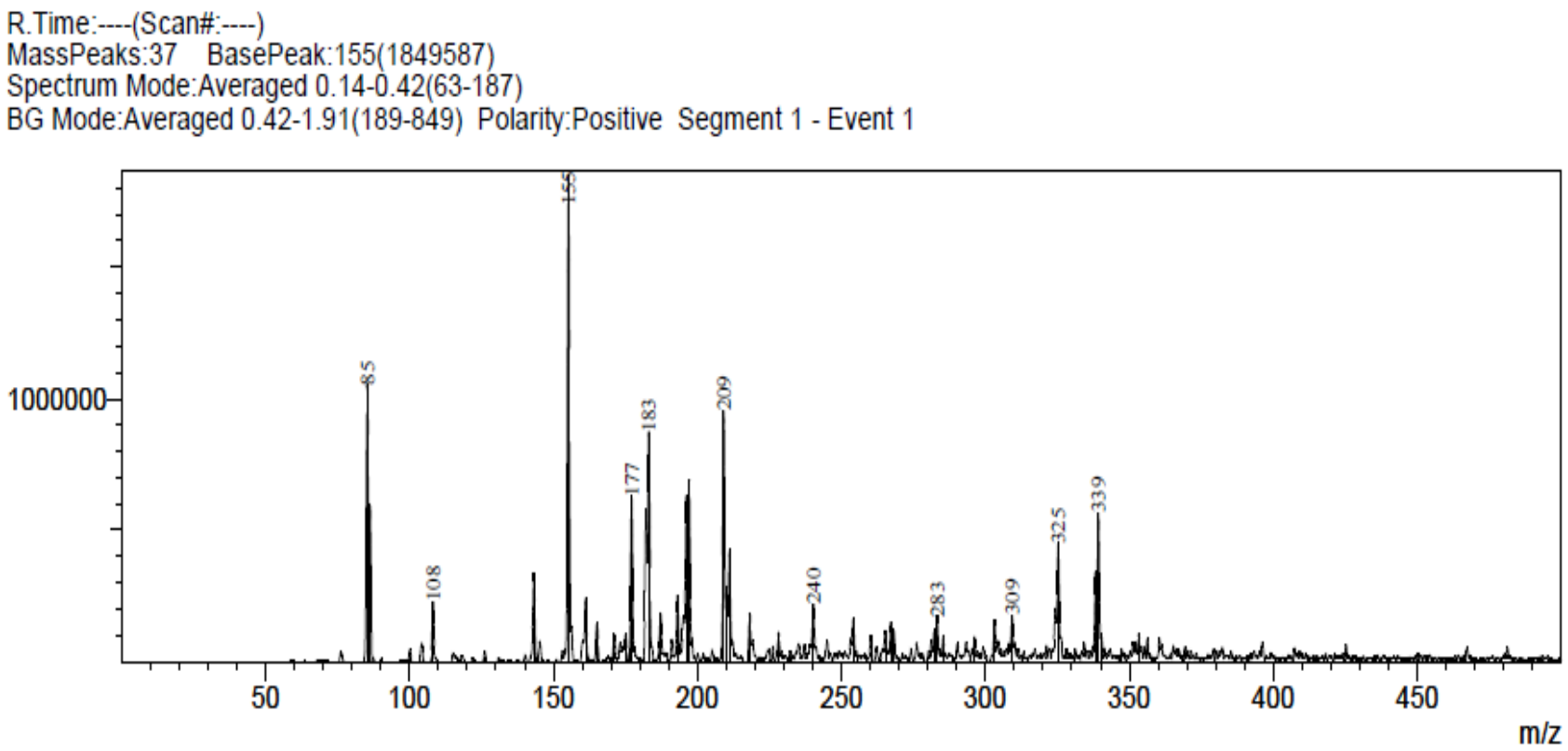

Figure 5.3.1.2 ESI mass spectrum of cyclo(Gly-Pro) (12)

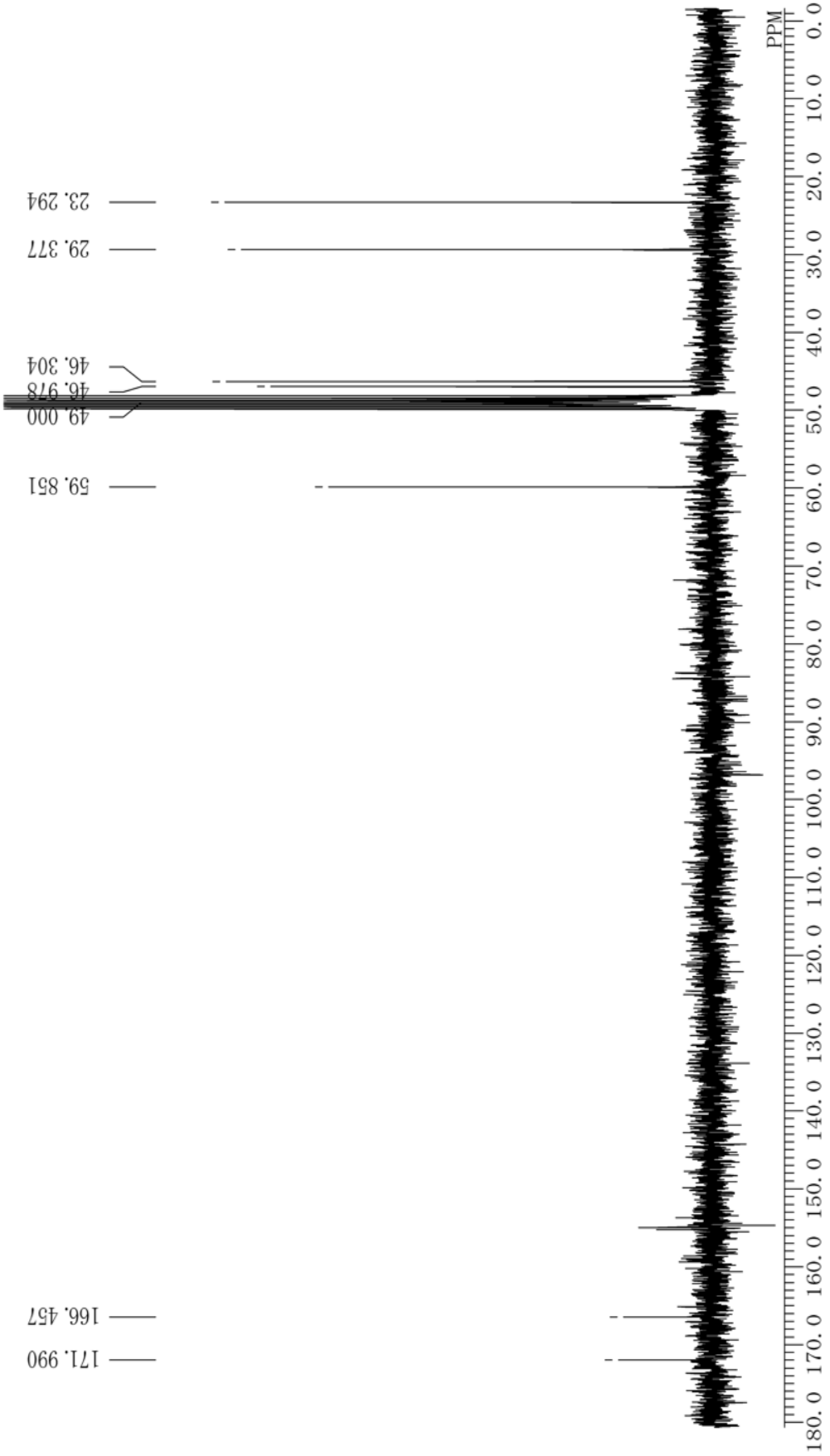

Figure 5.3.1.3 ^{13}C NMR (75 MHz; CD_3OD) spectrum of cyclo(Gly-Pro) (12)

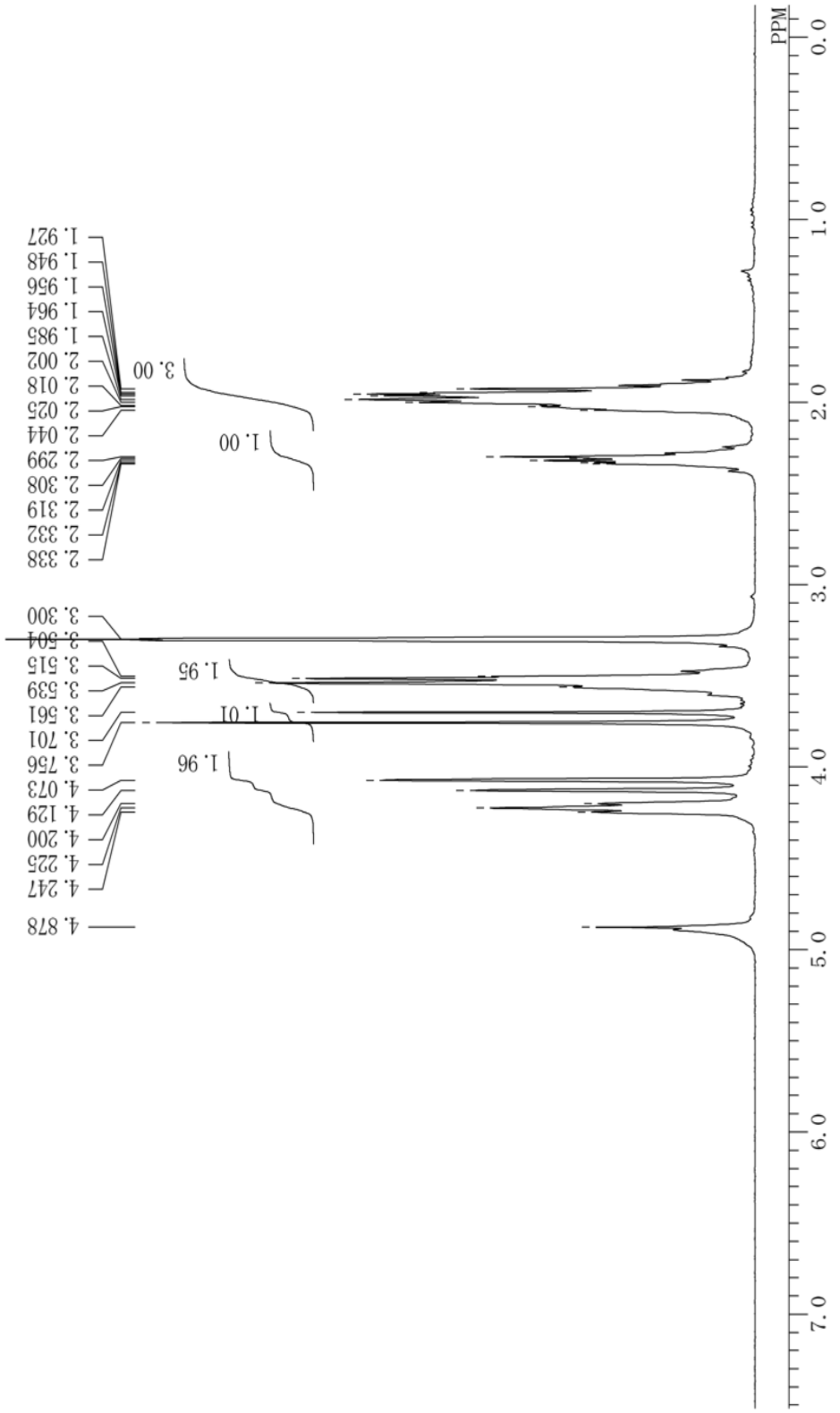

Figure 5.3.1.4 ^{1}H NMR (300 MHz; CD_3OD) spectrum of cyclo(Gly-Pro) (12)

5.3.2. Characterisation of compound 11

Compound 11 was obtained as white amorphous powder showing single spot under TLC study when the plates were developed under different solvent systems followed by spraying the plates with 10% methanolic sulphuric acid. This compound was found to be insoluble in hexane, sparingly soluble in water and freely soluble in MeOH, EtOAc and $CHCl_3$. Interpretation of the carbon NMR spectrum (75 MHz; $CDCl_3$) revealed the presence of eight carbon signals constituting two amide carbonyl groups (CONH, δ_C 166.4 and 170.5 ppm), three methylene groups (δ_C 45.4, 28.1 and 22.7 ppm), two methine groups (δ_C 51.1 and 59.2 ppm) and one methyl group (δ_C 15.9 ppm). On comparing the carbon NMR spectrum of compound **11** (Figure 5.3.2.1) with that of compound **12** (Figure 5.3.1.3), it was identified as a proline based cyclic dipeptide. However, the presence of an additional methyl carbon signal at 15.9 ppm and variation in the chemical shift value of C-3 signal (51.1 ppm) suggested the cyclic dipeptide as cyclo(Ala-Pro). This determination gained further evidence from the ^1H NMR spectrum (Figure 5.3.2.2) measured using $CDCl_3$, which showed a clear three proton doublet at 1.48 ppm due to methyl substituent, six methylene proton multiplets ranging between 4.18 – 1.73 ppm overlapping the methine proton signal and a broad singlet for N-H proton at 6.94 ppm. Finally, compound **11** was identified as *cis*-cyclo(Ala-Pro) by comparing the measured NMR data with the reported values (Stark *et al.* 2005, Campbell *et al.* 2009). The chemical structure of compound **11** was unequivocally assigned as **11** as shown below.

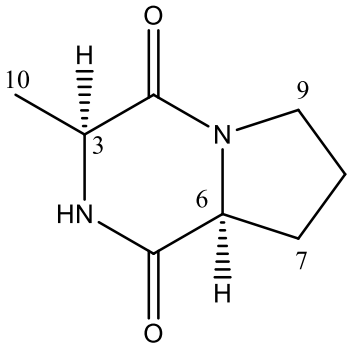

11

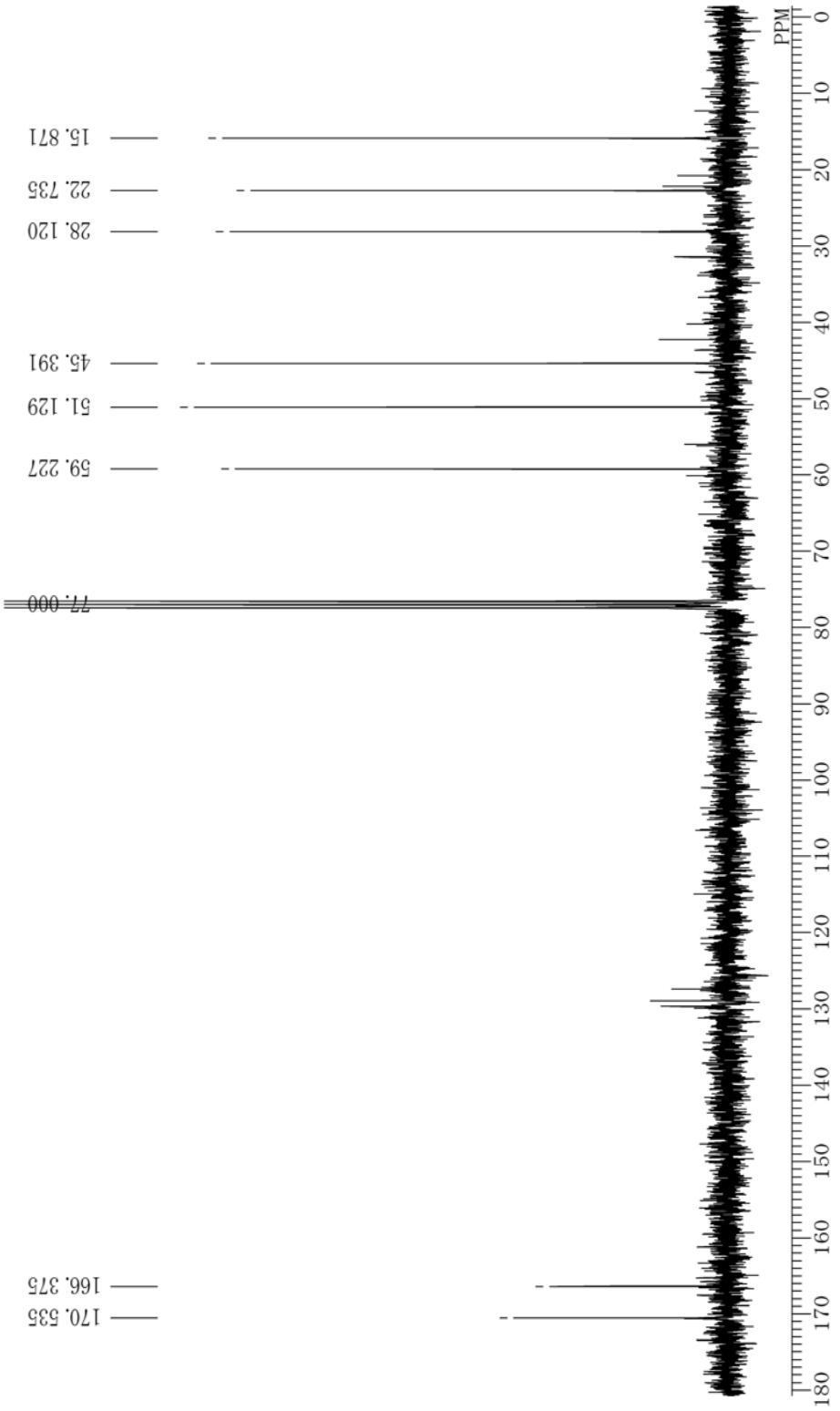

Figure 5.3.2.1 ^{13}C NMR (75 MHz; CD_3OD) spectrum of cyclo(Ala-Pro) (11)

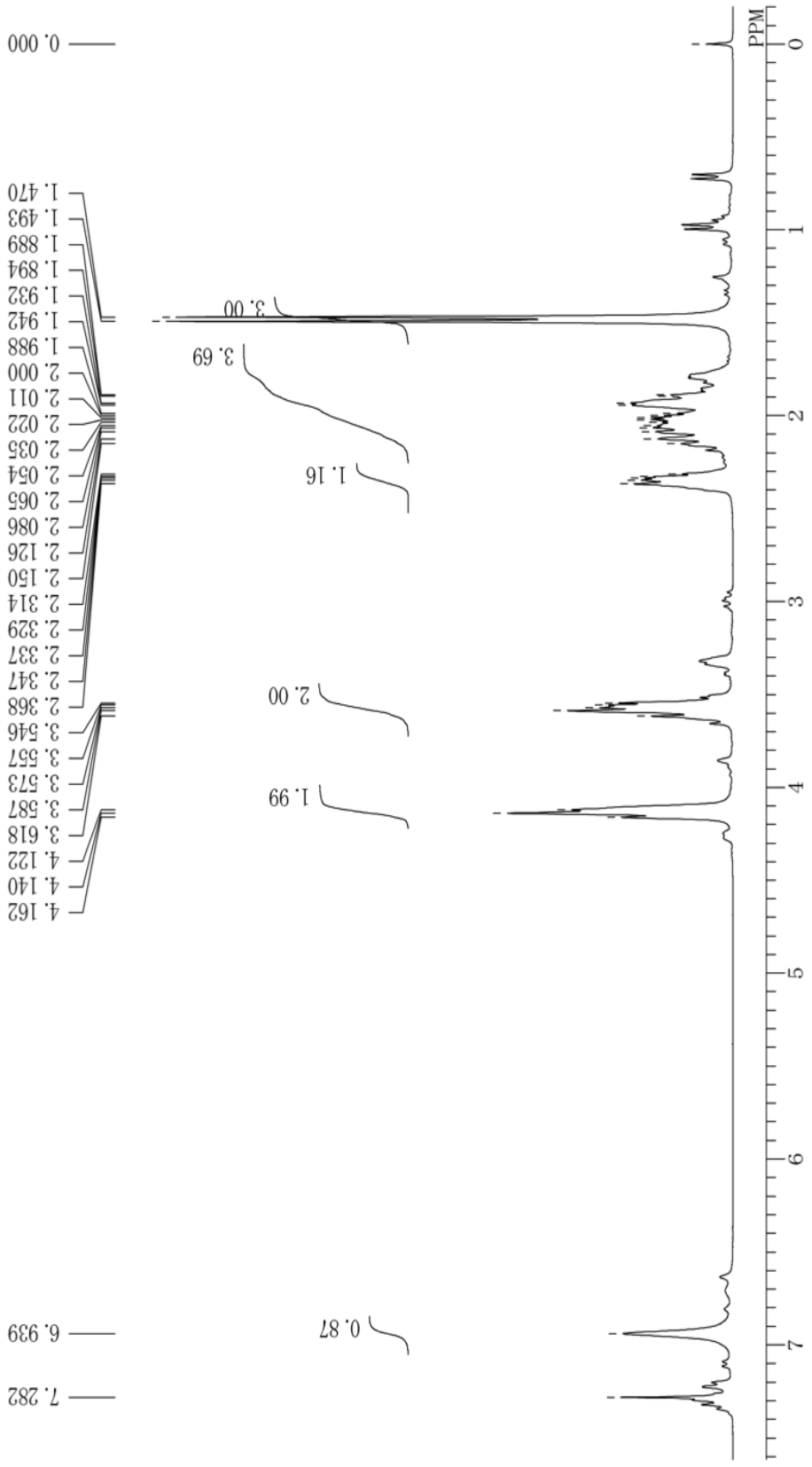

Figure 5.3.2.2 ^{1}H NMR (300 MHz; CD_3OD) spectrum of cyclo(Ala-Pro) (11)

5.3.3. Characterisation of compound 1

Compound **1** was obtained as colourless amorphous solid showing melting point of 170-172 ˚C. The singularity of the compound was assessed through TLC studies using different mobile phase systems ($CHCl_3$:acetone; 2:1; R_f 0.45 and $CHCl_3$:MeOH; 20:1; R_f 0.3) and spraying the plate with 10% methanolic sulphuric acid followed by heating the plate at 110 ˚C for 10 min. While the compound was found to be freely soluble in $CHCl_3$ and MeOH, it was insoluble in hexane and sparingly soluble in water.

Compound **1** exhibited $[M+H]^+$ ion peak at *m/z* 197 under ESI-MS (Figure 5.3.3.1) analysis which indicated the mass as 196 daltons with the molecular $C_{10}H_{16}N_2O_2$ identified from the congregated spectral data. The IR spectrum (Figure 5.3.3.2) showed the functionalities characteristic of cyclic peptides [3215, 2963, 1673, 1450, 1428, 1299, 1180 cm^{-1}). The 100 MHz ^{13}C NMR (Figure 5.3.3.3) and DEPT (Figure 5.3.3.4) spectra of compound **1** measured by dissolving in $CDCl_3$ revealed ten distinct carbon signals, which constituted two amide carbonyl carbons (CONH, δ_C 165.0 and 170.0 ppm), three methylene carbons (δ_C 45.2, 28.4 and 22.4 ppm), two deshielded methine carbons (δ_C 60.4 and 58.8 ppm) and three carbons of isopropyl group (28.5, 19.3 and 16.1 ppm). Comparison of the carbon NMR spectra of compounds **12**, **11** and **1** helped us in deducing compound **1** as a proline based cyclic dipeptide having isopropyl substitution at C-3. The presence of N-H proton as broad singlet at 6.03 ppm in the 400 MHz ^1H NMR spectrum (Figure 5.3.3.5) was further confirmed through D_2O shift (Figure 5.3.3.6). The broad methylene multiplets (3.70-3.53, 2.41-2.36 and 2.10-1.89 ppm), one proton integrated broad triplet at 4.10 ppm alongwith two methyl doublets integrating for three protons each (1.09 and 0.93 ppm) and a methine multiplet (2.67-2.63, 1H) signal found in the NMR spectrum of compound **1** confirmed it as cyclo(Val-Pro). The relative and absolute stereochemistry of the compound was established as cyclo(L-Val-L-Pro) by comparing the NMR data with those of the *cis*- and *trans*-isomers and based on the specific rotation, $[\alpha]_D^{25}$ -133 (*c*, 0.11, ethanol) (lit. -149 (c, 1.09, ethanol) (Campbell *et al.* 2009). Further, compound **1** was assigned as *cis*-cyclo(L-Val-L-Pro) by comparing the measured NMR data with the reported values (Furtado *et al.* 2005). Finally, the chemical structure of compound **1** was explicitly identified as **1** as shown below.

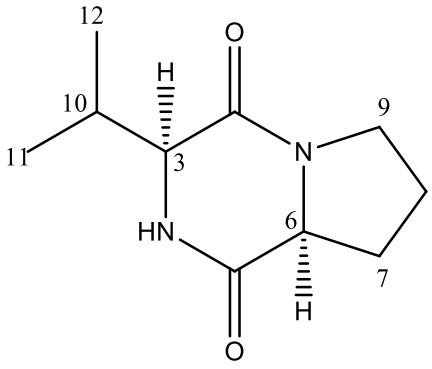

1

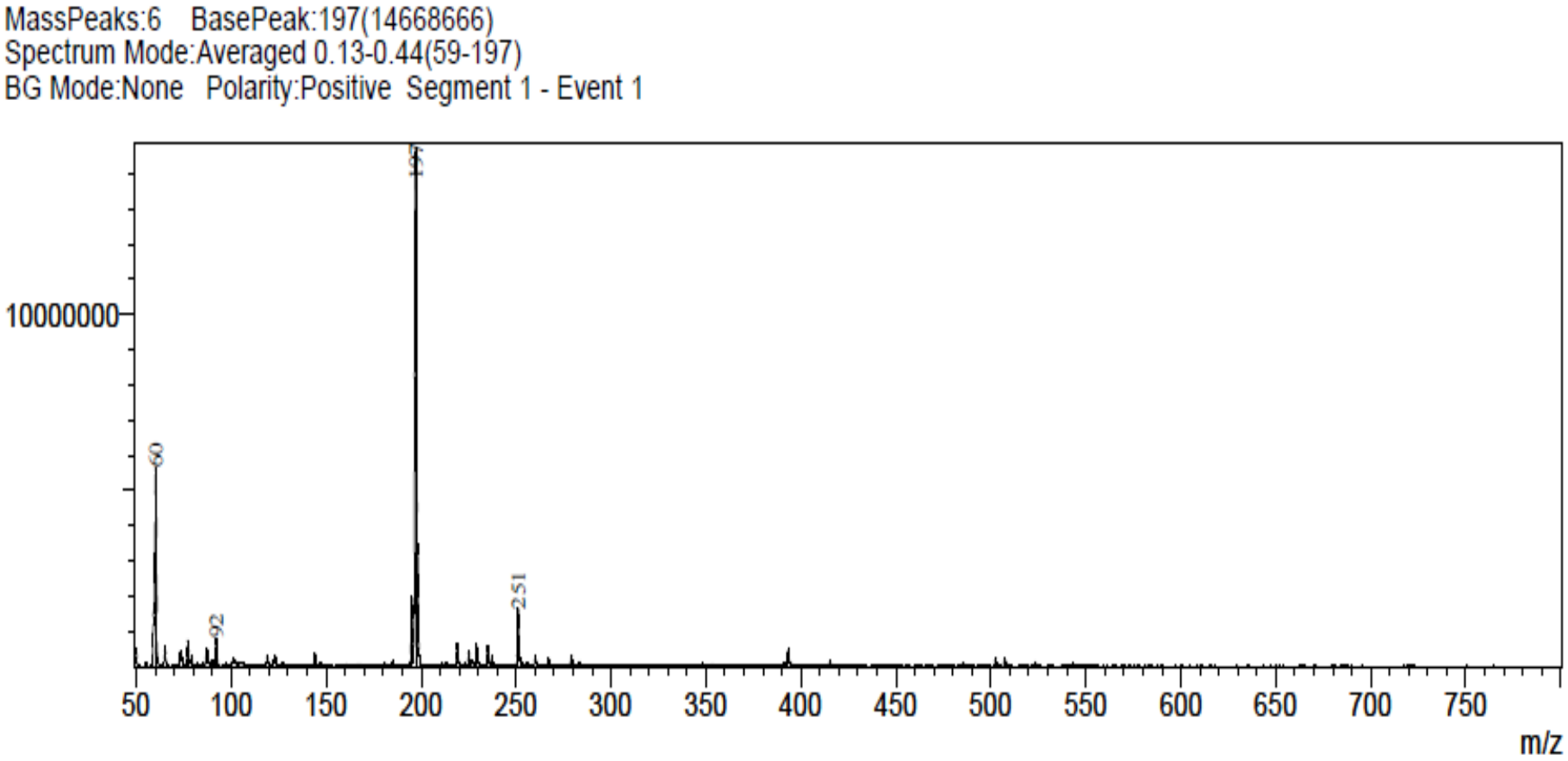

Figure 5.3.3.1 ESI mass spectrum of cyclo(Val-Pro) (1)

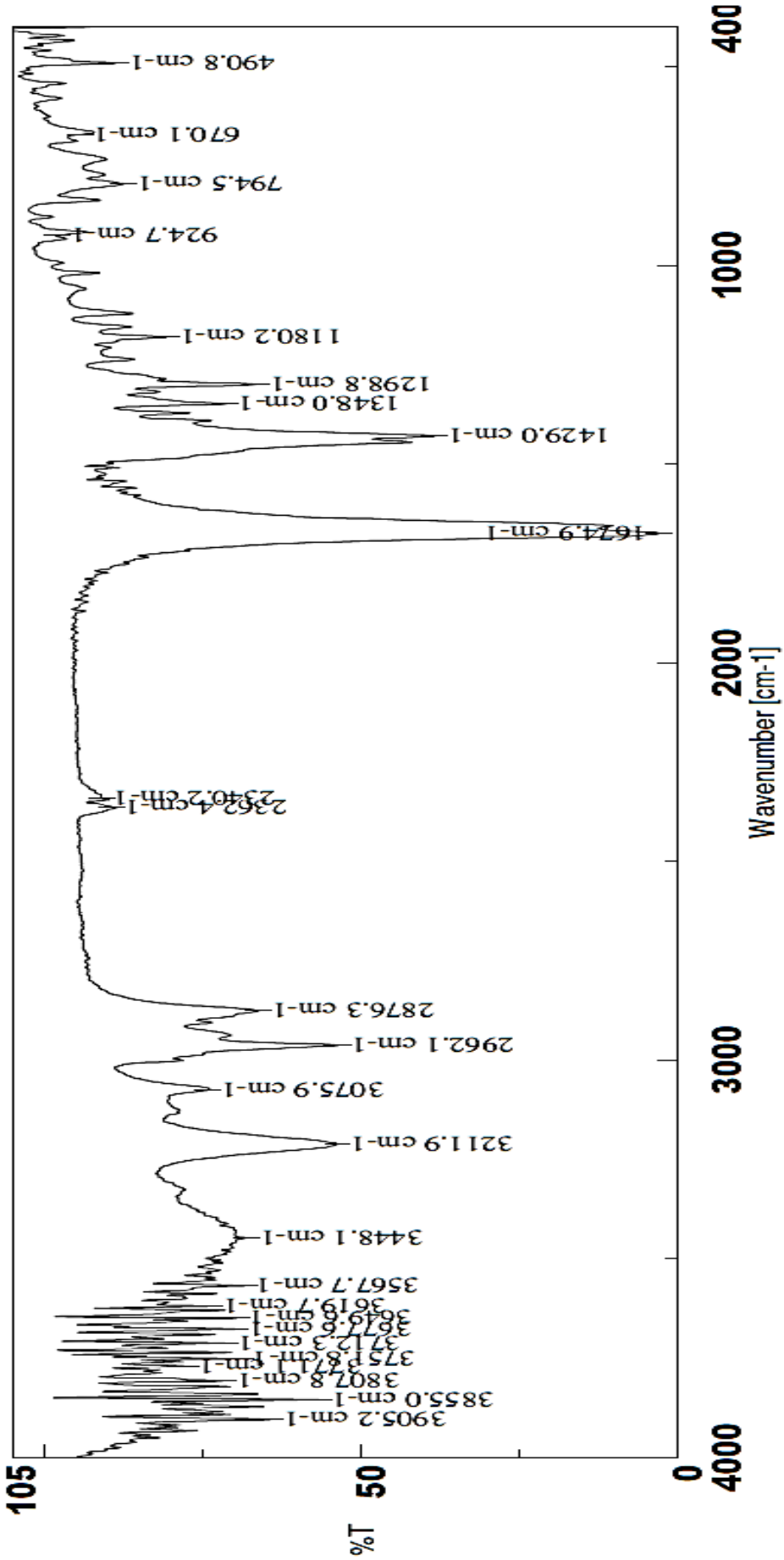

Figure 5.3.3.2 IR spectrum of cyclo(Val-Pro) (1)

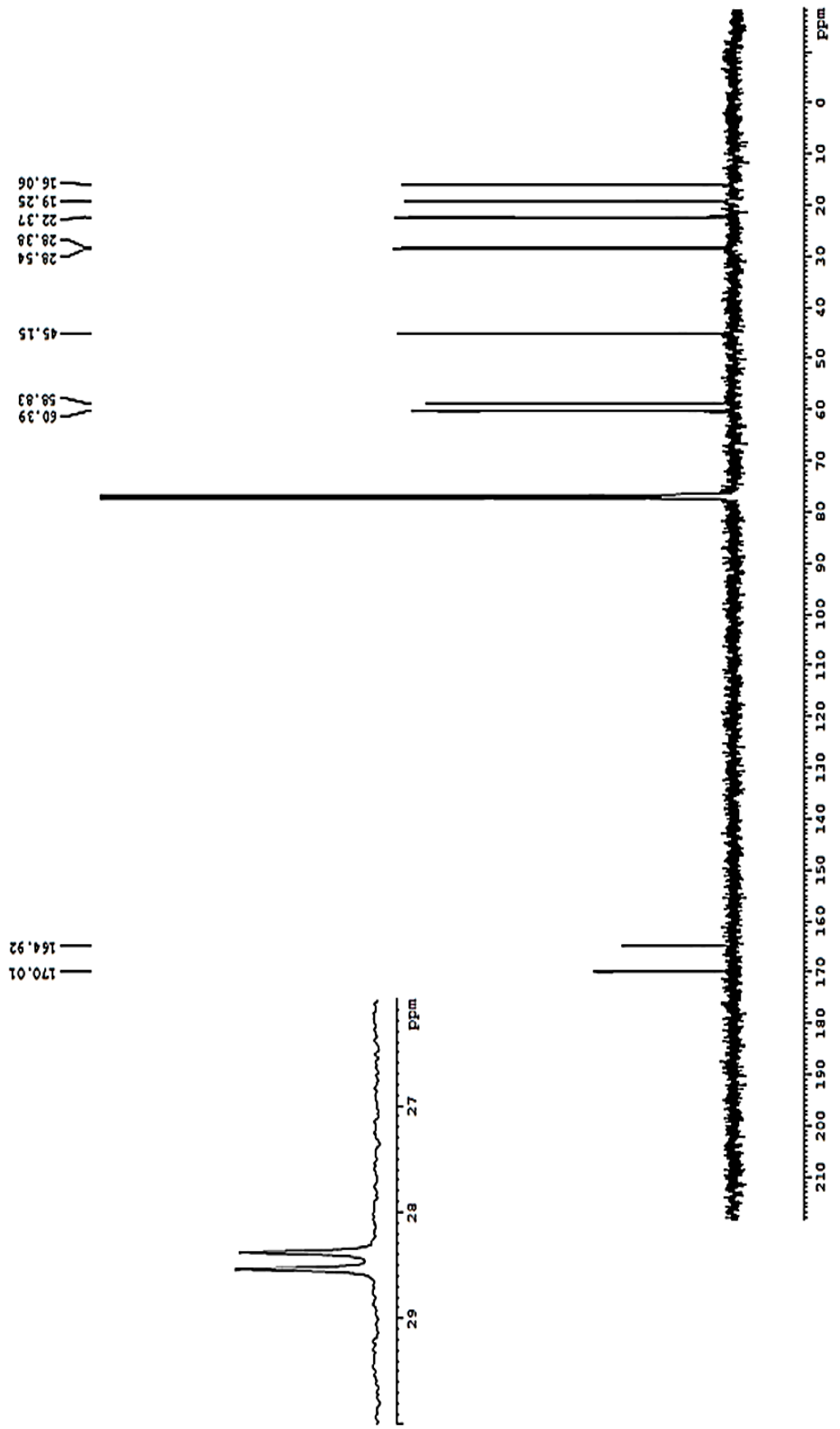

Figure 5.3.3.3 ^{13}C NMR (100 MHz; CD_3OD) spectrum of cyclo(Val-Pro) (1)

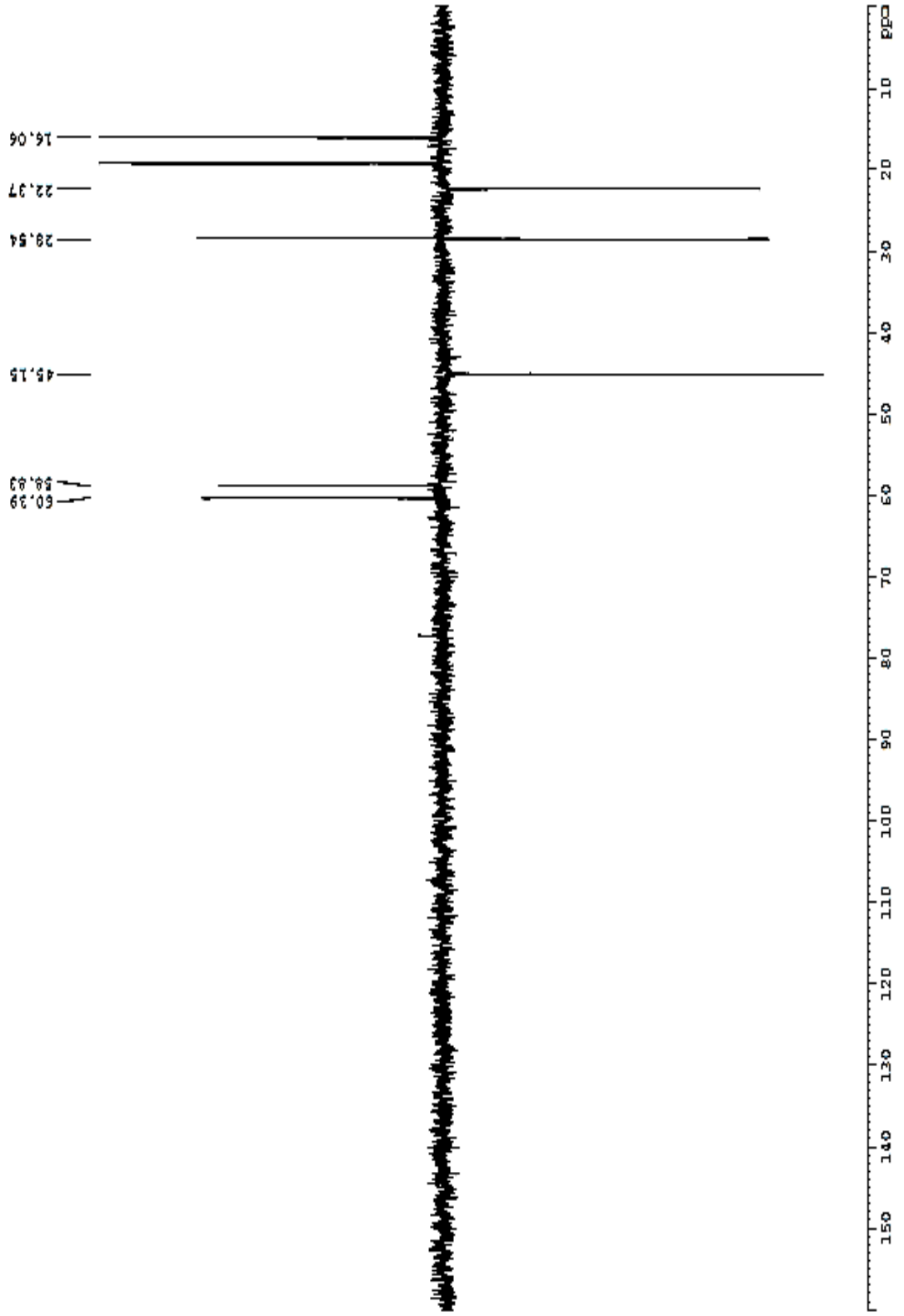

Figure 5.3.3.4 DEPT NMR spectrum of cyclo(Val-Pro) (1)

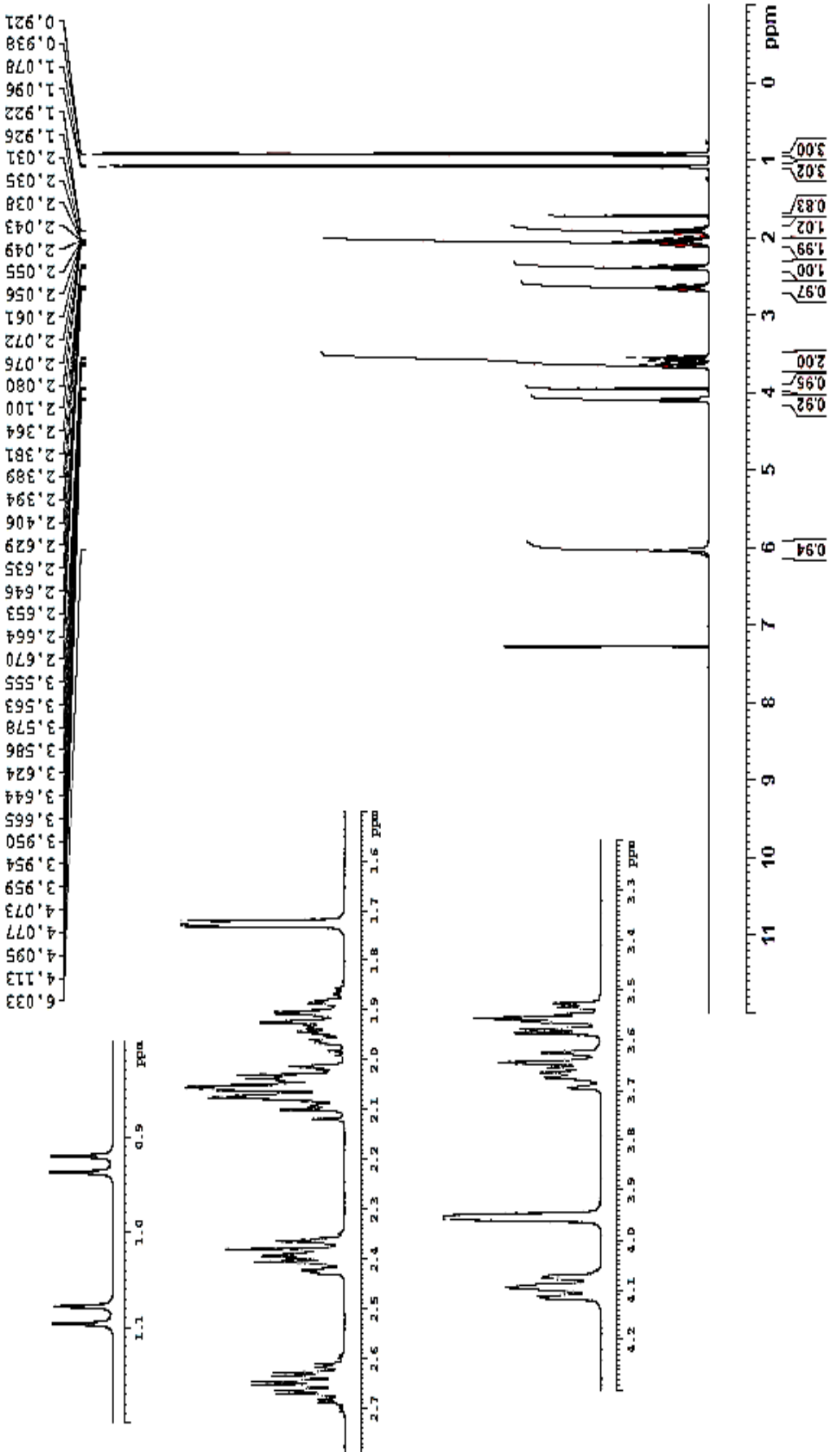

Figure 5.3.3.5 ^{1}H NMR (400 MHz, CD_3OD) spectrum of cyclo(Val-Pro) (1)

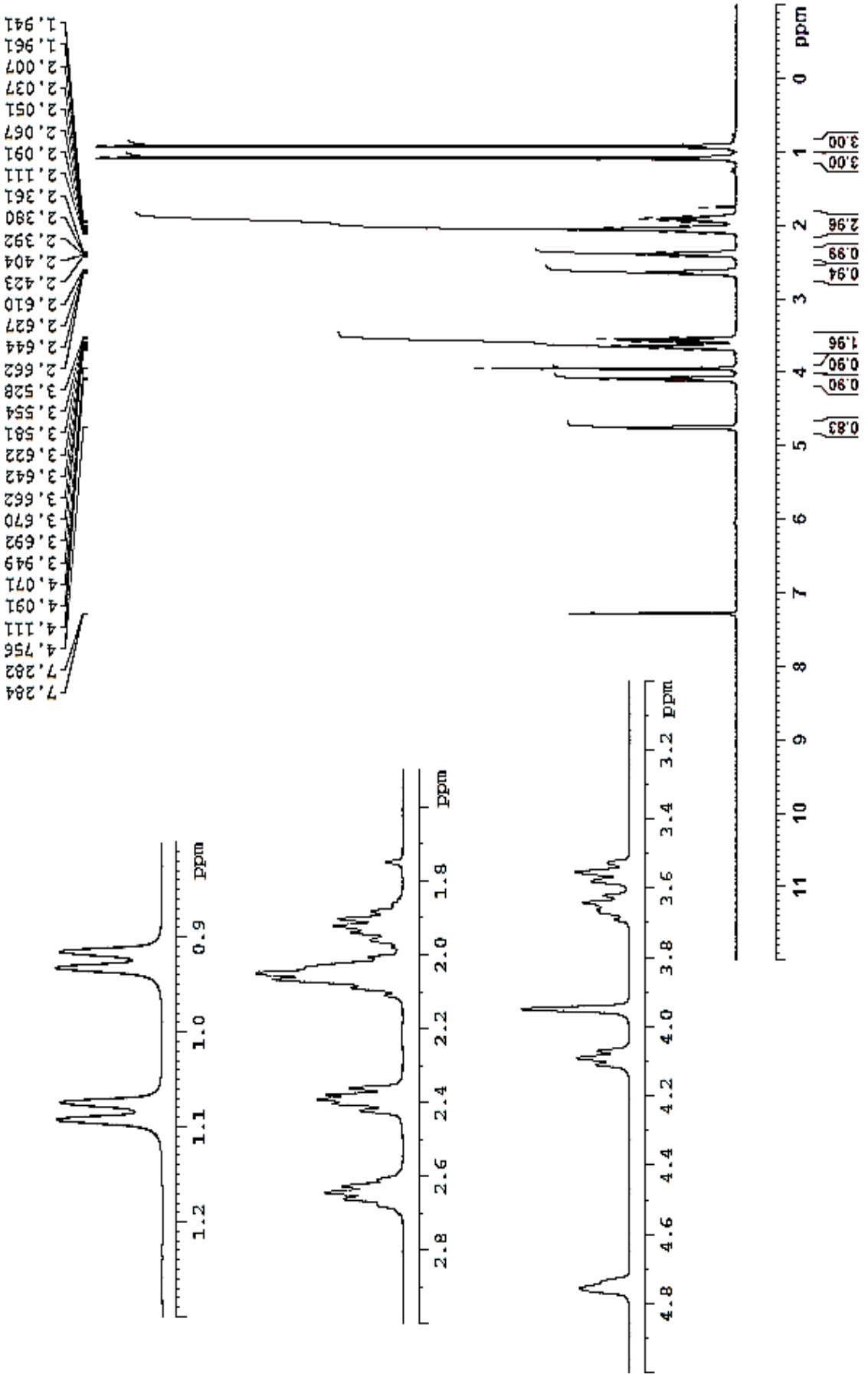

Figure 5.3.3.6 ^{1}H NMR (D_2O shift) spectrum of cyclo(Val-Pro) (1)

5.3.4. Characterisation of compound 2

Compound **2** was obtained as white amorphous powder, showing melting point of 163-165°C. After verifying the purity by TLC, the compound was subjected for ^{1}H and ^{13}C NMR analysis by dissolving in $CDCl_3$. Comparison of the measured carbon (Figure 5.3.4.1) and proton (Figure 5.3.4.2) NMR spectra with that of compound **1** (Figure 5.3.3.5 and Figure 5.3.3.3) revealed the similarity and lead to the identification of this compound too as a proline based cyclic dipeptide. However, some dissimilarity was observed in the carbon NMR spectrum of compound **2** (11 signals) due to the existence of peaks (δ_C 38.4, 24.5, 23.2 and 21.2 ppm) of isobutyl group [$(CH_3)_2$-CH-CH_2-] instead of isopropyl group [$(CH_3)_2$-CH-; δ_C 28.4, 19.1 and 16.0 ppm) as seen in compound **1**. This observation further gained support from the proton NMR spectrum (Figure 5.3.4.2) which confirmed the substituent as isobutyl group [(2.19-1.75 (5H, m, H-7b, H-8, H-10a, H-11), 1.54 (1H, ddd, *J*=14.3, 9.0, 5.1 Hz, H-10b), 1.00 (3H, d, *J*=6.6 Hz, H-12), 0.95 (d, *J*=6.3 Hz, H-13) ppm] in compound **2**. Thus compound **2** was identified as *cis*-cyclo(Leu-Pro) (**2**) by comparison of the measured proton and carbon NMR data with that of the reported data (Campbell *et al.* 2009).

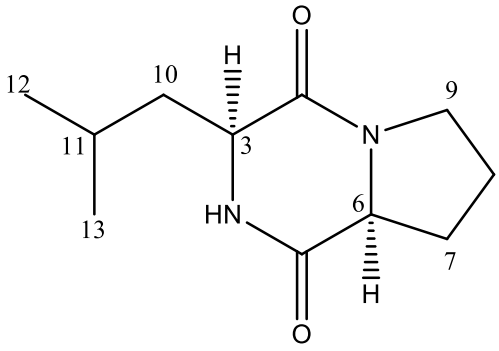

2

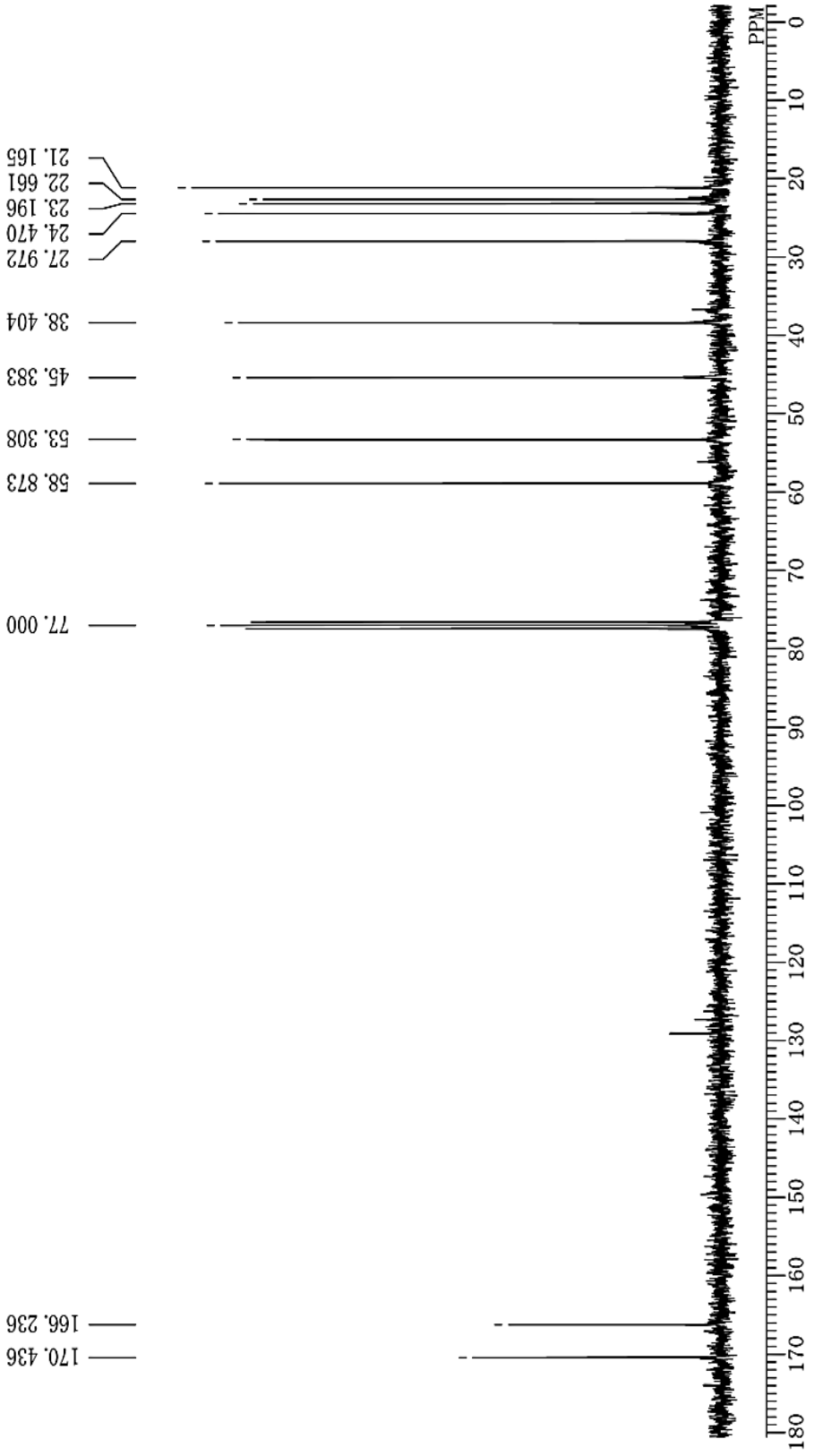

Figure 5.3.4.1 ^{13}C NMR (75 MHz; CD_3OD) spectrum of cyclo(Leu-Pro) (2)

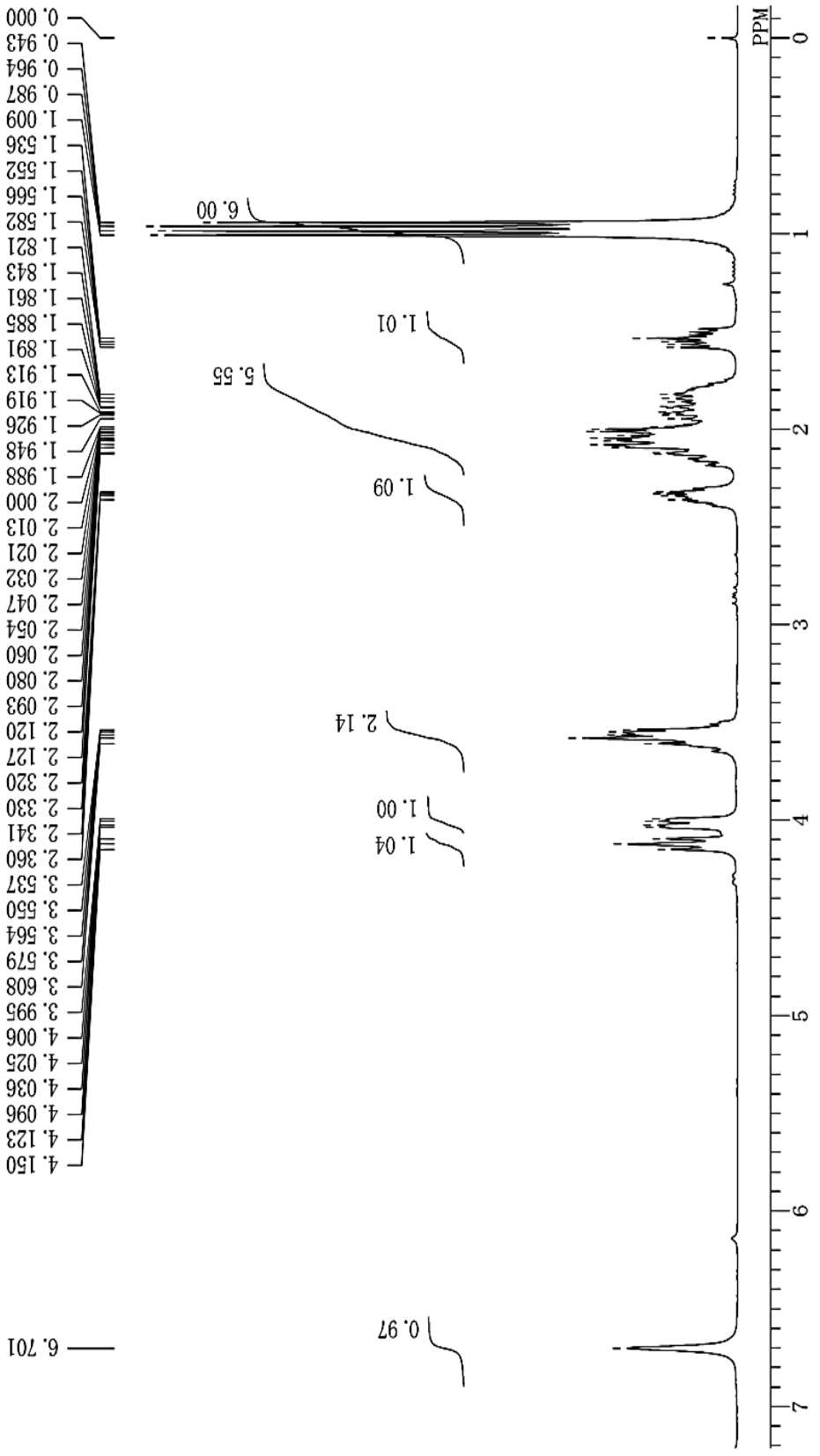

Figure 5.3.4.2 ^{1}H NMR (300 MHz; CD_3OD) spectrum of cyclo(Leu-Pro) (2)

5.3.5. Characterisation of compound 9

Compound **9** was isolated as white needle shaped crystals showing melting point of 178-179 ˚C. The purity was verified through TLC studies. The 75 MHz ^{13}C NMR spectrum of compound **9** (Figure 5.3.5.1) measured by dissolving in CD_3OD was found to display eleven signals which constituted two amide carbonyls (δ_C 171.6 and 167.6), three methylene carbons (δ_C 53.8, 38.0 and 36.8 ppm), four methine carbons (δ_C 67.7, 57.3, 53.2 and 24.4 ppm) along with two methyl carbons (δ_C 22.0 and 20.9 ppm) suggesting this compound also as a cyclic dipeptide derivative. The 300 MHz ^1H NMR spectrum (Figure 5.3.5.2) displayed the presence of signals due to protons of isobutyl group [1.94-1.85 (2H, m), 1.53-1.48 (1H, m), 0.95 (3H, d, *J*=6.3 Hz), 0.95 (3H, d, *J*=6.3 Hz)] similar to compound **2**. A careful interpretation of the spectrum revealed a difference in the signals due to methylene protons of proline part i.e. presence of a substitution at Pro-γ. The substituent was identified as a hydroxyl group from the IR spectrum which showed abroad absorption band at 3450 cm^{-1} (O-H str) (Figure 5.3.5.3). Compound **9** was finally identified as *cis*-Cyclo(Leu-hydroxy-Pro) (**9**) as drawn below. The stereochemistry was assigned by comparison of $[\alpha]_D^{25}$ [-135.2 (c, 0.71, MeOH)], ^{13}C and ^1H NMR data of reported compound (Furtado *et al.* 2005, De Hai *et al.* 2005).

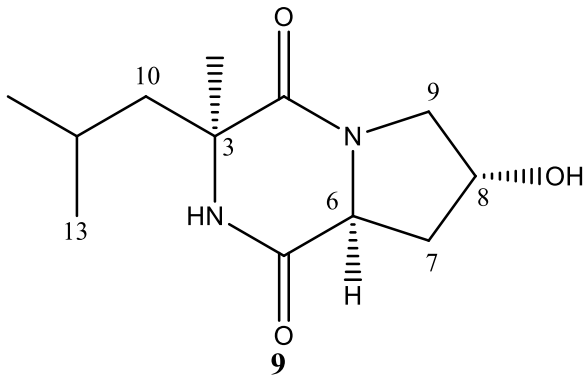

9

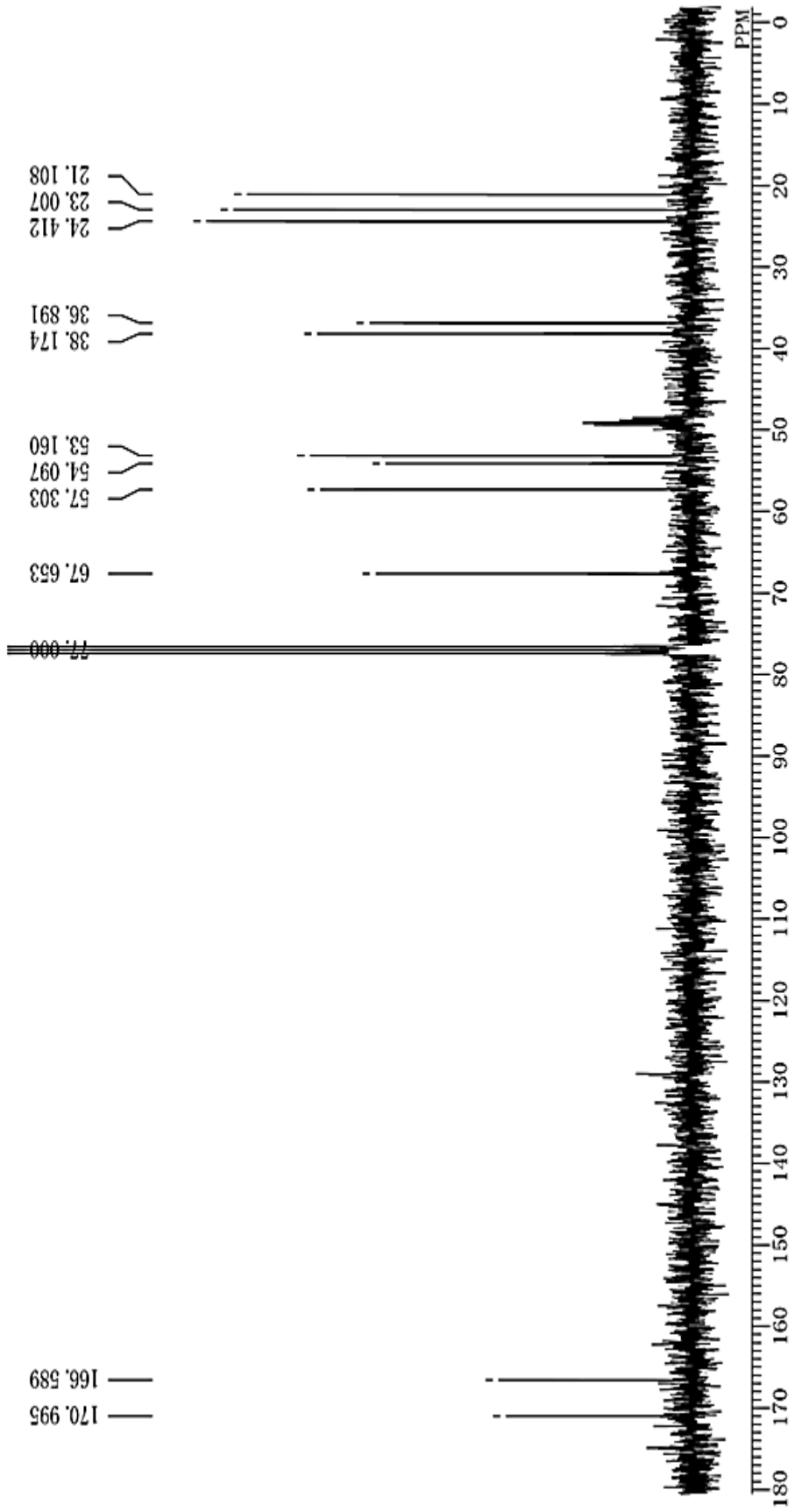

Figure 5.3.5.1 ^{13}C NMR (75 MHz; CD_3OD) spectrum of cyclo(Leu-Hydroxy-Pro) (9)

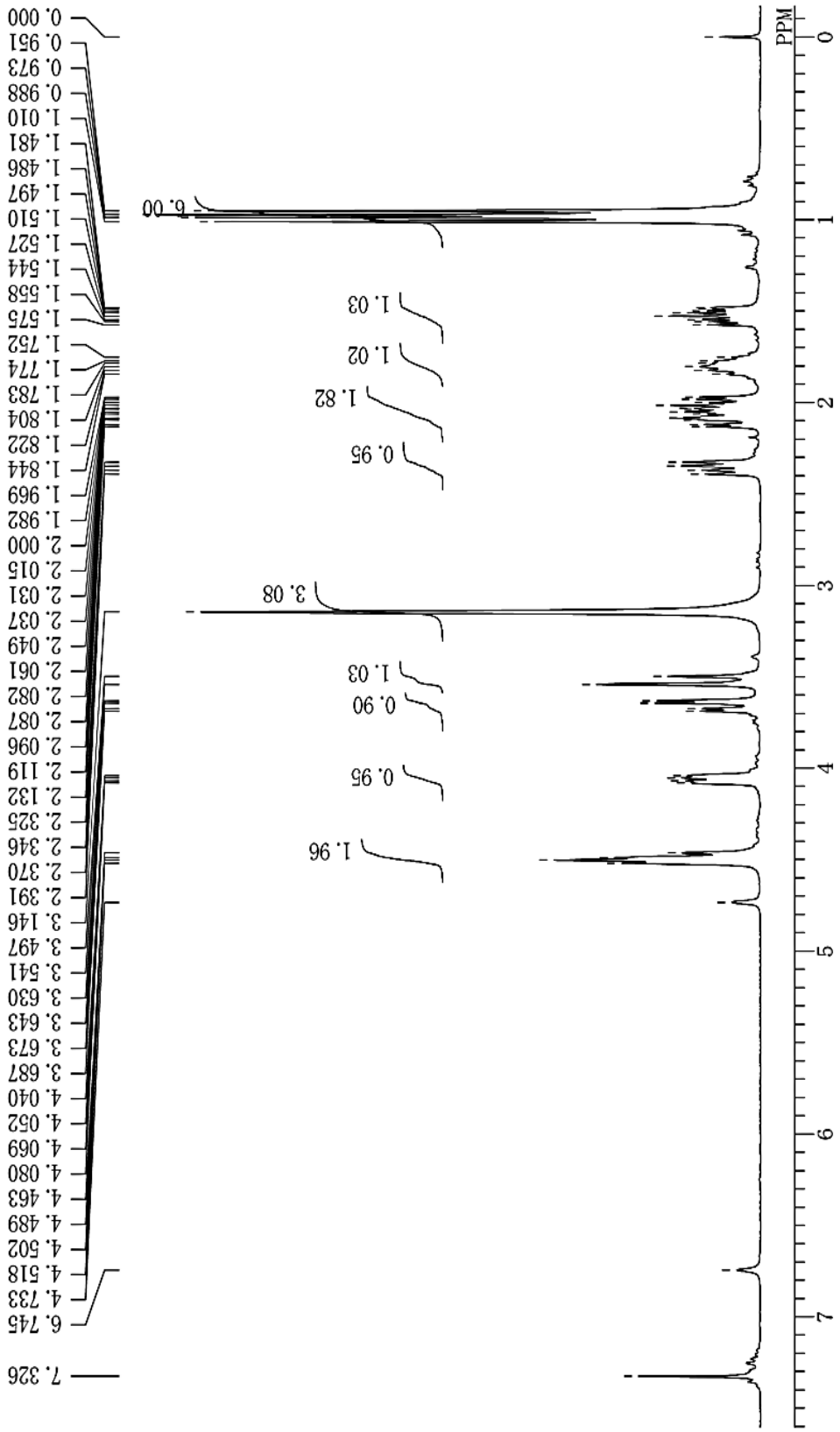

Figure 5.3.5.2 ^{1}H NMR (300 MHz; CD_3OD) spectrum of cyclo(Leu-Hydroxy-Pro) (9)

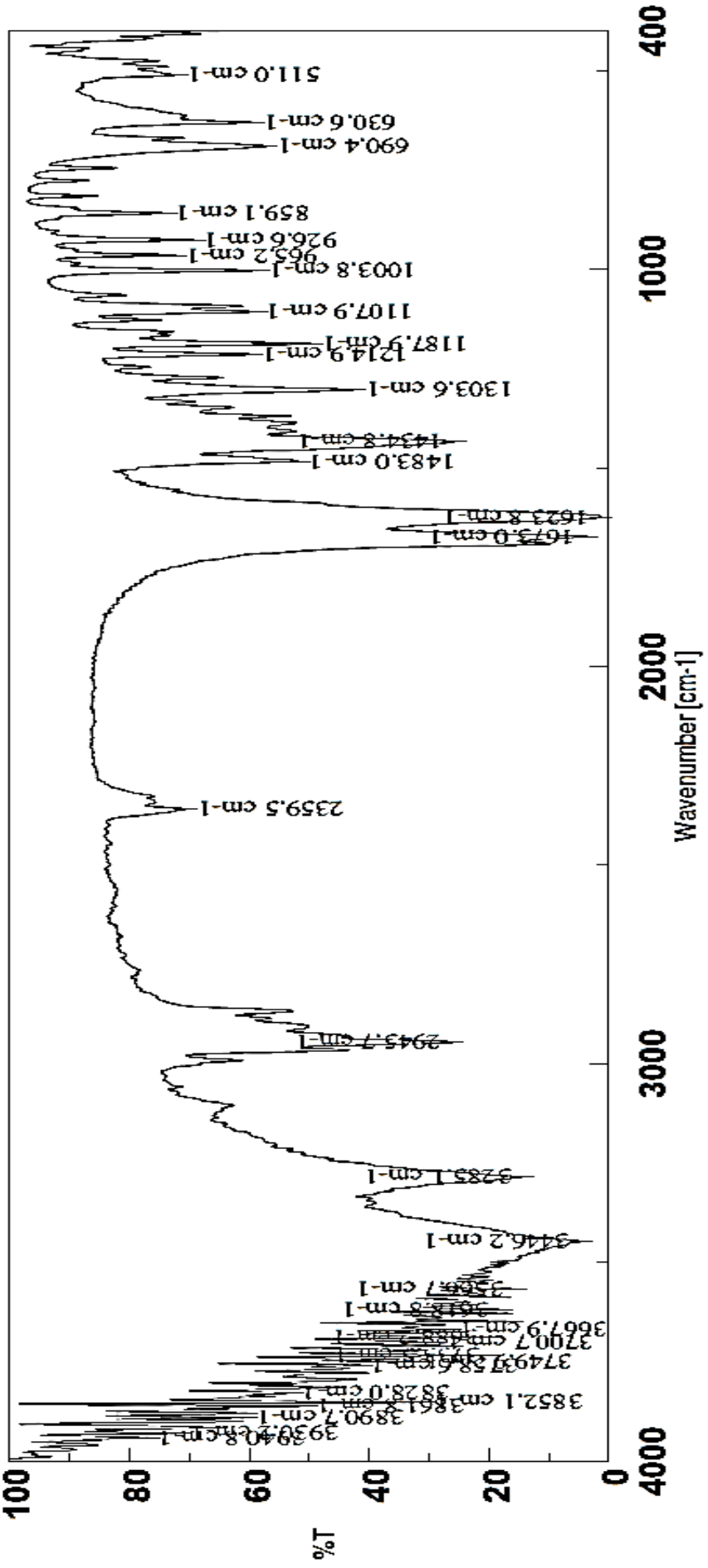

Figure 5.3.5.3 IR spectrum of cyclo(Leu-Hydroxy-Pro) (9)

5.3.6. Characterisation of compound 10

Compound **10** was obtained as white amorphous solid and its homogenous nature was accessed through TLC studies. Based on the ^{1}H and ^{13}C NMR spectral data, compound **10** was readily identified as a proline-based cyclic dipeptide. Interpretation of the proton NMR spectrum (Figure 5.3.6.1) disclosed the presence of a substituent at C-3 of diketopiperazine nucleus. The substituent was identified as *p*-hydroxy benzyl ring from the peaks which appeared at δ_H 7.52 (1H, br s), 7.05 (2H, d, *J*= 8.3 Hz) and 6.78 (2H, d, *J*=8.3 Hz) ppm. The benzylic proton signals were found at δ_H 3.43 (dd, J=14.4, 3.6 Hz) and 2.80 (dd, J=9.5, 4.8 Hz). Thus, the proton NMR data suggested, compound **10** to be built with proline and tyrosine. Further confirmation of this assumption was attained from the ^{13}C NMR (Figure 5.3.6.2) spectrum which showed twelve signals including aromatic carbon signals [169.7 (C=O), 165.2 (C=O), 155.7 (Ar-C-), 130.3(2 x Ar-CH-), 126.6 (Ar-C-), 116.0 (2 x Ar-CH-), 59.1 (OC-CH-N-), 56.3 (OC-CH-NH-), 45.4 (–CH_2-N-), 35.9 (Ar-CH_2-), 28.3 (-CH_2-), 22.4 (-CH_2-) ppm]. Finally, based on the good agreement between the measured NMR data of compound **10** and reported NMR data of *cis*-cyclo(Pro-Tyr), the structure of compound **10** was elucidated and it is shown below.

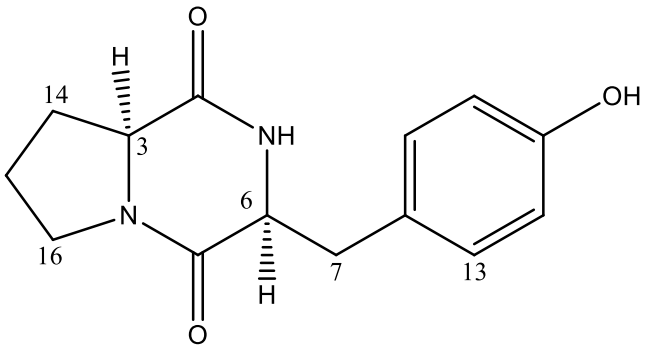

10

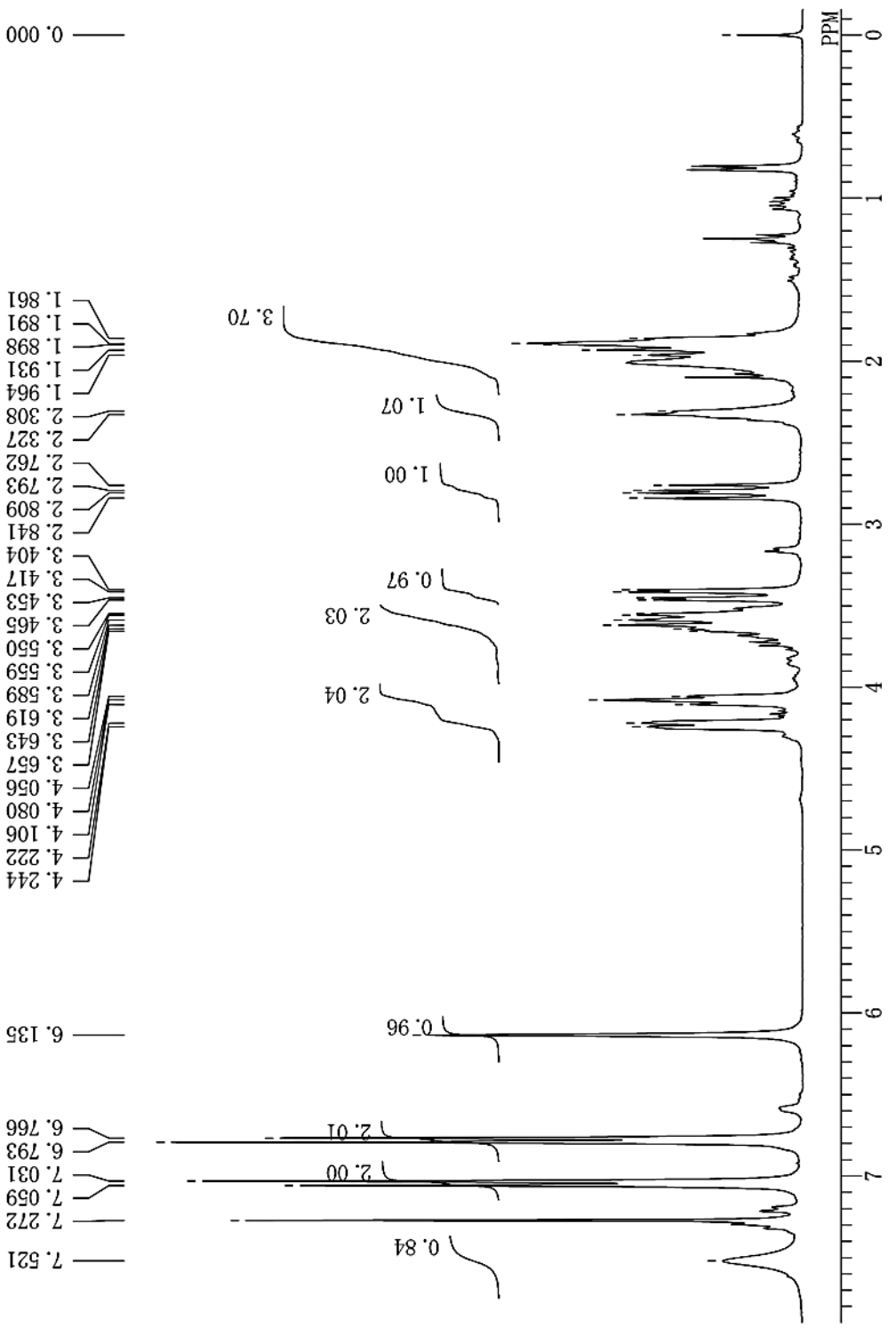

Figure 5.3.6.1 ^{1}H NMR (300 MHz; CD_3OD) spectrum of cyclo(Pro-Tyr) (10)

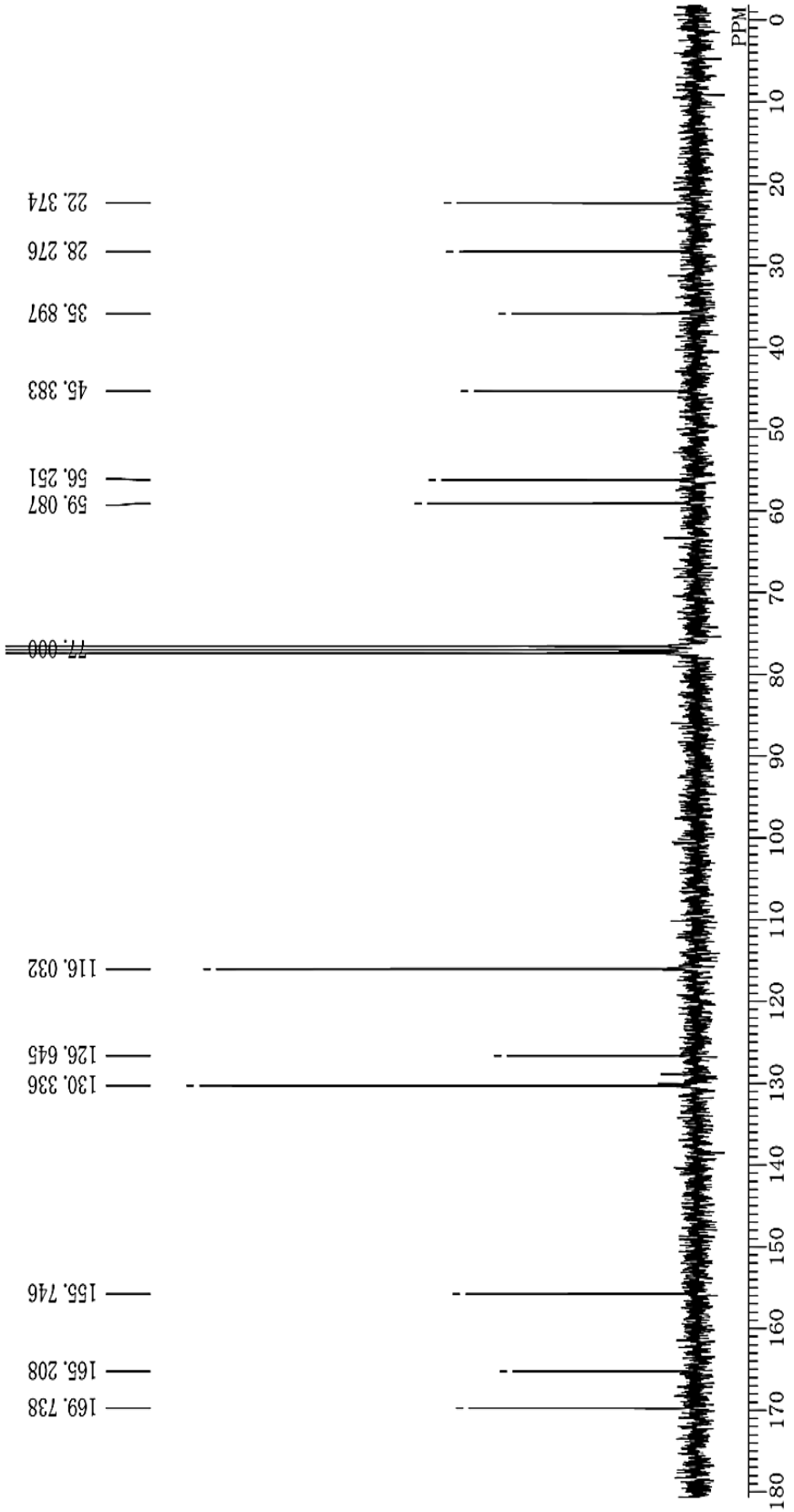

Figure 5.3.6.2 ^{13}C NMR (75 MHz CD_3OD) spectrum of cyclo(Pro-Tyr) (10)

5.3.7. Characterisation of compounds 3-8

Based on the careful interpretation of measured ^{1}H and ^{13}C NMR spectra of compounds **3-8**, they were identified as cyclic dipeptides. The identity of the compounds was established based on the comparison of measured NMR data with that of reported data. Compounds **3-8** were characterised as cyclo(Val-Leu) (**3**) (Li *et al.* 2006), cyclo(Phe-Pro) (**4**) (Stark *et al.* 2005), cyclo(Val-Phe) (**5**) (Tullberg *et al.* 2006), cyclo(Ile-Phe) (**6**) (Laville *et al.* 2015), cyclo(Leu-Ile) (**7**) (Laville *et al.* 2015) and cyclo(Leu-Leu) (**8**) (Ostermeier *et al.* 2009). The NMR data of compound **4** was not consistent with that of *cis*-cyclo(Phe-Pro), but in good agreement with that of *trans*-cyclo(Phe-Pro). Compound **4** was determined to be cyclo(L-Phe-D-Pro) based on the specific rotation, $[\alpha]_D^{25}$ 69.3 (*c*, 0.75, ethanol) (lit. 67 (methanol) for cyclo(L-Phe-D-Pro) (Wang *et al.* 2010) and (lit. -79 (c, 0.94, ethanol) for cyclo(D-Phe-L-Pro)) (Campbell *et al.* 2009). Figure 5.3.7.1 to Figure 5.3.7.12 presents the ^{1}H and ^{13}C NMR spectra of compounds **3-8**. The pragmatic δ_C and δ_H values are depicted around the structures and presented in Figure 5.3.7.13.

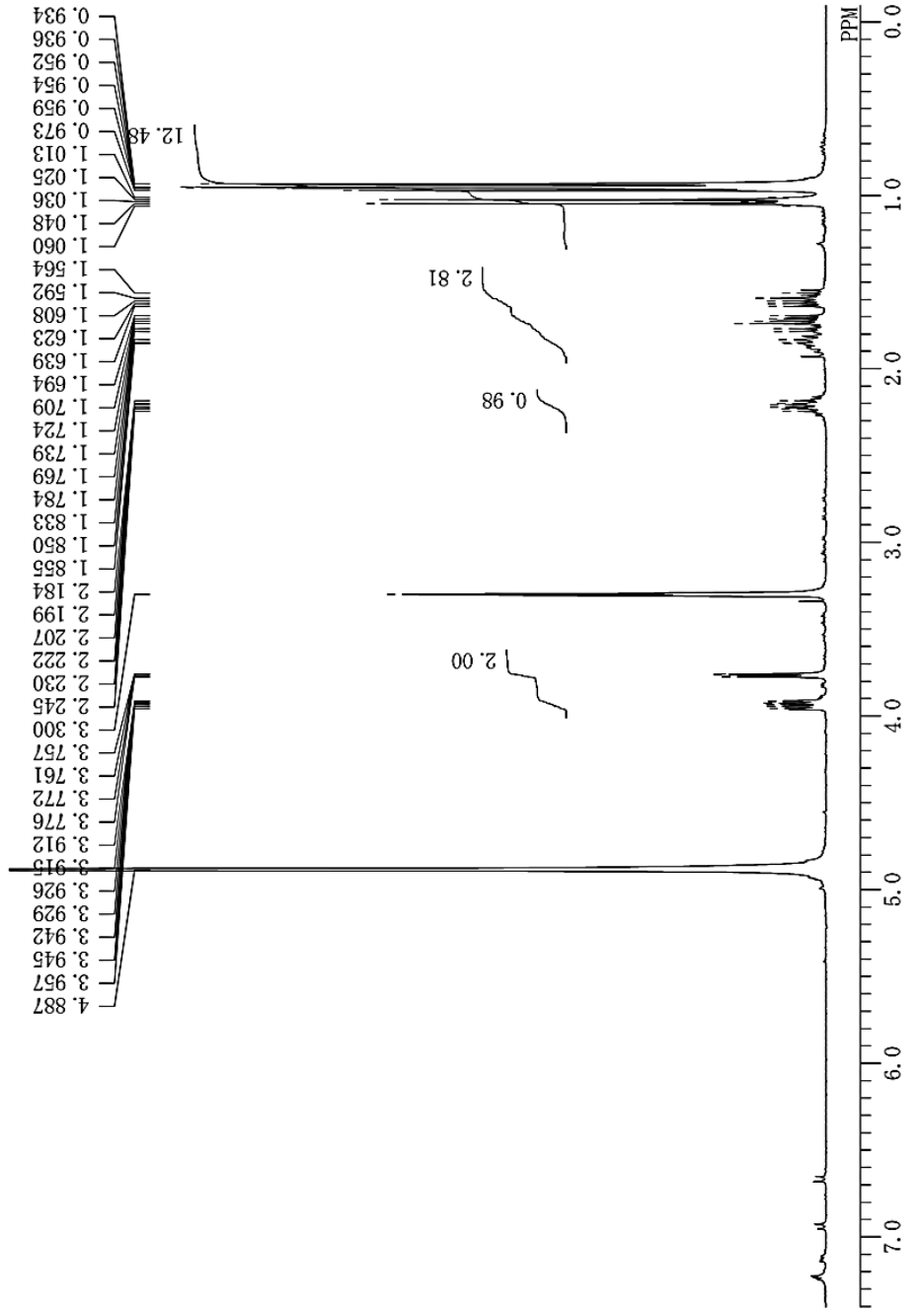

Figure 5.3.7.1 ^{1}H NMR (300 MHz; CD_3OD) spectrum of cyclo(Val-Leu) (3)

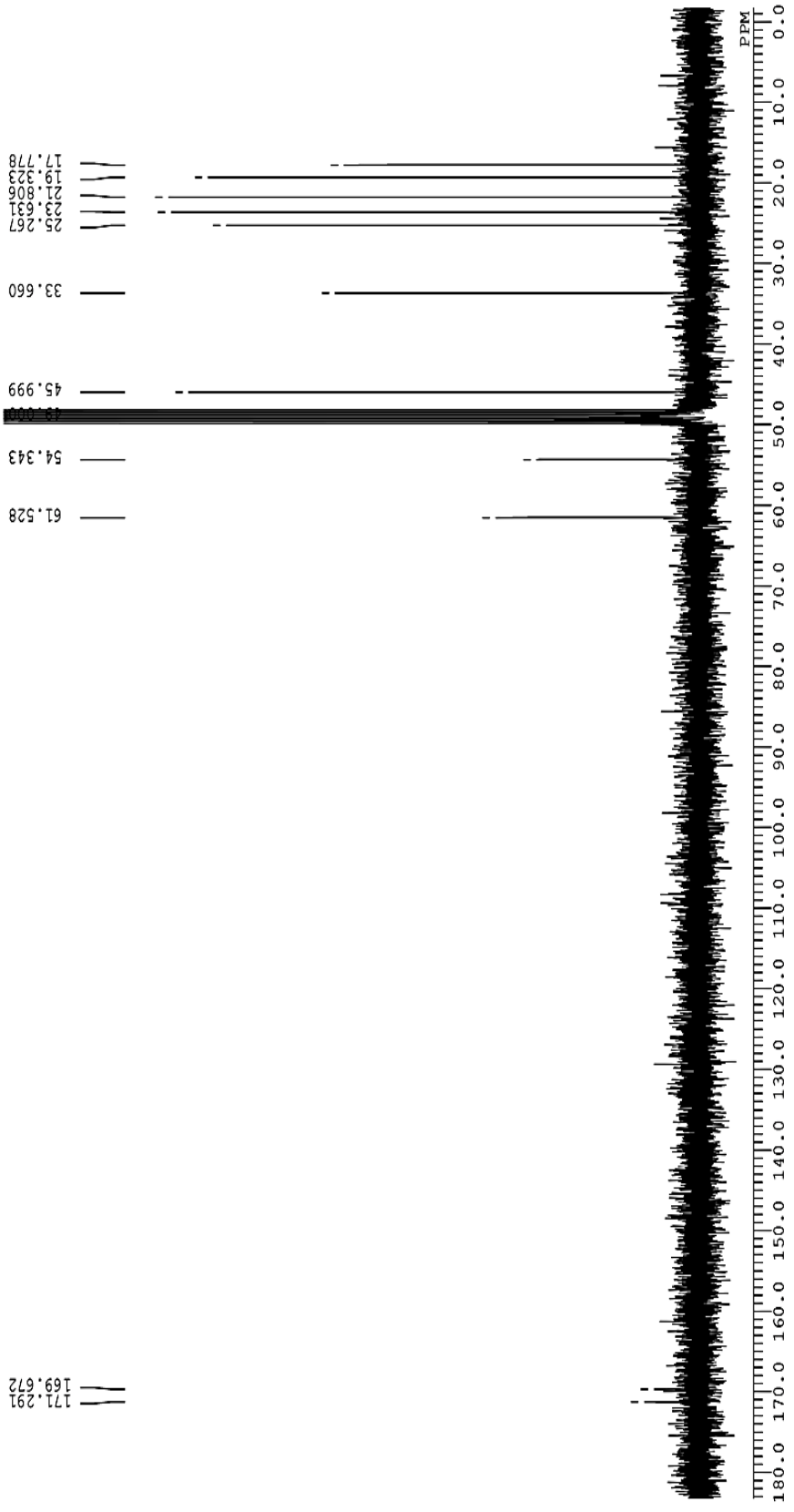

Figure 5.3.7.2 ^{13}C NMR (75 MHz; CD_3OD) spectrum of cyclo(Val-Leu) (3)

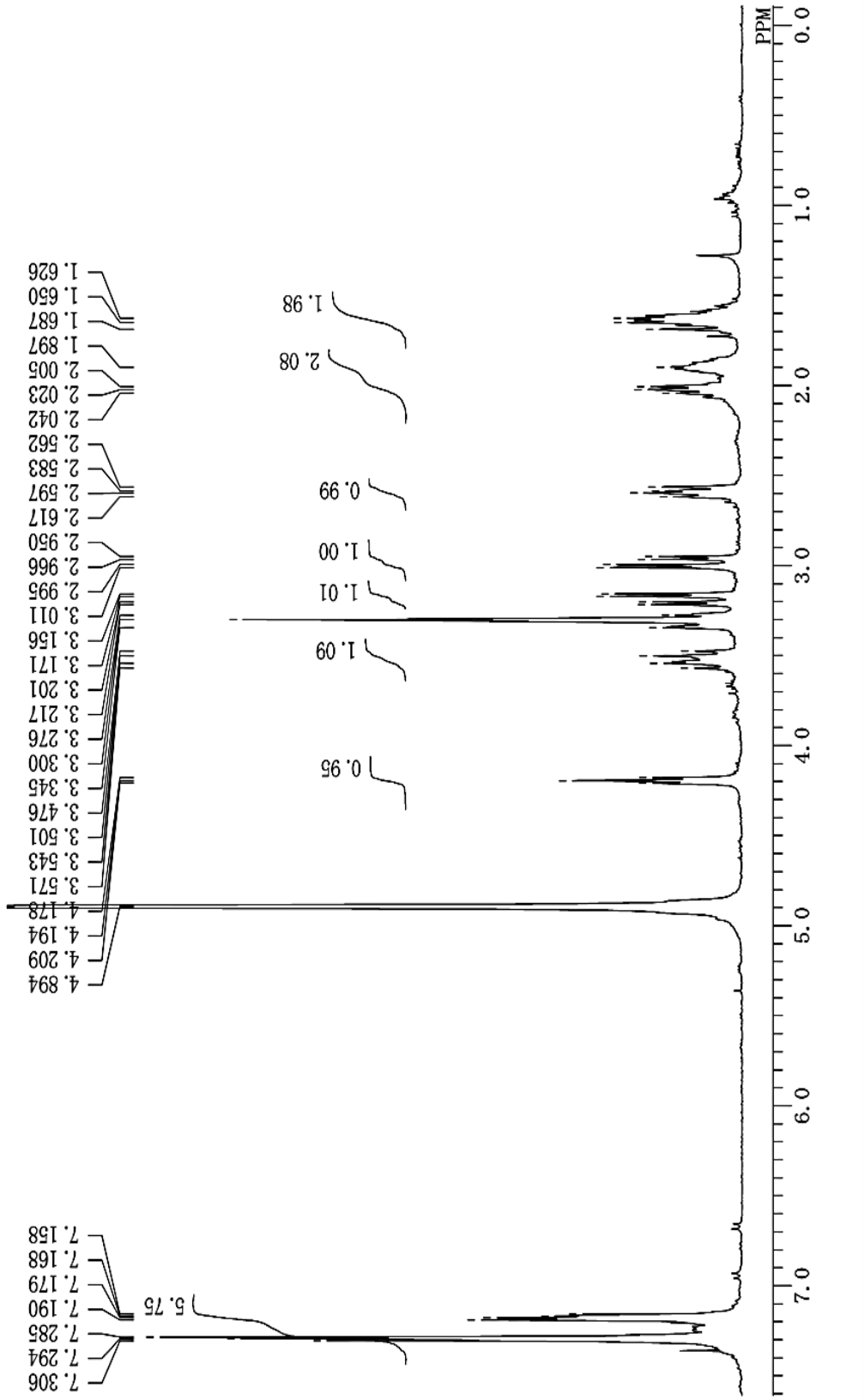

Figure 5.3.7.3 ^{1}H NMR (300 MHz; CD_3OD) spectrum of cyclo(Phe-Pro) (4)

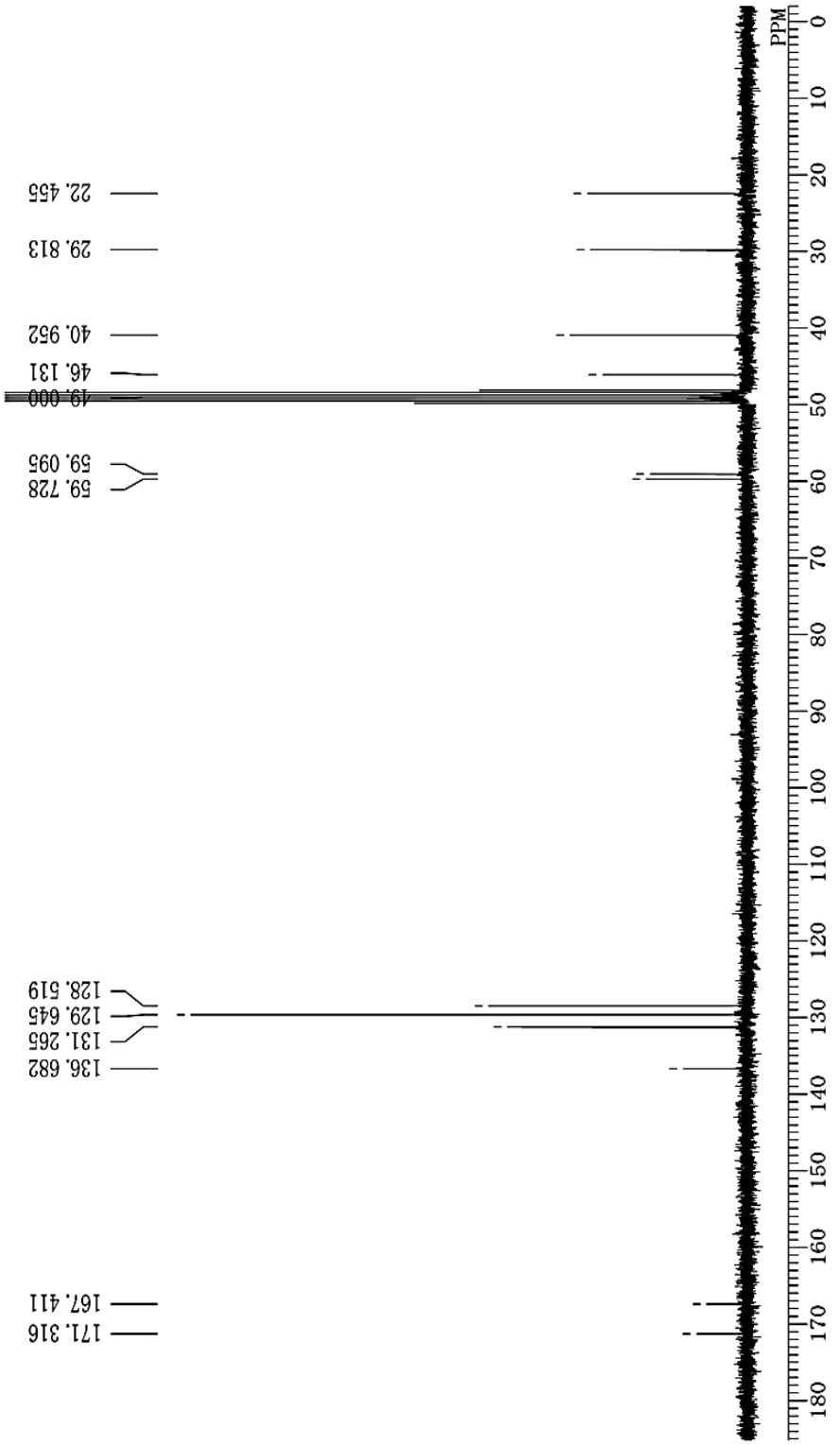

Figure 5.3.7.4 ^{13}C NMR (75 MHz; CD_3OD) spectrum of cyclo(Phe-Pro) (4)

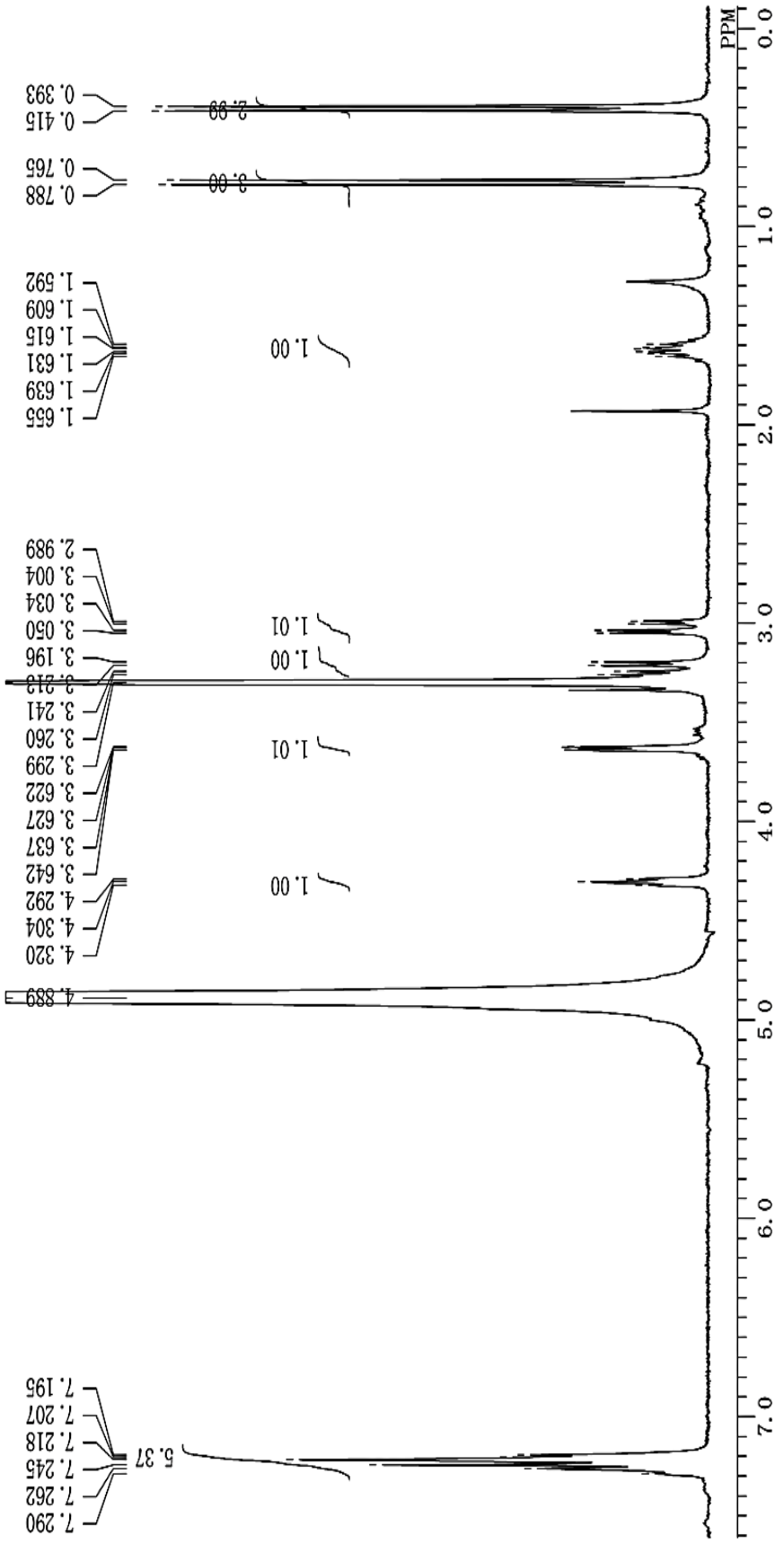

Figure 5.3.7.5 ^{1}H NMR (300 MHz; CD_3OD) spectrum of cyclo(Val-Phe) (5)

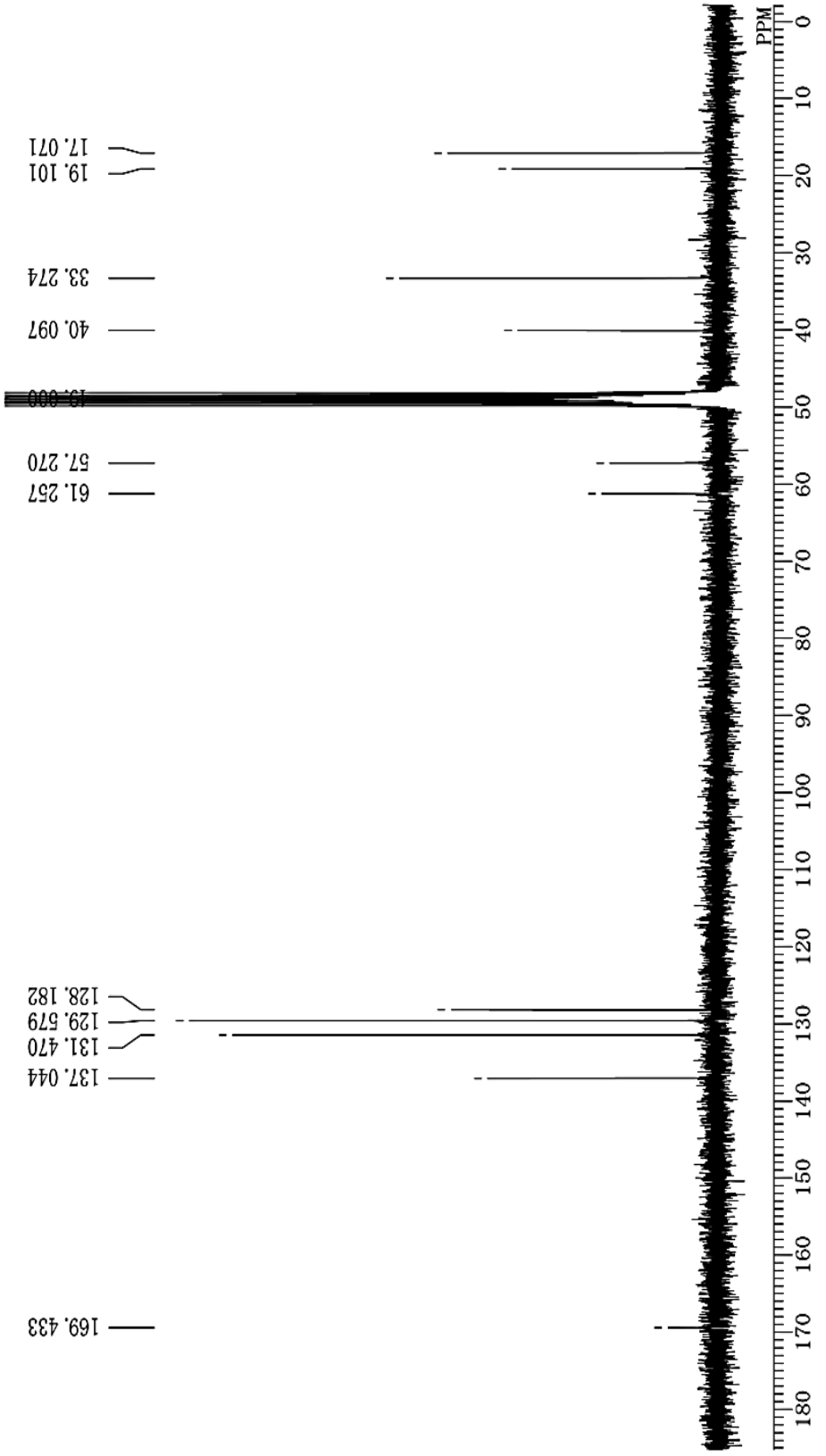

Figure 5.3.7.6 ^{13}C NMR (75 MHz; CD_3OD) spectrum of cyclo(Val-Phe) (5)

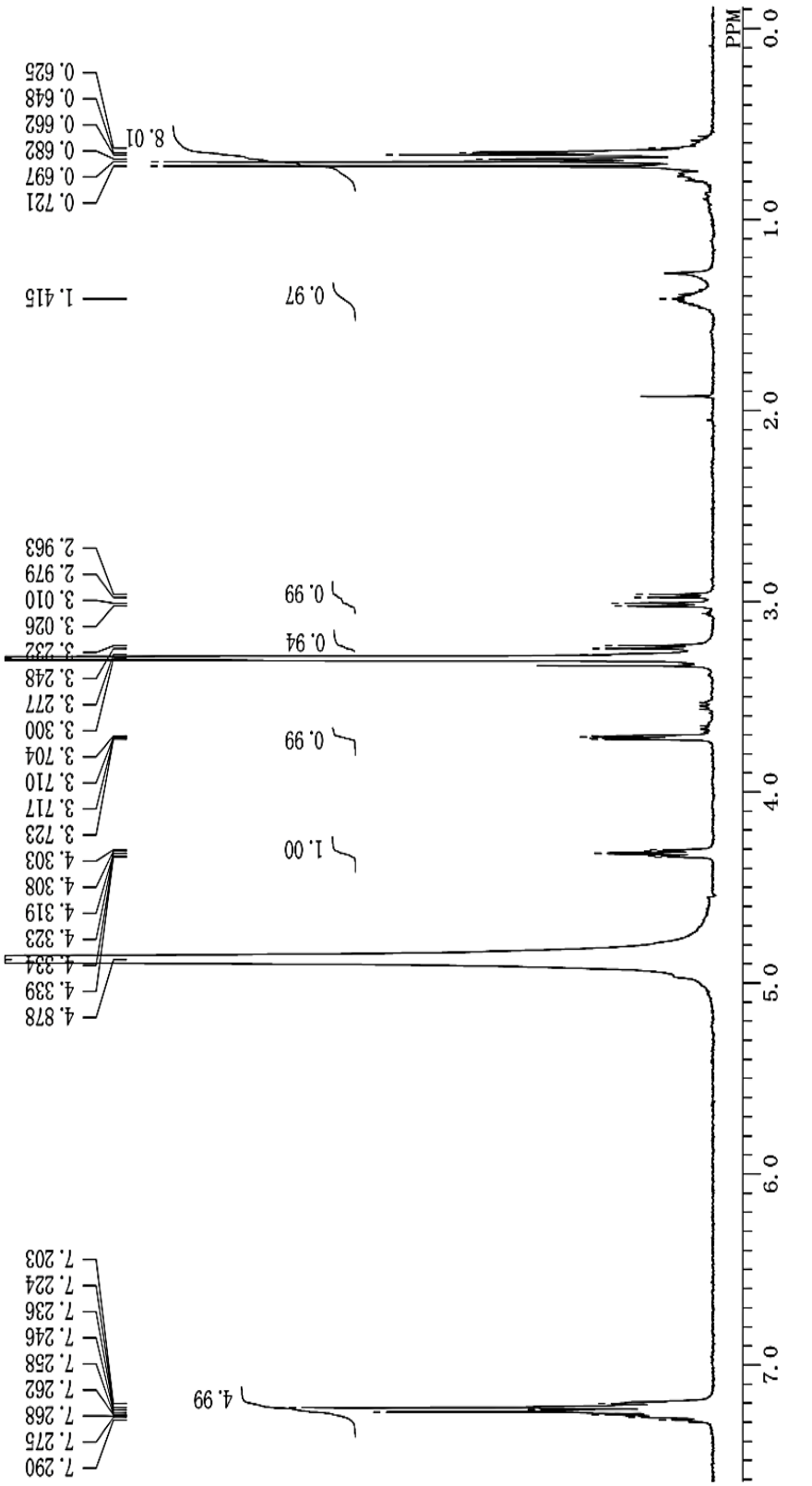

Figure 5.3.7.7 ^{1}H NMR (300 MHz; CD_3OD) spectrum of cyclo(Ile-Phe) (6)

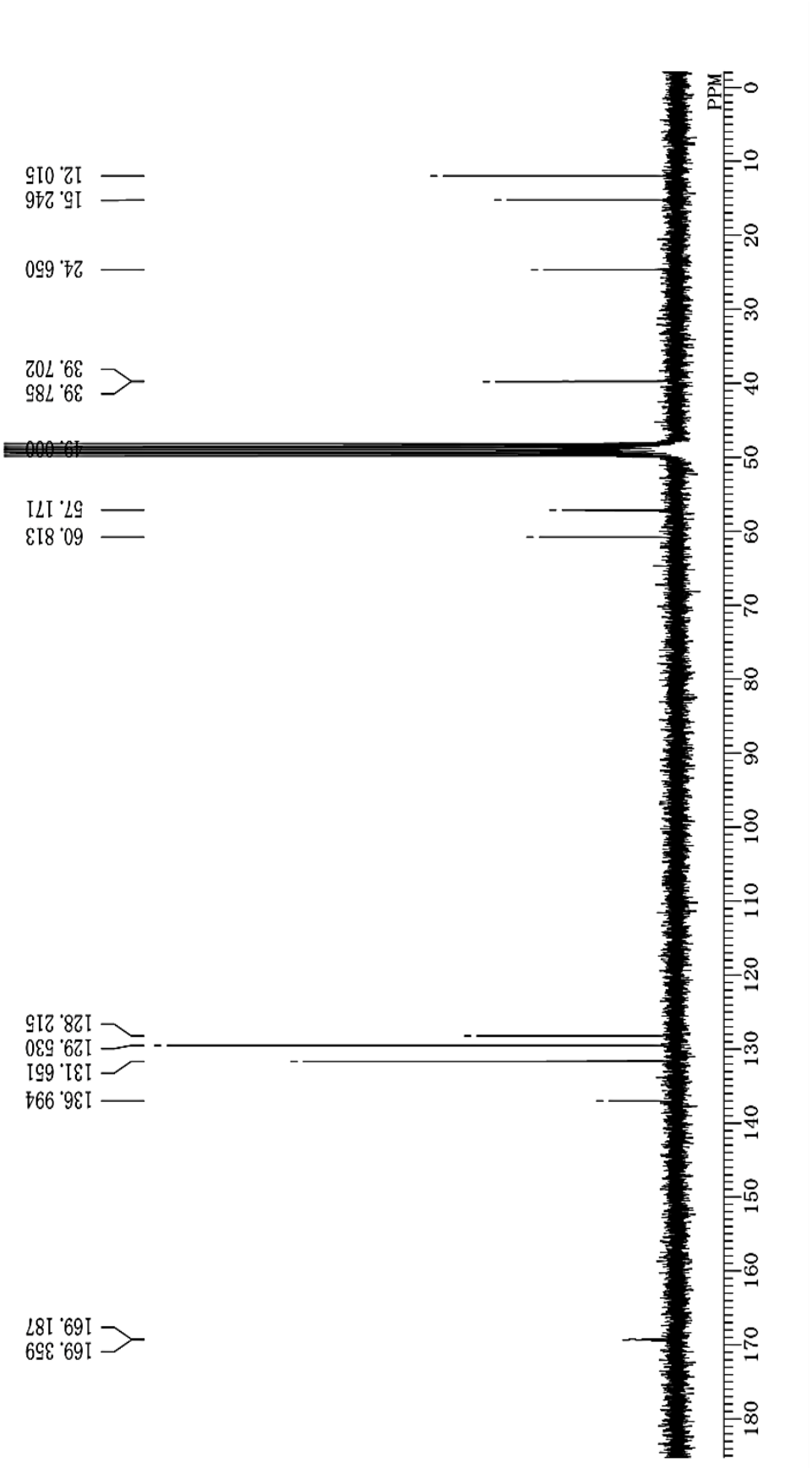

Figure 5.3.7.8 ^{13}**C NMR (75 MHz; CD_3OD) spectrum of cyclo(Ile-Phe) (6)**

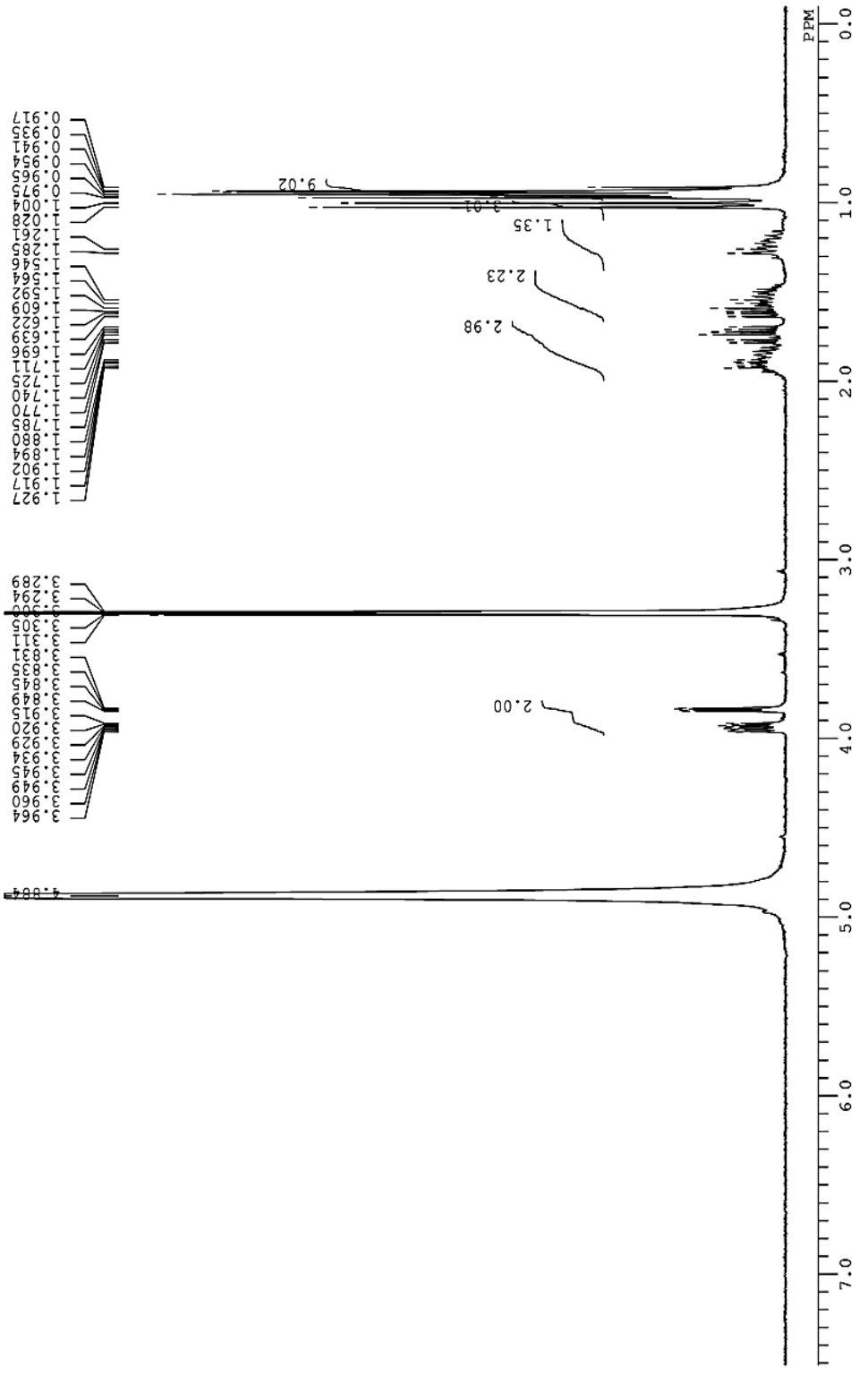

Figure 5.3.7.9 ^{1}H NMR (300 MHz CD_3OD) spectrum of cyclo(Leu-Ile) (7)

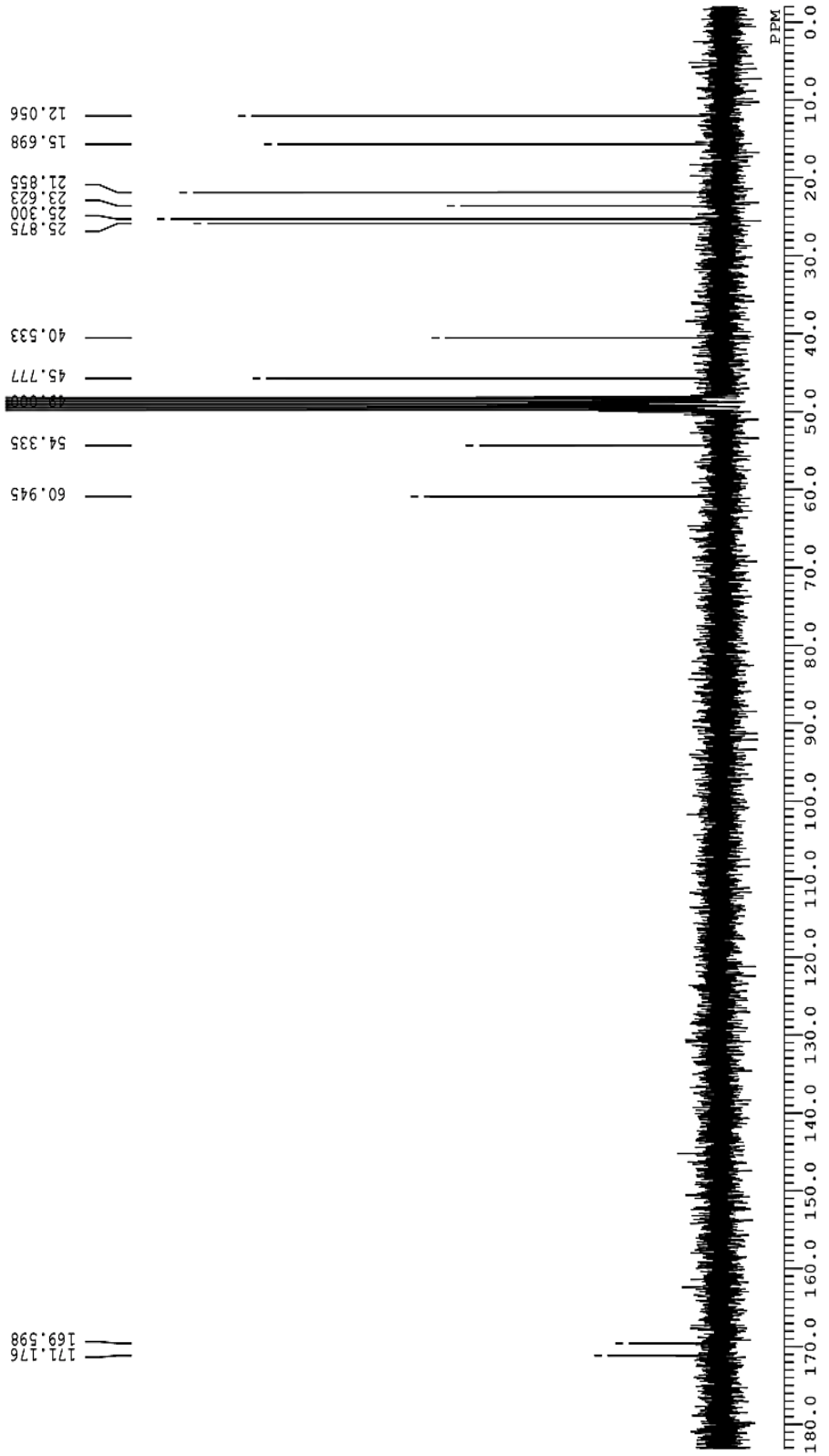

Figure 5.3.7.10 ^{13}C NMR (75 MHz; CD_3OD) spectrum of cyclo(Leu-Ile) (7)

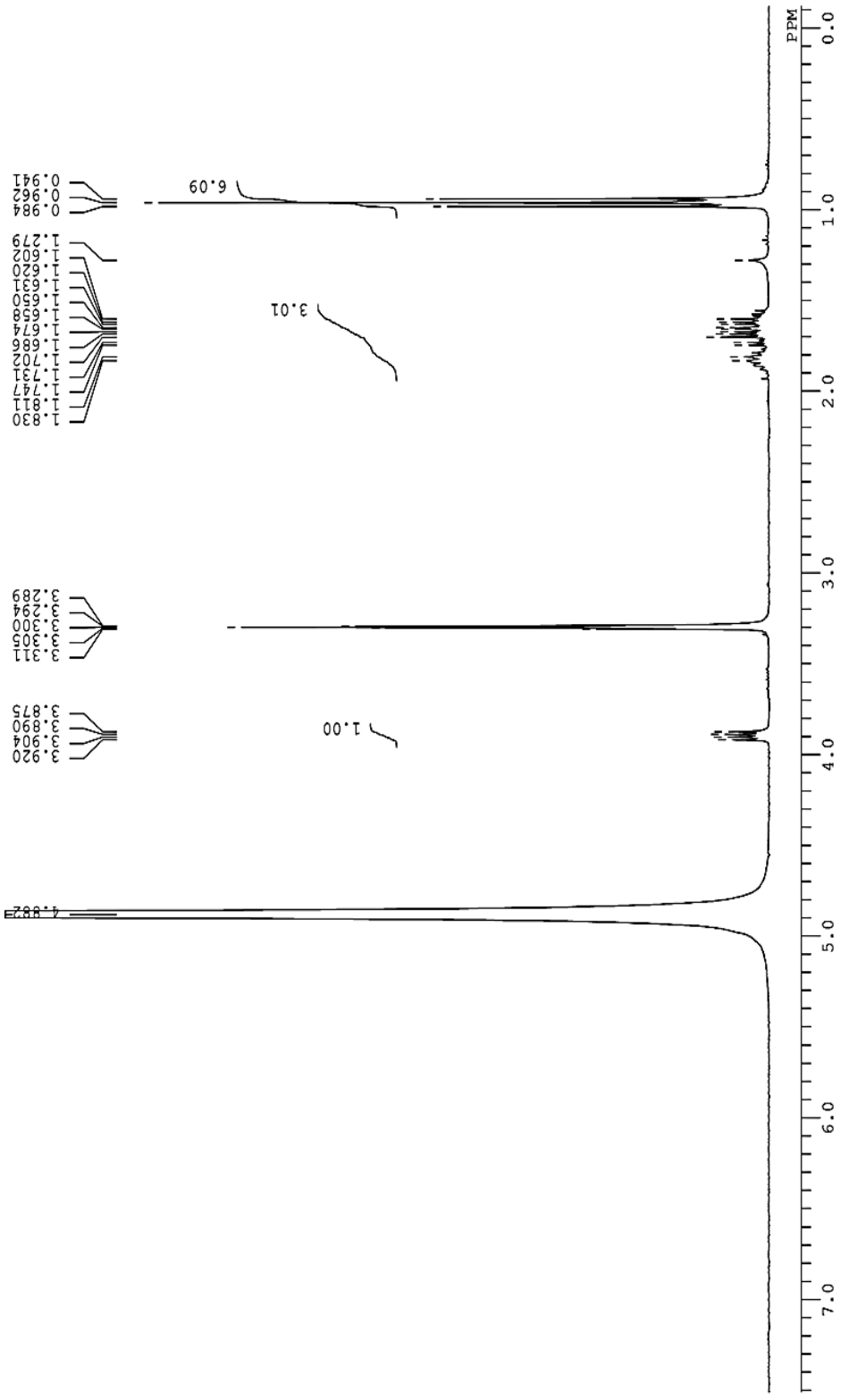

Figure 5.3.7.11 ^{1}H NMR (300 MHz; CD_3OD) spectrum of cyclo(Leu-Leu) (8)

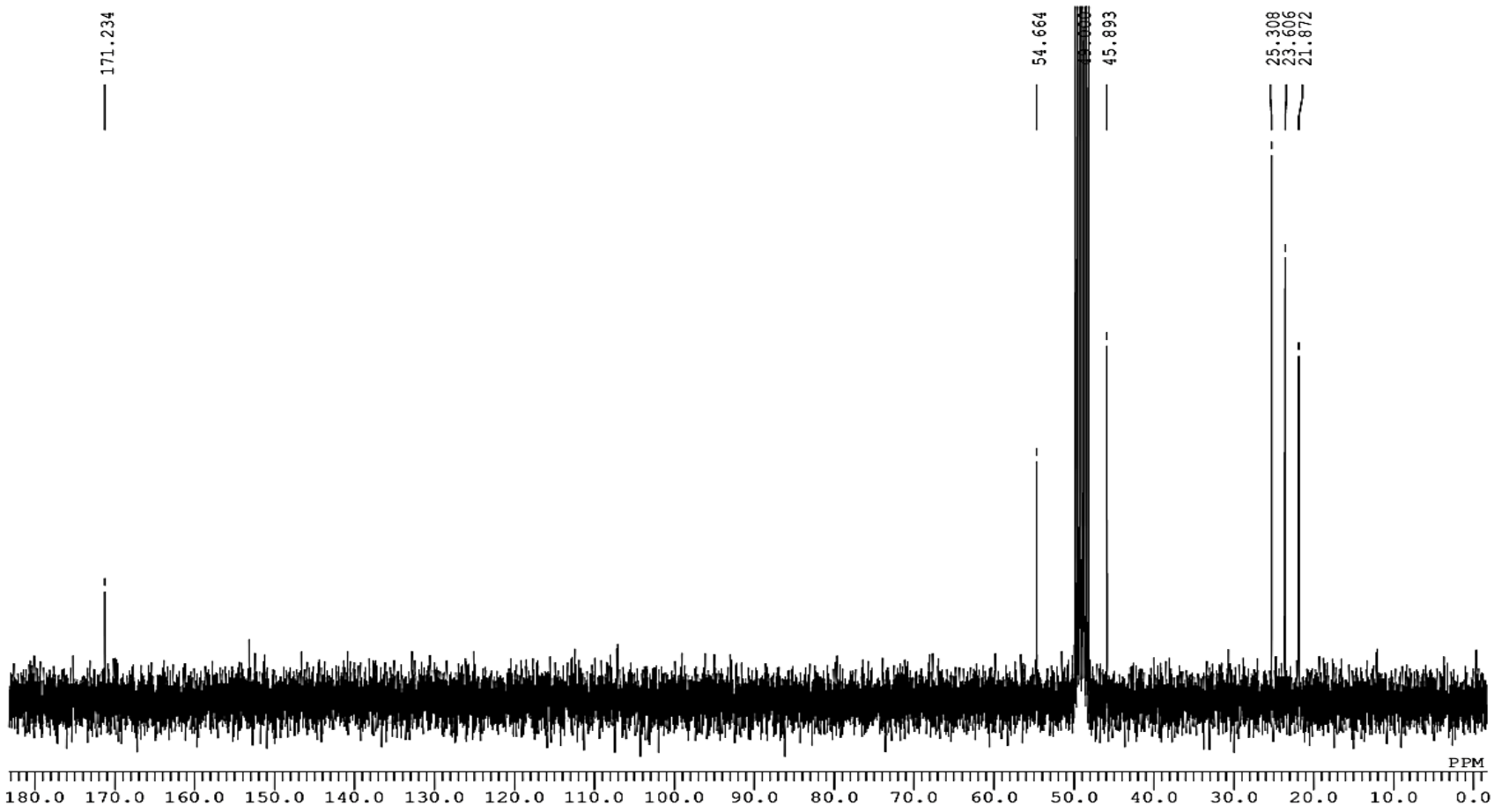

Figure 5.3.7.12 ^{13}C NMR (75 MHz; CD_3OD) spectrum of cyclo(Leu-Leu) (8)

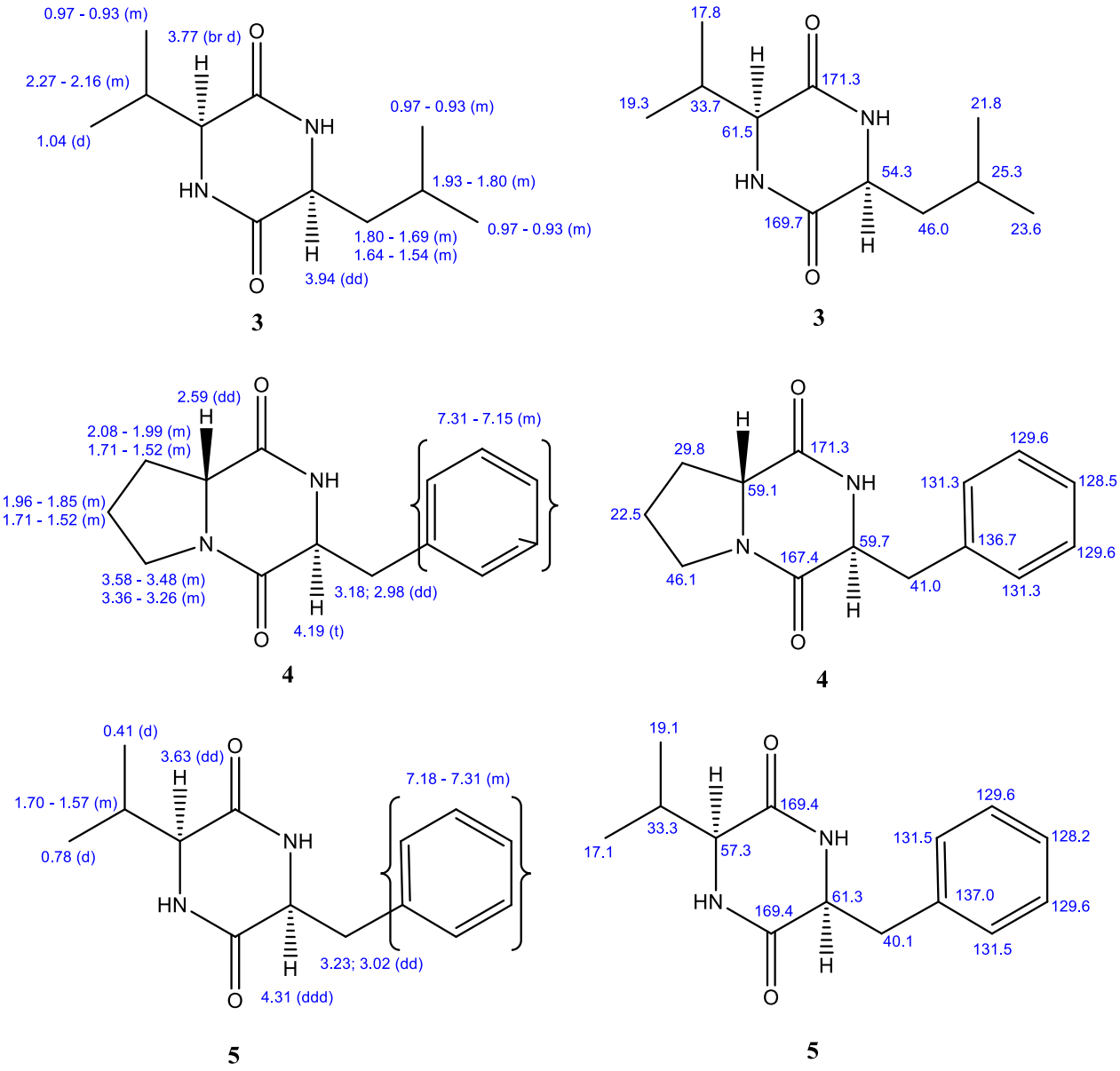

Figure 5.3.7.13a The chemical shift (δ_C and δ_H) values of compounds 3-5

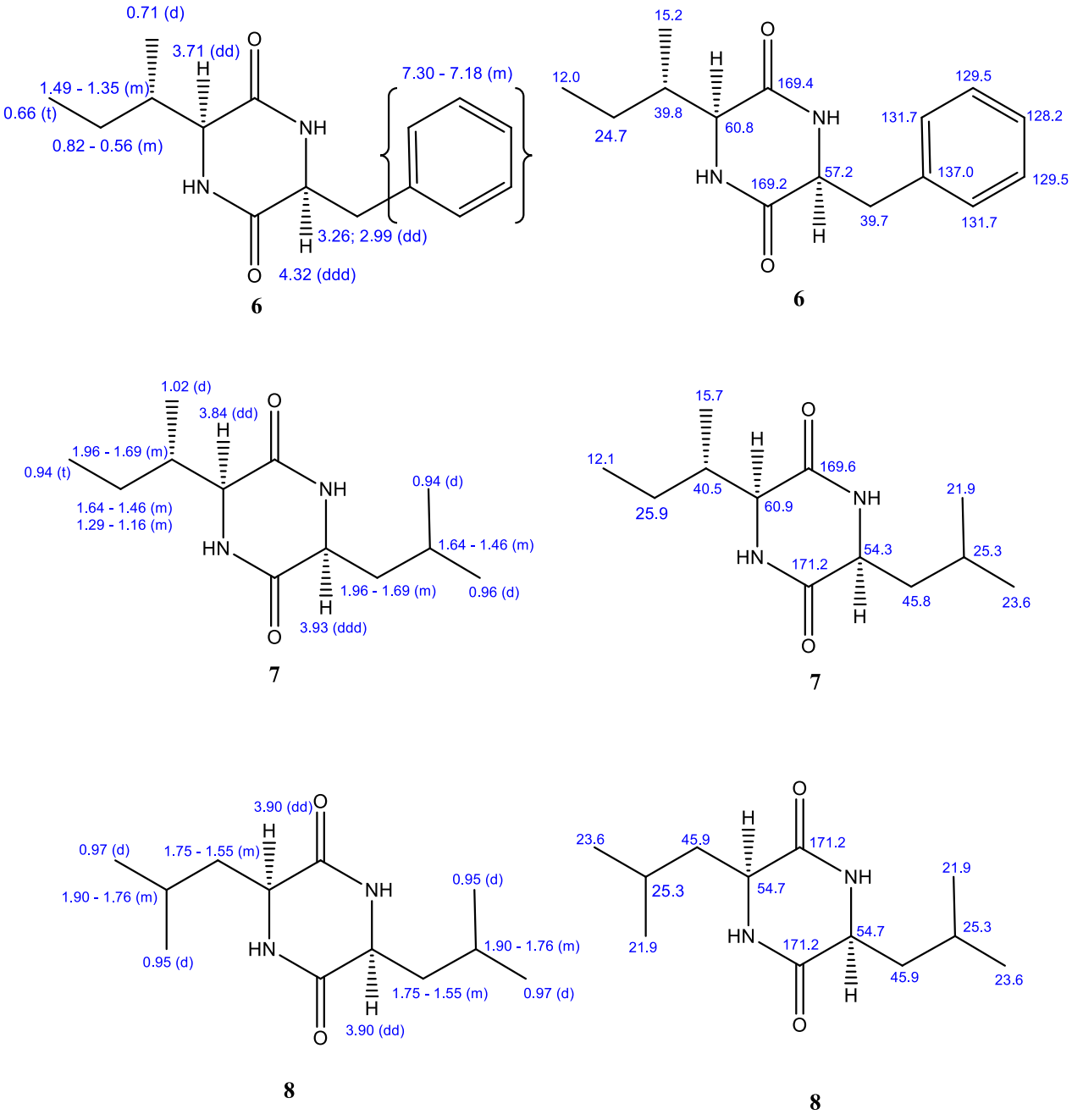

Figure 5.3.7.13b The chemical shift (δ_C and δ_H) values of compounds 6-8

5.3.8. Characterisation of compounds 13-20

Interpretation of proton and carbon NMR spectra of compounds **13-20** revealed them as cyclic dipeptides. The identity of the compounds was established based on the comparison of measured NMR data with that of the reported data. Compounds **13-20** were characterised as cyclo(Gly-Phe) **(13)** (De-Hai *et al.* 2005, Coursindel *et al.* 2010), cyclo(Ala-Phe) **(14)** (Stark *et al.* 2005, De-Hai *et al.* 2005), cyclo(Ala-Ile) (**15**) (Stark *et al.* 2005, De-Hai *et al.* 2005), cyclo(Gly-Tyr)(**16**) (Chen *et al.* 2018), cyclo(Ala-Tyr) (**17**) (Stark *et al.* 2005), cyclo(Val-Tyr)

(**18**) (Stark *et al.* 2005), cyclo(Leu-Tyr) (**19**) (Tullberg *et al.* 2006) and cyclo(Ala-Ala) **(20**) (Xu-Tao *et al.* 2009). Figure 5.3.8.1 to Figure 5.3.8.15 presents the ^{1}H and ^{13}C NMR spectra of compounds **13-20**. The pragmatic δ_C and δ_H values depicted around the structures of compounds **13-20** are presented in Figure 5.3.8.16a and Figure 5.3.8.16b. Compounds **14-15** and **17-20** were assigned as *cis*-cyclic dipeptides by comparing their NMR data with that of the reported data and assumed to be common natural L, L-forms.

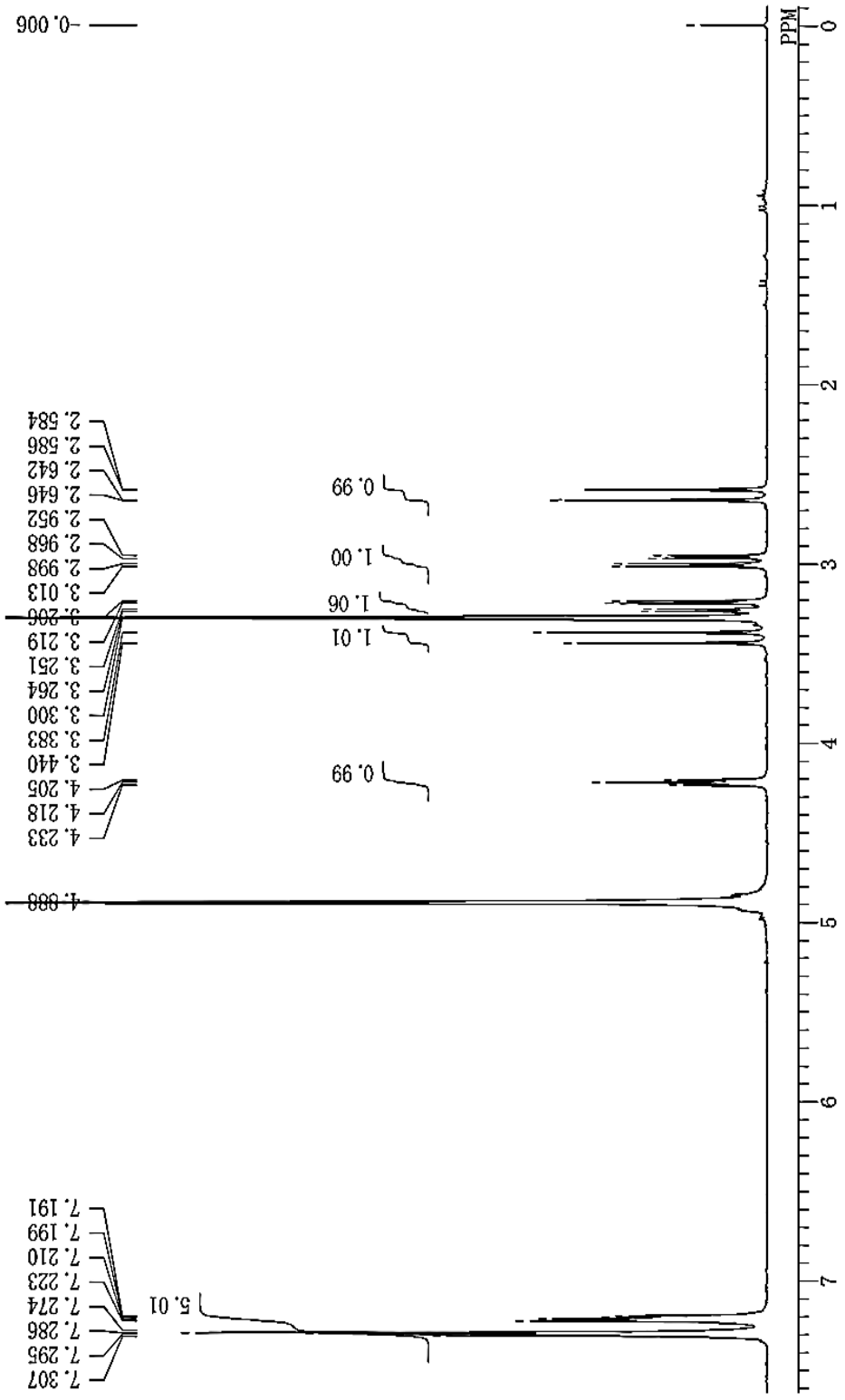

Figure 5.3.8.1 ^{1}H NMR (300 MHz; CD_3OD) spectrum of cyclo(Gly-Phe) (13)

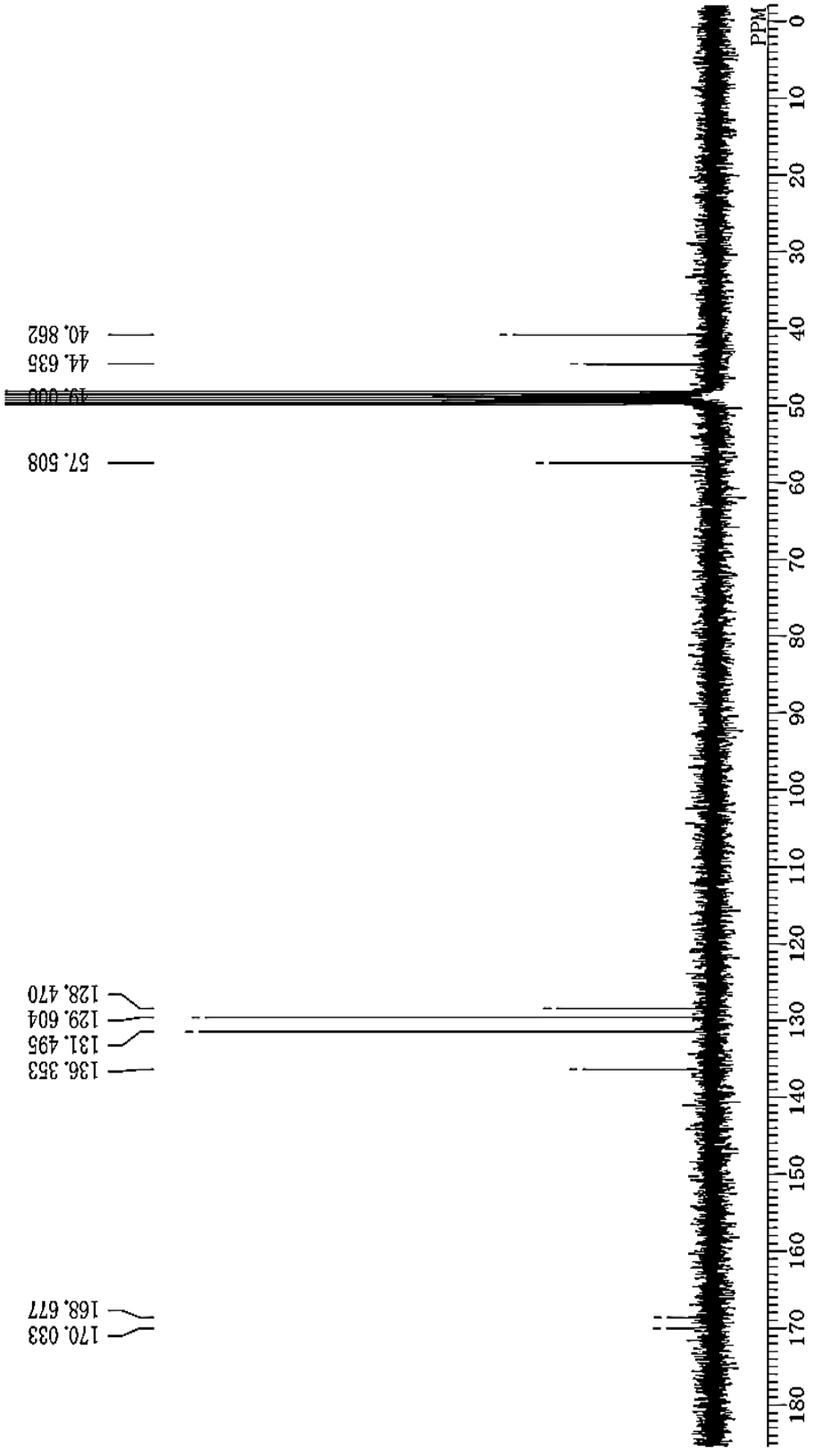

Figure 5.3.8.2 ^{13}C NMR (75 MHz, CD_3OD) Spectrum of cyclo(Gly-Phe)

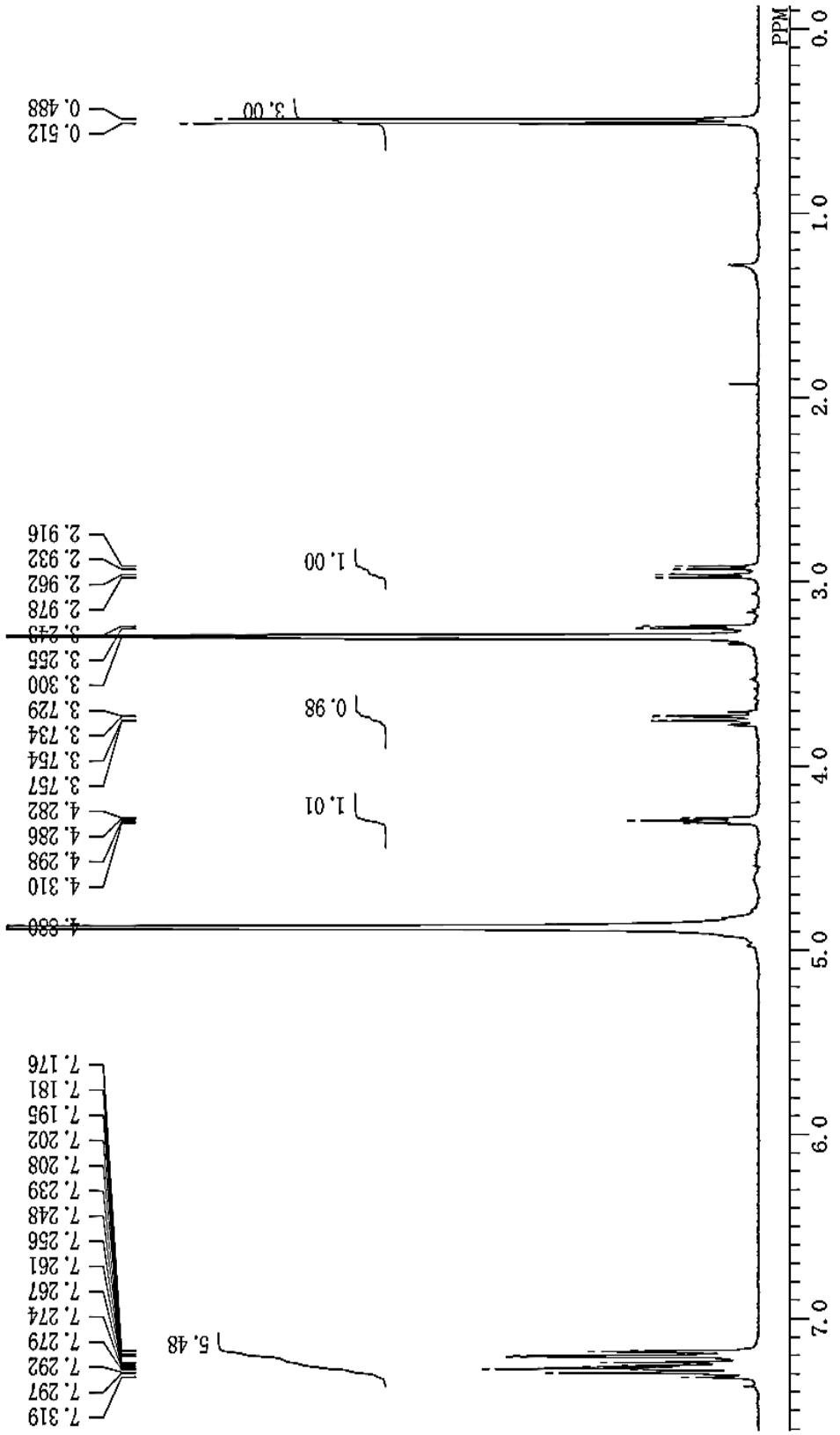

Figure 5.3.8.3 ^{1}H NMR (300 MHz; CD_3OD) spectrum of cyclo(Ala-Phe) (14)

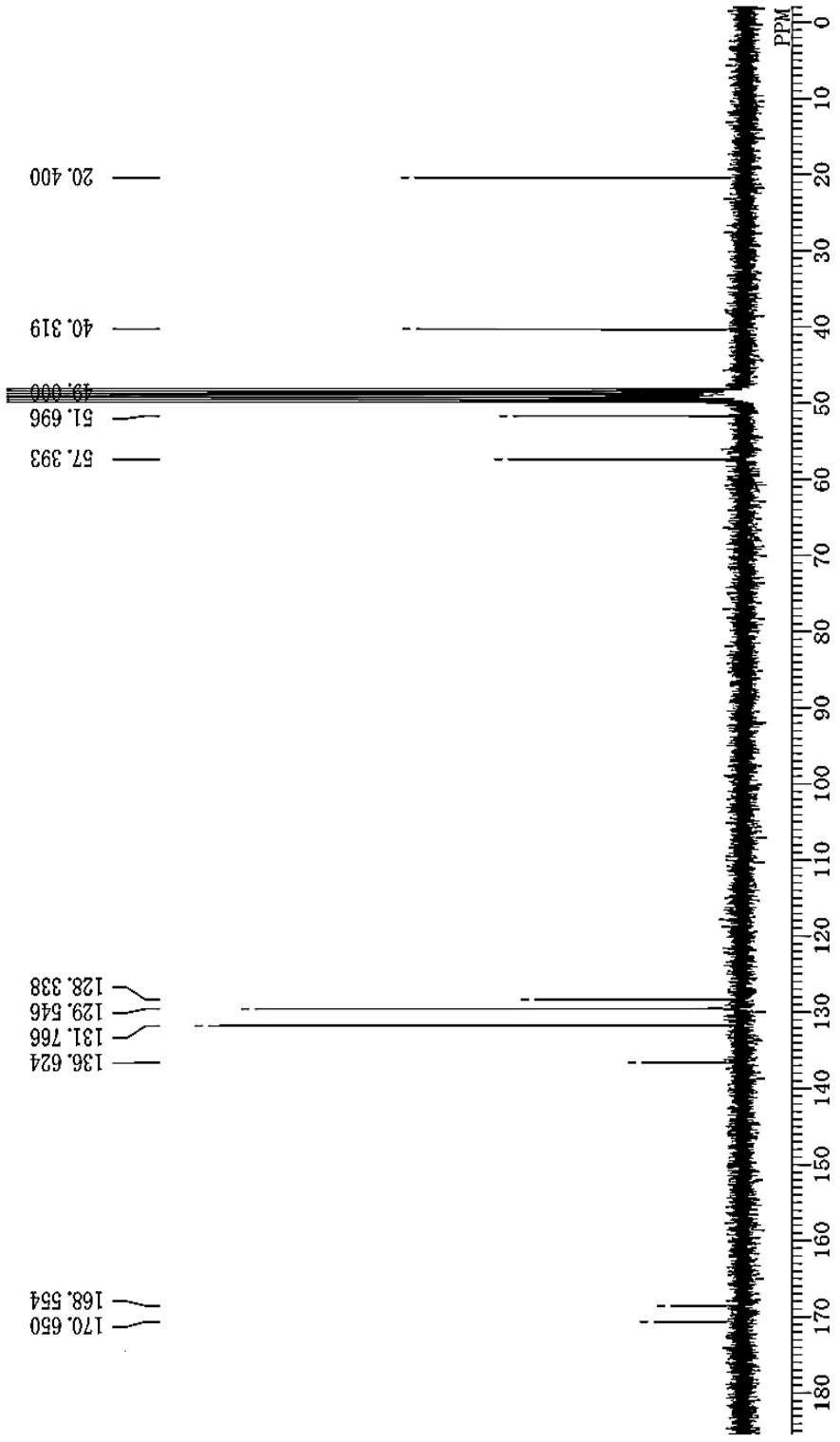

Figure 5.3.8.4 ^{13}C NMR (75 MHz, CD_3OD) Spectrum of cyclo(Ala-Phe) (14)

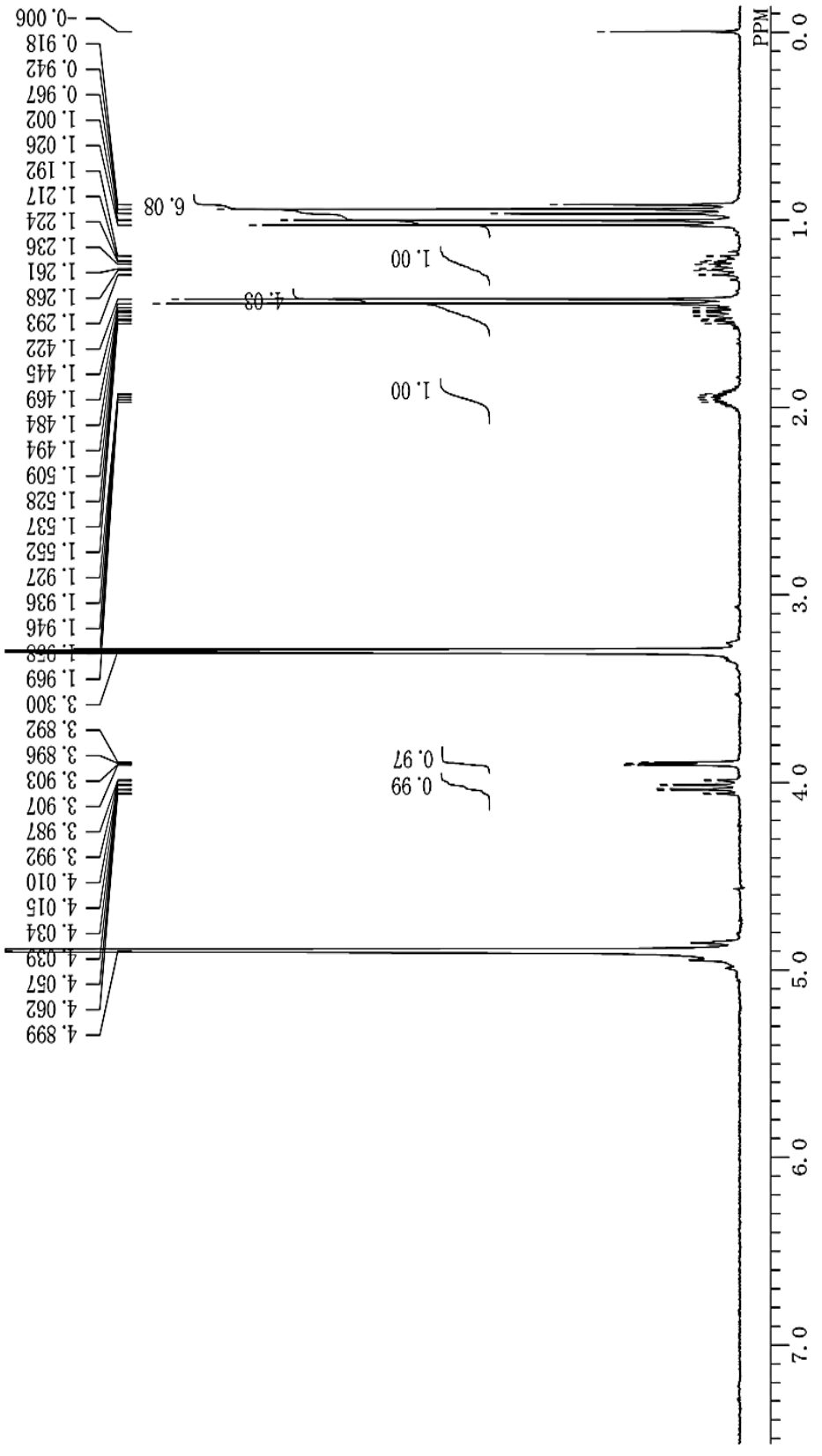

Figure 5.3.8.5 ^{1}H NMR (300 MHz; CD_3OD) spectrum of cyclo(Ala-Ile) (15)

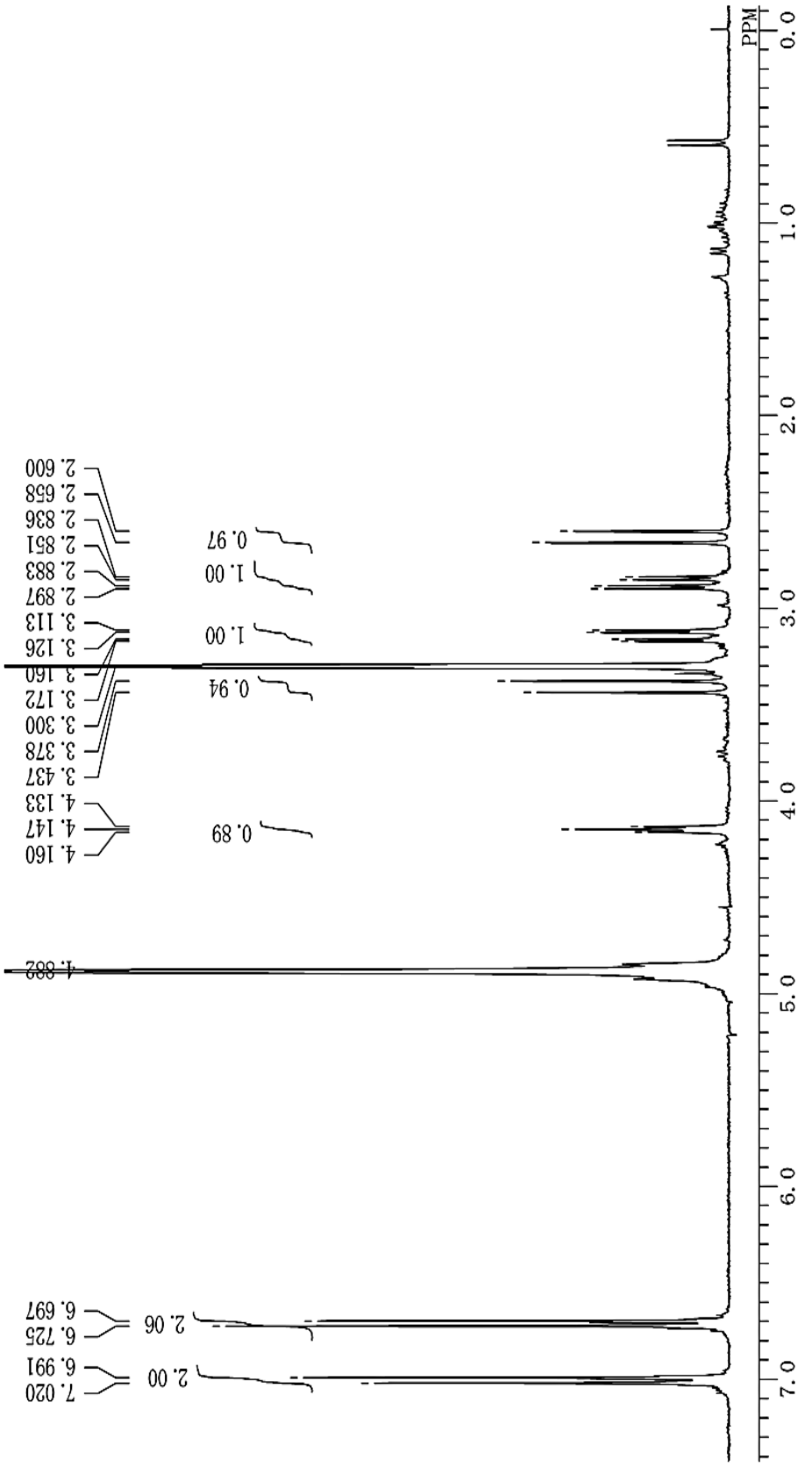

Figure 5.3.8.6 ^{1}H NMR (300 MHz; CD_3OD) spectrum of cyclo(Gly-Tyr) (16)

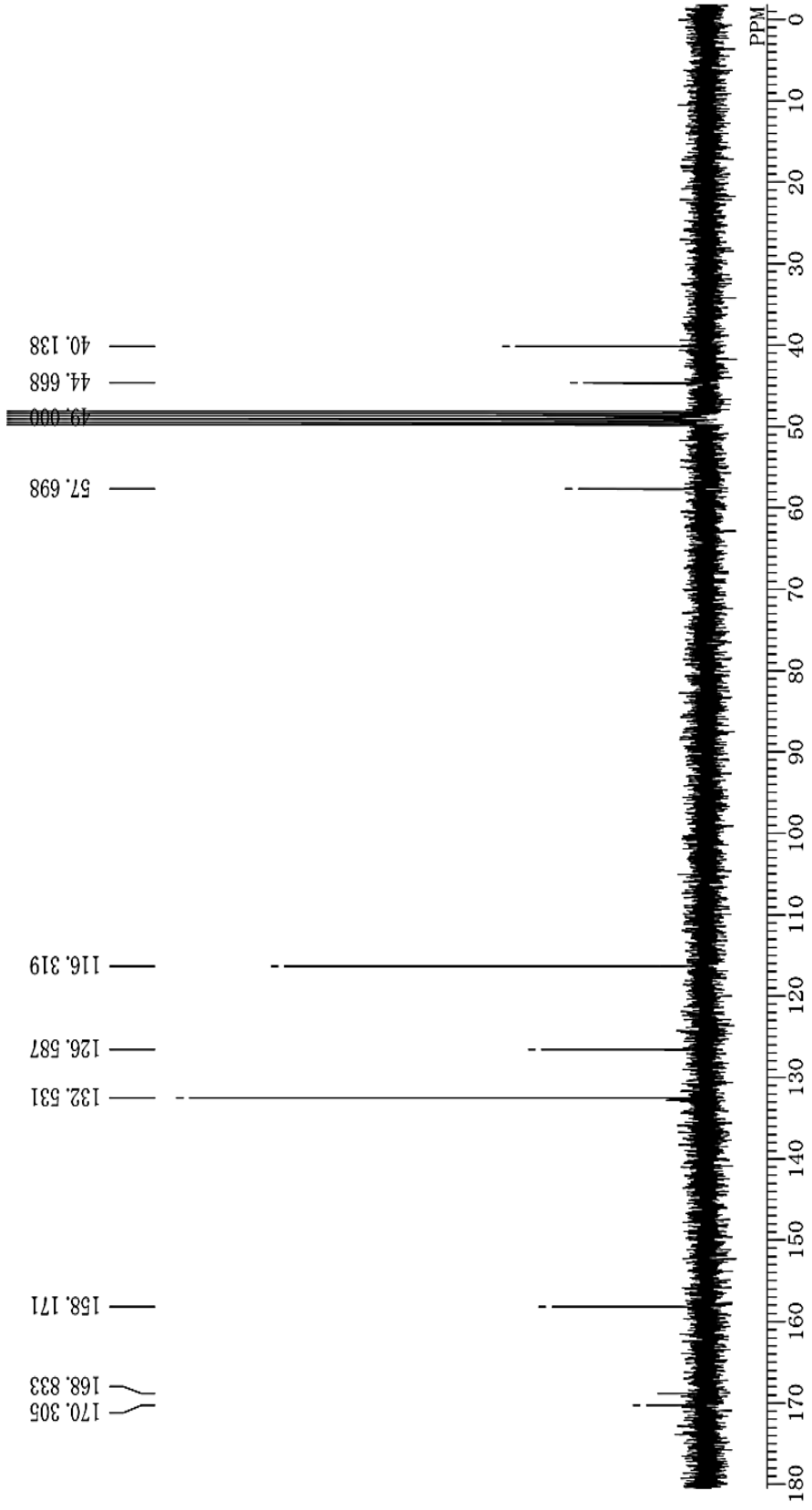

Figure 5.3.8.7 ^{13}C NMR (75 MHz, CD_3OD) Spectrum of cyclo(Gly-Tyr) (16)

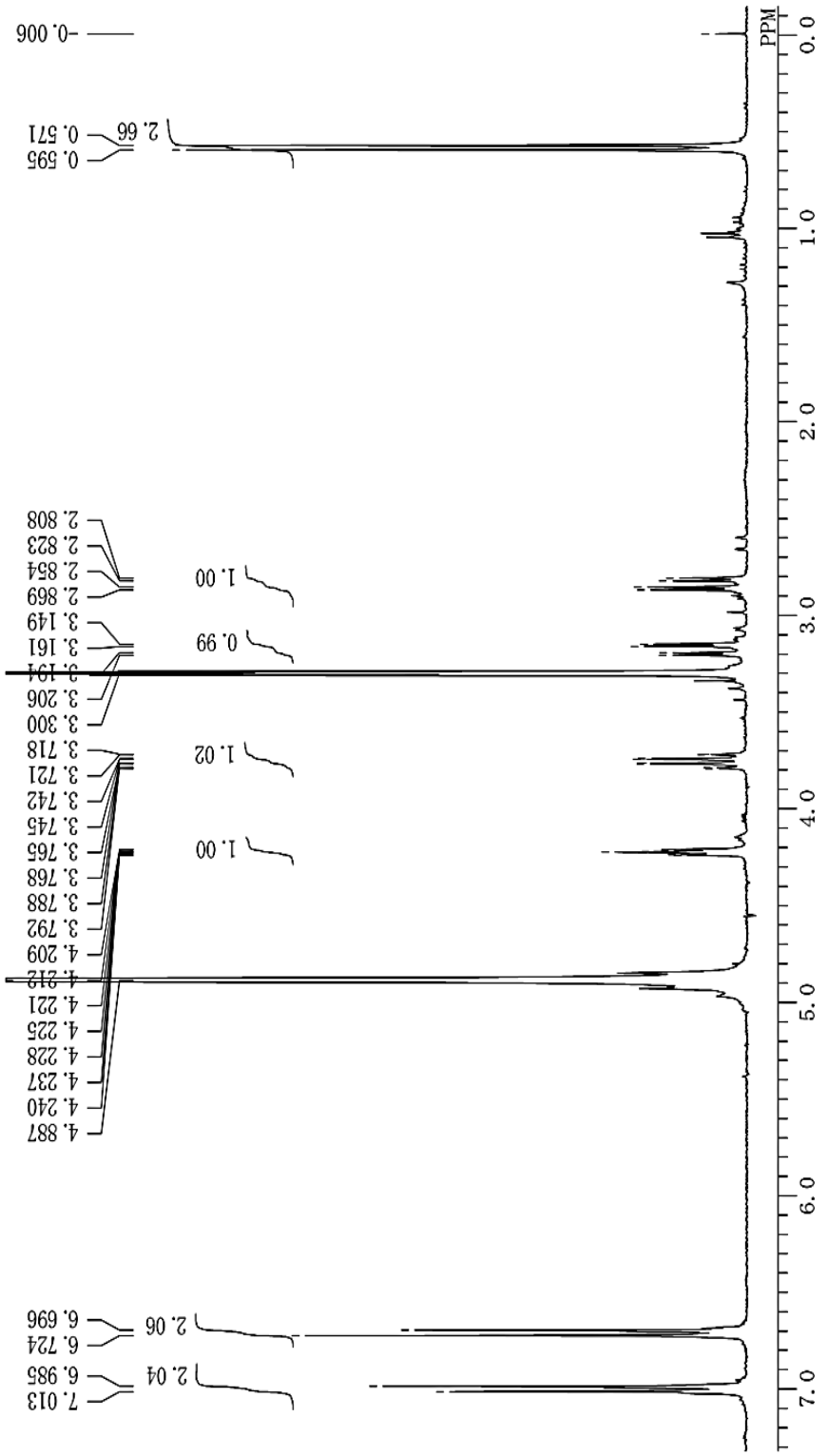

Figure 5.3.8.8 ^{1}H NMR (300 MHz, CD_3OD) Spectrum of cyclo(Ala-Tyr) (17)

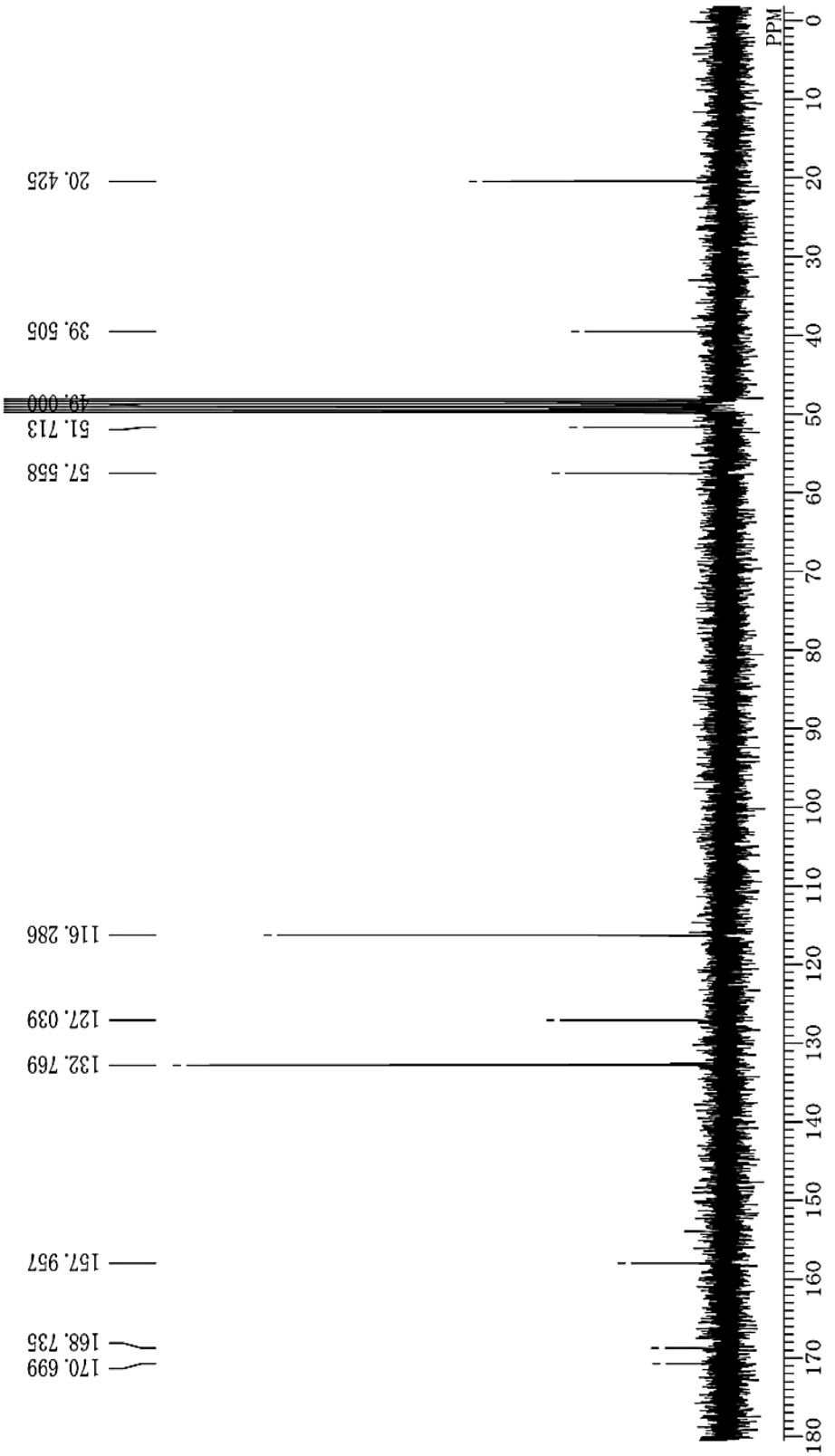

Figure 5.3.8.9 ^{13}C NMR (75 MHz, CD_3OD) Spectrum of cyclo(Ala-Tyr) (17)

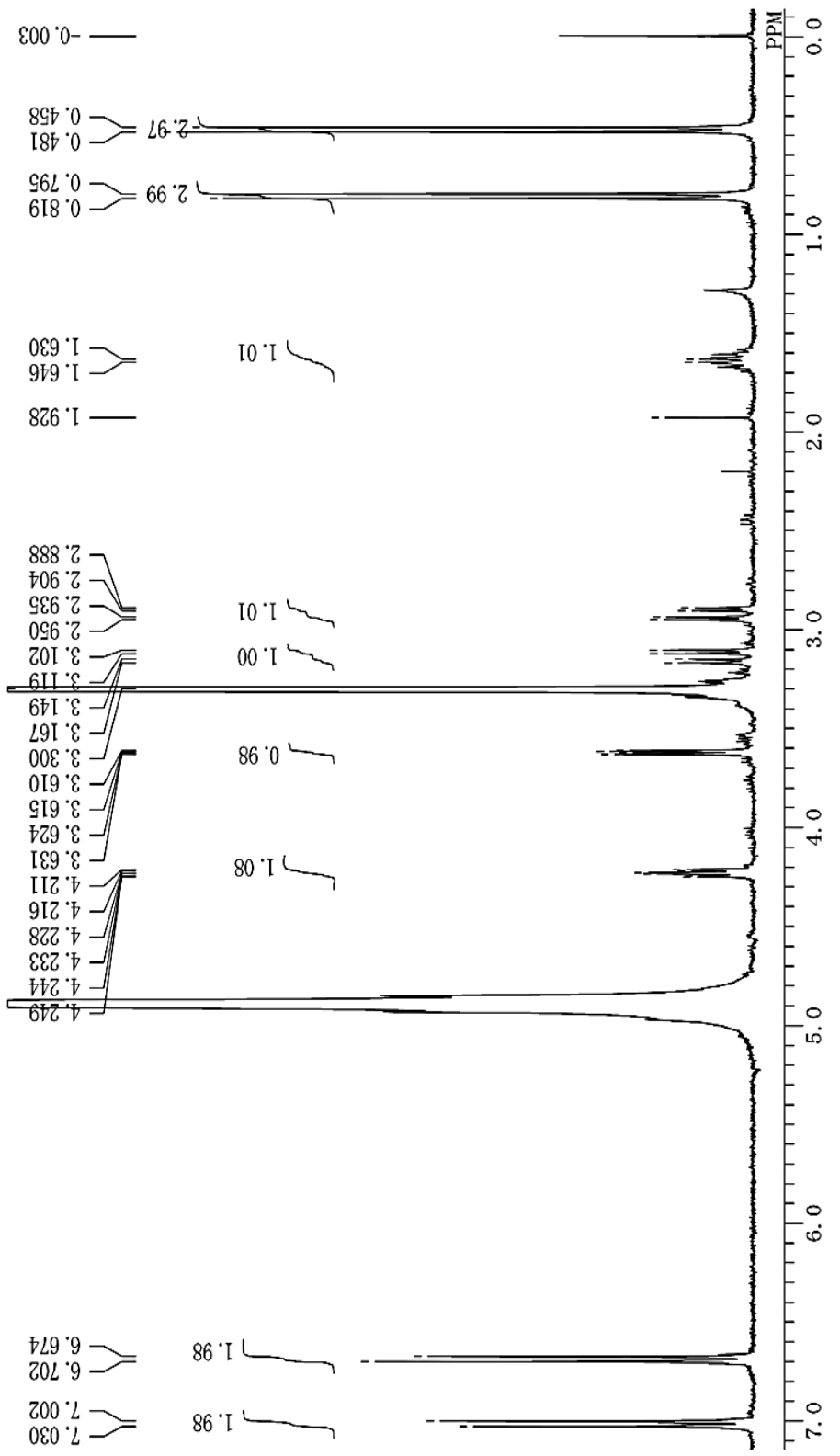

Figure 5.3.8.10 ^{1}H NMR (300 MHz, CD_3OD) Spectrum of cyclo(Val-Tyr) (18)

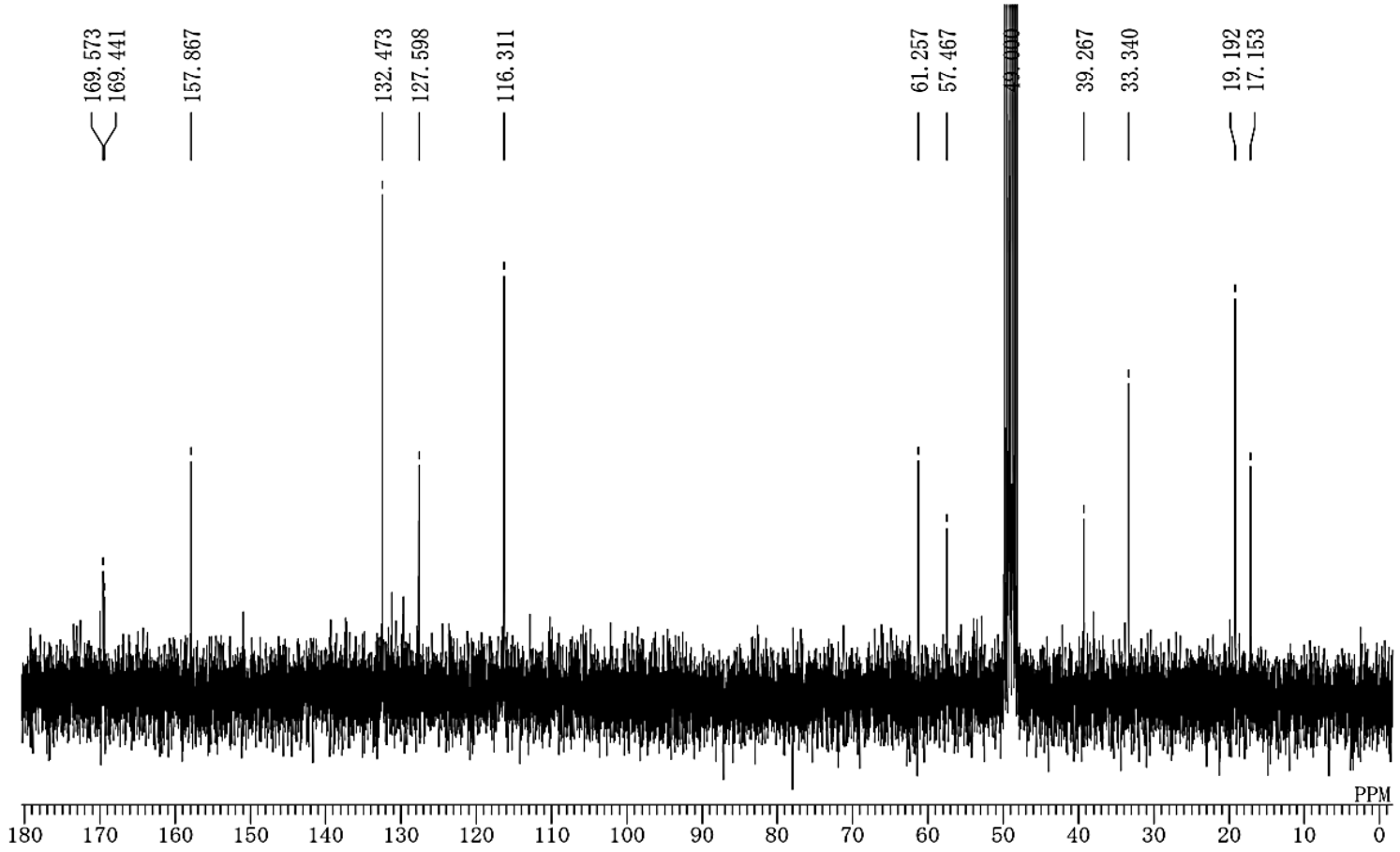

Figure 5.3.8.11 ^{13}C NMR (75 MHz, CD_3OD) Spectrum of cyclo(Val-Tyr) (18)

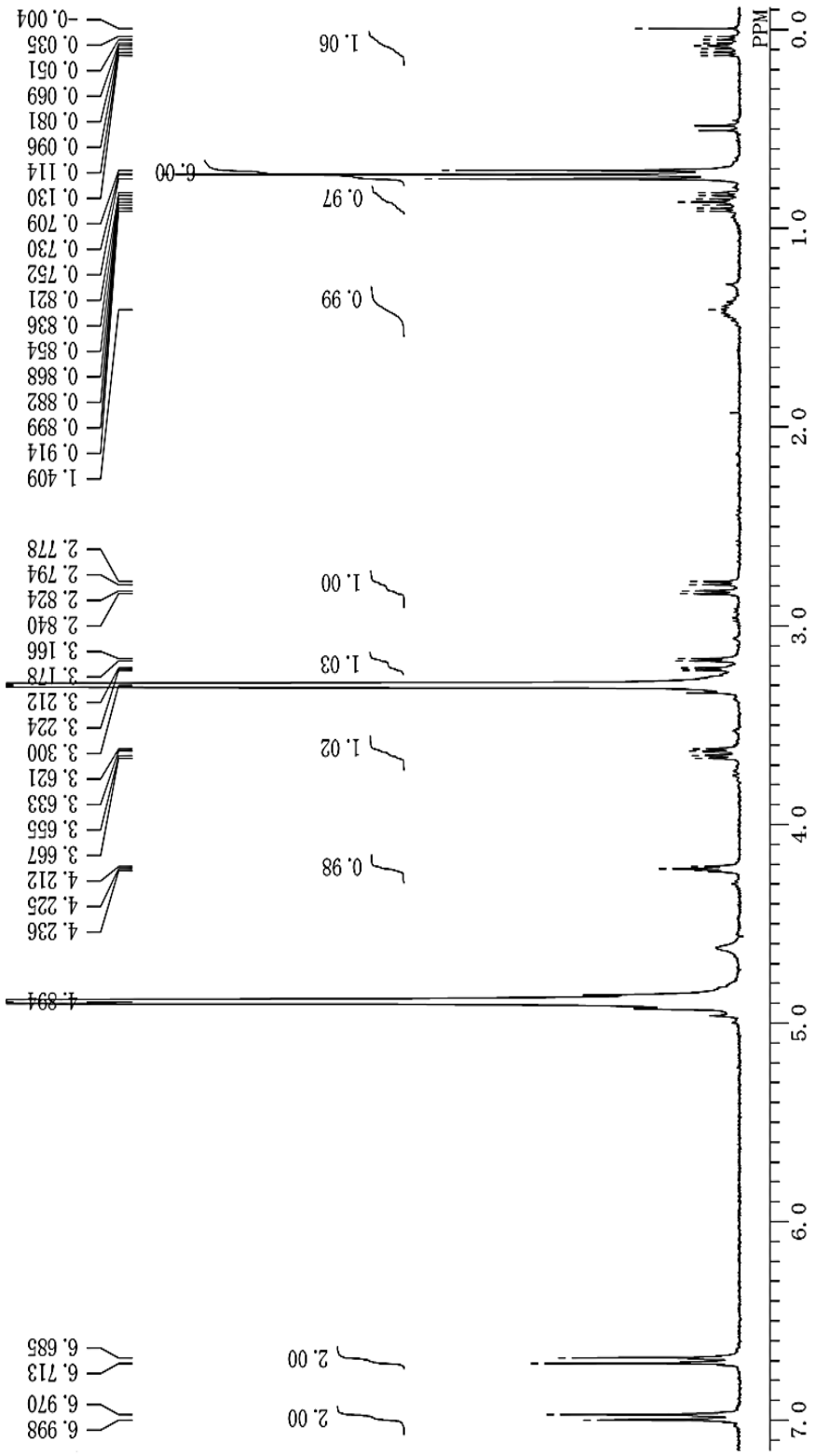

Figure 5.3.8.12 ^{1}H NMR (300 MHz, CD_3OD) Spectrum of cyclo(Leu-Tyr) (19)

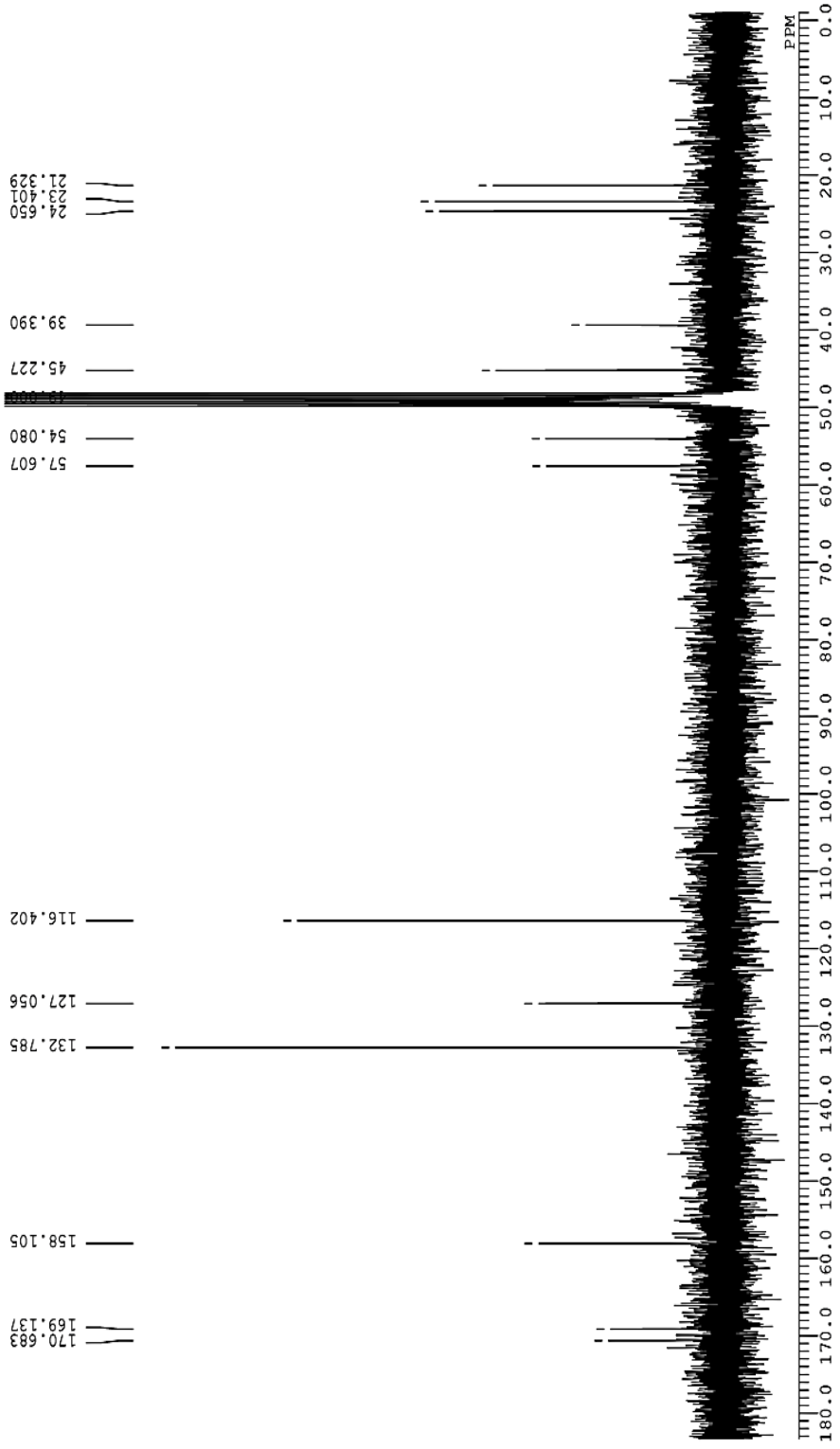

Figure 5.3.8.13 ^{13}C NMR (75 MHz, CD_3OD) Spectrum of cyclo(Leu-Tyr) (19)

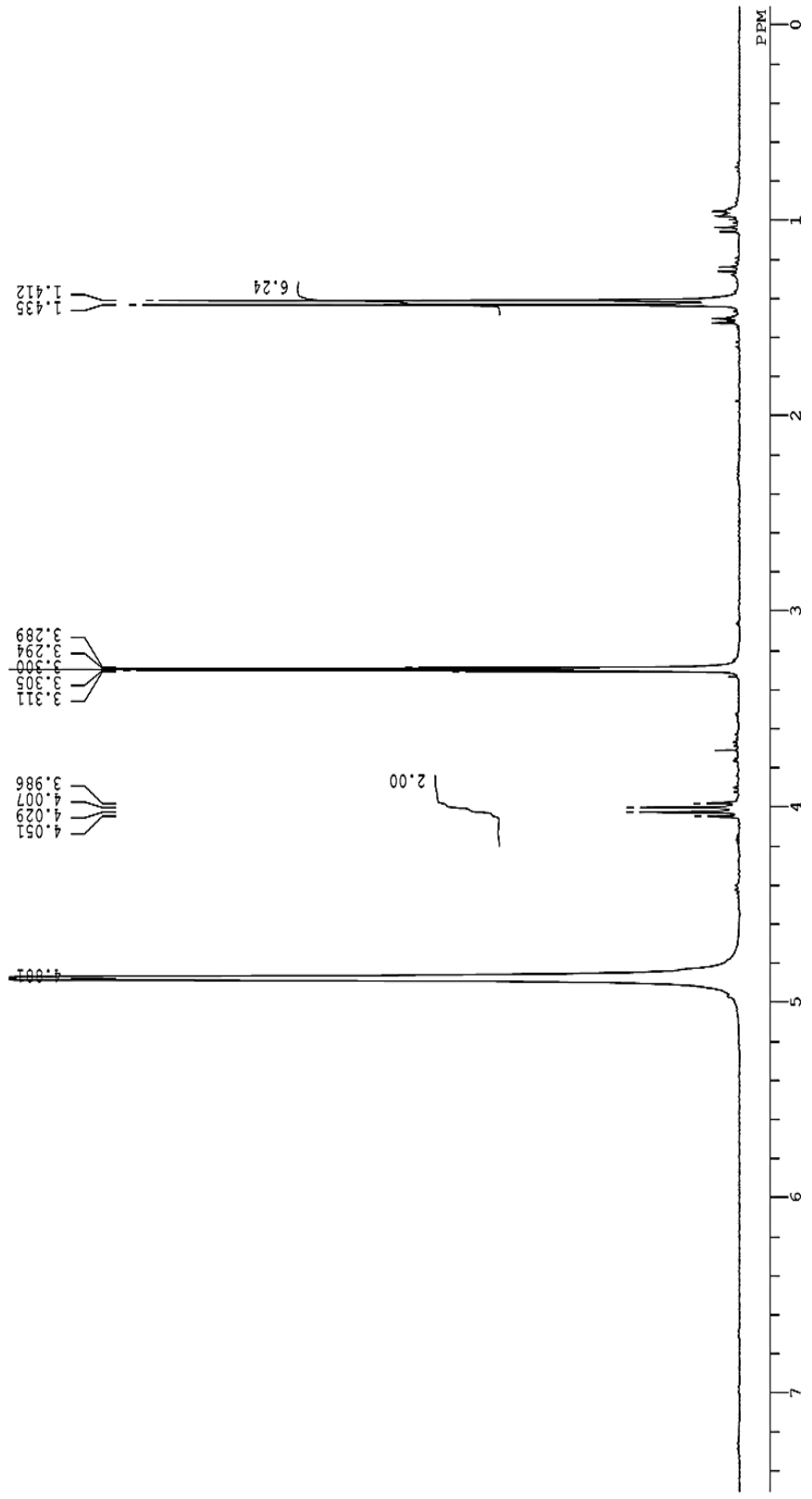

Figure 5.3.8.14 ^{1}H NMR (300 MHz, CD_3OD) Spectrum of cyclo(Ala-Ala) (20)

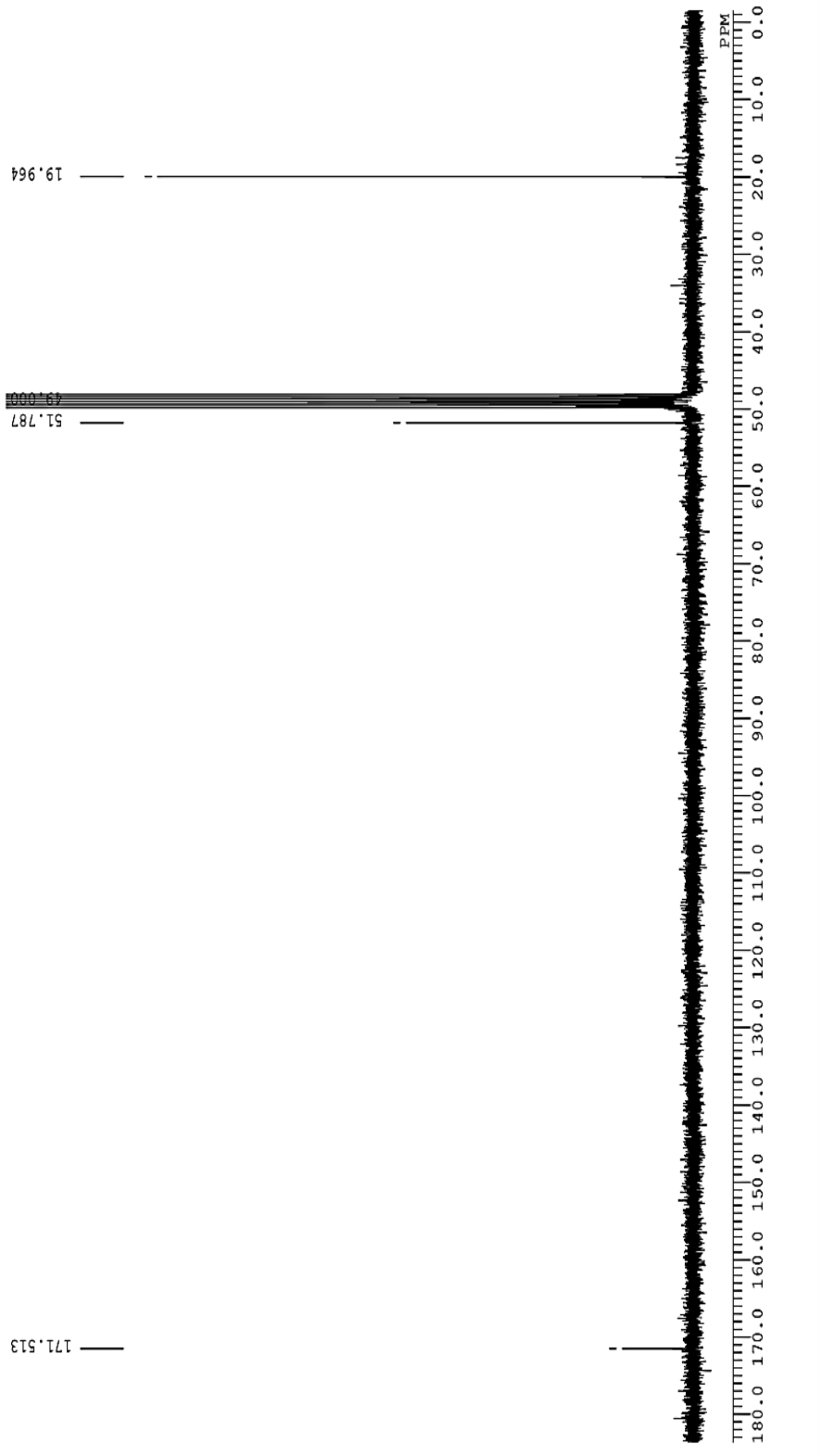

Figure 5.3.8.15 ^{13}C NMR (75 MHz, CD_3OD) Spectrum of cyclo(Ala-Ala) (20)

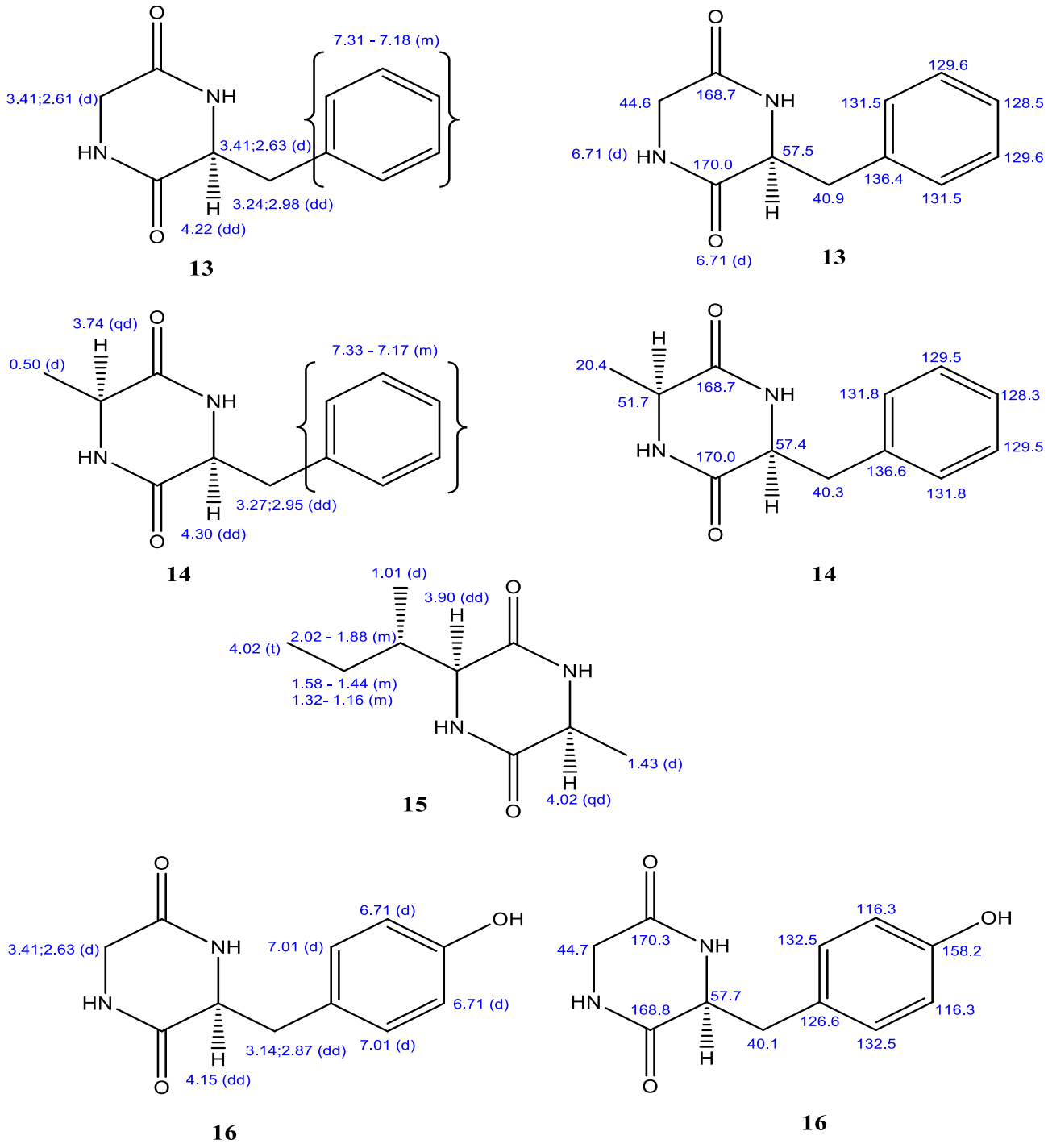

Figure 5.3.8.16a The chemical shift (δ_C and δ_H) values of compounds 13-16

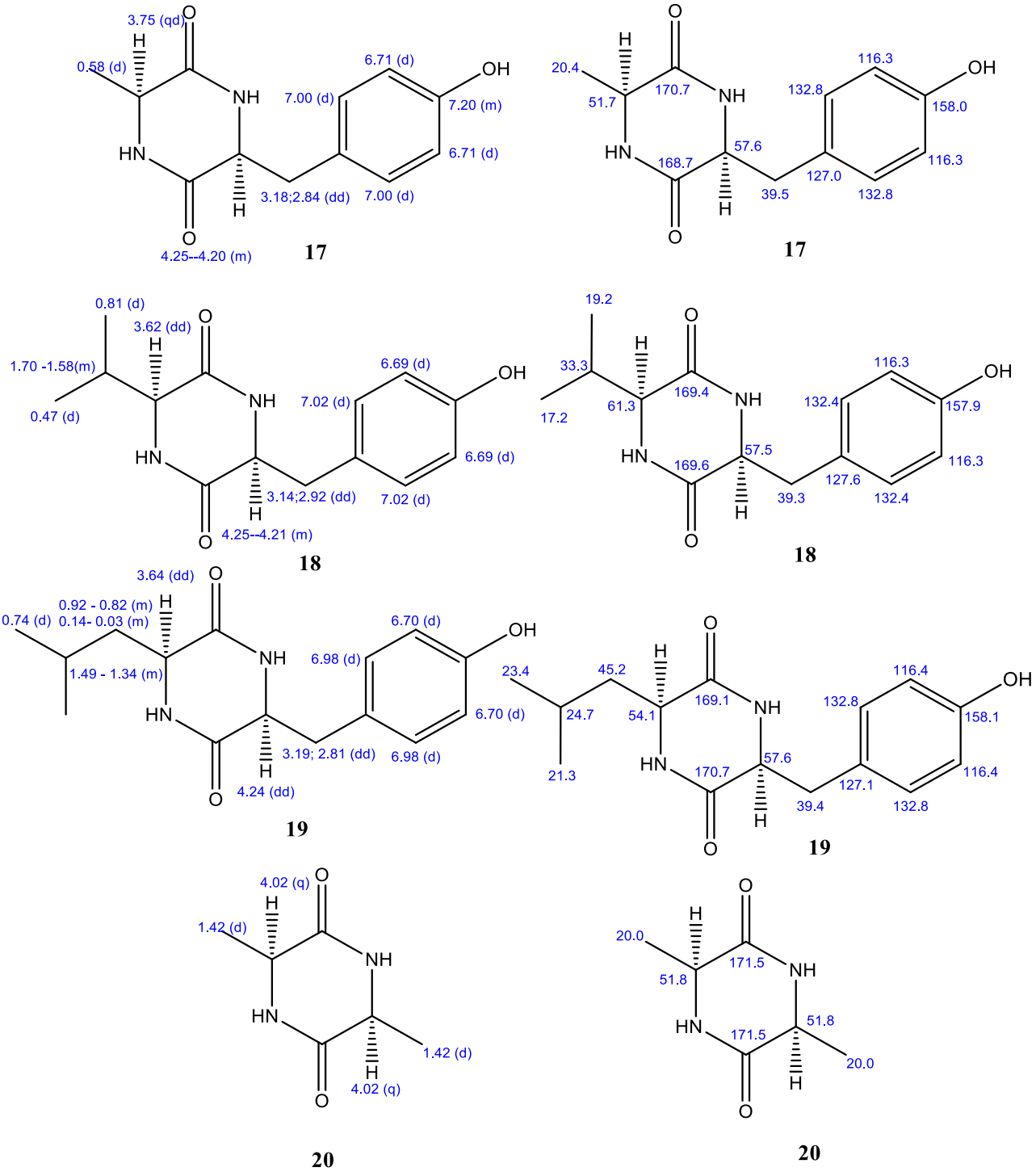

Figure 5.3.8.16b The chemical shift (δ_C and δ_H) values of compounds 17-20

Several reports describe the isolation of cyclic dipeptides from natural sources particularly those of microbial origin are found in the literature. Studies by Wei *et al.*, and his group reported the isolation of cyclo(Val-Pro), cyclo(Gly-Phe), cyclo(Phe-Tyr), cyclo(Leu-Tyr) and cyclo(Val-Leu) from *Streptomyces kunmingensis*, showing cytotoxicity against MCF-7 cancer cell line

(Wei *et al.* 2017). *Actinomycetes* and *Pencillium oxalicum* HSY-P-17 species had been reported as good sources for cyclic dipeptides (Liu *et al.* 2007). *Pseudomonas aurantiaca* derived cyclo(Pro-Tyr), cyclo(Val-Pro) and cyclo(Pro-Met) exhibited antifungal properties (Mehnaz *et al.* 2013). Cyclo(Val-Pro) obtained from *Asperigillus oryzae* (Shaaban *et al.* 2014) and *Nigrospora* species demonstrated cytotoxic action on HCT-116 cell lines (Chen *et al.* 2012). Furthermore, cyclic dipeptides extracted from *Bacillus cereus* exhibited antifungal activities (Xu *et al.* 2011). *Actinomycetes* 11014-originated cyclic dipeptides were found to possess antitumor properties (De-Hai *et al.* 2005) while cyclo(Val-Pro), cyclo (Leu-Pro) and cyclo(Phe-Pro) from *Streptomyces* demonstrated antineoplastic activity (Pettit *et al.* 2006). In addition, literature reports of secretions of cyclo(Val-Pro) and cyclo(Pro-Tyr) from *Pseudomonas fluorescens* (Guo *et al.* 2007), *Halobacillus litoralis* (Yang *et al.* 2002) and sponge *Tedania anhelans* (Parameswaran *et al.* 1997) substantiate the emerging interest on these compounds to develop as lead molecules. Nalli *et al.* described anti-inflammatory potential of isolated cyclic dipeptides cyclo(L-Pro-L-Val), cyclo(L-lle-D-Pro), cyclo(L-Leu-L-Pro), cyclo(D-Pro-L-Phe) from *Streptomyces sp*. (Nalli *et al.* 2017). Cyclo (L-Pro-L-Tyr), cyclo(L-Pro-L-Phe) and cyclo(L-Pro-L-Val) from *Pseudomonas aeruginosa* PAO1 showed anti-proliferative capacity by preventing phosphorylation of AKT and S6k kinases (Hernandez *et al.* 2017). Also, cyclo (L-Pro-D-Val) and cyclo (L-Pro-L-Tyr) isolated from *Bacillus sp*. HC001 and cyclo (L-Pro-D-Leu) derived from *Piscicoccus sp*. 12L081 effectively ameliorated LPS induced expression of HMGB-1 in sepsis (Lee *et al.* 2016).

Through the present study, *Pseudomonas sp.* (ABS-36) have been identified as a new source for seventeen cyclic dipeptides which include cyclo(Val-Pro) (**1**), cyclo(Val-Leu) (**3**), cyclo(Val-Phe) (**5**), cyclo(Leu-Leu) (**8**), cyclo(Pro-Tyr) (**10**), cyclo(Ala-Pro) (**11**), cyclo(Gly-Phe) (**13**), cyclo(Ala-Phe) (**14**), cyclo(Ala-Ile) (**15**), cyclo(Gly-Tyr) (**16**), cyclo(Ala-Tyr) (**17**), cyclo(Val-Tyr) (**18**), cyclo(Leu-Tyr) (**19**) and cyclo(Ala-Ala) (**20**). Proline based cyclic dipeptides were found to be major peptides secreted by *Pseudomonas* sp. They were further evaluated for *in vitro* and *in vivo* anti-inflammatory evaluations.

5.4 Cyclic dipeptides as potential pro-inflammatory cytokine inhibitors

The six proline based cyclic dipeptides, cyclo(Val-Pro) (**1**), cyclo(Leu-Pro) (**2**), cyclo(Leu-hydroxy-Pro) (**9**), cyclo(Pro-Tyr) (**10**), cyclo(Ala-Pro) (**11**), cyclo(Gly-Pro) (**12**) were first evaluated for their cytotoxicity in the LPS stimulated environment followed by the determination of their anti-inflammatory potential using supernatant from the same LPS

induced *RAW 264.7* cell lines. Mouse macrophages were treated with different concentrations of the compounds i.e. 3 μM, 10 μM, 30 μM and 100 μM.

5.4.1 Cell viability evaluation of isolated compounds in stimulated cells

Cell viability of cyclic dipeptides **1, 2, 9-12** was tested on LPS-stimulated RAW 264.7 mouse macrophages using rapid colorimetric MTT assay in order to confirm the anti-inflammatory nature of the compounds. Cells were treated with different concentration of compounds ranging from 3 μM to 100 μM as per the experimental design. Results of ELISA study and MTT assay revealed cyclic dipeptides to be non-cytotoxic in LPS-stimulated RAW 264.7 cell lines with IC_{50} values ranging from 270-450 μM. Figure 5.4.1 presents the detailed result of % cell viability effect of tested compounds.

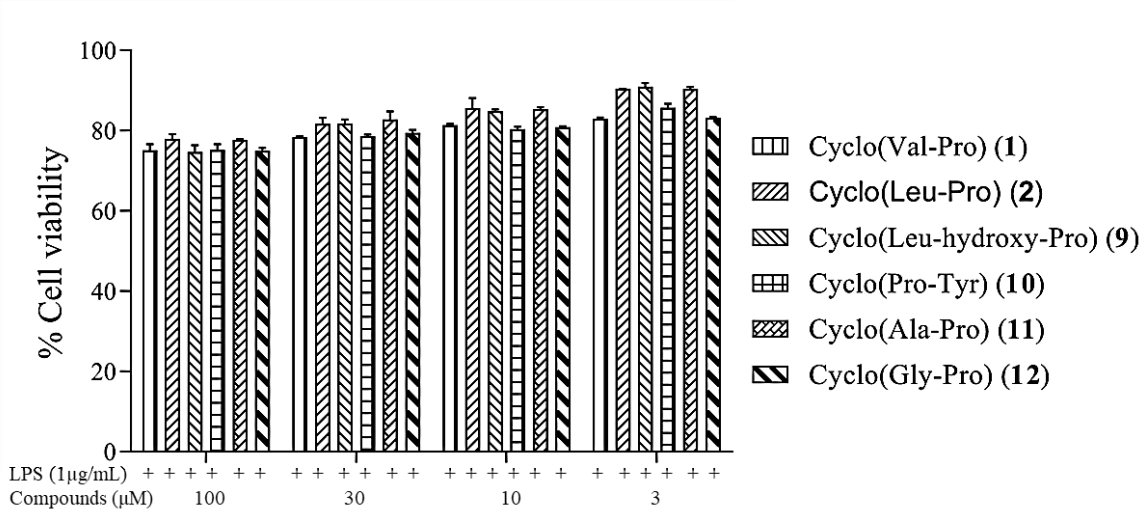

Figure 5.4.1: Effect of cyclic dipeptides on cell viability of LPS-stimulated RAW cells. Figure shows the effect of treatment of cells with the varied concentration (3, 10, 30, 100 μM) of cyclic dipeptides **1, 2, 9-12**, followed by LPS stimulation for 24 h through MTT assay. The values are presented as mean ± SEM from triplicate

5.4.2 *In vitro* IL-1β inhibitory effect of cyclic dipeptides in LPS and calcium oxalate induced model

The supernatant collected from the treated cells was subjected to IL-1β ELISA estimations and the results were found to be significant with IC_{50} values ranging from 44 to 62 μM (Table 5.3.1). At 100 μM concentration, cyclo(Ala-Pro) (**11**), cyclo(Pro-Tyr) (**10**) and cyclo(Gly-Pro) (**12**) attenuated IL-1β level by 69.65%, 69.45% and 67.77%, respectively. Nevertheless, compounds cyclo(Val-Pro) (**1**), cyclo(Leu-hydroxy-Pro) (**9**) and cyclo(Leu-Pro) (**2**) caused downregulation of IL-1β by 66.12%, 63.28% and 61.42%, respectively at the same concentration (Figure 5.4.2) (Table 5.4.1). Prednisolone, corticosteroid prescribed for the treatment of a wide range of

inflammatory and autoimmune diseases, was used as a reference standard at 10 μM dose, which showed 60.70% inhibition of IL-1β (Table 5.4.1).

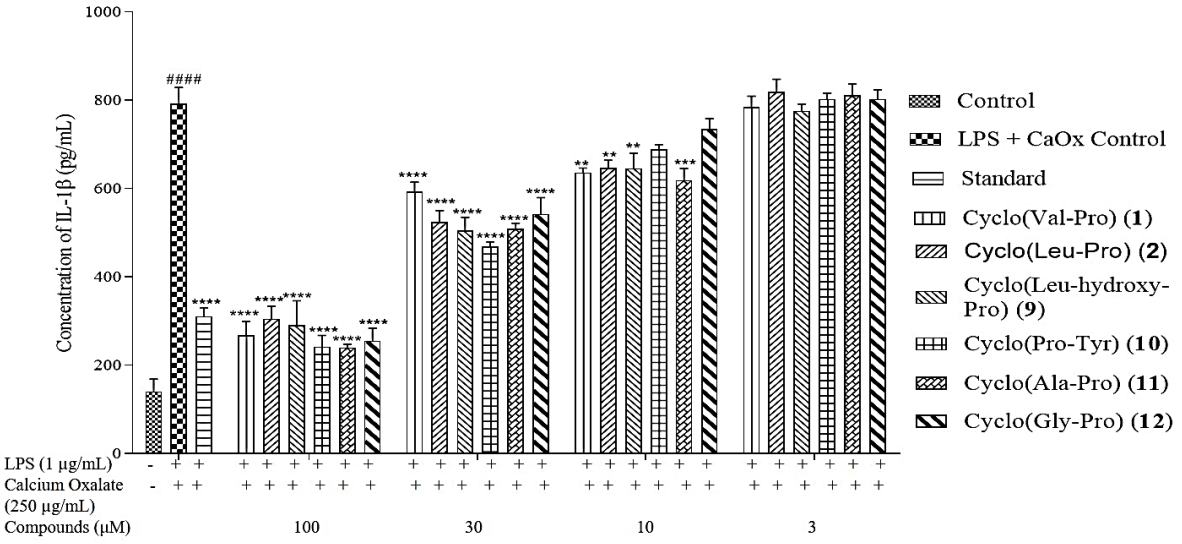

Figure 5.4.2 Inhibitory effect of compounds 1, 2, 9-12 on LPS and oxalate-crystal induced IL-1β in RAW 264.7 cells. Cells were treated with the indicated concentrations of cyclic dipeptides for 1 h and then incubated with LPS (1 μg/mL) and calcium oxalate crystals (250 μg/mL) for 24 h. Supernatant collected after incubation was used for estimating IL-1β levels using ELISA kit. The values are presented as mean ± SEM from triplicate. $^{####}P < 0.0001$ vs. Normal control, $^{****}P < 0.0001$ vs. LPS and calcium oxalate control, $^{***}P < 0.001$ vs. LPS calcium oxalate control, $^{**}P < 0.01$ vs. LPS and calcium oxalate control.

5.4.3 Effect of cyclic dipeptides on LPS-induced TNF-α and IL-6 levels using ELISA studies

Mouse macrophages were treated with different concentrations of the cyclic dipeptides **1, 2, 9-12** as per the experimental protocol. ELISA assay was carried out on the collected supernatant to estimate the TNF-α and IL-6 production. Cyclic dipeptides revealed promising results in attenuating pro-inflammatory cytokines. At 100 μM concentration, cyclo(Val-Pro) (**1**), cyclo(Gly-Pro) (**12**) and cyclo(Ala-Pro) (**11**) exhibited 47.85%, 44.33% and 43.10% reduction in TNF-α levels, respectively. Other compounds, cyclo(Leu-Pro) (**2**), cyclo(Leu-hydroxy-Pro) (**9**) and cyclo(Pro-Tyr) (**10**) reduced TNF-α levels by 37.68%, 35.96% and 35.90%, respectively at 100 μM concentration (Figure 5.4.3.1) (Table 5.4.1). The reference drug prednisolone showed 43.71% downregulation in TNF-α levels at 10 μM concentration. The IC_{50} values of tested compounds are presented in Table 5.4.2.

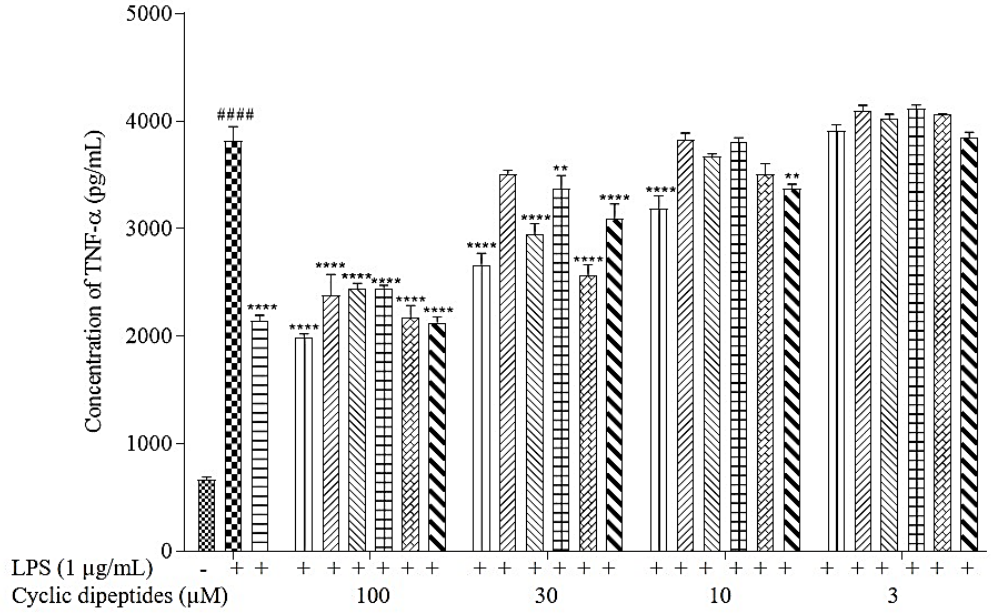

Figure 5.4.3.1: TNF-α inhibitory effect of cyclic dipeptides 1, 2, 9-12 on LPS induced RAW 264.7 cells. The cells were treated with the indicated concentrations of cyclic dipeptides **1**, **2**, **9-12** for 1 h and then incubated with LPS (1 μg/mL) for 24 h. Collected supernatant was used for determining TNF-α levels using ELISA kit. The values are presented as mean ± SEM from triplicate. $^{####}P < 0.0001$ vs. Normal control, $^{****}P < 0.0001$ vs. LPS control, $^{**}P < 0.01$ vs. LPS control.

Cyclic dipeptides significantly abrogated IL-6 levels with IC_{50} values ranging from 40-105 μM (Table 5.4.1). Cyclo(Val-Pro) (**1**) exhibited IC_{50} of 40.2 μM and 62.04% reduction in IL-6 levels at 100 μM concentration. On the other hand, prednisolone reduced IL-6 by 57.47% at 10 μM. Cyclo(Leu-Pro) (**2**), cyclo(Leu-hydroxy-Pro) (**9**), cyclo(Pro-Tyr) (**10**), cyclo(Ala-Pro) (**11**) and cyclo(Gly-Pro) (**12**) decreased IL-6 levels by 61.20%, 56.84%, 66.89%, 50.97% and 53.44%, respectively at 100 μM concentration (Figure 5.4.3.2) (Table 5.4.1).

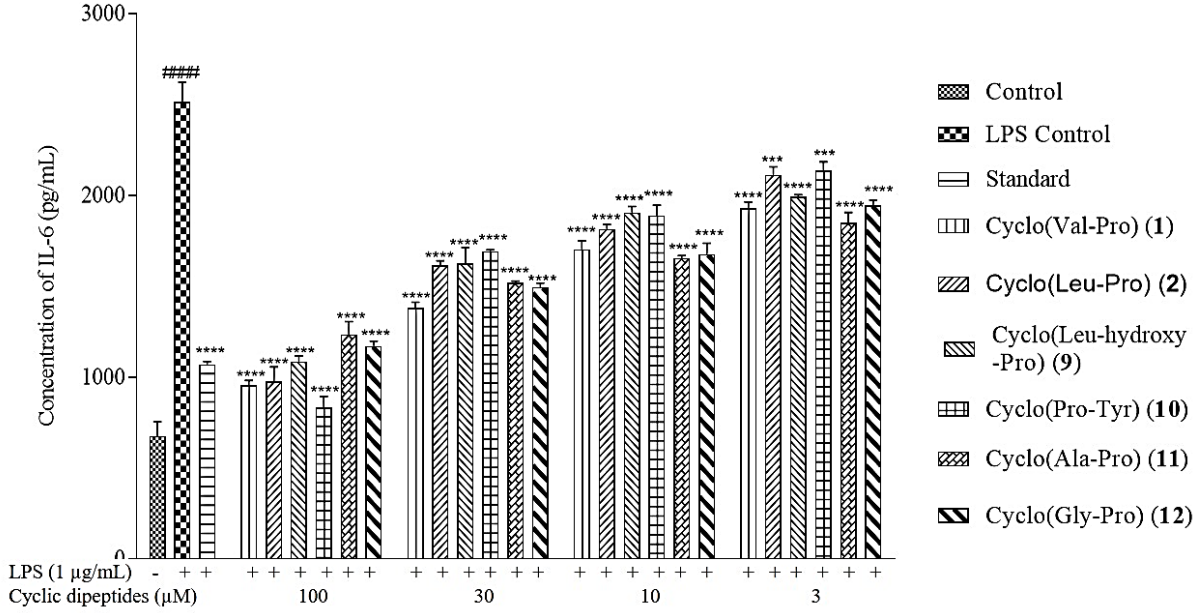

Figure 5.4.3.2: Effect of cyclic dipeptides 1, 2, 9-12 on LPS induced IL-6 levels in mouse macrophages using ELISA estimations. Cells were treated with the indicated concentrations 3, 10, 30 and 100 μM of cyclic dipeptides **1**, **2**, **9-12** for 1 h and then primed with LPS (1 μg/mL) for 24 h. Collected supernatant was used for estimating IL-6 levels using ELISA kit. The values are presented as mean ± SEM from triplicate. $^{\#\#\#\#}P < 0.0001$ vs. Normal control, $^{****}P < 0.0001$ vs. LPS control, $^{***}P < 0.001$ vs. LPS control.

In vitro assays were designed to test the efficacy of the isolated compounds in attenuating pro-inflammatory cytokine levels. LPS used in the assays exerts inflammatory action by binding to TLR4 receptor. Cyclic dipeptides showed significant alleviation of the LPS-induced cytokine levels at 10, 30 and 100 μM concentrations and the effect was comparable to that of standard prednisolone tested at 10 μM concentration. Prednisolone inhibited IL-1β, TNF-α and IL-6 levels by 60.70%, 43.71% and 57.47%, respectively. Thus, treatment with cyclic dipeptides elicited protective anti-inflammatory effect by suppressing pro-inflammatory cytokines IL-1β, TNF-α and IL-6.

5.4.4 Evaluation of inhibitory effect of cyclic dipeptides 1, 2, 9-12 on LPS-induced nitric oxide (NO) production

Cyclic dipeptides significantly lowered LPS-induced NO levels in RAW 264.7 cell lines ($P < 0.01$ vs. LPS control) at 100 μM concentration. Cyclo(Leu-hydroxy-Pro) (**9**) exhibited IC_{50} value of 75.13 μM and cyclo(Pro-Tyr) (**10**) showed 42.69 μM (Table 5.4.1). Percentage inhibition by all cyclic dipeptides **1, 2, 9-12** is summarised and presented in Table 5.4.1 and Figure 5.4.4. All

these results yielded a positive indication to further evaluate the efficacy of these compounds under *in vivo* models of inflammation.

Table 5.4.1 Percentage cell viability and percentage inhibition of TNF-α, IL-6, IL-1β and NO by cyclic dipeptides

Compounds	Concentration (µM)	% Cell viability	% Inhibition			
			TNF-α	IL-6	IL-1β	NO
Standard (Prednisolone)	10	-	43.71±1.22	57.47±1.08	60.70±4.13	59.20±8.03
1	100	75.16±3.72	47.85±3.75	62.04±1.83	66.12±6.62	38.84±3.98
	30	78.40±4.01	30.22±3.01	45.07±2.05	25.11±4.70	21.53±3.19
	10	81.35±3.98	16.53±2.93	32.30±3.22	19.64±2.22	ND
	3	82.95±3.21	ND	23.32±2.33	0.96±5.49	ND
2	100	77.96±4.74	37.68±2.93	61.20±5.44	61.42±1.87	40.88±1.06
	30	81.72±5.33	8.03±4.01	35.75±1.62	33.77±0.35	23.65±5.25
	10	85.61±3.75	ND	27.83±1.65	18.34±1.62	16.44±1.42
	3	90.44±7.05	ND	16.00±2.90	ND	ND
9	100	74.72±2.01	35.96±4.09	56.84±2.09	63.28±1.10	55.28±5.97
	30	81.77±5.10	22.72±5.01	35.40±6.11	36.21±6.5	31.24±2.74
	10	84.87±6.33	3.84±2.07	24.24±2.25	18.50±7.5	18.79±2.54
	3	90.93±4.03	ND	20.80±0.74	1.98±3.10	ND
10	100	75.2±1.95	35.90±2.87	66.89±4.22	69.45±2.34	60.77±3.84
	30	78.61±1.94	11.76±2.88	32.76±0.65	40.76±2.45	44.40±3.03
	10	80.39±5.05	0.41±3.96	24.89±3.87	13.05±3.87	36.26±2.01
	3	85.72±4.92	ND	15.09±3.31	ND	ND
11	100	77.67±4.92	43.10±2.97	50.97±4.99	69.65±3.05	53.48±1.97
	30	82.8±4.3	32.76±3.42	39.67±0.75	35.68±3.89	25.05±2.35
	10	85.39±2.74	8.18±2.96	34.25±1.02	21.88±4.05	2.19±0.24
	3	90.41±2.01	ND	26.50±3.87	ND	ND
12	100	74.98±4.02	44.33±4.74	53.44±1.88	67.77±6.32	31.01±1.75
	30	79.48±0.7	19.01±5.06	40.58±1.47	31.51±8.12	23.96±3.94
	10	80.87±2.07	11.69±6.34	33.35±4.09	7.16±5.11	16.36±2.03
	3	83.18±2.56	ND	22.63±1.88	ND	ND

ND: Not detected

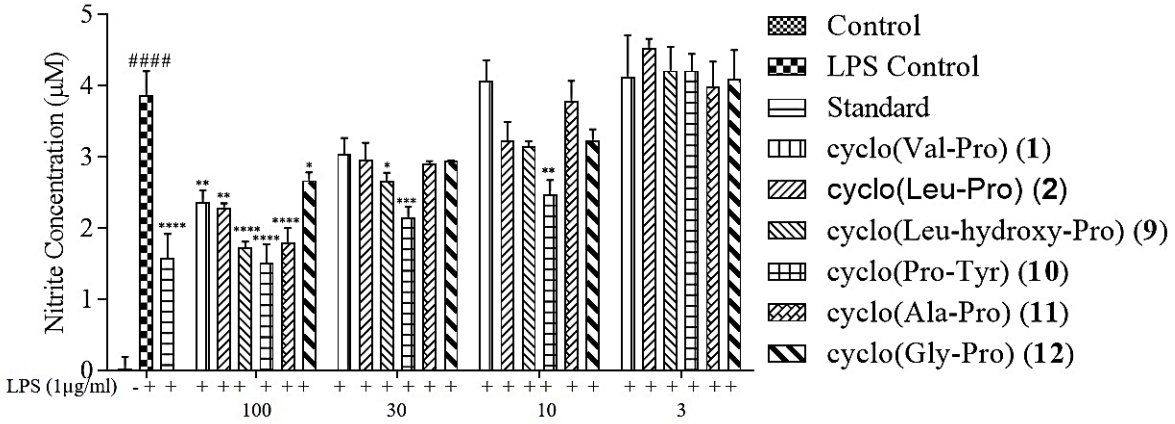

Figure 5.4.4: Inhibitory effect of cyclic dipeptides 1, 2, 9-12 on LPS induced NO production in RAW 264.7 cells. Cells were treated with the predetermined concentration of cyclic dipeptides **1**, **2**, **9-12** one hour prior to the stimulation with LPS (1 μg/mL) for 24 h. Collected supernatant was assessed for NO levels using Griess method. The values are presented as mean ± SEM from triplicate. $^{\#\#\#\#}P < 0.0001$ vs. Normal control, ****$P < 0.0001$vs. LPS control, *** $P < 0.001$ vs. LPS control, ** $P < 0.01$ vs. LPS control, * $P < 0.05$ vs. LPS control.

Table 5.4.2 IC_{50} values of 1, 2, 9-12 cyclic dipeptides determined under LPS-induced pro-inflammatory cytokines assay, Griess assay and cell viability assay

Estimated parameter	IC_{50} values (μM) of compounds					
	1	**2**	**9**	**10**	**11**	**12**
IL-1β	61.77	60.09	54.96	**44.70**	44.82	56.4
TNF-α	**115.38**	457.83	318.56	449.64	136.01	223.22
IL-6	**40.2**	57.53	80.0	50.71	104.05	74.59
NO	259.17	153.07	75.13	**42.69**	110.07	473.85
Cell viability	439.45	355.94	270.36	392.68	348.44	431.07

5.5 Evaluation of anti-inflammatory efficacy of cyclic dipeptides (1, 2, 9-12) using renal injury models

On perceiving the beneficial role of cyclic dipeptides **1**, **2** and **9**–**12** in effectively suppressing pro-inflammatory cytokines (IL-1β, TNF-α and IL-6) and NO secretions under LPS- induced *in vitro* model, their anti-inflammatory potential was further examined under various mouse model of renal injury. All compounds showed significant activity in alleviating IL-1β levels (IC_{50} values ranging between 44.7 – 61.8 μM) and as IL-1β plays putative role in pathophysiology

of various inflammatory disorders especially in renal injury, these compounds might effectively control renal disorders. The *in vivo* study was done in accordance with the protocols prepared as per standard guidelines and approved by Institutional Animal Ethical Committee [IAEC approval number: BITS-Hyd/IAEC/2017/10].

5.5.1 Oxalate induced renal nephropathy model

Renal nephropathy developed using sodium oxalate crystals is characterised by the formation of calcium oxalate crystals in renal tubular and interstitial region that causes damage to tubules, induces inflammation and subsequently progresses to renal failure. Briefly, in oxalate nephropathy model, C57/BL6 male mice were categorised into eight different groups: group-1 (normal control), group 2 (oxalate treatment), group 3 (Cyclo(Val-Pro) (**1**) treatment), group 4 (Cyclo (Leu-Pro) (**2**) treatment), group 5 (Cyclo(Leu-Hydroxy-Pro) (**9**) treatment), group 6 (Cyclo (Pro-Tyr) (**10**) treatment), group 7 (Cyclo (Pro-Ala) (**11**) treatment) and group 8 (Cyclo (Gly-Pro) (**12**) treatment). All compounds were prepared as suspension in 9:1 methylcellulose and Tween 20 mixture and administered at 50 mg/kg body weight dose using oral gavage one hour prior to administration of sodium oxalate crystals. A random dose of 50 mg/kg was selected for initial testing of efficiency. Renal nephropathy was induced by injecting 75 mg/kg body weight dose of sodium oxalate by intraperitoneal route. After 24 h of induction, mice were sacrificed and their blood samples and kidney tissue samples were collected for evaluation. Damage to kidney tissue by oxalate crystals was assessed by determining the IL-1β and blood urea nitrogen (BUN) levels in plasma, expression of KIM-1 (kidney injury marker) and expression of inflammatory markers IL-1β, IL-6 and TNF-α in renal tissue. Also, histological evaluation was carried out in renal tissue using H&E staining.

5.5.1.1 Estimation of plasma IL-1β levels using ELISA assay in oxalate-induced renal nephropathy model

Cyclic dipeptides cyclo(Val-Pro) (**1**), cyclo(Leu-Pro) (**2**), cyclo(Leu-hydroxy-Pro) (**9**), cyclo(Pro-Tyr) (**10**), cyclo(Ala-Pro) (**11**), cyclo(Gly-Pro) (**12**) significantly attenuated oxalate induced plasma IL-1β levels ($P < 0.001$ vs. oxalate control). Cyclo(Val-Pro) (**1**) showed 57% reduction in elevated plasma IL-1β levels, cyclo(Leu-Pro) (**2**) lowered it by 48.12% and cyclo(Leu-Hydroxy-Pro) (**9**) showed 36.97% inhibition as indicated in ELISA studies (Figure 5.5.1.1). Table 5.5.1 demonstrates the percentage inhibition of plasma IL-1β levels by all cyclic dipeptides.

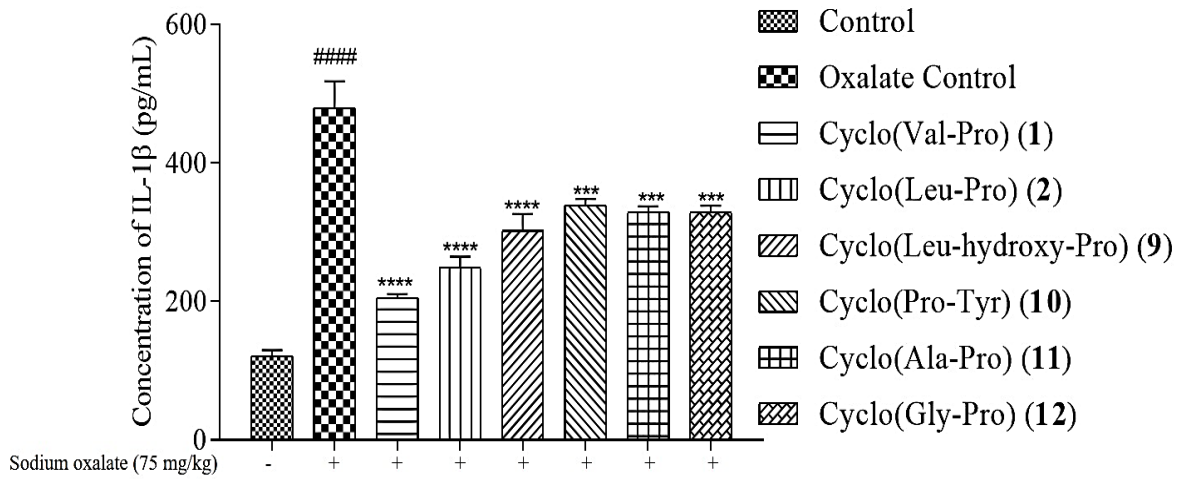

Figure 5.5.1.1 Inhibitory effect on plasma IL-1β levels by cyclic dipeptides 1, 2, 9-12 treatment in oxalate crystal induced renal nephropathy model. Figure demonstrates the inhibition effect of cyclic dipeptides **1**, **2**, **9-12** on plasma IL-1β levels at 50 mg/kg oral dose in oxalate crystals-treated animals. All values were presented as mean ± SEM (n=6). ($^{####}P$<0.0001 vs. Normal control, ***P<0.001 vs. oxalate control, ****P<0.0001 vs. oxalate control).

Table 5.5.1 Percentage inhibition of plasma IL-1β levels by all cyclic dipeptides under oxalate induced renal nephropathy model

S. No.	Compounds	% Inhibition of plasma IL-1β
1.	Cyclo(Val-Pro) (**1**)	**57.07**
2.	Cyclo(Leu-Pro) (**2**)	48.12
3.	Cyclo(Leu-hydroxy-Pro) (**9**)	36.97
4.	Cyclo(Pro-Tyr) (**10**)	29.30
5.	Cyclo(Ala-Pro) (**11**)	31.49
6.	Cyclo(Gly-Pro) (**12**)	31.46

5.5.1.2 Attenuation of blood urea nitrogen levels

Cyclic dipeptides markedly lowered plasma BUN levels (a renal functional marker) indicating the protection against the damage induced by oxalate nephropathy. Cyclo(Leu-Pro) (**2**) attenuated BUN levels by 19.57%, while compound cyclo(Val-Pro) (**1**) significantly attenuated BUN levels with P value of < 0.05 and 35.21% inhibition at 50 mg/kg body weight dose as illustrated in Figure 5.5.1.2.

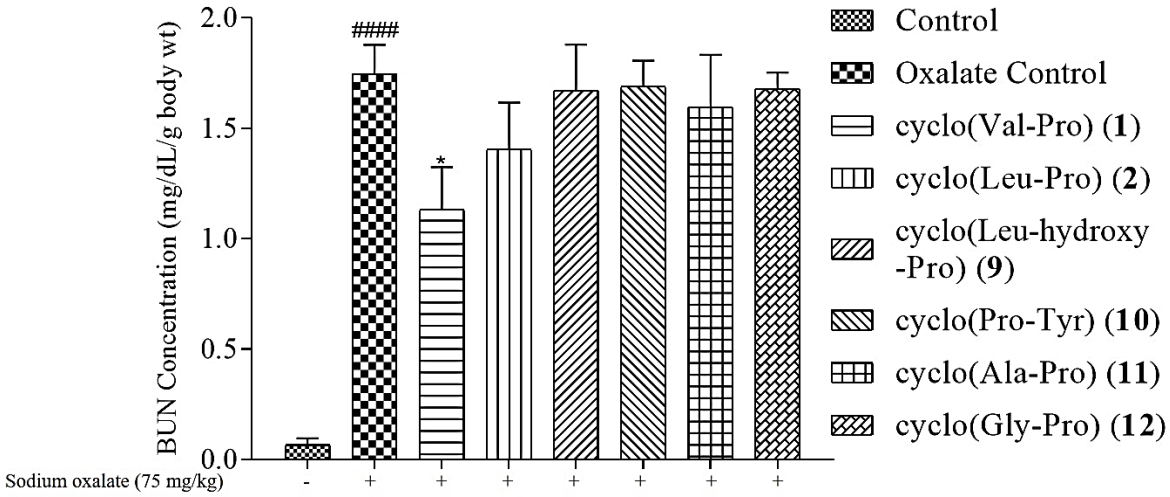

Figure 5.5.1.2 Plasma BUN inhibition effect of cyclic dipeptides in oxalate crystal induced renal nephropathy model. Figure demonstrates the inhibition effect of **1, 2, 9-12** at the dose of 50 mg/kg on plasma BUN levels induced by oxalate crystals. (The values are presented as mean ±SEM (n=6). $^{####}P<0.0001$ vs. Normal control, $^{*}P < 0.05$ vs. oxalate control)

5.5.1.3 Assessment of mRNA gene expression of renal injury markers and inflammatory markers

Among the tested cyclic dipeptide, cyclo(Val-Pro) (**1**) was found to be most effective in controlling the secretions of plasma IL-1β and BUN levels. Hence, cyclo(Val-Pro) (**1**) treatment group samples were evaluated for mRNA expression study of kidney injury marker KIM-1 and pro-inflammatory markers IL-1β, TNF-α and IL-6 levels. Cyclo(Val-Pro) (**1**) alleviated oxalate induced renal nephropathy as evidenced by significant reduction in the renal RNA expression of IL-1β ($P < 0.01$), which is a prime cytokine released during oxalate injury. Levels of other cytokines TNF-α and IL-6 were also lowered significantly ($P < 0.05$). Also, expression of KIM-1 was reduced significantly ($P < 0.001$) (Figure 5.5.1.3).

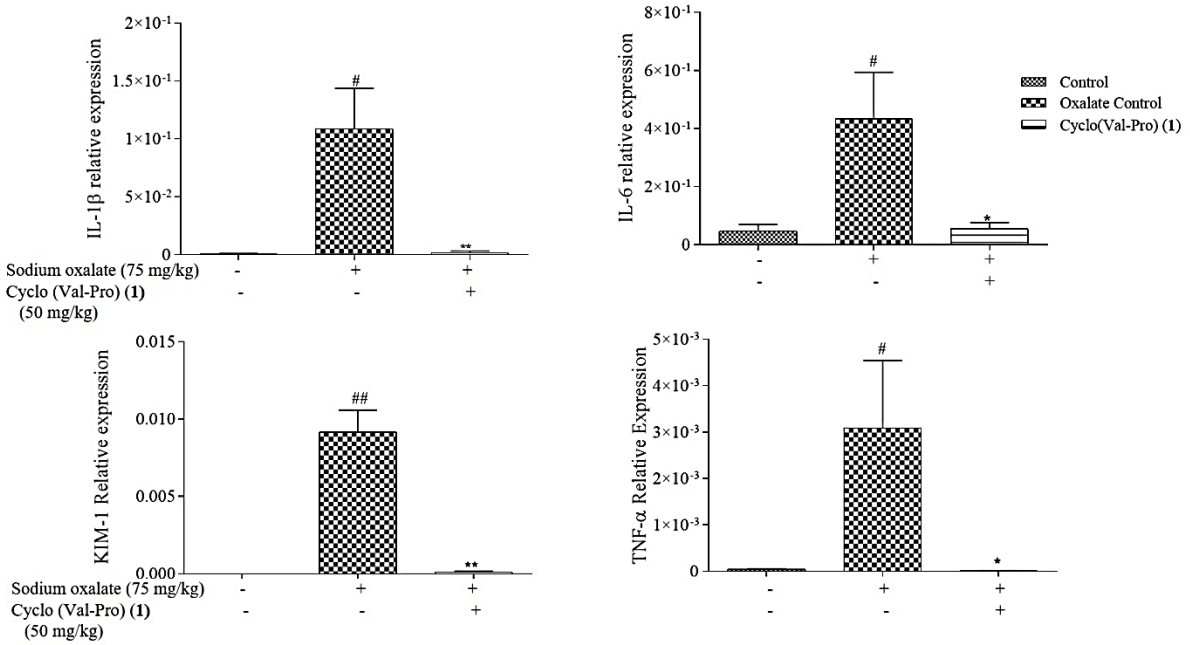

Figure 5.5.1.3 Inhibition effect of compound cyclo(Val-Pro) (1) on renal mRNA expression under oxalate crystal induced renal nephropathy model using RTPCR. Figure illustrates the inhibitory effect of cyclo(Val-Pro) (**1**) at the dose of 50 mg/kg on renal RNA expression of TNF-α, IL-1β, IL-6 (proinflammatory markers) and KIM-1 (renal injury markers) induced by oxalate crystals in renal nephropathy model done using RTPCR. The values are presented as mean ±SEM (n=6). $^{\#}P<0.05$ vs. Normal control, $^{\#\#}P<0.01$vs. Normal control, $^{*}P<0.05$ vs. oxalate control, $^{**}P<0.01$ vs. oxalate control, $^{***}P<0.001$ vs. oxalate control).

5.5.1.4 Histological analysis

Renal tissues of active compound cyclo(Val-Pro) (**1**) was sliced to 5 µm sections and stained with H and E dye to study the impact of treatment on renal architecture damage. Tubular injury index was scored in semi-quantitative method based on tubular necrosis, tubular dilation and tubular cast. Scoring was given on the scale of 0-5 with 0 showing no /nil damage and 5 to those showing severe renal damage. Tubular necrosis involves loss of brush border, flattening of cells, disruption and detachment of tubular cells from basement membrane. Tubular cast develops as a result of protein precipitation and tubular dilation is characterized by widening of luminal tubular tissue (Ahil et al 2019, Mulay et al 2012). Cyclo(Val-Pro) (**1**) markedly protected renal tissues against oxalate nephropathy as delineated by histological data (Figure 5.5.1.4).

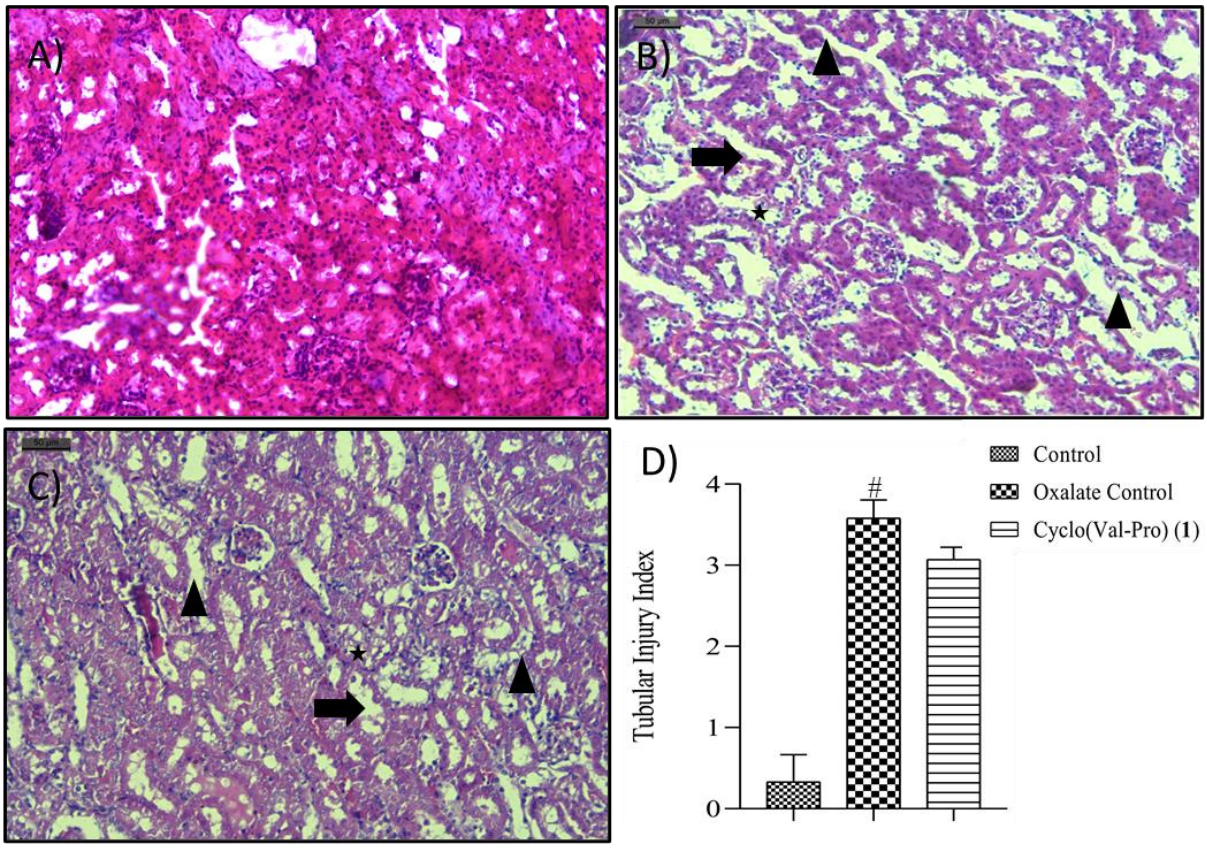

Figure 5.5.1.4 Renal Histology of cyclo(Val-Pro) (1) treatment on calcium oxalate induced nephropathy model. Figure illustrates the protective role of cyclo(Val-Pro) (**1**) at a dose of 50 mg/kg on renal histology in calcium oxalate nephropathy model. Representative photomicrograph of renal histological sections (H & E) at 40x from (A) control group (B) oxalate crystal control group (C) cyclo(Val-Pro) (**1**) group and (D) Tubular injury index which was quantified by semi-quantitative scoring [Tubular dilation (thick arrows), Tubular necrosis (triangle) and Tubular casts (star)]. ($^{\#}P<0.05$ vs. Normal control).

Treatment with cyclic dipeptides in calcium oxalate induced renal nephropathy model, particularly cyclo(Val-Pro) **(1)** indicated positive effects in alleviating renal injury and results were found to be consistent with *in vitro* LPS-induced inflammatory model.

5.5.1.5 *In vitro* mechanistic study on cyclo(Val-Pro) (1)

On viewing the positive effect of cyclic dipeptides in alleviating pro-inflammatory cytokines levels, further *in vitro* mechanistic studies were carried out on cyclo(Val-Pro) (**1**) at 100 µM concentration using LPS and calcium oxalate induced inflammatory model on RAW 264.7 cell lines. Since**,** IL-1β plays a primary role in the development of calcium oxalate-induced renal nephropathy, mRNA gene expression study of pro-inflammatory cytokines mainly IL-1β and protein expression study of pro as well as mature form of IL-1β was done.

5.5.1.5.1 Effect of cyclo(Val-Pro) (1) on mRNA expression levels of pro-inflammatory cytokines

Cyclo(Val-Pro) (**1**) treatment group samples were evaluated for mRNA expression study of pro-inflammatory markers IL-1β, TNF-α and IL-6 levels. Cyclo(Val-Pro) (**1**) alleviated LPS and oxalate crystals induced IL-1β expression levels ($P < 0.001$), which is a prime cytokine released during oxalate injury. Levels of other cytokines TNF-α and IL-6 were also lowered significantly ($P < 0.05$) as shown in Figure 5.5.1.5.1.

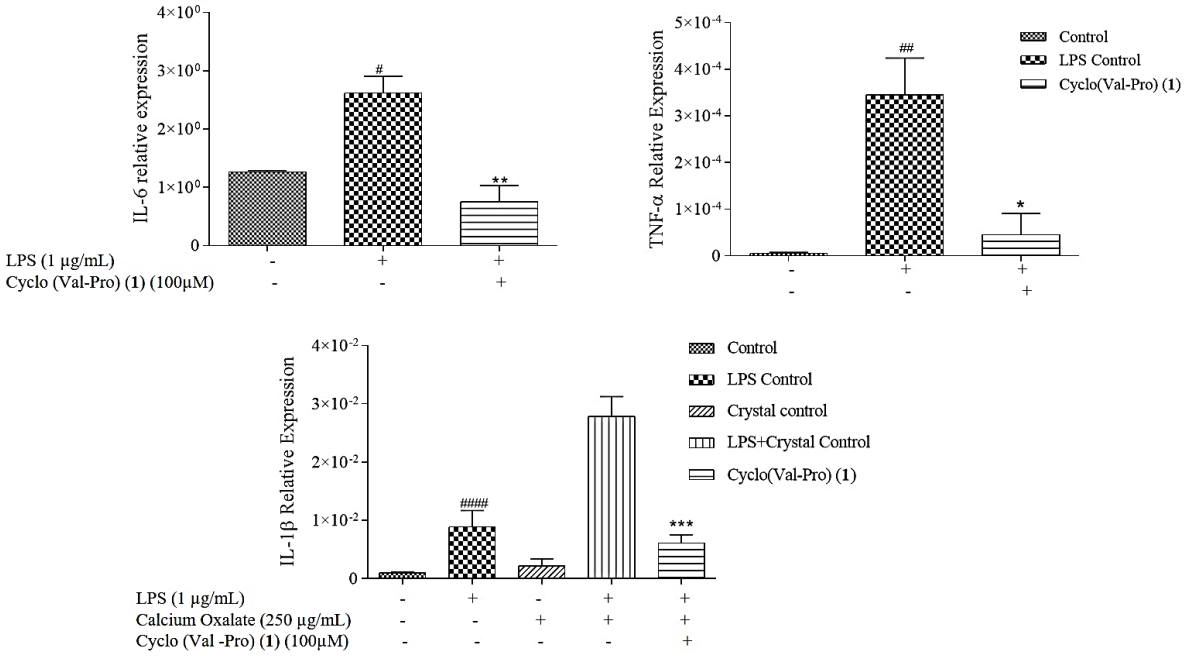

Figure 5.5.1.5.1. Inhibition effect of compound cyclo(Val-Pro) (1) on mRNA expression levels of pro-inflammatory cytokines using RTPCR. Figure illustrates the inhibitory effect of cyclo(Val-Pro) (**1**) at 100 µM concentration. mRNA expression levels of TNF-α, IL-1β, IL-6 (proinflammatory markers) were induced by LPS or LPS + oxalate crystals in *in vitro* model done using RTPCR. The values are presented as mean ±SEM (n=3). $^{\#}P<0.05$ vs. Normal control, $^{\#\#}P<0.01$ vs. Normal control, $^{*}P<0.05$ vs. LPS control, $^{**}P<0.01$ vs. LPS control, $^{***}P<0.001$ vs. LPS + oxalate control).

5.5.1.5.2 Effect of cyclo(Val-Pro) (1) on protein expression levels of pro-inflammatory cytokine IL-1β

Cyclo(Val-Pro) (**1**) treatment significantly reduced the protein expression level of pro-inflammatory markers IL-1β. Both pro as well as mature forms of IL-1β were considerably reduced upon treatment with Cyclo(Val-Pro) (**1**) as demonstrated in Figure 5.5.1.5.2.

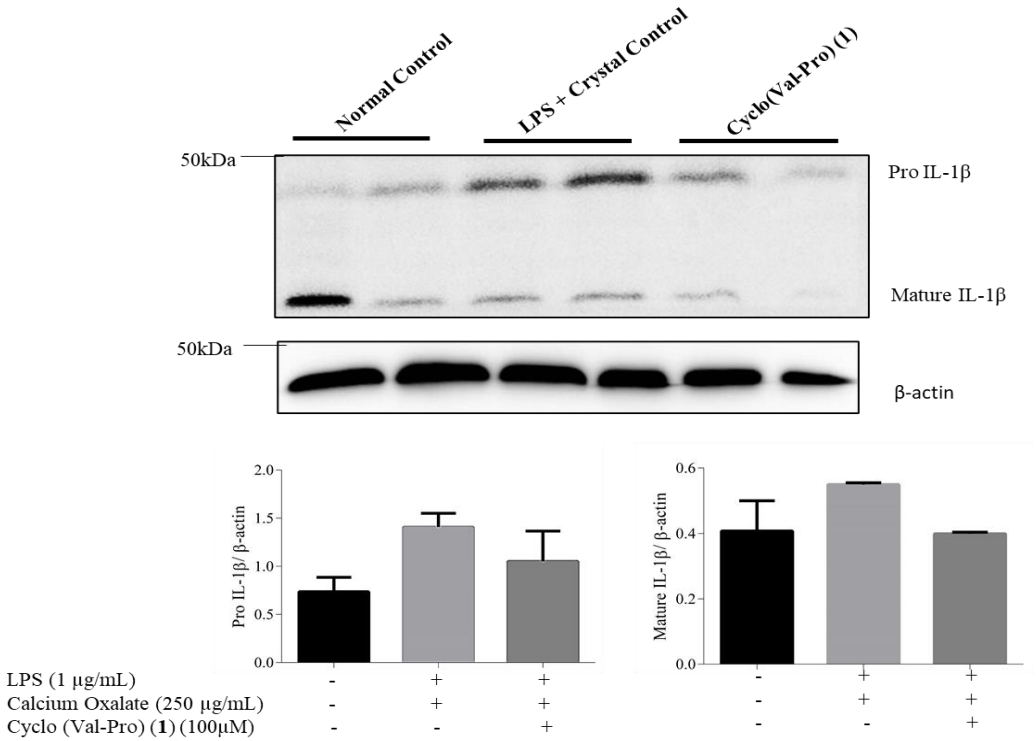

Figure 5.5.1.5.2 Effect of cyclo(Val-Pro) (1) treatment on IL-1β at 100 µM concentration under LPS and oxalate crystal induced *in vitro* model. Figure illustrates the protective effect of cyclo(Val-Pro) (**1**) in alleviating IL-1β at 100 µM concentration on protein expression of pro- IL-1β and mature IL-1β in RAW 264.7 cells. (The values are presented as mean ±SEM (n=2).

5.5.2 Ischemic-reperfusion model of renal injury

Based on the results observed under oxalate nephropathy model, cyclic dipeptide cyclo(Val-Pro) (**1**) and cyclo(Leu-Hydroxy-Pro) (**9**) was further assessed for its anti-inflammatory potential in another model of acute renal injury i.e. Ischemic reperfusion model. Apperceiving their favourable effects at tested dose of 50 mg/kg body weight under oxalate nephropathy model, compounds were tested at different doses i.e. 25, 50 and 75 mg/kg body weight to see their protective activity.

Briefly, C57BL/6 male mice were used for the study and compounds **1** and **9** were administered at 25, 50 and 75 mg/kg body weight dose prior to injury induction. Ischemic injury was induced by clamping left renal artery for 45 min and then reperfusion was allowed by removing the clamp. Mice were sacrificed after 24 h of ischemic injury to collect blood and renal tissue samples for further assessment of injury.

5.5.2.1 Protective effect of cyclo(Val-Pro) (1) on ischemic reperfusion model

5.5.2.1.1 Effect of cyclo(Val-Pro) (1) on ischemia induced IL-1β secretions

Isolated plasma samples from treated mice were used for estimating the levels of IL-1β using ELISA assay. IL-1β levels were significantly reduced at 75 mg/kg and at 50 mg/kg dose with 49.78% and 64.47% inhibition, respectively and $P<0.05$. Further, marked inhibitory effect was observed even at a low dose of 25 mg/kg body weight of cyclo(Val-Pro) (**1**) (25.00%) (Figure 5.5.2.1.1).

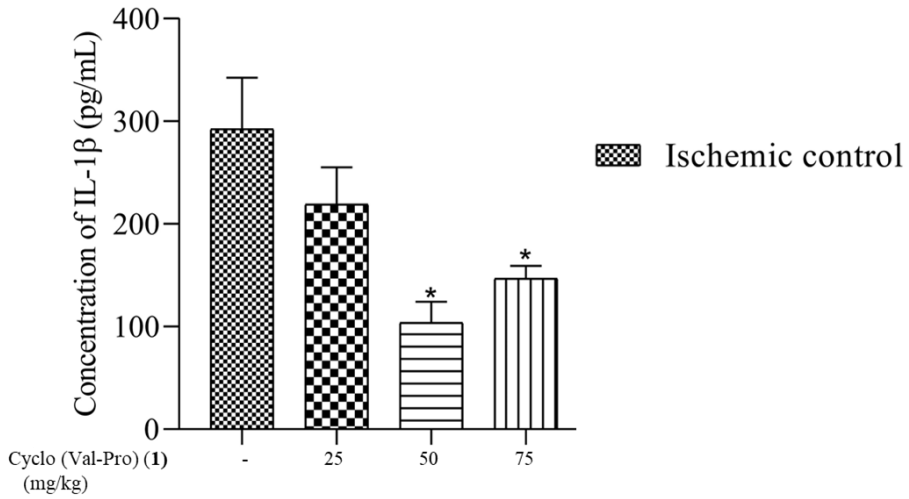

Figure 5.5.2.1.1 Effect of cyclo(Val-Pro) (1) on plasma IL-1β levels at various doses (25, 50 and 75 mg/kg) using ELISA studies. Figure demonstrates the inhibitory effect of cyclo(Val-Pro) (**1**) on plasma IL-1β levels at 25, 50 and 75 mg/kg dose in ischemic reperfusion animals. All values were presented as mean ± SEM (n=6). (*$P<0.05$ vs. ischemic control).

5.5.2.1.2 Effect of cyclo(Val-Pro) (1) on mRNA expression levels of pro-inflammatory cytokines and kidney injury markers

mRNA samples isolated from renal tissues were evaluated for the gene expression study of pro-inflammatory cytokines and kidney injury markers. At 75 mg/kg dose of cyclo(Val-Pro) (**1**), KIM-1 levels were significantly attenuated from 12.23 ± 4.38 to 1.93 ± 0.75 and NGAL levels were diminished from 2.20 ± 1.48 to 0.17 ± 0.15. Also, compound **1** showed significant abrogation of α-GST and π-GST expression level at 75 mg/kg and 50 mg/kg (Figure 5.5.2.1.2a).

Significant downregulation of mRNA expression levels of pro-inflammatory cytokines (TNF-α, IL-6 and IL-1β) was observed at 75 mg/kg and 50 mg/kg dose ($P<0.05$). IL-1β mRNA expression levels were diminished from 0.21 ± 0.04 to 0.04 ± 0.04, TNF-α was lessened from 1.15±1.35 to 0.03 ± 0.03 and IL-6 from 0.33 ± 0.25 to 0.05 ± 0.03 in 75 mg/kg cyclo(Val-Pro)

(**1**) treated group. Also, 25 mg/kg dose showed significant alleviation in expression levels of TNF-α (P<0.05) (Figure 5.5.2.1.2b).

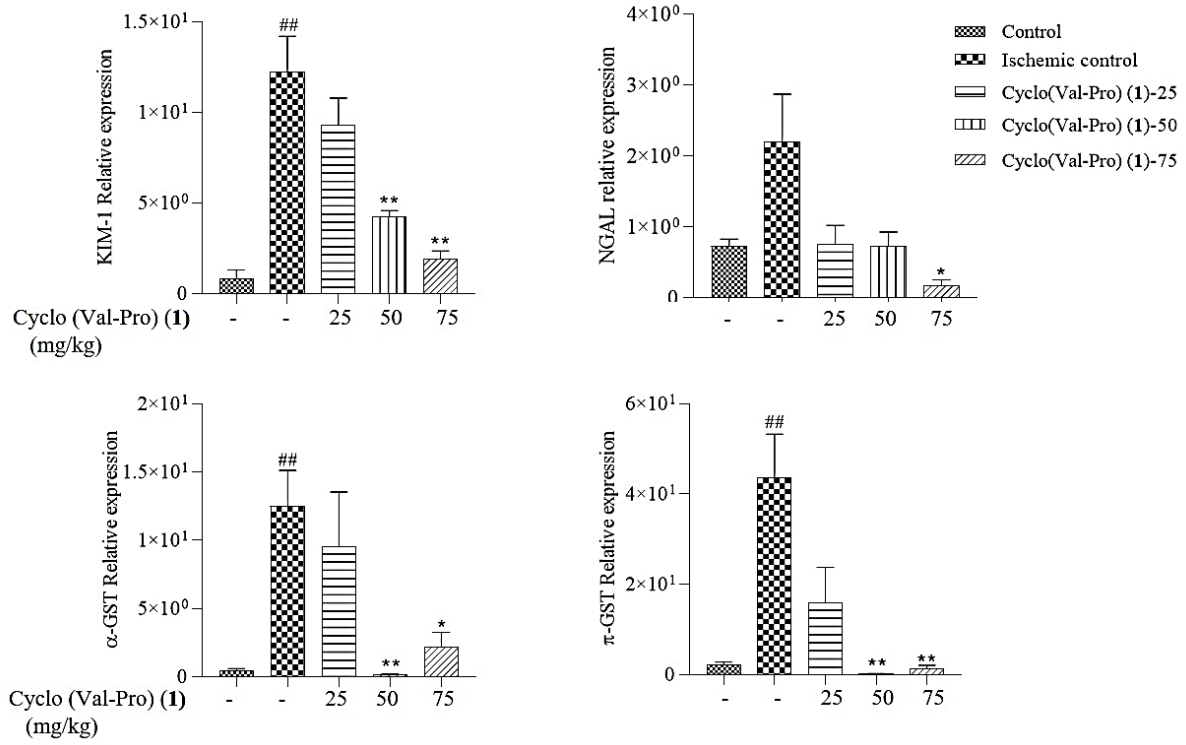

Figure 5.5.2.1.2a Inhibitory effect of cyclo(Val-Pro) (1) administration at 25, 50 and 75 mg/kg doses on mRNA expression levels of kidney injury markers. Figure shows alleviation of mRNA expression levels of renal injury markers *viz*., KIM-1, NGAL, α-GST, π-GST by cyclo(Val-Pro) (**1**) at 25, 50 and 75 mg/kg dose. (The values are presented as mean ±SEM (n=6). $^{\#\#}P$<0.01 vs. control, *P<0.05 vs. ischemic control, **P<0.01vs. ischemic control)

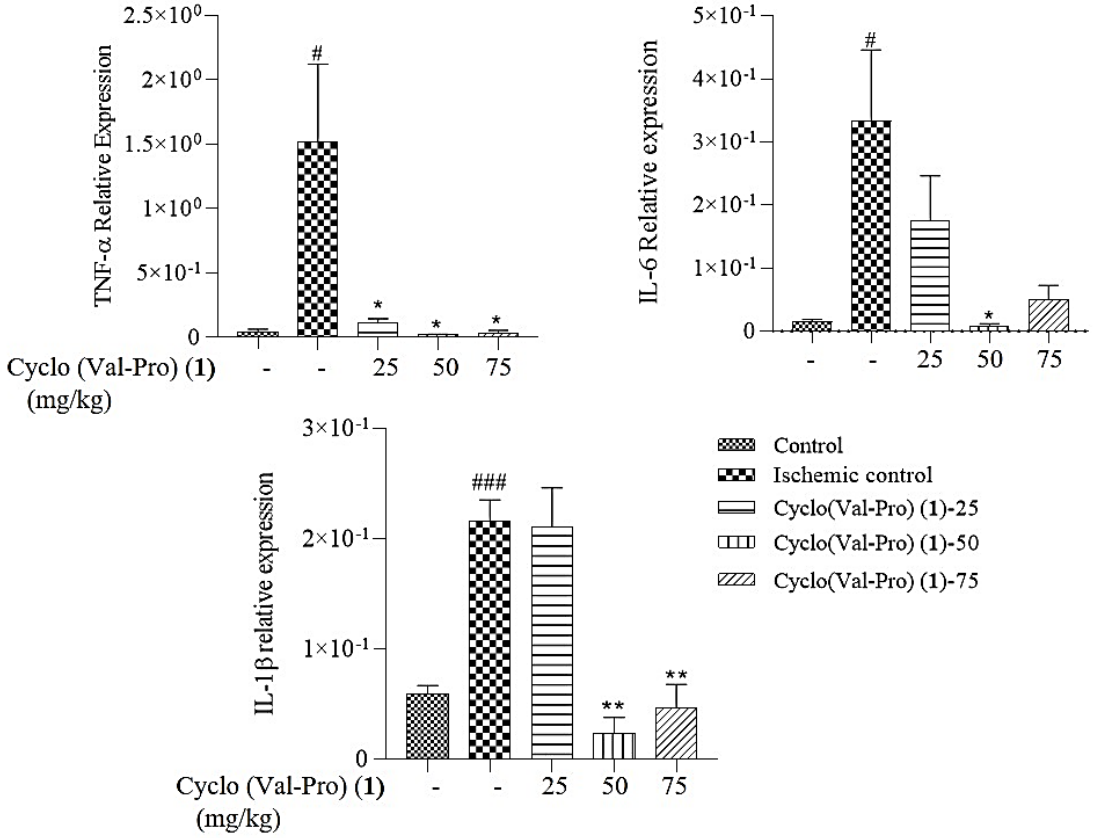

Figure 5.5.2.1.2b Inhibitory effect of cyclo(Val-Pro) (1) administration at 25, 50 and 75 mg/kg doses on mRNA expression levels of pro-inflammatory cytokines. Figure shows alleviation of mRNA expression level of inflammatory markers TNF-α, IL-6 and IL-1β by cyclo(Val-Pro) (**1**) at 25, 50 and 75 mg/kg dose. (The values are presented as mean ±SEM (n=6). $^{\#}P<0.05$ vs. control, $^{\#\#\#}P<0.001$ vs. control, $^{*}P<0.05$ vs. ischemic control, $^{**}P<0.01$vs. ischemic control)

5.5.2.1.3 Effect of cyclo(Val-Pro) (1) on histopathology of ischemia-induced damaged renal tissue

Observation was made for renal tissue damage in terms of tubular dilation, cast formation and necrosis using H and E staining. Histopathology of renal tissue indicated the attenuation of damage caused by ischemia upon treatment with compound **1**. As shown in Figure 5.5.2.1.3 tubular injury index analysed on the basis of tubular dilation, tubular cast and necrosis was found to be improved to significant extent when treated with cyclo(Val-Pro) (**1**) at 75 mg/kg and 50 mg/kg.

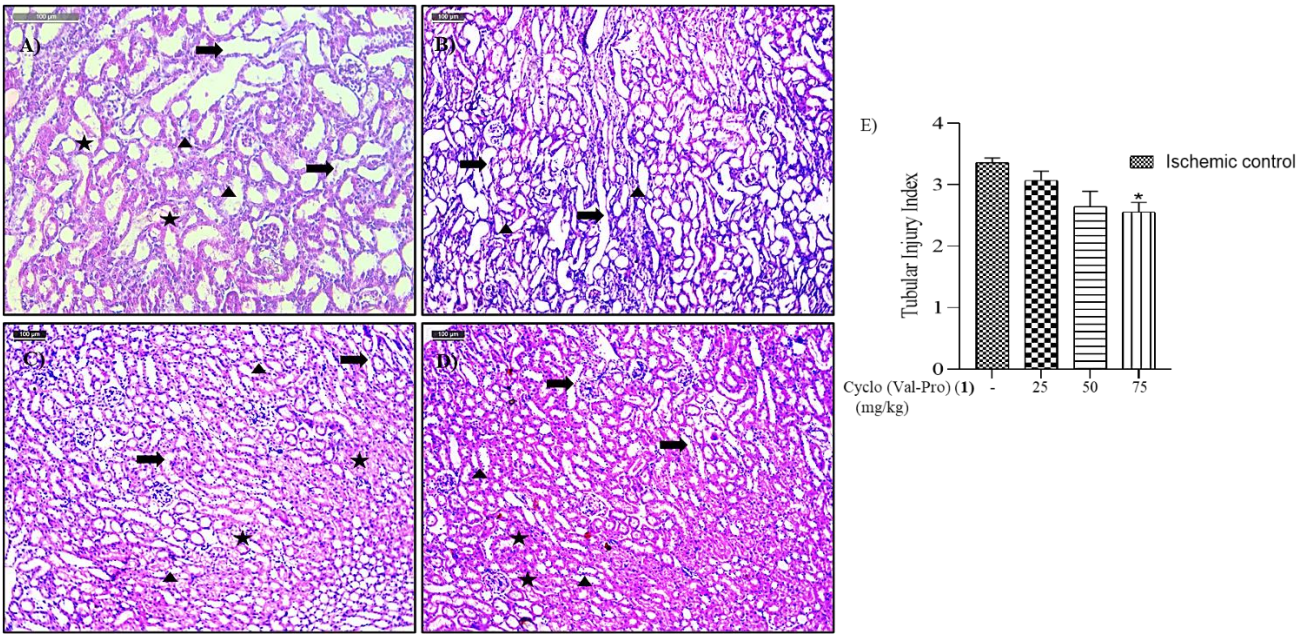

Figure 5.5.2.1.3 Effect of cyclo(Val-Pro) (1) on renal tissue at 25, 50 and 75 mg/kg doses in ischemic reperfusion model. Figure depicts the protective role of cyclo(Val-Pro) (**1**) at 25, 50 and 75 mg/kg body weight dose on renal tissue. Representative photomicrograph of renal histological sections (H & E) at 40x from (A) Ischemic control group (B) cyclo(Val-Pro) (**1**) treated group at 25 mg/kg dose (C) cyclo(Val-Pro) (**1**) treated group at 50 mg/kg dose (D) cyclo(Val-Pro) (**1**) treated group at 75 mg/kg dose and (E) represents tubular injury index characterised by tubular dilation (thick arrows), tubular necrosis (triangle) and tubular casts (star).

5.5.2.2 Protective effect of cyclo(Leu-Hydroxy-Pro) (9) on ischemia induced IL-1β secretions

5.5.2.2.1 Effect of cyclo(Leu-Hydroxy-Pro) (9) on ischemia induced IL-1β secretions

Isolated plasma samples from treated mice were used for estimating the levels of IL-1β using ELISA assay. IL-1β levels were significantly reduced in all treatment groups i.e. 25, 50 and 75 mg/kg dose with $P<0.05$. Also the effect was comparable to that of standard Bay given at the dose of 10 mg/kg. (Figure 5.5.2.2.1).

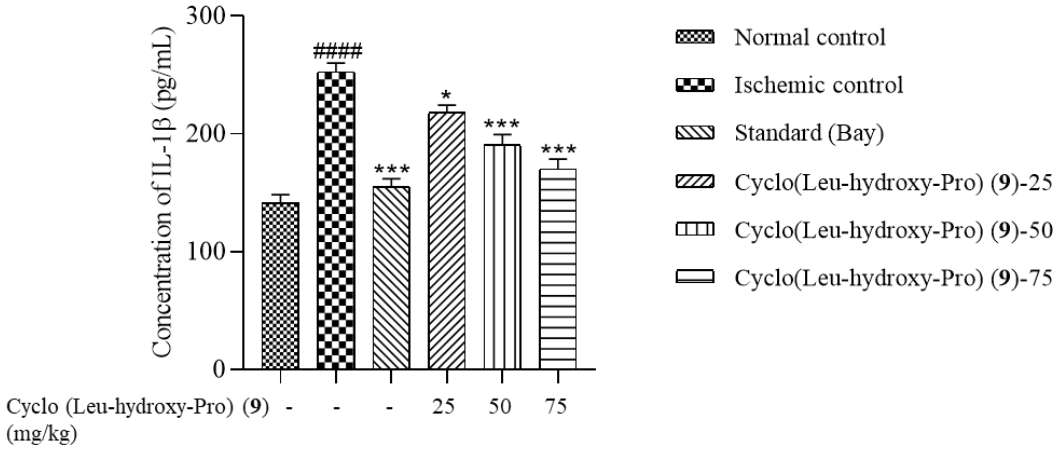

Figure 5.5.2.2.1 Effect of standard (Bay((10 mg/kg) and cyclo(Leu-Hydroxy-Pro) (9) on plasma IL-1β levels at various doses (25, 50 and 75 mg/kg) using ELISA studies. Figure demonstrates the inhibitory effect of Bay (10 mg/kg) and cyclo(Leu-Hydroxy-Pro) **(9)** on plasma IL-1β levels at 25, 50 and 75 mg/kg dose in ischemic reperfusion animals. All values were presented as mean ± SEM (n=6). (**P*<0.05 vs. ischemic control, ****P*<0.001 vs. ischemic control, $^{###}$*P*<0.001 vs. Normal control).

5.5.2.2.2 Effect of cyclo(Leu-Hydroxy-Pro) (9) on mRNA expression levels of pro-inflammatory cytokines and kidney injury markers

mRNA samples isolated from renal tissues were evaluated for the gene expression study of pro-inflammatory cytokines and kidney injury markers. At 50 and 75 mg/kg dose of cyclo(Leu-Hydroxy-Pro) (**9**), KIM-1 levels were significantly attenuated (*P*<0.01) and NGAL levels were significantly reduced at 75 mg/kg dose (*P*<0.01). Also, compound **9** showed significant abrogation of α-GST and π-GST expression level at 75 mg/kg dose (Figure 5.5.2.2.2a).

Significant downregulation of mRNA expression levels of pro-inflammatory cytokines (TNF-α, IL-6 and IL-1β) was observed at 75 mg/kg dose (*P*<0.05). IL-1β mRNA expression levels were significantly reduced at 25, 50 and 75 mg/kg dose (*P*<0.05). Further there was a reduction in the levels of TNF-α and IL-6 levels were lessened in 75 mg/kg cyclo(Leu-Hydroxy-Pro) (**9**) treated group (Figure 5.5.2.2.2b).

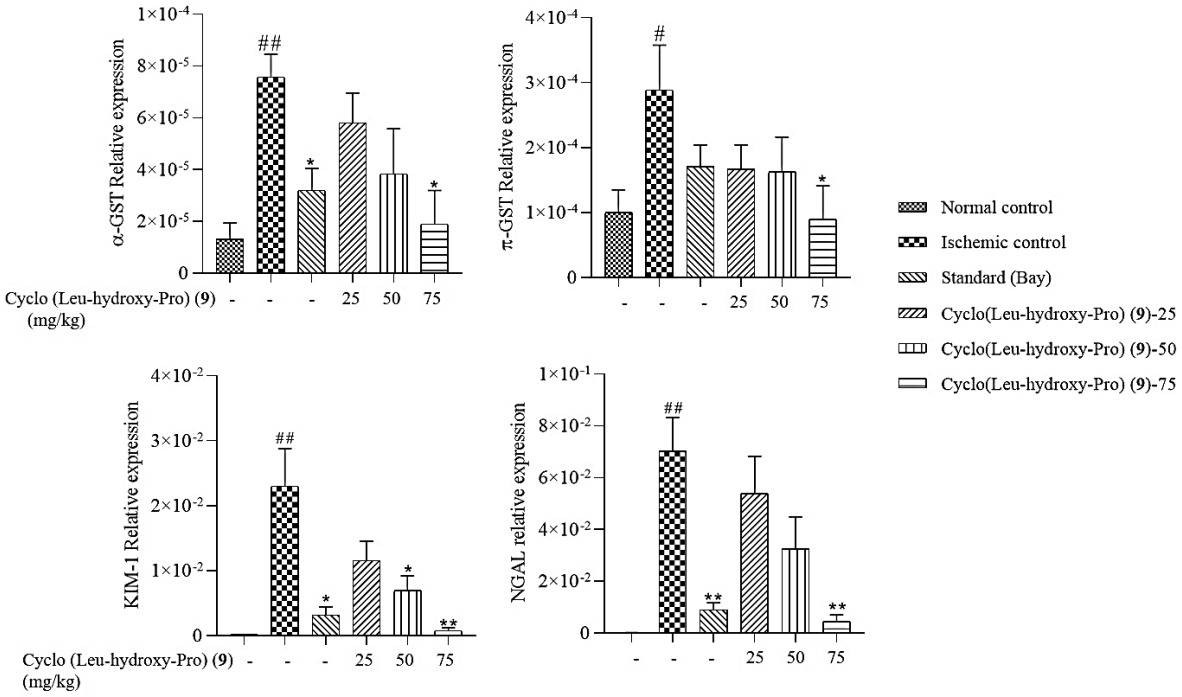

Figure 5.5.2.2.2a Inhibitory effect of standard Bay (10 mg/kg) and cyclo(Leu-Hydroxy-Pro) (9) administration at 25, 50 and 75 mg/kg doses on mRNA expression levels of kidney injury markers. Figure shows alleviation of mRNA expression levels of renal injury markers *viz*., KIM-1, NGAL, α-GST, π-GST by Bay at 10 mg/kg and cyclo(Leu-Hydroxy-Pro) **(9)** at 25, 50 and 75 mg/kg dose. (The values are presented as mean ±SEM (n=6). **P*<0.05 vs. ischemic control, ***P*<0.01 vs. ischemic control, $^{\#}P$<0.05 vs. normal control, $^{\#\#}P$<0.01vs. normal control)

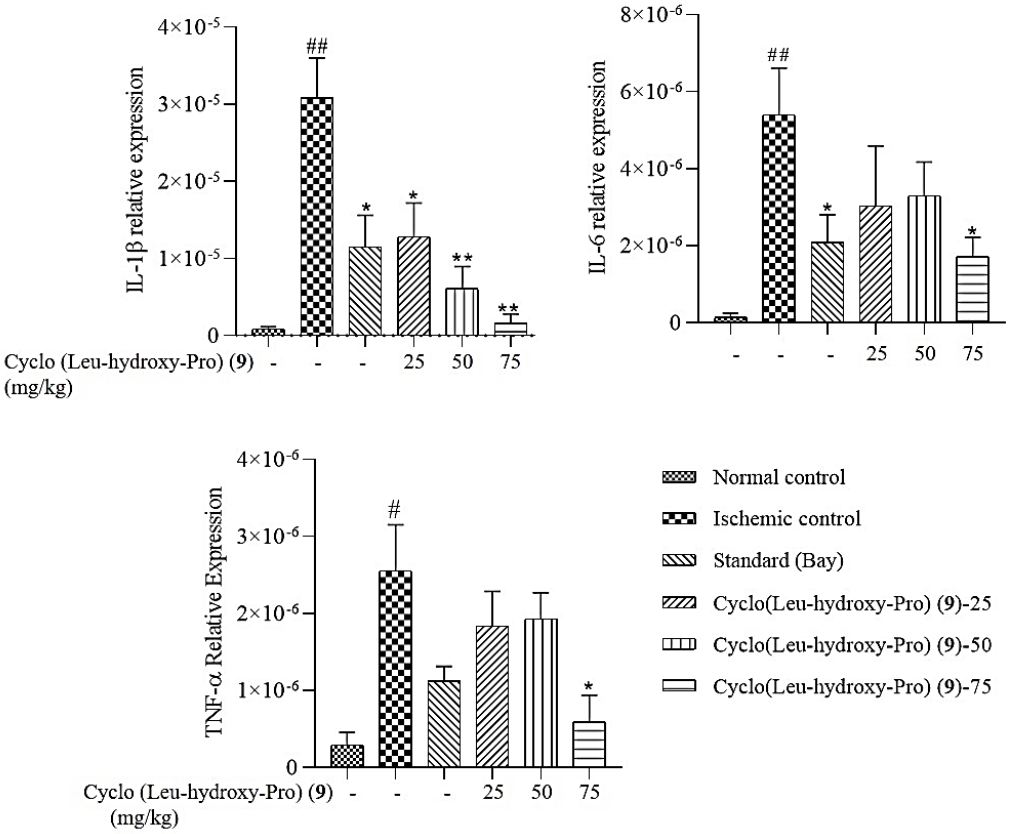

Figure 5.5.2.2.2b Inhibitory effect of cyclo(Leu-Hydroxy-Pro) (9) administration at 25, 50 and 75 mg/kg doses and standard (Bay) at 10 mg/kg dose on mRNA expression levels of pro-inflammatory cytokines level. Figure shows alleviation of mRNA expression level of inflammatory markers TNF-α, IL-6 and IL-1β by Bay and cyclo(Leu-Hydroxy-Pro) (**9**) at 25, 50 and 75 mg/kg dose. (The values are presented as mean ±SEM (n=6). **P*<0.05 vs. ischemic control, ***P*<0.01 vs. ischemic control, $^{\#}P$<0.05 vs. normal control, $^{\#\#}P$<0.01 vs. normal control)

5.5.2.2.3 Effect of cyclo(Leu-Hydroxy-Pro) (9) on histopathology of ischemia-induced damaged renal tissue

Observation was made for renal tissue damage in terms of tubular dilation, cast formation and necrosis using H and E staining. Histopathology of renal tissue indicated the attenuation of damage caused by ischemia upon treatment with compound **9**. As shown in Figure 5.5.2.2.3 tubular injury index analysed on the basis of tubular dilation, tubular cast and necrosis was found to be improved to significant extent when treated with cyclo(Leu-Hydroxy-Pro) (**9**) at 75 mg/kg dose.

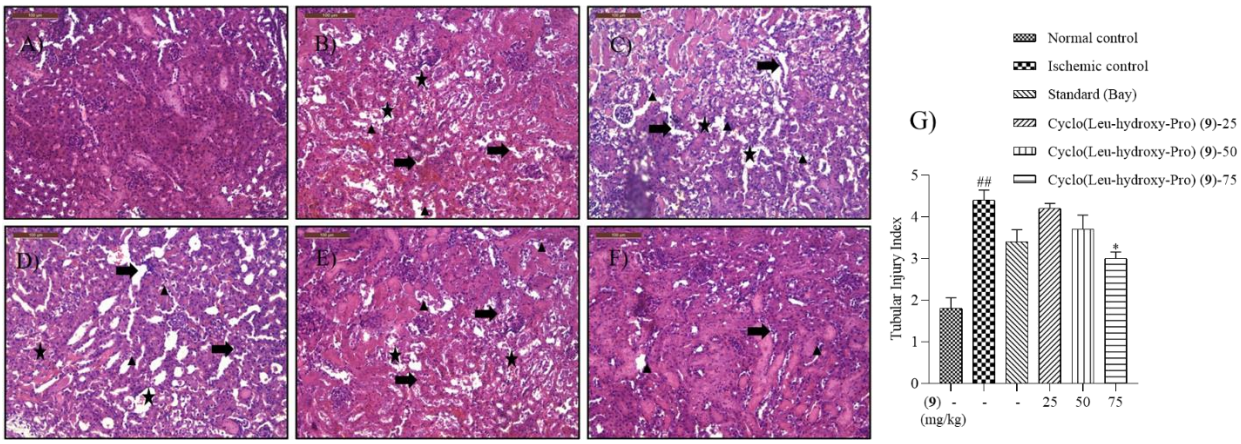

Figure 5.5.2.2.3 Effect of Bay at 10 mg/kg and cyclo(Leu-Hydroxy-Pro) (9) on renal tissue at 25, 50 and 75 mg/kg doses in ischemic reperfusion model. Figure depicts the protective role of Bay at 10 mg/kg dose and cyclo(Leu-Hydroxy-Pro) (**9**) at 25, 50 and 75 mg/kg body weight dose on renal tissue. Representative photomicrograph of renal histological sections (H & E) at 20x from (A) Normal control group (B) Ischemic control group (C) cyclo(Leu-Hydroxy-Pro) (**9**) treated group at 25 mg/kg dose (D) cyclo(Leu-Hydroxy-Pro) (**9**) treated group at 50 mg/kg dose (E) cyclo(Leu-Hydroxy-Pro) (**9**) treated group at 75 mg/kg dose and (F) Standard (Bay) treated group at 10 mg/kg dose and (G) represents tubular injury index characterised by tubular dilation (thick arrows), tubular necrosis (triangle) and tubular casts (star).

5.5.2.3 *In vitro* mechanistic studies

Model of ischemia was mimicked in kidney epithelial cell lines NRK 52E using antimycin, an inhibitor of ATP at the dose of 3 μM/mL and further *in vitro* mechanistic studies were carried out on cyclo(Val-Pro) (**1**) and cyclo(Leu-Hydroxy-Pro) (**9**) at different doses of 300, 100, 30, 10 and 3 μM.

5.5.2.3.1 Cell viability studies using MTT reagent

Compound cyclo(Val-Pro) (**1**) significantly improved cell viability in antimycin treated NRK 52E cell lines at the doses of 300, 100, 30 and 10 μM (P<0.05) whereas cyclo(Leu-Hydroxy-Pro) (**9**) showed significant protection against antimycin induced cytotoxicity at the dose of 300 μM (P<0.01) as depicted in Figure 5.5.2.3.1.

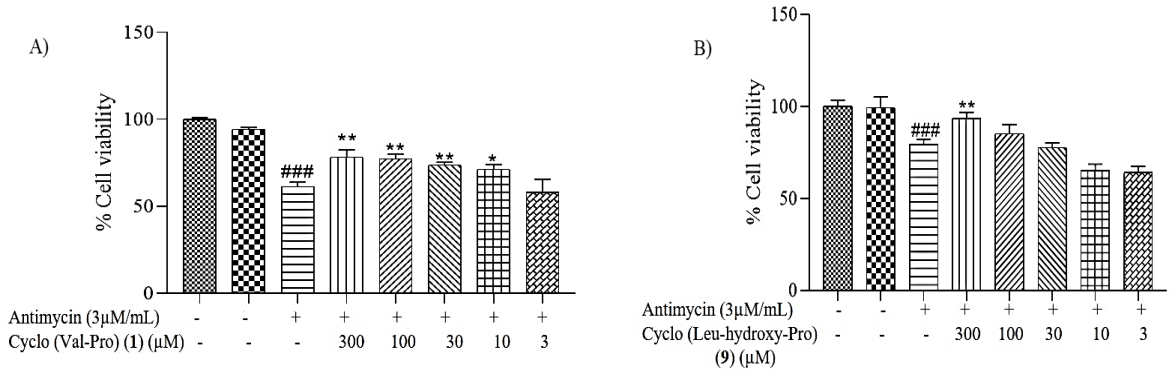

Figure 5.5.2.3.1 Inhibitory effect of cyclo (Val-Pro) (1) (A) and cyclo(Leu-Hydroxy-Pro) (9) (B) at 300, 100, 30, 10 and 3 µM concentrations on antimycin induced cytotoxicity using MTT assay. Figure shows decline in the antimycin induced cytotoxicity by cyclo (Val-Pro) **(1)** and cyclo(Leu-Hydroxy-Pro) **(9)** at different concentrations of 300, 100, 30, 10 and 3 µM on NRK 52E cells. (The values are presented as mean ±SEM (n=5). **P*<0.05 vs. antimycin control, ***P*<0.01 vs. antimycin control, #*P*<0.05 vs. normal control, ##*P*<0.01 vs. normal control)

5.5.2.3.2 Antimycin induced cytotoxicity studies using flow cytometry

Further, 100 µM dose of cyclo(Val-Pro) (**1**) and cyclo(Leu-Hydroxy-Pro) (**9**) was selected to carry out antimycin induced cytotoxicity studies on NRK 52E cell lines using flow cytometry. Compounds cyclo(Val-Pro) (**1**) and cyclo(Leu-Hydroxy-Pro) (**9**) significantly reduced percentage cell death to 2.3% (*P*<0.05) (Figure 5.5.2.3.2).

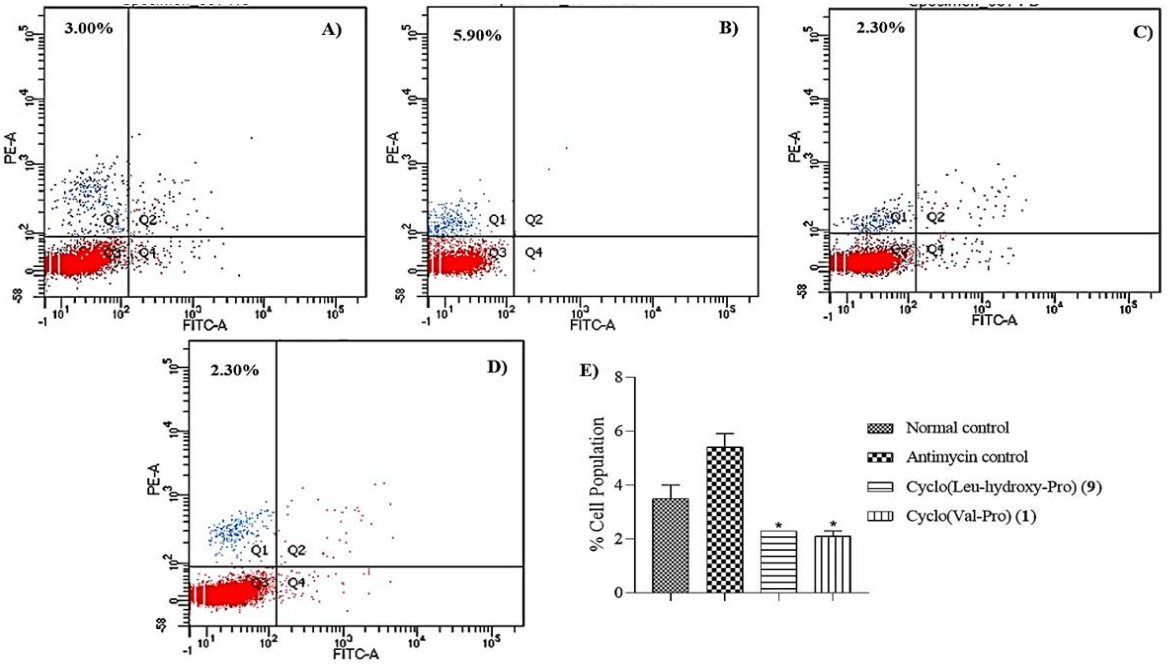

Figure 5.5.2.3.2 Inhibitory effect of cyclo (Val-Pro) (1) and cyclo(Leu-Hydroxy-Pro) (9) at 100 µM concentrations on antimycin induced cytotoxicity using flow cytometry assay. Figure shows decline in the antimycin induced cytotoxicity by cyclo (Val-Pro) (**1**) and cyclo(Leu-Hydroxy-Pro) (**9**) at 100 µM. (A) represents normal control group, (B) antimycin A control group, (C) represents cyclo (Val-Pro)

(**1**) treated group, (D) represents cyclo(Leu-Hydroxy-Pro) (**9**) treated group and (E) represents % cell population. (The values are presented as mean ±SEM (n=3). (**P*<0.05 vs. antimycin control)

5.5.2.3.3 Western blot analysis of pro-apoptotic protein Bax and anti-apoptotic protein BCL2

Compounds cyclo(Val-Pro) (**1**) and cyclo(Leu-Hydroxy-Pro) (**9**) were tested at the dose of 100 µM to estimate the levels of pro-apoptotic protein Bax and anti-apoptotic protein BCL2 using western blot analysis. Compounds significantly reduced antimycin induced elevated levels of pro-apoptotic protein Bax and increased the levels of anti-apoptotic protein BCL2 as presented in Figure 5.5.2.3.3.

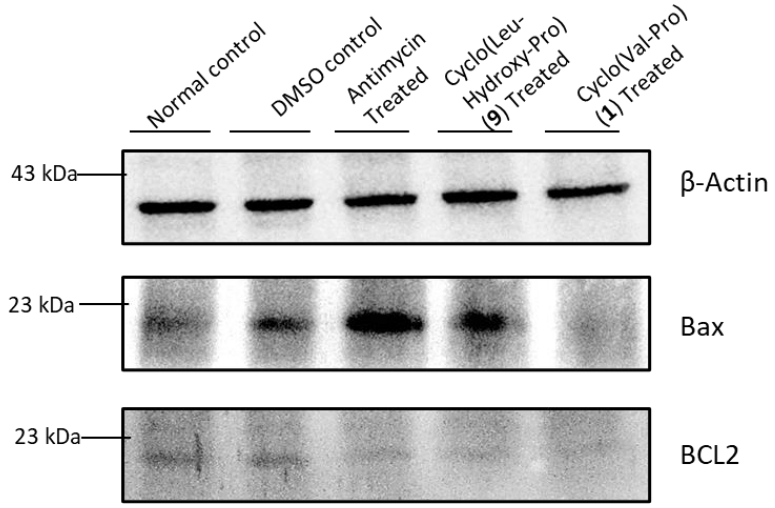

Figure 5.5.2.3.3 Effect of cyclo(Val-Pro) (1) and cyclo(Leu-Hydroxy-Pro) (9) on antimycin B induced apoptosis. Figure depicts the protective role of cyclo(Val-Pro) (**1**) and cyclo(Leu-Hydroxy-Pro) (**9**) at 100 µ.M concentration on protein expression of Bax and BCL 2 in NRK 52E using western blot

5.5.3 Unilateral ureter obstruction induced renal injury

Anti-inflammatory efficacy of cyclo(Val-Pro) (**1**) under two acute kidney injury models further motivated us to test its activity in a chronic renal injury model. Cyclo(Val-Pro) (**1**) was tested in UUO model at 50 mg/kg body weight dose. Compound administration was done on alternate days till sacrifice i.e. tenth day of the ligation. Antifibrotic activity of cyclo(Val-Pro) (**1**) was compared with that of standard NFκB inhibitor 'bay' administered at 5 mg/kg dose given on alternate days until the day of sacrifice. Bay 117082, a selective inhibitor for nod-like receptor family pyrin domain containing 3 (NLRP3) and inhibitor of nuclear factor-kappa B (NF-kB) was used as standard to compare the activity of the compounds (Lee *et al.* 2005).

Kidney tissues were evaluated for the expression of fibrotic markers such as α-SMA, TGF-β and collagen-1. TGF-β plays a putative role in the development of interstitial fibrosis by promoting phenotypic transformation of tubular epithelial cells to myofibroblast and

stimulating extracellular matrix synthesis. Collagen-1 is a predominant component of extracellular matrix produced by fibroblast (Kishimoto *et al.* 2011). Figure 5.6.3 presents the appearance of kidneys on the tenth day of ligation of unilateral ureter.

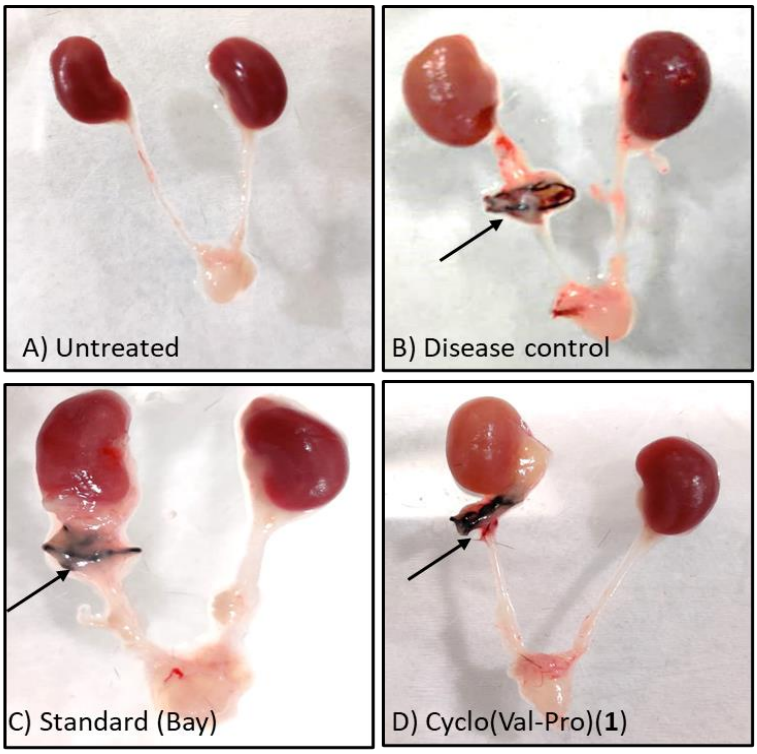

Figure 5.5.3 Photographs displaying the appearance of kidneys of different groups on the tenth day of ligation of unilateral ureter (Arrow indicates ligated kidney)

5.5.3.1 Effect of administration of cyclo(Val-Pro) (1) on fibrotic markers

Isolated proteins from renal tissue were studied for the expression of fibrotic markers (α-SMA, TGF-β and collagen-1) using western blot analysis. The α-SMA present in the smooth muscle cells of renal arterioles, was found to be strikingly upregulated after tenth day of renal obstruction. Administration of cyclo(Val-Pro) (**1**) suppressed the protein expression of α-SMA (P<0.05) and the effect was more pronounced as compared to standard 'bay' which exhibited marginal protection in attenuating α-SMA levels (Figure 5.5.3.1). Also, Figure 5.5.3.1 demonstrates the significant protection (P<0.01) by cyclo(Val-Pro) (**1**) in abating renal fibrosis by lowering the expression of TGF-β and collagen-1 while bay treated group exhibited marginal protection in alleviating interstitial fibrosis.

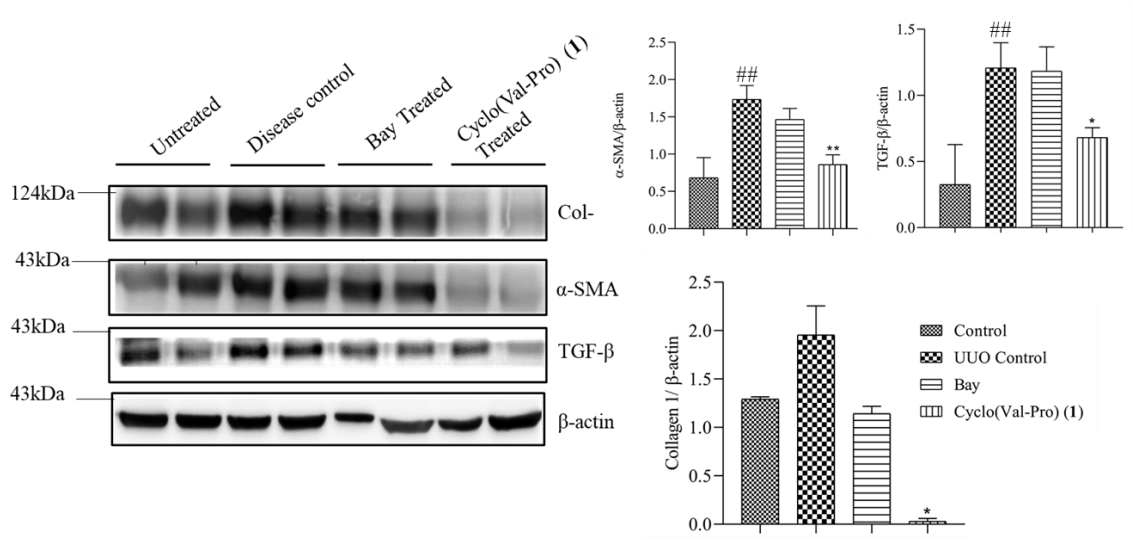

Figure 5.5.3.1 Effect of cyclo(Val-Pro) (1) treatment on fibrotic markers at 50 mg/kg dose under unilateral ureteral obstruction model. Figure illustrates the protective effect of cyclo(Val-Pro) (**1**) in alleviating interstitial fibrosis by reducing expression of α-SMA, TGF-β and collagen-1 at 50 mg/kg dose. (The values are presented as mean ±SEM (n=6). $^{\#\#}P<0.01$ vs. normal control, $^{*}P<0.05$ vs. disease control, $^{**}P<0.01$ vs. diseases control)

5.5.3.2 Effect of cyclo(Val-Pro) (1) on renal tissue fibrosis using Picro-sirius red staining

The presence of interstitial fibrosis was assessed in slides using picro- sirius red staining. Renal tissues obtained from control, disease control, bay and cyclo(Val-Pro) (**1**) treatment groups were stained using picro-sirius red. Sirius red stains collagen, which is a key marker of fibrosis. Renal tissues stained with sirius red staining showed fibrotic area. Figure 5.5.3.2 depicts the favourable effect of cyclo(Val-Pro) (**1**) treatment on attenuation of renal fibrosis.

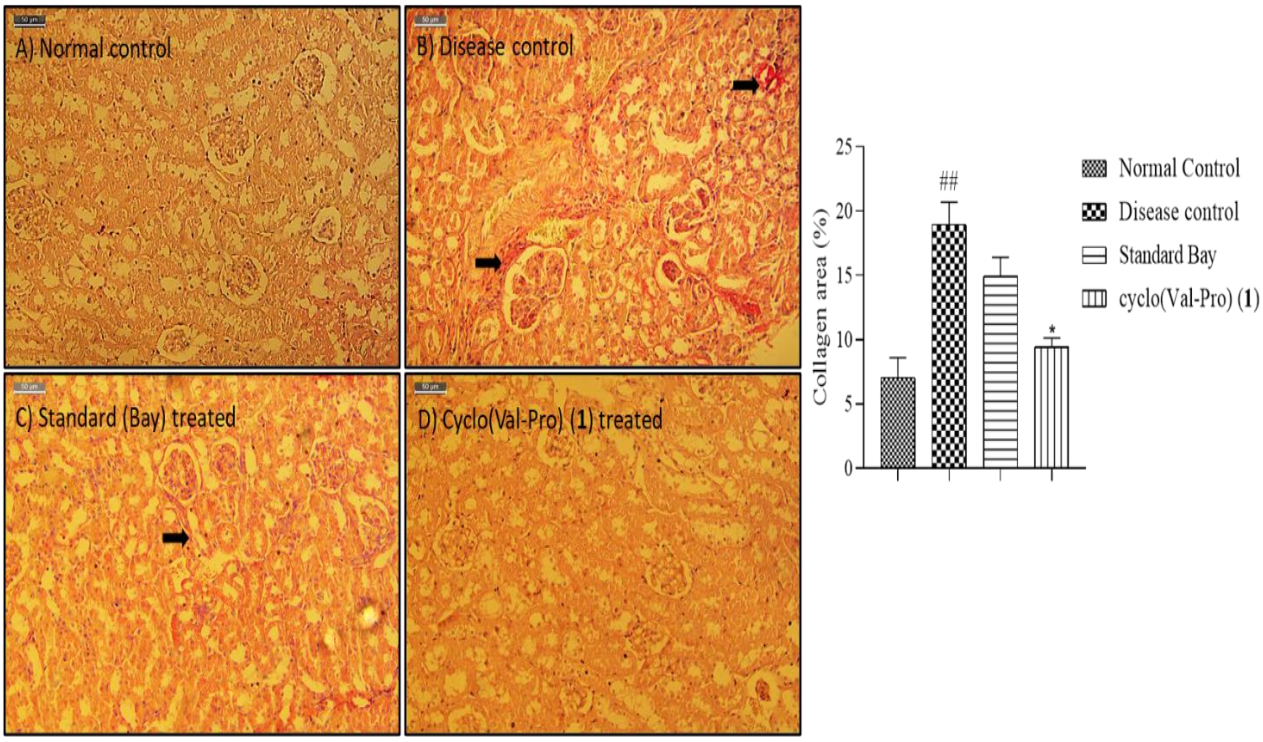

Figure 5.5.3.2 Effect of cyclo(Val-Pro) (1) on fibrosis observed under picro sirius red staining in unilateral ureter obstruction model. Figure depicts the protective role of cyclo(Val-Pro) (**1**) at 50 mg/kg body weight dose on fibrosis in renal tissues of cyclo(Val-Pro) (**1**) treated animals. (A) represents normal control, (B) represents disease control group (C) represents bay treated group (5 mg/kg) (D) indicates cyclo(Val-Pro) (**1**) group. Arrows show fibrosis. (**P*<0.05 vs. Disease control, $^{\#\#}P$<0.01 vs. Normal control).

5.5.3.3 *In vitro* mechanistic studies on cyclo(Val-Pro) (1)

On perceiving the positive role of cyclo(Val-Pro) (**1**) in fibrotic model, it was further subjected to TGF-β induced fibrotic model in NRK-49F cell lines at different doses of 300, 100, 30, 10 and 3 µM. Cyclo(Val-Pro) (**1**) significantly improved TGF-β induced proliferation of NRK-49F at dose of 100 µM (**P*<0.05) (Figure 5.5.3.3).

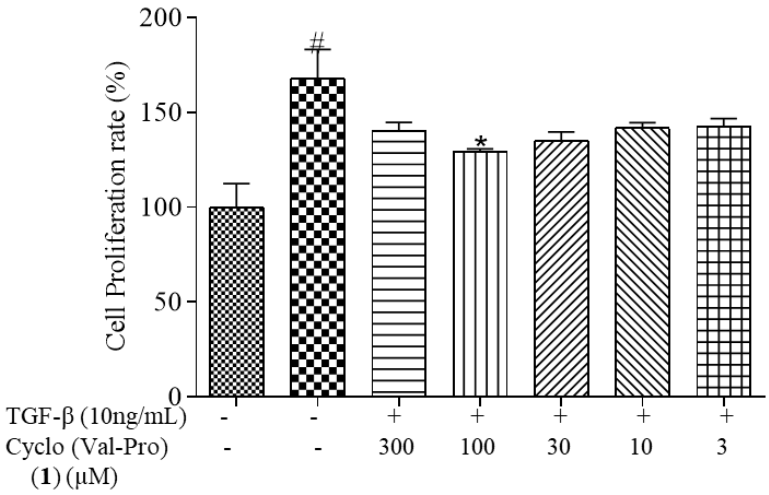

Figure 5.5.3.3 Effect of cyclo(Val-Pro) (1) treatment on TGF-β induced cell proliferation at different concentrations of 300, 100, 30, 10 and 3 µM. Figure illustrates the protective effect of cyclo(Val-Pro) (**1**) in attenuating TGF-β induced cell proliferation in NRK 49F cells. (The values are presented as mean ±SEM (n=6). $^{*}P<0.05$ vs. TGF-β control, $^{\#}P<0.01$ vs. normal control)

Investigation of the constituents of bioactive culture broth extract (PCBE) of *Pseudomonas sp*. (ABS-36) explored the secretion of an array of cyclic dipeptides. This study reports the isolation of seventeen cyclic dipeptides (**1**–**3**, **5**–**8**, **10**, **11**, **13**–**20**) from this source for the first time. Cyclic dipeptides isolated from other sources have shown tremendous therapeutic potential for treatment of various disorders. Some findings also suggest their positive role in attenuation of inflammation but so far, no study has been reported on the efficacy of the cyclic dipeptides in mitigating renal inflammation. Proline based cyclic dipeptides were further evaluated for their anti-inflammatory efficacy in *in vitro* inflammatory models and acute as well as chronic renal inflammatory model. All results collectively disclosed the favourable effects of cyclic dipeptides particularly cyclo(Val-Pro) (**1**) in attenuating renal injury by downregulating pro-inflammatory cytokines.

Chapter 6

Summary and Conclusions

Extensive study of literature revealed *Pseudomonas* species as promising source of components with advantageous role in attenuating several disorders. Therefore, *Pseudomonas* species was selected for exploring new small molecular weight leads targeting pro-inflammatory cytokines. Fluorescing bacterial strain earlier identified as *Pseudomonas* species by comparison of 16S rDNA sequence and registered as ABS-36 strain, was selected for the study. Culture broth was then prepared in bulk using King's B media and extracted with ethyl acetate. The culture broth extract (PCBE) was screened for anti-inflammatory effect using cell based LPS model using RAW 267.4 cells. Cell viability studies conferred PCBE to be non-cytotoxic (IC_{50} value of 1867.25 µg/mL). IL-1β levels were diminished by 63.76% at 500 µg/mL concentrations, IL-6 concentration by 94.15% and TNF-α by 88.67%. Parallelly, estimation of NO levels using Griess assay also showed significant decline of 53.47% at 500 µg/mL concentrations. These *in vitro* results corroborated the anti-inflammatory efficacy of PCBE and motivated the investigator to continue the chemical investigation of bioactive chemical constituents on it. PCBE was then subjected to various chromatographic techniques for the isolation and identification of potential leads for the treatment of various inflammatory diseases.

Around twenty compounds were isolated from PCBE and they were characterised as cyclic dipeptides using various spectroscopic techniques. Among them, seventeen cyclic dipeptides [(cyclo(Val-Pro) (**1**), cyclo(Leu-Pro) (**2**), cyclo(Val-Leu) (**3**), cyclo(Val-Phe) (**5**), cyclo(Ile-Phe) (**6**), cyclo(Leu-Ile) (**7**), cyclo(Leu-Leu) (**8**), cyclo(Pro-Tyr) (**10**), cyclo(Ala-Pro) (**11**), cyclo(Gly-Phe) (**13**), cyclo(Ala-Phe) (**14**), cyclo(Ala-Ile) (**15**), cyclo(Gly-Tyr)(**16**), cyclo(Ala-Tyr) (**17**), cyclo(Val-Tyr) (**18**), cyclo(Leu-Tyr) (**19**) and cyclo(Ala-Ala) (**20**)] are being reported for the first time from *Pseudomonas* species. Furthermore, proline-based cyclic dipeptides were obtained as major compounds which were screened for pharmacological activity using *in vitro* and *in vivo* models of inflammation. Compounds **1**, **2**, **9-12** were examined for pro-inflammatory cytokine inhibition potential using LPS-induced *in vitro* model of inflammation at logarithmic doses of 3, 10, 30 and 100 µM. Cyclic dipeptides were found to be non-cytotoxic in RAW 264.7 cell lines with IC_{50} values ranging from 270-450 µM. Cyclic dipeptides significantly suppressed IL-1β, TNF-α and IL-6 levels with IC_{50} values ranging from 44-62 µM, 115-458 µM and 40-104 µM, respectively. Likewise, nitrite levels were also suppressed by compounds **1**, **2**, **9-12** to considerable extent. Together it can be inferred from these results that proline based cyclic dipeptides effectively controlled pro-inflammatory cytokines mediated inflammation.

The effect of these six cyclic dipeptides **1**, **2**, **9**, **10**, **11** and **12** were then screened in *in vivo* model of oxalate induced nephropathy at a randomly selected 50 mg/kg body weight dose. Compounds **1**, **2**, **9**, **10**, **11** and **12** significantly attenuated oxalate induced plasma IL-1β levels ($P < 0.001$). Cyclo(Val-Pro) (**1**) showed 57% suppression of plasma IL-1β levels, cyclo(Leu-Pro) (**2**) reduced by 48.12% while cyclo(Leu-Hydroxy-Pro) (**9**) showed 36.97% inhibition in ELISA studies. Cyclo(Leu-Pro) (**2**) lowered blood urea nitrogen (BUN) by 19.57%, while cyclo(Val-Pro) (**1**) significantly reduced BUN by 35.21% inhibition. Based on the results of plasma IL-1β and BUN levels, further mRNA expression and histopathology studies were done on compound **1**. Cyclo(Val-Pro) (**1**) significantly attenuated mRNA expression of kidney injury marker KIM-1 ($P < 0.001$) and pro-inflammatory markers IL-1β ($P < 0.01$), TNF-α and IL-6 levels ($P < 0.05$). Compound **1** markedly protected the renal tissues architecture against oxalate nephropathy. *In vitro* mechanistic study done on compound **1** showed significant reduction of mRNA gene expression of pro-inflammatory cytokines and marked reduction of protein expression levels of pro-IL-1β and mature IL-1β.

In view of the favourable effects of cyclo(Val-Pro) (**1**) and cyclo(Leu-Hydroxy-Pro) (**9**) in improving oxalate induced renal nephropathy, compound **1** and **9** were further screened under ischemic reperfusion model at different doses of 25, 50 and 75 mg/kg body weight. The plasma IL-1β levels were considerably downregulated at 75 mg/kg dose. Even at a low dose of 25 mg/kg, 25.00% inhibition effect was observed in compound **1**. Furthermore, compound **1** and compound **9** showed significant abrogation of mRNA levels of kidney injury markers KIM-1, NGAL, α-GST and π-GST and IL-1β, TNF-α and IL-6 cytokines at 75 mg/kg and 50 mg/kg body weight doses. Even, low dose of 25 mg/kg also showed marked decline in the levels of pro-inflammatory cytokines and renal injury markers. Histopathological studies showed significant improvement in healing of the damage to renal tissue caused by ischemia. *In vitro* mechanistic study done using antimycin induced ischemia in NRK-52 E cell lines showed significant improvement in cell survivability rate in MTT as well as Flow cytometry assays while significant attenuation of pro-apoptotic protein Bax and anti-apoptotic protein BCL2 was observed in cyclo(Val-Pro) (**1**) and cyclo(Leu-Hydroxy-Pro) (**9**) treated cells.

Cyclo(Val-Pro) (**1**) was further tested in a chronic renal injury model of unilateral ureter obstruction model at 50 mg/kg body weight. Compound **1** showed significant abrogation of obstruction mediated renal fibrosis as depicted by protein expression study of fibrosis markers collagen-1, α-sma and TGF-β. Also, histopathological evaluation done using sirius red staining showed marked alleviation of renal fibrosis. In-vitro mechanistic study done using TGF-β

induced fibrotic model in NRK-49F cell lines, showed significant improvement in cell survivability rate. Collectively all results suggested a positive role of cyclic dipeptides derived from *Pseudomonas sp*. ABS-36 in attenuating cytokine mediated inflammation.

In conclusion, investigation of the constituents of PCBE revealed the secretion of a wide array of cyclic dipeptides by *Pseudomonas sp*. ABS-36. Six proline based cyclic dipeptides were tested for their anti-inflammatory efficacy in acute and chronic renal injury models for the first time. Also, cyclo(Val-Pro) (**1**) tested in detail under three different renal injury models was proved to be the most effective compound and thus explored as a lead molecule for developing therapeutic agent against renal inflammation.

Chapter 7

Future Perspectives

Future perspectives

1. In the present work, attempts were made to isolate secondary metabolites secreted by *Pseudomonas sp.* ABS-36 and they were characterised as cyclic dipeptides. Proline based cyclic dipeptides were tested for their efficacy under *in vitro* LPS-induced inflammation model, *in vivo* acute and chronic models of renal inflammation. The culture broth extract as well as the isolated constituents revealed tremendous potential in attenuating pro-inflammatory cytokine induced inflammation. The work could be continued to evaluate pharmacokinetic properties of these cyclic dipeptides in order to maximise the effect at lower doses.
2. Further, these compounds can be used as leads for synthesizing more active moieties in future.
3. Toxicity studies can be performed on these cyclic dipeptides.
4. Mechanistic study could be performed to evaluate the pathway involved.
5. Formulations can be developed for these compounds to improve pharmacokinetic and therapeutic profile.

References

References

1. Abbas, N. A., Salem, A. E., & Awad, M. M. (2018). Empagliflozin, SGLT 2 inhibitor, attenuates renal fibrosis in rats exposed to unilateral ureteric obstruction: potential role of klotho expression. *Naunyn-Schmiedeberg's Archives of Pharmacology*, 391(12), 1347-1360.
2. Abdulkhaleq, L. A., Assi, M. A., Abdullah, R., Zamri-Saad, M., Taufiq-Yap, Y. H., & Hezmee, M. N. M. (2018). The crucial roles of inflammatory mediators in inflammation: A review. *Veterinary World*, 11(5), 627.
3. Abou El-Ghar, M. E., Shokeir, A. A., Refaie, H. F., & El-Diasty, T. A. (2008). MRI in patients with chronic obstructive uropathy and compromised renal function: a sole method for morphological and functional assessment. *The British Journal of Radiology*, 81(968), 624-629.
4. Adnan, A. Z., Taher, M. U. H. A. M. M. A. D., Afriani, T. I. K. A., Fauzana, A. N. N. I. S. A., Roesma, D. I., & Putra, A. E. (2018). Anti-inflammatory activity of tinocrisposide by inhibiting nitric oxide production in lipopolysaccharides-stimulated raw 264.7 cells. *Asian Journal of Pharmaceutical and Clinical Research*, *11*(4), 149-153.
5. Ahil, S. B., Hira, K., Shaik, A. B., Pal, P. P., Kulkarni, O. P., Araya, H., & Fujimoto, Y. (2019). L-Proline-based-cyclic dipeptides from Pseudomonas sp.(ABS-36) inhibit pro-inflammatory cytokines and alleviate crystal-induced renal injury in mice. *International Immunopharmacology*, *73*, 395-404.
6. Allam, R., Kumar, S. V., Darisipudi, M. N., & Anders, H. J. (2014). Extracellular histones in tissue injury and inflammation. *Journal of Molecular Medicine*, *92*(5), 465-472.
7. Altaee, N., Kadhim, M. J., & Hameed, I. H. (2017). Detection of volatile compounds produced by Pseudomonas aeruginosa isolated from UTI patients by gas chromatography-mass spectrometry. *International Journal of Current Pharmaceutical Review and Research*, 7(6), 8-24.
8. Ashley, N. T., Weil, Z. M., & Nelson, R. J. (2012). Inflammation: mechanisms, costs, and natural variation. *Annual Review of Ecology, Evolution, and Systematics*, 43, 385-406.

9. Bagga, A., Bakkaloglu, A., Devarajan, P., Mehta, R. L., Kellum, J. A., Shah, S. V., ... & Levin, A. (2007). Improving outcomes from acute kidney injury: report of an initiative. *Pediatric Nephrology*, 22(10), 1655.
10. Bao, L., Yu, J., Zhong, H., Huang, D., & Lu, Q. (2017). Expression of toll-like receptors in T lymphocytes stimulated with N-(3-oxododecanoyl)-L-homoserine lactone from Pseudomonas aeruginosa. *Acta Pathologica, Microbiologica, et Immunologica Scandinavica*, 125(6), 553-557.
11. Bellezza, I., Grottelli, S., Mierla, A. L., Cacciatore, I., Fornasari, E., Roscini, L., ... & Minelli, A. (2014). Neuroinflammation and endoplasmic reticulum stress are coregulated by cyclo (His-Pro) to prevent LPS neurotoxicity. *The International Journal of Biochemistry & Cell Biology*, *51*, 159-169.
12. Bhardwaj, M., Sali, V. K., Mani, S., & Vasanthi, H. R. (2020). Neophytadiene from Turbinaria ornata Suppresses LPS-Induced Inflammatory Response in RAW 264.7 Macrophages and Sprague Dawley Rats. *Inflammation*, 1-14.
13. Bhargava, H. N., & Ritzmann, R. F. (1980). Inhibition of neuroleptic-induced dopamine receptor supersensitivity by cyclo (Leu-Gly). *Pharmacology Biochemistry and Behavior*, *13*(5), 633-636.
14. Biernacka, A., Dobaczewski, M., & Frangogiannis, N. G. (2011). TGF-β signaling in fibrosis. *Growth Factors*, 29(5), 196-202.
15. Bilbault, H., & Haymann, J. P. (2016). Experimental models of renal calcium stones in rodents. *World Journal of Nephrology*, *5*(2), 189.
16. Bina, X. R., & Bina, J. E. (2010). The cyclic dipeptide cyclo (Phe-Pro) inhibits cholera toxin and toxin-coregulated pilus production in O1 El Tor Vibrio cholerae. *Journal of Bacteriology*, 192(14), 3829-3832.
17. Blondin, J., Purkerson, M. L., Rolf, D., Schoolwerth, A. C., & Klahr, S. (1975). Renal function and metabolism after relief of unilateral ureteral obstruction. *Proceedings of the Society for Experimental Biology and Medicine*, 150(1), 71-76.
18. Bonegio, R., & Lieberthal, W. (2002). Role of apoptosis in the pathogenesis of acute renal failure. *Current Opinion in Nephrology and Hypertension*, *11*(3), 301-308.
19. Bonventre, J. V., & Yang, L. (2011). Cellular pathophysiology of ischemic acute kidney injury. *The Journal of Clinical Investigation*, 121(11), 4210-4221.
20. Böttinger, E. P. (2007). TGF-β in renal injury and disease. *In Seminars in Nephrology* (Vol. 27, No. 3, pp. 309-320). WB Saunders.

21. Bratchkova, A., & Ivanova, V. (2017). Isolation, identification and biological activities of cyclic dipeptides from antarctic microorganisms. *Comptes Rendus de l'Académie bulgare des Sciences*, 70(10), 1389-1399.
22. Brenner, P. S., & Krakauer, T. (2003). Regulation of inflammation: A review of recent advances in anti-inflammatory strategies. *Current Medicinal Chemistry-Anti-Inflammatory & Anti-Allergy Agents*, 2(3), 274-283.
23. Budzikiewicz, H. (1993). Secondary metabolites from fluorescent pseudomonads. *FEMS Microbiology Letters*, *104*(3-4), 209-228.
24. Campbell, J., Lin, Q., Geske, G. D., & Blackwell, H. E. (2009). New and unexpected insights into the modulation of LuxR-type quorum sensing by cyclic dipeptides. *ACS Chemical Biology*, 4(12), 1051-1059**.**
25. Chang, Y. K., Choi, H., Jeong, J. Y., Na, K. R., Lee, K. W., Lim, B. J., & Choi, D. E. (2016). Dapagliflozin, SGLT2 inhibitor, attenuates renal ischemia-reperfusion injury. *PloS one*, *11*(7).
26. Chawla, L. S., Eggers, P. W., Star, R. A., & Kimmel, P. L. (2014). Acute kidney injury and chronic kidney disease as interconnected syndromes. *New England Journal of Medicine*, 371(1), 58-66.
27. Chen, G., Tian, L., Wu, H. H., Bai, J., Lu, X., Xu, Y., & Pei, Y. H. (2012). Secondary metabolites from fungus Nigrospora sp. *Journal of Asian Natural Products Research*, 14(8), 759-763.
28. Chen, Guangjian(2016). *Chinese Patent No. CN 105288585 A 20160203.*
29. Chen, L., Deng, H., Cui, H., Fang, J., Zuo, Z., Deng, J., ... & Zhao, L. (2018). Inflammatory responses and inflammation-associated diseases in organs. *Oncotarget*, 9(6), 7204.
30. Chen, L., Guo, Q. F., Ma, J. W., & Kang, W. Y. (2018). Chemical constituents of *Bacillus coagulans* LL1103. *Chemistry of Natural Compounds*, 54(2), 419-420.
31. Chen, T. K., Knicely, D. H., & Grams, M. E. (2019). Chronic kidney disease diagnosis and management: A review. *Jama*, 322(13), 1294-1304.
32. Cheng, C., Othman, E. M., Stopper, H., Edrada-Ebel, R., Hentschel, U., & Abdelmohsen, U. R. (2017). Isolation of petrocidin A, a new cytotoxic cyclic dipeptide from the marine sponge-derived bacterium *Streptomyces* sp. SBT348. *Marine drugs*, 15(12), 383.

33. Chevalier, R. L., Thornhill, B. A., Forbes, M. S., & Kiley, S. C. (2010). Mechanisms of renal injury and progression of renal disease in congenital obstructive nephropathy. *Pediatric nephrology*, 25(4), 687-697.
34. Chevalier, R. L., Forbes, M. S., & Thornhill, B. A. (2009). Ureteral obstruction as a model of renal interstitial fibrosis and obstructive nephropathy. *Kidney International*, *75*(11), 1145-1152.
35. Choi, H., Ku, S. K., & Bae, J. S. (2016). Inhibitory Effect of Three Diketopiperazines from Marine-derived Bacteria on Secretory Group IIA Phospholipase A2. *Natural Product Communications*, 11(9), 1934578X1601100919.
36. Chung, A. C., Huang, X. R., Meng, X., & Lan, H. Y. (2010). miR-192 mediates TGF-β/Smad3-driven renal fibrosis. *Journal of the American Society of Nephrology*, 21(8), 1317-1325.
37. Coursindel, T., Restouin, A., Dewynter, G., Martinez, J., Collette, Y., & Parrot, I. (2010). Stereoselective ring contraction of 2, 5-diketopiperazines: an innovative approach to the synthesis of promising bioactive 5-membered scaffolds. *Bioorganic Chemistry*, 38(5), 210-217.
38. Daemen, M. A., van de Ven, M. W., Heineman, E., & Buurman, W. A. (1999). Involvement of endogenous interleukin-10 and tumor necrosis factor-α in renal ischemia-reperfusion injury1, 2. *Transplantation*, *67*(6), 792-800.
39. de Vries, B., Köhl, J., Leclercq, W. K., Wolfs, T. G., van Bijnen, A. A., Heeringa, P., & Buurman, W. A. (2003). Complement factor C5a mediates renal ischemia-reperfusion injury independent from neutrophils. *The Journal of Immunology*, 170(7), 3883-3889.
40. Deepa, I., Kumar, S. N., Sreerag, R. S., Nath, V. S., & Mohandas, C. (2015). Purification and synergistic antibacterial activity of arginine derived cyclic dipeptides, from *Achromobacter* sp. associated with a rhabditid entomopathogenic nematode against major clinically relevant biofilm forming wound bacteria. *Frontiers in Microbiology*, 6, 876.
41. De-hai, L., Qian-qun, G., Wei-ming, Z., Hong-bing, L., Yu-chun, F., & Tian-jiao, Z. (2005). Antitumor components from marine actinomycete 11014 I. Cyclic dipeptides. *Chinese Journal of Antibiotics*, 30(8), 449.
42. Denning, G. M., Iyer, S. S., Reszka, K. J., O'Malley, Y., Rasmussen, G. T., & Britigan, B. E. (2003). Phenazine-1-carboxylic acid, a secondary metabolite of Pseudomonas aeruginosa, alters expression of immunomodulatory proteins by human airway

epithelial cells. *American Journal of Physiology-Lung Cellular and Molecular Physiology*, 285(3), L584-L592.

43. Devarajan, P. (2008). Neutrophil gelatinase-associated lipocalin (NGAL): a new marker of kidney disease. *Scandinavian journal of clinical and laboratory investigation*, 68(sup241), 89-94.
44. Di Sole, F., Hu, M. C., Zhang, J., Babich, V., Bobulescu, I. A., Shi, M., ... & Moe, O. W. (2011). The reduction of Na/H exchanger-3 protein and transcript expression in acute ischemia–reperfusion injury is mediated by extractable tissue factor (s). *Kidney International*, 80(8), 822-831.
45. Donnahoo, K. K., Shames, B. D., Harken, A. H., & Meldrum, D. R. (1999). The role of tumor necrosis factor in renal ischemia-reperfusion injury. *The Journal of Urology*, *162*(1), 196-203.
46. Fan, J. M., Huang, X. R., Ng, Y. Y., Nikolic-Paterson, D. J., Mu, W., Atkins, R. C., & Lan, H. Y. (2001). Interleukin-1 induces tubular epithelial-myofibroblast transdifferentiation through a transforming growth factor-β1-dependent mechanism in vitro. *American Journal of Kidney Diseases*, *37*(4), 820-831
47. Fang, T., Koo, T. Y., Lee, J. G., Jang, J. Y., Xu, Y., Hwang, J. H., ... & Kim, S. Y. (2019). Anti-CD45RB Antibody Therapy Attenuates Renal Ischemia-Reperfusion Injury by Inducing Regulatory B Cells. *Journal of the American Society of Nephrology*, *30*(10), 1870-1885.
48. Ferro, J. N. D. S., de Aquino, F. L. T., de Brito, R. G., dos Santos, P. L., Quintans, J. D. S. S., de Souza, L. C., ... & Barreto, E. (2015). Cyclo-Gly-Pro, a cyclic dipeptide, attenuates nociceptive behaviour and inflammatory response in mice. *Clinical and Experimental Pharmacology and Physiology*, *42*(12), 1287-1295.
49. Fiorentino, M., Grandaliano, G., Gesualdo, L., & Castellano, G. (2018). Acute kidney injury to chronic kidney disease transition. *In Acute Kidney Injury-Basic Research and Clinical Practice* (Vol. 193, pp. 45-54). Karger Publishers.
50. Fischer, R., Kontermann, R. E., & Maier, O. (2015). Targeting sTNF/TNFR1 signaling as a new therapeutic strategy. *Antibodies*, 4(1), 48-70.
51. Frikha Dammak, D., Zarai, Z., Najah, S., Abdennabi, R., Belbahri, L., Rateb, M. E., ... & Maalej, S. (2017). Antagonistic properties of some halophilic thermoactinomycetes isolated from superficial sediment of a solar saltern and production of cyclic antimicrobial peptides by the novel isolate *Paludifilum halophilum*. *BioMed Research International*, 2017.

52. Fry, A. C., & Farrington, K. (2006). Management of acute renal failure. *Postgraduate Medical journal*, 82(964), 106-116.
53. Fukasawa, H., Yamamoto, T., Suzuki, H., Togawa, A., Ohashi, N., Fujigaki, Y., ... & Hishida, A. (2004). Treatment with anti-TGF-β antibody ameliorates chronic progressive nephritis by inhibiting Smad/TGF-β signaling. *Kidney International*, 65(1), 63-74.
54. Furtado, N. A., Pupo, M. T., Carvalho, I., Campo, V. L., Duarte, M. C. T., & Bastos, J. K. (2005). Diketopiperazines produced by an *Aspergillus fumigatus* Brazilian strain. *Journal of the Brazilian Chemical Society*, 16(6B), 1448-1453.
55. Furuichi, K., Wada, T., Iwata, Y., Kokubo, S., Hara, A., Yamahana, J., ... & Yokoyama, H. (2006). Interleukin-1-dependent sequential chemokine expression and inflammatory cell infiltration in ischemia-reperfusion injury. *Critical Care Medicine*, 34(9), 2447-2455
56. Furukawa, T., Akutagawa, T., Funatani, H., Uchida, T., Hotta, Y., Niwa, M., & Takaya, Y. (2012). Cyclic dipeptides exhibit potency for scavenging radicals. *Bioorganic & Medicinal Chemistry*, 20(6), 2002-2009.
57. Garaud, S., Le Dantec, C., Jousse-Joulin, S., Hanrotel-Saliou, C., Saraux, A., Mageed, R. A., ... & Renaudineau, Y. (2009). IL-6 modulates CD5 expression in B cells from patients with lupus by regulating DNA methylation. *The Journal of Immunology*, 182(9), 5623-5632.
58. Ghaly, A., & Marsh, D. R. (2010). Ischaemia–reperfusion modulates inflammation and fibrosis of skeletal muscle after contusion injury. *International Journal of Experimental Pathology*, 91(3), 244-255.
59. Ghasemi, A., Hedayati, M., & Biabani, H. (2007). Protein precipitation methods evaluated for determination of serum nitric oxide end products by the Griess assay. *Journal of Medical Sciences Research*, 2(15), 29-32.
60. Kumar, S. S., Hira, K., Ahil, S. B., Kulkarni, O. P., Araya, H., & Fujimoto, Y. (2020). New synthetic coumarinolignans as attenuators of pro-inflammatory cytokines in LPS-induced sepsis and carrageenan-induced paw oedema models. *Inflammopharmacology*.
61. Glucksam-Galnoy, Y., Sananes, R., Silberstein, N., Krief, P., Kravchenko, V. V., Meijler, M. M., & Zor, T. (2013). The bacterial quorum-sensing signal molecule N-3-oxo-dodecanoyl-L-homoserine lactone reciprocally modulates pro-and anti-

inflammatory cytokines in activated macrophages. *The Journal of Immunology*, 191(1), 337-344.

62. Grande, M. T., Pérez-Barriocanal, F., & López-Novoa, J. M. (2010). Role of inflammation in tubulo-interstitial damage associated to obstructive nephropathy. *Journal of Inflammation*, 7(1), 1-14.
63. Gross, H., & Loper, J. E. (2009). Genomics of secondary metabolite production by Pseudomonas spp. *Natural Product Reports*, *26*(11), 1408-1446.
64. Grottelli, S., Ferrari, I., Pietrini, G., Peirce, M. J., Minelli, A., & Bellezza, I. (2016). The role of cyclo (His-Pro) in neurodegeneration. *International Journal of Molecular Sciences*, 17(8), 1332.
65. Guo, G., Morrissey, J., McCracken, R., Tolley, T., Liapis, H., & Klahr, S. (2001). Contributions of angiotensin II and tumor necrosis factor-α to the development of renal fibrosis. *American Journal of Physiology-Renal Physiology*, *280*(5), F777-F785.
66. Guo, Q., Guo, D., Zhao, B., Xu, J., & Li, R. (2007). Two cyclic dipeptides from *Pseudomonas fluorescens* GcM5-1A carried by the pine wood nematode and their toxicities to Japanese black pine suspension cells and seedlings in vitro. *Journal of Nematology*, 39(3), 243.
67. Guo, R., Wang, Y., Minto, A. W., Quigg, R. J., & Cunningham, P. N. (2004). Acute renal failure in endotoxemia is dependent on caspase activation. *Journal of the American Society of Nephrology*, *15*(12), 3093-3102.
68. Hameed, R. H., Abbas, F. M., & Hameed, I. H. (2018). Analysis of Secondary Metabolites Released by *Pseudomonas fluorescens* Using GC-MS Technique and Determination of Its Anti-Fungal Activity. *Indian Journal of Public Health Research & Development*, 9(5), 449-455.
69. Han, W. K., Bailly, V., Abichandani, R., Thadhani, R., & Bonventre, J. V. (2002). Kidney Injury Molecule-1 (KIM-1): a novel biomarker for human renal proximal tubule injury. *Kidney International*, 62(1), 237-244.
70. Haq, M., Norman, J., Saba, S. R., Ramirez, G., & Rabb, H. (1998). Role of IL-1 in renal ischemic reperfusion injury. *Journal of the American Society of Nephrology*, *9*(4), 614-619.
71. Hayakawa, Y., Akimoto, M., Ishikawa, A., Izawa, M., & Shin-Ya, K. (2016). Curromycin A as a GRP78 downregulator and a new cyclic dipeptide from Streptomyces sp. *The Journal of Antibiotics*, 69(3), 187-188.

72. He, W. M., Yin, J. Q., Cheng, X. D., Lu, X., Ni, L., Xi, Y., ... & Wei, M. G. (2018). Oleanolic acid attenuates TGF-β1-induced epithelial-mesenchymal transition in NRK-52E cells. *BMC Complementary and Alternative Medicine*, 18(1), 1-8.
73. Hernández-Padilla, L., Vázquez-Rivera, D., Sánchez-Briones, L. A., Díaz-Pérez, A. L., Moreno-Rodríguez, J., Moreno-Eutimio, M. A., ... & Campos-García, J. (2017). The antiproliferative effect of cyclodipeptides from *Pseudomonas aeruginosa* PAO1 on HeLa cells involves inhibition of phosphorylation of Akt and S6k kinases. *Molecules*, 22(6), 1024.
74. Hira, K., Shaik, A., Kumar, S., & Ahil, S. B (2017). Pseudomonas-A potential Source for Drug Lead Discovery. *Current Trends in Biomedical Engineering & Biosciences*, 5(5), 555674.
75. Hooi, D. S., Bycroft, B. W., Chhabra, S. R., Williams, P., & Pritchard, D. I. (2004). Differential immune modulatory activity of Pseudomonas aeruginosa quorum-sensing signal molecules. *Infection and Immunity*, 72(11), 6463-6470.
76. Hoque, F., Abraham, T. J., & Jaisankar, P. (2019). Isolation and partial characterisation of secondary metabolites from fish-borne bacterium, *Pseudomonas aeruginosa*. *Indian Journal of Fisheries*, 66(1), 81-91.
77. Horii, Y., Muraguchi, A., Iwano, M., Matsuda, T., Hirayama, T., Yamada, H., ... & Ohmoto, Y. (1989). Involvement of IL-6 in mesangial proliferative glomerulonephritis. *The Journal of Immunology*, 143(12), 3949-3955.
78. Hosseinian, S., Rad, A. K., Bideskan, A. E., Soukhtanloo, M., Sadeghnia, H., Shafei, M. N., ... & Beheshti, F. (2017). Thymoquinone ameliorates renal damage in unilateral ureteral obstruction in rats. *Pharmacological Reports*, 69(4), 648-657.
79. https://www.thermofisher.com/in/en/home/references/ambion-tech-support/rna-isolation/tech-notes/is-your-rna-intact.html. Accessed 14 May 2020.
80. Huang, D., Zhou, H., & Gao, J. (2015). Nanoparticles modulate autophagic effect in a dispersity-dependent manner. *Scientific Reports*, *5*, 14361.
81. Jarvis, F. G., & Johnson, M. J. (1949). A glyco-lipide produced by Pseudomonas aeruginosa. *Journal of the American Chemical Society*, 71(12), 4124-4126.
82. Jeong, S., Ku, S. K., Min, G., Choi, H., Park, D. H., & Bae, J. S. (2016). Suppressive effects of three diketopiperazines from marine-derived bacteria on polyphosphate-mediated septic responses. *Chemico-Biological Interactions*, 257, 61-70.

83. Jin, W. U., Xiao-ming, L. U., & Ya-le, D. U. A. N. (2013). Cyclo (L-Pro-L-Phe) dipeptide: the potential phosphodiesterase inhibitors. *Journal of East China Normal University (Natural Science)*, *2013*(2), 84.
84. Jo, S. K., Rosner, M. H., & Okusa, M. D. (2007). Pharmacologic treatment of acute kidney injury: why drugs haven't worked and what is on the horizon. *Clinical Journal of the American Society of Nephrology*, 2(2), 356-365.
85. Jones, S. A., Fraser, D. J., Fielding, C. A., & Jones, G. W. (2015). Interleukin-6 in renal disease and therapy. *Nephrology Dialysis Transplantation*, 30(4), 564-574.
86. Kahn, S. A., Gulmi, F. A., Chou, S. Y., Mooppan, U. M., & Kim, H. (1997). Contribution of endothelin-1 to renal vasoconstriction in unilateral ureteral obstruction: reversal by verapamil. *The Journal of Urology*, 157(5), 1957-1962.
87. Kang, H., Ku, S. K., Choi, H., & Bae, J. S. (2016). Three diketopiperazines from marine-derived bacteria inhibit LPS-induced endothelial inflammatory responses. *Bioorganic & Medicinal Chemistry Letters*, 26(8), 1873-1876.
88. Karkar, A. M., Tam, F. W., Steinkasserer, A., Kurrle, R., Langner, K., Scallon, B. J., ... & Rees, A. J. (1995). Modulation of antibody-mediated glomerular injury in vivo by IL-1ra, soluble IL-1 receptor, and soluble TNF receptor. *Kidney International*, 48(6), 1738-1746.
89. Khaled, J. M., Al-Mekhlafi, F. A., Mothana, R. A., Alharbi, N. S., Alzaharni, K. E., Sharafaddin, A. H., ... & Benelli, G. (2018). Brevibacillus laterosporus isolated from the digestive tract of honeybees has high antimicrobial activity and promotes growth and productivity of honeybee's colonies. *Environmental Science and Pollution Research*, 25(11), 10447-10455.
90. Khambati, I., Han, S., Pijnenburg, D., Jang, H., & Forsythe, P. (2017). The bacterial quorum-sensing molecule, N-3-oxo-dodecanoyl-L-homoserine lactone, inhibits mediator release and chemotaxis of murine mast cells. *Inflammation Research*, 66(3), 259-268.
91. Khan, R., Basha, A., Goverdhanam, R., Rao, P. C., Tanemura, Y., Fujimoto, Y., & Begum, A. S. (2015). Attenuation of TNF-α secretion by l-proline-based cyclic dipeptides produced by culture broth of *Pseudomonas aeruginosa. Bioorganic & Medicinal Chemistry Letters*, 25(24), 5756-5761.
92. Khan, S. B., Cook, H. T., Bhangal, G., Smith, J., Tam, F. W., & Pusey, C. D. (2005). Antibody blockade of TNF-α reduces inflammation and scarring in experimental crescentic glomerulonephritis. *Kidney International*, 67(5), 1812-1820.

93. Khan, S. R. (1997). Animal models of kidney stone formation: an analysis. *World Journal of Urology*, 15(4), 236-243.
94. Khan, S. R., Pearle, M. S., Robertson, W. G., Gambaro, G., Canales, B. K., Doizi, S., ... & Tiselius, H. G. (2016). Kidney stones. *Nature Reviews Disease Primers*, *2*(1), 1-23.
95. Kiberd, B. A. (1993). Interleukin-6 receptor blockage ameliorates murine lupus nephritis. *Journal of the American Society of Nephrology*, 4(1), 58-61.
96. Kielar, M. L., John, R., Bennett, M., Richardson, J. A., Shelton, J. M., Chen, L., ... & Nagami, G. T. (2005). Maladaptive role of IL-6 in ischemic acute renal failure. *Journal of the American Society of Nephrology*, 16(11), 3315-3325.
97. Kilian, G., Davids, H., & Milne, P. J. (2013). Anticancer activity of the liposome-encapsulated cyclic dipeptides, cyclo (His-Gly) and cyclo (His-Ala). *Die Pharmazie-An International Journal of Pharmaceutical Sciences*, 68(3), 207-211.
98. Kim, E. H., Choi, Y. S., & Kim, Y. M. (2019). Antioxidative and anti-inflammatory effect of Phellinus igniarius on RAW 264.7 macrophage cells. *Journal of Exercise Rehabilitation*, 15(1), 2
99. Kim, Y. S., Park, J. J., Sakoda, Y., Zhao, Y., Hisamichi, K., Kaku, T. I., & Tamada, K. (2010). Preventive and therapeutic potential of placental extract in contact hypersensitivity. *International Immunopharmacology*, 10(10), 1177-1184.
100. Kishimoto, K., Kinoshita, K., Hino, S., Yano, T., Nagare, Y., Shimazu, H., ... & Funauchi, M. (2011). Therapeutic effect of retinoic acid on unilateral ureteral obstruction model. *Nephron Experimental Nephrology*, 118(3), e69-e78.
101. Kolisnikova, K. N., Gudasheva, T. A., Nazarova, G. A., Antipov, T. A., Voronina, T. A., & Seredenin, S. B. (2012). Similarity of cycloprolylglycine to piracetam in antihypoxic and neuroprotective effects. *Eksperimental'naia i Klinicheskaia Farmakologiia*, 75(9), 3-6.
102. Kolyasnikova, K., Nazarova, G., Gudasheva, T., Voronina, T., & Seredenin, S. (2015). Antihypoxic activity of cycloprolylglycine analogs. *Bulletin of Experimental Biology & Medicine*, 158(4).
103. Komada, T., Usui, F., Kawashima, A., Kimura, H., Karasawa, T., Inoue, Y., ... & Muto, S. (2015). Role of NLRP3 inflammasomes for rhabdomyolysis-induced acute kidney injury. *Scientific Reports*, 5, 10901.
104. Kravchenko, V. V., Kaufmann, G. F., Mathison, J. C., Scott, D. A., Katz, A. Z., Grauer, D. C., ... & Ulevitch, R. J. (2008). Modulation of gene expression via disruption of NF-κB signaling by a bacterial small molecule. *Science*, 321(5886), 259-263.

105. Kumar, S. S., Begum, A. S., Hira, K., Niazi, S., Kumar, B. P., Araya, H., & Fujimoto, Y. (2019). Structure-based design and synthesis of new 4-methylcoumarin-based lignans as pro-inflammatory cytokines (TNF-α, IL-6 and IL-1β) inhibitors. *Bioorganic Chemistry*, 89, 102991.
106. Kwak, M. K., Liu, R., Kim, M. K., Moon, D., Kim, A. H., Song, S. H., & Kang, S. O. (2014). Cyclic dipeptides from lactic acid bacteria inhibit the proliferation of pathogenic fungi. *Journal of Microbiology*, 52(1), 64-70.
107. Kwak, M. K., Liu, R., Kwon, J. O., Kim, M. K., Kim, A. H., & Kang, S. O. (2013). Cyclic dipeptides from lactic acid bacteria inhibit proliferation of the influenza A virus. *Journal of Microbiology*, 51(6), 836-843.
108. Lan, H. Y. (2011). Diverse roles of TGF-β/Smads in renal fibrosis and inflammation. *International Journal of Biological Sciences*, 7(7), 1056.
109. Lan, H. Y., Nikolic-Paterson, D. J., Zarama, M., Vannice, J. L., & Atkins, R. C. (1993). Suppression of experimental crescentic glomerulonephritis by the interleukin-1 receptor antagonist. *Kidney International*, 43(2), 479-485.
110. Laville, R., Nguyen, T. B., Moriou, C., Petek, S., Debitus, C., & Al-Mourabit, A. (2015). Marine natural occurring 2, 5-diketopiperazines: isolation, synthesis and optical properties. *Heterocycles*, 90(2), 1351-1366.
111. Laxmi, M., & Bhat, S. G. (2016). Characterization of pyocyanin with radical scavenging and antibiofilm properties isolated from *Pseudomonas aeruginosa* strain BTRY1. 3 *Biotech*, 6(1), 27.
112. Lee, M. C. I., Velayutham, M., Komatsu, T., Hille, R., & Zweier, J. L. (2014). Measurement and characterization of superoxide generation from xanthine dehydrogenase: a redox-regulated pathway of radical generation in ischemic tissues. *Biochemistry*, 53(41), 6615-6623.
113. Lee, W., Ku, S. K., Choi, H., & Bae, J. S. (2016). Inhibitory effects of three diketopiperazines from marine-derived bacteria on endothelial protein C receptor shedding in human endothelial cells and mice. *Fitoterapia*, 110, 181-188.
114. Lee, W., Ku, S. K., Park, S., Kim, K. M., Choi, H., & Bae, J. S. (2016). Inhibitory Effect of Three Diketopiperazines from Marine-Derived Bacteria on HMGB1-Induced Septic Responses in vitro and in vivo. *The American journal of Chinese medicine*, 44(06), 1145-1166.
115. Lee, Y. J., & Han, H. J. (2005). Effect of adenosine triphosphate in renal ischemic injury: Involvement of NF-κB. *Journal of Cellular Physiology*, 204(3), 792-799.

116. Lei, Y., Devarapu, S. K., Motrapu, M., Cohen, C., Lindenmeyer, M. T., Moll, S., ... & Anders, H. J. (2019). Interleukin-1β inhibition for chronic kidney disease in obese mice with type 2 diabetes. *Frontiers in Immunology*, 10, 1223.
117. Li, X., Dobretsov, S., Xu, Y., Xiao, X., Hung, O. S., & Qian, P. Y. (2006). Antifouling diketopiperazines produced by a deep-sea bacterium, *Streptomyces fungicidicus*. *Biofouling*, 22(3), 187-194.
118. Liang, X., Schnaper, H. W., Matsusaka, T., Pastan, I., Ledbetter, S., & Hayashida, T. (2016). Anti-TGF-β Antibody, 1D11, Ameliorates Glomerular Fibrosis in Mouse Models after the Onset of Proteinuria. *PloS one*, 11(5).
119. Lin, W. X., Xie, C. L., Zhou, M., Xia, M. L., Zhou, T. T., Chen, H. F., ... & Yang, Q. (2018). Chemical constituents from the deep sea-derived *Streptomyces xiamenensis* MCCC 1A01570 and their effects on RXRα transcriptional regulation. *Natural Product Research*, 1-4.
120. Lindeberg, M., Myers, C. R., Collmer, A., & Schneider, D. J. (2008). Roadmap to new virulence determinants in Pseudomonas syringae: insights from comparative genomics and genome organization. *Molecular Plant-Microbe Interactions*, 21(6), 685-700.
121. Linkermann, A., Hackl, M. J., Kunzendorf, U., Walczak, H., Krautwald, S., & Jevnikar, A. M. (2013). Necroptosis in immunity and ischemia-reperfusion injury. *American Journal of Transplantation*, 13(11), 2797-2804.
122. Liu, H. B., Gao, H., Wang, N. L., Lin, H. P., Hong, K., & Yao, X. S. (2007). Cyclic dipeptide constituents from the mangrove fungus *Penicillium oxalicum* (No. 092007)[J]. *Journal of Shenyang Pharmaceutical University*, 8, 006.
123. Liu, Z., Xiao, Y., Chen, W., Wang, Y., Wang, B., Wang, G., ... & Tang, R. (2014). Calcium phosphate nanoparticles primarily induce cell necrosis through lysosomal rupture: the origination of material cytotoxicity. *Journal of Materials Chemistry B*, 2(22), 3480-3489.
124. López-Hernández, F. J., & López-Novoa, J. M. (2012). Role of TGF-β in chronic kidney disease: an integration of tubular, glomerular and vascular effects. *Cell and Tissue Research*, 347(1), 141-154.
125. Ludwig-Portugall, I., Bartok, E., Dhana, E., Evers, B. D., Primiano, M. J., Hall, J. P., ... & Boor, P. (2016). An NLRP3-specific inflammasome inhibitor attenuates crystal-induced kidney fibrosis in mice. *Kidney International*, 90(3), 525-539.
126. Makris, K., & Spanou, L. (2016). Acute kidney injury: definition, pathophysiology and clinical phenotypes. *The Clinical Biochemist Reviews*, 37(2), 85.

127. Malek, M., & Nematbakhsh, M. (2015). Renal ischemia/reperfusion injury; from pathophysiology to treatment. *Journal of Renal Injury Prevention*, 4(2), 20.
128. Mangamuri, U. K., Muvva, V., Poda, S., Chitturi, B., & Yenamandra, V. (2016). Bioactive natural products from *Pseudonocardia endophytica* VUK-10. *Journal of Genetic Engineering and Biotechnology*, 14(2), 261-267.
129. Marreiro de Sales-Neto, J., Lima, É. A., Cavalcante-Silva, L. H. A., Vasconcelos, U., & Rodrigues-Mascarenhas, S. (2019). Anti-inflammatory potential of pyocyanin in LPS-stimulated murine macrophages. *Immunopharmacology and Immunotoxicology*, 41(1), 102-108.
130. Masola, V., Carraro, A., Granata, S., Signorini, L., Bellin, G., Violi, P., ... & Zaza, G. (2019). In vitro effects of interleukin (IL)-1 beta inhibition on the epithelial-to-mesenchymal transition (EMT) of renal tubular and hepatic stellate cells. *Journal of Translational Medicine*, 17(1), 1-11.
131. McDaniel, B. L., & Bentley, M. L. (2015). The role of medications and their management in acute kidney injury. *Integrated Pharmacy Research & Practice*, 4, 21.
132. McMahon, B. A., Koyner, J. L., & Murray, P. T. (2010). Urinary glutathione S-transferases in the pathogenesis and diagnostic evaluation of acute kidney injury following cardiac surgery: a critical review. *Current Opinion in Critical Care*, 16(6), 550.
133. Mehnaz, S., Saleem, R. S. Z., Yameen, B., Pianet, I., Schnakenburg, G., Pietraszkiewicz, H., ... & Gross, H. (2013). Lahorenoic acids A–C, ortho-dialkyl-substituted aromatic acids from the biocontrol strain *Pseudomonas aurantiaca* PB-St2. *Journal of Natural Products*, 76(2), 135-141.76(2), 135-141.
134. Mehta, R. L., Kellum, J. A., Shah, S. V., Molitoris, B. A., Ronco, C., Warnock, D. G., & Levin, A. (2007). Acute Kidney Injury Network: report of an initiative to improve outcomes in acute kidney injury. *Critical Care*, 11(2), R31.
135. Meldrum, D. R., & Donnahoo, K. K. (1999). Role of TNF in mediating renal insufficiency following cardiac surgery: evidence of a postbypass cardiorenal syndrome. *Journal of Surgical Research*, 85(2), 185-199.
136. Meldrum, K. K., Misseri, R., Metcalfe, P., Dinarello, C. A., Hile, K. L., & Meldrum, D. R. (2007). TNF-α neutralization ameliorates obstruction-induced renal fibrosis and dysfunction. *American Journal of Physiology-Regulatory, Integrative and Comparative Physiology*, 292(4), R1456-R1464.

137. Mendes, A. F., Cruz, M. T., & Gualillo, O. (2018). The Physiology of Inflammation—The Final Common Pathway to Disease. *Frontiers in Physiology*, 9, 1741.
138. Mezaache-Aichour, S., Guechi, A., Zerroug, M. M., Nicklin, J., & Strange, R. N. (2013). Antimicrobial activity of *Pseudomonas* secondary metabolites. *Pharmacognosy Communications*, 3(3).
139. Mihai, S., Codrici, E., Popescu, I. D., Enciu, A. M., Albulescu, L., Necula, L. G., ... & Tanase, C. (2018). Inflammation-related mechanisms in chronic kidney disease prediction, progression, and outcome. *Journal of Immunology Research*, 2018.
140. Minelli, A., Bellezza, I., Grottelli, S., Pinnen, F., Brunetti, L., & Vacca, M. (2006). Phosphoproteomic analysis of the effect of cyclo-[His-Pro] dipeptide on PC12 cells. *Peptides*, 27(1), 105-113.
141. Mitsui-Saitoh, K., Furukawa, T., Akutagawa, T., Hasada, K., Mizutani, H., Sugimoto, Y., ... & Takaya, Y. (2011). Protective effects of cyclo (L-Leu-L-Tyr) against postischemic myocardial dysfunction in guinea-pig hearts. *Biological and Pharmaceutical Bulletin*, 34(3), 335-342.
142. Miyajima, A., Chen, J., Lawrence, C., Ledbetter, S., Soslow, R. A., Stern, J., ... & Vaughan Jr, E. D. (2000). Antibody to transforming growth factor-β ameliorates tubular apoptosis in unilateral ureteral obstruction. *Kidney International*, 58(6), 2301-2313.
143. MnIAs, N. E. (1995). Interleukin-1 in crescentic glomerulonephritis. *Kidney International*, 48, 576-586.
144. Mosmann, T. (1983). Rapid colorimetric assay for cellular growth and survival: application to proliferation and cytotoxicity assays. *Journal of Immunological Methods*, 65(1-2), 55-63.
145. Mulay, S. R., & Anders, H. J. (2017). Crystal nephropathies: mechanisms of crystal-induced kidney injury. *Nature Reviews Nephrology*, 13(4), 226-240.
146. Mulay, S. R., Eberhard, J. N., Desai, J., Marschner, J. A., Kumar, S. V., Weidenbusch, M., ... & Hans, W. (2017). Hyperoxaluria requires TNF receptors to initiate crystal adhesion and kidney stone disease. *Journal of the American Society of Nephrology*, 28(3), 761-768
147. Mulay, S. R., Eberhard, J. N., Pfann, V., Marschner, J. A., Darisipudi, M. N., Daniel, C., ... & Rathkolb, B. (2016). Oxalate-induced chronic kidney disease with its uremic and cardiovascular complications in C57BL/6 mice. *American Journal of Physiology-Renal Physiology*, *310*(8), F785-F795.

148. Mulay, S. R., Evan, A., & Anders, H. J. (2014). Molecular mechanisms of crystal-related kidney inflammation and injury. Implications for cholesterol embolism, crystalline nephropathies and kidney stone disease. *Nephrology Dialysis Transplantation*, 29(3), 507-514.
149. Mulay, S. R., Kulkarni, O. P., Rupanagudi, K. V., Migliorini, A., Darisipudi, M. N., Vilaysane, A., ... & Anders, H. J. (2012). Calcium oxalate crystals induce renal inflammation by NLRP3-mediated IL-1β secretion. *The Journal of Clinical Investigation*, 123(1).
150. Nalli, Y., Gupta, S., Khajuria, V., Singh, V. P., Sajgotra, M., Ahmed, Z., ... & Ali, A. (2017). TNF-α and IL-6 inhibitory effects of cyclic dipeptides isolated from marine bacteria *Streptomyces* sp. *Medicinal Chemistry Research*, 26(1), 93-100.
151. Nauta, R. J., Tsimoyiannis, E. V. A. N. G. E. L. O. S., Uribe, M. A. R. I. O., Walsh, D. B., Miller, D. E. B. O. R. A. H., & Butterfield, A. R. T. H. U. R. (1991). The role of calcium ions and calcium channel entry blockers in experimental ischemia-reperfusion-induced liver injury. *Annals of Surgery*, 213(2), 137.
152. Nechemia-Arbely, Y., Barkan, D., Pizov, G., Shriki, A., Rose-John, S., Galun, E., & Axelrod, J. H. (2008). IL-6/IL-6R axis plays a critical role in acute kidney injury. *Journal of the American Society of Nephrology*, 19(6), 1106-1115.
153. Nilov, D. K., Yashina, K. I., Gushchina, I. V., Zakharenko, A. L., Sukhanova, M. V., Lavrik, O. I., & Švedas, V. K. (2018). 2, 5-Diketopiperazines: a new class of poly (ADP-ribose) polymerase inhibitors. *Biochemistry* (Moscow), 83(2), 152-158.
154. Nishanth Kumar, S., & Mohandas, C. (2014). Antimycobacterial activity of cyclic dipeptides isolated from *Bacillus* sp. N strain associated with entomopathogenic nematode. *Pharmaceutical Biology*, 52(1), 91-96.
155. Nishanth Kumar, S., Dileep, C., Mohandas, C., Nambisan, B., & Ca, J. (2014). Cyclo (d-Tyr-d-Phe): a new antibacterial, anticancer, and antioxidant cyclic dipeptide from Bacillus sp. N strain associated with a rhabditid entomopathogenic nematode. *Journal of Peptide Science*, 20(3), 173-185.
156. Nishanth, S. K., Nambisan, B., & Dileep, C. (2014). Three bioactive cyclic dipeptides from the *Bacillus* sp. N strain associated with entomopathogenic nematode. *Peptides*, 53, 59-69.
157. Ohshima, T., & Sato, Y. (1998). Time-dependent expression of interleukin-10 (IL-10) mRNA during the early phase of skin wound healing as a possible indicator of wound vitality. *International Journal of Legal Medicine*, 111(5), 251-255.

158. Ortega, L. M., & Fornoni, A. (2010). Role of cytokines in the pathogenesis of acute and chronic kidney disease, glomerulonephritis, and end-stage kidney disease. International Journal of Interferon, *Cytokine and Mediator Research*, 2(1), 49-62.
159. Ostermeier, M., Limberg, C., Herwig, C., & Ziemer, B. (2009). Stabilizing the Boat Conformation of Piperazines Coordinated to Iron (II): iso-Butyl Substituents Lead to Robust Oxidation Catalysts via Hyperconjugation. *Zeitschrift Für Anorganische und Allgemeine Chemie*, 635(12), 1823-1830.
160. Palleroni, N. J. (2015). Pseudomonas. *Bergey's Manual of Systematics of Archaea and Bacteria*, 1-1.
161. Pandey, A. (2019). Pharmacological potential of marine microbes. *In Pharmaceuticals from Microbes* (pp. 1-25). Springer, Cham.
162. Pat, B., Yang, T., Kong, C., Watters, D., Johnson, D. W., & Gobe, G. (2005). Activation of ERK in renal fibrosis after unilateral ureteral obstruction: modulation by antioxidants. *Kidney International*, 67(3), 931-943.
163. Pecoits-Filho, R., Lindholm, B., Axelsson, J., & Stenvinkel, P. (2003). Update on interleukin-6 and its role in chronic renal failure. *Nephrology Dialysis Transplantation*, 18(6), 1042-1045.
164. Pérez-Picaso, L., Olivo, H. F., Argotte-Ramos, R., Rodríguez-Gutiérrez, M., & Rios, M. Y. (2012). Linear and cyclic dipeptides with antimalarial activity. *Bioorganic & Medicinal Chemistry Letters*, 22(23), 7048-7051.
165. Pettit, G. R., Du, J., Pettit, R. K., Richert, L. A., Hogan, F., Mukku, V. J., & Hoard, M. S. (2006). Antineoplastic Agents. 554. The Manitoba Bacterium *Streptomyces* sp., 1. *Journal of Natural Products*, 69(5), 804-806.
166. Prasad, C. (1995). Bioactive cyclic dipeptides. *Peptides*, 16(1), 151-164.
167. Qian, H. S., Weldon, S. M., Matera, D., Lee, C., Yang, H., Fryer, R. M., ... & Reinhart, G. A. (2016). Quantification and comparison of anti-fibrotic therapies by polarized SRM and SHG-based morphometry in rat UUO model. *PloS one*, 11(6).
168. R & D Systems (2020) https://www.rndsystems.com/products/mouse-tnf-alpha-duoset-elisa_dy410. Accessed on 14 May 2020.
169. Ra, K. S., Suh, H. J., & Choi, J. W. (2012). Hypoglycemic effects of Cyclo (His-Pro) in streptozotocin-induced diabetic rats. *Biotechnology and Bioprocess Engineering*, 17(1), 176-184.

170. Rabb, H., Griffin, M. D., McKay, D. B., Swaminathan, S., Pickkers, P., Rosner, M. H., ... & Ronco, C. (2016). Inflammation in AKI: current understanding, key questions, and knowledge gaps. *Journal of the American Society of Nephrology*, 27(2), 371-379.
171. Ragab, D., Abdallah, D. M., & El-Abhar, H. S. (2014). Cilostazol renoprotective effect: Modulation of PPAR-γ, NGAL, KIM-1 and IL-18 underlies its novel effect in a model of ischemia-reperfusion. *Plos one*, 9(5).
172. Rahimi, K., Lotfabad, T. B., Jabeen, F., & Ganji, S. M. (2019). Cytotoxic effects of mono-and di-rhamnolipids from *Pseudomonas aeruginosa* MR01 on MCF-7 human breast cancer cells. *Colloids and Surfaces B: Biointerfaces*, 181, 943-952.
173. Raj, D. S., Pecoits-Filho, R., & Kimmel, P. L. (2020). Inflammation in chronic kidney disease. *In Chronic Renal Disease* (pp. 355-373). Academic Press.
174. Ramesh, G., & Reeves, W. B. (2002). TNF-α mediates chemokine and cytokine expression and renal injury in cisplatin nephrotoxicity. *The Journal of Clinical Investigation*, 110(6), 835-842.
175. Ravanan, R., & Tomson, C. R. (2007). Natural history of postobstructive nephropathy: a single-center retrospective study. *Nephron Clinical Practice*, 105(4), c165-c170.
176. Romagnani, P., Remuzzi, G., Glassock, R., Levin, A., Jager, K. J., Tonelli, M., ... & Anders, H. J. (2017). Chronic kidney disease. *Nature Reviews Disease Primers*, 3(1), 1-24.
177. Rupesh, K. R., Priya, A. M., Prashanth, K., & Jayachandran, S. (2012). Inhibitory effects of bioactive leads isolated from *Pseudomonas aeruginosa* PS3 and *Pseudomonas fluorescens* PS7 on MAP kinases and down regulation of pro inflammatory cytokines (TNF-α, IL-1β) and mediators (NO, iNOS and COX). *Toxicology in vitro*, 26(4), 571-578.
178. Ryan, G. B., & Majno, G. (1977). Acute inflammation. A review. *The American Journal of Pathology*, 86(1), 183.
179. Sakai, K., Nozaki, Y., Murao, Y., Yano, T., Ri, J., Niki, K., ... & Matsumura, I. (2019). Protective effect and mechanism of IL-10 on renal ischemia–reperfusion injury. *Laboratory Investigation*, 99(5), 671-683.
180. Saleki, M., Colgin, N., Kirby, J. A., Cobb, S. L., & Ali, S. (2013). Evaluation of two cyclic di-peptides as inhibitors of CCL2 induced chemotaxis. *Med Chem Comm*, 4(5), 860-864.
181. Scheller, J., Grötzinger, J., & Rose-John, S. (2006). Updating interleukin-6 classic-and trans-signaling. *Signal Transduction*, 6(4), 240-259.

182. Schnaper, H. W., Jandeska, S., Runyan, C. E., Hubchak, S. C., Basu, R. K., Curley, J. F., ... & Hayashida, T. (2009). TGF-beta signal transduction in chronic kidney disease. *Frontiers in Bioscience* (Landmark edition), 14, 2448.
183. Selvakumar, S., Sivasankaran, D., & Singh, V. K. (2009). Enantioselective Henry reaction catalyzed by C 2-symmetric chiral diamine–copper (II) complex. *Organic & Biomolecular Chemistry*, 7(15), 3156-3162.
184. Serhan, C. N., & Savill, J. (2005). Resolution of inflammation: the beginning programs the end. *Nature Immunology*, 6(12), 1191-1197.
185. Shaaban, M., El-Metwally, M. M., & Nasr, H. (2014). A new diketopiperazine alkaloid from Aspergillus oryzae. *Natural Product Research*, 28(2), 86-94.
186. Sharfuddin, A. A., & Molitoris, B. A. (2011). Pathophysiology of ischemic acute kidney injury. *Nature Reviews Nephrology*, 7(4), 189.
187. Sinha, A., Bajpai, M., Panda, S., Ranjan, S., & Sharma, M. C. (2012). Unilateral ureteric obstruction: Role of renin angiotensin system blockade on renal recovery: An experimental study. *Journal of Indian Association of Pediatric Surgeons*, 17(2), 49.
188. Skibba, M., Hye Khan, M., Kolb, L. L., Yeboah, M. M., Falck, J. R., Amaradhi, R., & Imig, J. D. (2017). Epoxyeicosatrienoic acid analog decreases renal fibrosis by reducing epithelial-to-mesenchymal transition. *Frontiers in Pharmacology*, 8, 406.
189. Smith, P. E., Krohn, R. I., Hermanson, G. T., Mallia, A. K., Gartner, F. H., Provenzano, M., ... & Klenk, D. C. (1985). Measurement of protein using bicinchoninic acid. *Analytical Biochemistry*, 150(1), 76-85.
190. Solecka, J., Rajnisz-Mateusiak, A., Guspiel, A., Jakubiec-Krzesniak, K., Ziemska, J., Kawęcki, R., ... & Wietrzyk, J. (2018). Cyclo (Pro-DOPA), a third identified bioactive metabolite produced by *Streptomyces* sp. 8812. *The Journal of Antibiotics*, 71(8), 757-761.
191. Song, S., Fu, S., Sun, X., Li, P., Wu, J. E., Dong, T., ... & Deng, Y. (2018). Identification of cyclic dipeptides from Escherichia coli as new antimicrobial agents against Ralstonia solanacearum. *Molecules*, 23(1), 214.
192. Stark, T., & Hofmann, T. (2005). Structures, sensory activity, and dose/response functions of 2, 5-diketopiperazines in roasted cocoa nibs (*Theobroma cacao*). *Journal of Agricultural and Food Chemistry*, 53(18), 7222-7231.
193. Staugas, R. E., Harvey, D. P., Ferrante, A., Nandoskar, M., & Allison, A. C. (1992). Induction of tumor necrosis factor (TNF) and interleukin-1 (IL-1) by *Pseudomonas aeruginosa* and exotoxin A-induced suppression of lymphoproliferation and TNF,

lymphotoxin, gamma interferon, and IL-1 production in human leukocytes. *Infection and Immunity*, 60(8), 3162-3168.

194. Su, H., Lei, C. T., & Zhang, C. (2017). Interleukin-6 signaling pathway and its role in kidney disease: an update. *Frontiers in Immunology*, 8, 405.
195. Sun, J., Zhang, X., Broderick, M., & Fein, H. (2003). Measurement of nitric oxide production in biological systems by using Griess reaction assay. *Sensors*, 3(8), 276-284.
196. Sun-sang, J. S., Li, L., Huang, L., Lawler, J., Ye, H., Rosin, D. L., ... & Schrader, J. (2017). Proximal tubule CD73 is critical in renal ischemia-reperfusion injury protection. *Journal of the American Society of Nephrology*, 28(3), 888-902.
197. Tabacco, A., Meiattini, F., Moda, E., & Tarli, P. (1979). Simplified enzymic/colorimetric serum urea nitrogen determination. *Clinical Chemistry*, 25(2), 336-337.
198. Tan, M., & Epstein, W. (1972). Polymer formation during the degradation of human light chain and Bence-Jones proteins by an extract of the lysosomal fraction of normal human kidney. *Immunochemistry*, 9(1), 9-16.
199. Tang, W. W., Feng, L., Vannice, J. L., & Wilson, C. B. (1994). Interleukin-1 receptor antagonist ameliorates experimental anti-glomerular basement membrane antibody-associated glomerulonephritis. *The Journal of Clinical Investigation*, 93(1), 273-279.
200. Tattevin, P., Revest, M., Chapplain, J. M., Ratajczak-Enselme, M., Arvieux, C., & Michelet, C. (2013). Increased risk of renal stones in patients treated with atazanavir. *Clinical Infectious Diseases*, 56(8), 1186-1186.
201. Tesch, G. H., Yang, N., Yu, H., Lan, H. Y., Foti, R., Chadban, S. J., ... & Nikolic-Paterson, D. J. (1997). Intrinsic renal cells are the major source of interleukin-1 beta synthesis in normal and diseased rat kidney. *Nephrology, dialysis, transplantation: official publication of the European Dialysis and Transplant Association-European Renal Association*, 12(6), 1109-1115.
202. Therrien, F. J., Agharazii, M., Lebel, M., & Larivière, R. (2012). Neutralization of tumor necrosis factor-alpha reduces renal fibrosis and hypertension in rats with renal failure. *American Journal of Nephrology*, 36(2), 151-161.
203. Thurman, J. M. (2007). Triggers of inflammation after renal ischemia/reperfusion. *Clinical Immunology*, 123(1), 7-13.

204. Tian, X., Feng, J., Fan, S. M., Han, J. R., & Liu, S. X. (2016). Synthesis and activity evaluation of the cyclic dipeptides arylidene N-alkoxydiketopiperazines. *Bioorganic & Medicinal Chemistry*, 24(21), 5197-5205.
205. Timoshanko, J. R., Sedgwick, J. D., Holdsworth, S. R., & Tipping, P. G. (2003). Intrinsic renal cells are the major source of tumor necrosis factor contributing to renal injury in murine crescentic glomerulonephritis. *Journal of the American Society of Nephrology*, 14(7), 1785-1793.
206. Trof, R. J., Di Maggio, F., Leemreis, J., & Groeneveld, A. J. (2006). Biomarkers of acute renal injury and renal failure. *Shock*, 26(3), 245-253.
207. Tullberg, M., Grøtli, M., & Luthman, K. (2006). Efficient synthesis of 2, 5-diketopiperazines using microwave assisted heating. *Tetrahedron*, 62(31), 7484-7491.
208. Ucero, A. C., Benito-Martin, A., Izquierdo, M. C., Sanchez-Nino, M. D., Sanz, A. B., Ramos, A. M., ... & Ortiz, A. (2014). Unilateral ureteral obstruction: beyond obstruction. *International Urology and Nephrology*, 46(4), 765-776.
209. Ucero, A. C., Gonçalves, S., Benito-Martin, A., Santamaría, B., Ramos, A. M., Berzal, S., ... & Ortiz, A. (2010). Obstructive renal injury: from fluid mechanics to molecular cell biology. *Journal of Urology*, *2*, 41.
210. Ulmer, A. J., Pryjma, J., Tarnok, Z., Ernst, M., & Flad, H. D. (1990). Inhibitory and stimulatory effects of Pseudomonas aeruginosa pyocyanine on human T and B lymphocytes and human monocytes. *Infection and Immunity*, 58(3), 808-815.
211. Van Meerloo, J., Kaspers, G. J., & Cloos, J. (2011). Cell sensitivity assays: the MTT assay. In *Cancer Cell Culture* (pp. 237-245). Humana Press.
212. Vaughan, E. D., Marion, D., Poppas, D. P., & Felsen, D. (2004). Pathophysiology of unilateral ureteral obstruction: studies from Charlottesville to New York. *The Journal of Urology*, 172(6 Part 2), 2563-2569.
213. Vikram, A., Ante, V. M., Bina, X. R., Zhu, Q., Liu, X., & Bina, J. E. (2014). Cyclo (valine–valine) inhibits *Vibrio cholerae* virulence gene expression. *Microbiology*, 160(Pt 6), 1054.
214. Wang, G., Dai, S., Chen, M., Wu, H., Xie, L., Luo, X., & Li, X. (2010). Two diketopiperazine cyclo (pro-phe) isomers from marine bacteria *Bacillus subtilis* sp. 13-2. *Chemistry of Natural Compounds*, 46(4), 583-585.
215. Wang, N., Cui, C. B., & Li, C. W. (2016). A new cyclic dipeptide penicimutide: the activated production of cyclic dipeptides by introduction of neomycin-resistance in the

marine-derived fungus *Penicillium Purpurogenum* G59. *Archives of Pharmacal Research*, 39(6), 762-770.

216. Wattana-Amorn, P., Charoenwongsa, W., Williams, C., Crump, M. P., & Apichaisataienchote, B. (2016). Antibacterial activity of cyclo (L-Pro-L-Tyr) and cyclo (D-Pro-L-Tyr) from *Streptomyces* sp. strain 22-4 against phytopathogenic bacteria. *Natural Product Research*, 30(17), 1980-1983.
217. Wei, H. X., Fang, X. W., Xie, X. S., Zhang, S. P., Jiang, Y., & Wu, S. H. (2017). Secondary Metabolites of a Soil-Derived *Streptomyces kunmingensis*. *Chemistry of Natural Compounds*, 53(4), 794-796.
218. Wendt, M. K., Allington, T. M., & Schiemann, W. P. (2009). Mechanisms of the epithelial–mesenchymal transition by TGF-β. *Future Oncology*, 5(8), 1145–1168.
219. Wierenga, K. A., Wee, J., Gilley, K. N., Rajasinghe, L. D., Bates, M. A., Gavrilin, M. A., ... & Pestka, J. J. (2019). Docosahexaenoic Acid Suppresses Silica-Induced Inflammasome Activation and IL-1 Cytokine Release by Interfering with Priming Signal. *Frontiers in Immunology*, 10, 2130.
220. Wilber, J. F. (1995). *U.S. Patent No. 5,418,218*. Washington, DC: U.S. Patent and Trademark Office.
221. Wilson, P. D., Devuyst, O., Li, X., Gatti, L., Falkenstein, D., Robinson, S., ... & Burrow, C. R. (2000). Apical plasma membrane mispolarization of NaK-ATPase in polycystic kidney disease epithelia is associated with aberrant expression of the β2 isoform. *The American Journal of Pathology*, 156(1), 253-268.
222. Wolfs, T. G., Buurman, W. A., van Schadewijk, A., de Vries, B., Daemen, M. A., Hiemstra, P. S., & van't Veer, C. (2002). In vivo expression of Toll-like receptor 2 and 4 by renal epithelial cells: IFN-γ and TNF-α mediated up-regulation during inflammation. *The Journal of Immunology*, 168(3), 1286-1293.
223. Wong, W. W., Gentle, I. E., Nachbur, U., Anderton, H., Vaux, D. L., & Silke, J. (2010). RIPK1 is not essential for TNFR1-induced activation of NF-κ B. *Cell Death & Differentiation*, 17(3), 482-487.
224. Wu, M. Y., Yiang, G. T., Liao, W. T., Tsai, A. P. Y., Cheng, Y. L., Cheng, P. W., ... & Li, C. J. (2018). Current mechanistic concepts in ischemia and reperfusion injury. *Cellular Physiology and Biochemistry*, 46(4), 1650-1667.
225. Xing, L., Song, E., Yu, C. Y., Jia, X. B., Ma, J., Sui, M. S., ... & Gao, X. (2019). Bone marrow–derived mesenchymal stem cells attenuate tubulointerstitial injury through

multiple mechanisms in UUO model. *Journal of Cellular Biochemistry*, 120(6), 9737-9746.

226. Xu, Z., Zhang, Y., Fu, H., Zhong, H., Hong, K., & Zhu, W. (2011). Antifungal quinazolinones from marine-derived Bacillus cereus and their preparation. *Bioorganic & Medicinal Chemistry Letters*, 21(13), 4005-4007.
227. Xu-Tao, C. A. O., Dong, W. A. N. G., Na, W. A. N. G., & Zheng, C. U. I. (2009). Water-soluble constitutions from the skin of Bufo bufo gargarizans Cantor. *Chinese Journal of Natural Medicines*, 7(3), 181-183.
228. Yamazaki, Y., Kido, Y., Hidaka, K., Yasui, H., Kiso, Y., Yakushiji, F., & Hayashi, Y. (2011). Development of Chemical Probes towards the Elucidation of Binding Mechanism of Plinabulin, a Cyclicdipeptide Based Anti-microtubule Agent. *In Peptide Science: Proceedings of the... Japanese Peptide Symposium* (Vol. 2010, p. 56).
229. Yang, L., Tan, R. X., Wang, Q., Huang, W. Y., & Yin, Y. X. (2002). Antifungal cyclopeptides from *Halobacillus litoralis* YS3106 of marine origin. *Tetrahedron Letters*, 43(37), 6545-6548.
230. Yang, S. C., Sung, P. J., Lin, C. F., Kuo, J., Chen, C. Y., & Hwang, T. L. (2014). Anti-inflammatory effects of secondary metabolites of marine *Pseudomonas* sp. in human neutrophils are through inhibiting P38 MAPK, JNK, and calcium pathways. *PLoS one*, 9(12).
231. Zhai, Y., Shao, Z., Cai, M., Zheng, L., Li, G., Yu, Z., & Zhang, J. (2019). Cyclo (l-Pro–l-Leu) of Pseudomonas putida MCCC 1A00316 Isolated from Antarctic Soil: Identification and Characterization of Activity against *Meloidogyne incognita*. *Molecules*, 24(4), 768.
232. Zhang, H. (2011). Anti-IL-1 β Therapies. Recent patents on DNA & gene sequences, 5(2), 126-135.
233. Zhang, W., Wang, W., Yu, H., Zhang, Y., Dai, Y., Ning, C., ... & Xia, Y. (2012). Interleukin 6 underlies angiotensin II–induced hypertension and chronic renal damage. *Hypertension*, 59(1), 136-144.
234. Zhang, X. L., Topley, N., Ito, T., & Phillips, A. (2005). Interleukin-6 regulation of transforming growth factor (TGF)-β receptor compartmentalization and turnover enhances TGF-β1 signalling. *Journal of Biological Chemistry*, 280(13), 12239-12245.

235. Zhang, X., Song, Y., Ci, X., An, N., Ju, Y., Li, H., ... & Deng, X. (2008). Ivermectin inhibits LPS-induced production of inflammatory cytokines and improves LPS-induced survival in mice. *Inflammation Research*, 57(11), 524-529.
236. Zhao, J. Y., Ding, J. H., Li, Z. H., Feng, T., Zhang, H. B., & Liu, J. K. (2018). A new cyclic dipeptide from cultures of *Coprinus plicatilis*. *Natural Product Research*, 32(8), 972-976.
237. Zhong, J., Yang, H. C., & Fogo, A. B. (2017). A perspective on chronic kidney disease progression. *American Journal of Physiology-Renal Physiology*, 312(3), F375-F384.
238. Zhou, X., Fang, P., Tang, J., Wu, Z., Li, X., Li, S., ... & Yao, X. (2016). A novel cyclic dipeptide from deep marine-derived fungus Aspergillus sp. SCSIOW2. *Natural Product Research*, 30(1), 52-57.

LIST OF PUBLICATIONS FROM THESIS WORK

1. A. Sajeli Begum*****, **Kirti Hira**, Ameer Basha Shaik, Pragya P. P., Onkar P. Kulkarni, H. Araya and Y. Fujimoto. l-Proline-based-cyclic dipeptides from *Pseudomonas* sp. (ABS-36) inhibit pro-inflammatory cytokines and alleviate crystal-induced renal injury in mice. *International Immunopharmacology*, 2019, doi.org/10.1016/j.intimp.2019.05.044
2. **Kirti Hira**, Ameer Basha, Santosh Kumar, Sajeli Begum Ahil*. "*Pseudomonas* – a potential source for drug lead discovery" *Current Trends in Biomedical Engineering and Biosciences*, 2017, 5(5), 555674. DOI: 10.19080/CTBEB.2017.05.555674
3. **Kirti Hira**, Pravesh Sharma, Onkar Kulkarni, Sajeli Begum Ahil*. *"Pseudomonas* sp. (ABS-36) derived cyclic dipeptides alleviates acute renal injury in ischemic reperfusion"- Under Communication.

OTHER PUBLICATIONS

1. Sajeli Ahil Begum*, **Kirti Hira**, Pragya Paramita Pal, Samrun Nessa, Onkar P. Kulkarni, Jeyapragash Danaraj, Ameer Basha Shaik, Hiroshi Araya, Yoshinori Fujimoto. Halodule pinifolia (Seagrass) attenuated lipopolysaccharide-, carrageenan- and crystal-induced secretion of pro-inflammatory cytokines: Mechanism and Chemistry. Inflammopharmacology, 2020
2. Santhosh S Kumar, **Kirti Hira**, Sajeli Begum Ahil*, Onkar P Kulkarni, Hiroshi Araya and Yoshinori Fujimoto. New Synthetic Coumarinolignans as Attenuator of Pro-Inflammatory Cytokines under LPS-Induced Sepsis and Carrageenan-Induced Paw Oedema Models. Inflammopharmacology, 2020, https://doi.org/10.1007/s10787-020-00710-w
3. S. Santhosh Kumar, Ahil Sajeli Begum***, Kirti Hira**, Sarfaraj Niazi, B.R. Parshantha Kumar, Hiroshi Araya and Yoshinori Fujimoto. Structure-based design and synthesis of new 4-methylcoumarin-based lignans as pro-inflammatory cytokines (TNF-<alpha>, IL-6 and IL-1<beta>) inhibitors. *Bioorganic Chemistry*, 2019, DOI 10.1016/j.bioorg.2019.102991
4. Ahil Sajeli Begum*, Santosh Kumar, Suryanarayana G, **Kirti Hira**. "O-Glucoside of natural cleomiscosin-A: An attenuator of pro-inflammatory cytokine production" *Phytochemistry Letters*, 2018, 26, 83-8. https://doi.org/10.1016/j.phytol.2018.05.022
5. Pabbati Sanjana, **Hira Kirti** and Sajeli Begum*. "Medical devices and their approval procedure in India" *Int. J. Drug Reg. Affairs* 2016, 4(3), 19-29 (DOI: http://dx.doi.org/10.22270/ijdra.v4i3.186).

PAPER PRESENTED AT NATIONAL AND INTERNATIONAL CONFERENCES

1. Cyclo (Val-Pro) attenuates renal injury by inhibiting pro-inflammatory cytokines in mice renal ischemic model. **Cytokines 2019- International Cytokines And Interferon Society, Vienna, Austria**. Oct 20-23,2019.
2. Natural Diketopiperazines as TNF α and IL 6 inhibitors. **Pharmacology 2018 – British Pharmacological Society**, London, UK. Dec 18 – 20, 2018.
3. Tumor Necrosis Factor-alpha inhibitory activity of *H.pinifolia*. **24th ISCB International Conference**, Manipal University, India. 11-13th Jan 2018.
4. MTT assay-guided isolation of a cytotoxic lead from *Hedyotic umbellata* and its mechanism of action against non-small cell lung cancer A549 cells. **International Conference on Drug Development Technology** (Dubai), Oct 16-17, 2017, 19(10) Part VIII, 891.
5. Screening of phyto-compounds to identify cytotoxic lead molecules against A549, MDA-MB and HT-29 cell lines and their isolation methods. **68th Indian Pharmaceutical Congress**, 2016, Dec 16-18, Visakhapatnam.

Biography of Kirti

Kirti completed her B.Pharm degree in the year 2014 from Delhi Institute of Pharmaceutical Sciences and Research (DIPSAR), New Delhi and her M.S Pharm degree in the year 2016 from National Institute of Pharmaceutical Education and Research (NIPER), Mohali. In August 2016, she got admitted for PhD program in Department of Pharmacy, BITS-Pilani, Hyderabad campus under the supervision of Prof. A. Sajeli Begum. Later in the same year, she was awarded with CSIR-JRF Fellowship from CSIR, New Delhi. As a part of research achievements, she has contributed to seven international publications, two patents and one book chapter till date. She has presented her work in several National and International conferences. She was also awarded with travel grant from CSIR, New Delhi and Milstein Travel Grant Award, in 2019, to present her research work entitled "Cyclo(Val-Pro) attenuates renal injury by inhibiting pro-inflammatory cytokines in mice renal ischemic model" at Cytokines 2019- International Cytokines And Interferon Society at Vienna, Austria (Oct 20-23,2019).

Biography of Prof. A. Sajeli Begum

Prof. Ahil Sajeli Begum is currently an Associate Professor and Head of the Department of Pharmacy, Birla Institute of Technology and Science, Pilani-Hyderabad Campus. She received her B. Pharm degree (1999) from Dr. M.G.R. Medical University, Chennai and M. Pharm degree (2001) in Pharmaceutical Chemistry from Indian Institute of Technology-Banaras Hindu University (IIT-BHU), Varanasi. She was awarded with Ph.D. degree (2005) from IMS-BHU. Prof. A.S. Begum is a recipient of the Deutscher Akademischer Austausch Dienst (DAAD) Fellowship (2004) to pursue research at Eberhard Karls University, Tubingen, Germany. Soon after completing her Ph.D. program, she joined in Department of Pharmaceutics at IIT-BHU, Varanasi as an Assistant Professor and then moved to BITS-Pilani Hyderabad in mid-2010. She has 15 years of experience in teaching and research. She has successfully completed 4 research projects funded by University Grants Commission (UGC) – New Delhi, Council of Scientific and Industrial Research (CSIR)-New Delhi, Department of Science and Technology (DST) and Indian Council of Medical Research (ICMR) - Indian Council of Social Science Research (ICSSR). She has 45 publications and 2 patents to her credit and authored a book chapter in "Progress in the Chemistry of Organic Natural Products" published by Springer Wien New York. Prof A.S. Begum is a life time member of various scientific forums like Association of Pharmaceutical Teachers of India (APTI), Indian Pharmacy Graduates Association (IPGA), Indian Chemical Society, Society for Ethno pharmacology, Member of Indian Phytopathological Society and Member of International Cytokine and Interferon Society. She has successfully guided 4 PhD students and currently supervising 5 students for their doctoral thesis work.

Biography of Prof. Onkar Prakash Kulkarni

Prof. Onkar Prakash Kulkarni is currently an Associate Professor in the Department of Pharmacy, Birla Institute of Technology and Science, Pilani-Hyderabad Campus. He received his B. Pharm degree (2002) from College of Pharmacy, Solapur, Shivaji University and M. Pharm degree (2004) from College of Pharmaceutical Sciences Manipal, MAHE University. He has completed his Ph.D. and Post-Doc in the area of renal inflammatory diseases in Ludwig Maximilians University Munich, Germany. He has published more than 40 research articles in peer reviewed journals. He has completed 3 projects as principal investigator and has 2 ongoing projects as co-principal investigator to his credit. He was awarded with the prestigious Har Govind Singh Khorana- Innovative Young Biotechnologist Award by DBT in the year 2015 in the category of chronic kidney disease. He is currently supervising 6 students for their doctoral thesis work.